Combined Reactions and Separations

Using

Ionic Liquids and Carbon Dioxide

Maaike Christine KROON

Combined Reactions and Separations

Using

Ionic Liquids and Carbon Dioxide

Proefschrift

ter verkrijging van de graad van doctor
aan de Technische Universiteit Delft,
op gezag van de Rector Magnificus Prof. dr. ir. J. T. Fokkema,
voorzitter van het College voor Promoties,
in het openbaar te verdedigen op maandag 11 december 2006 om 15:00 uur

door

Maaike Christine KROON

scheikundig ingenieur
geboren te Rotterdam

"The world is more complicated than the truths about it"
Stefan Themerson

Summary

Combined Reactions and Separations Using Ionic Liquids and Carbon Dioxide

The chemical industry is under considerable pressure to drastically reduce the huge amounts of chemical waste produced and energy consumed. Efforts to increase the resource-efficiency in chemical processing include the replacement of stoichiometric reactions by catalytic alternatives, the minimization of solvent losses and the integration of several unit operations into one process step. The main objective of this thesis is to develop a new methodology to design processes using ionic liquids and carbon dioxide as combined reaction and separation media in order to minimize waste generation and energy consumption. Bottlenecks concerning reaction and separation rates, selectivities, (electro)chemical and thermal stabilities, prediction of thermodynamic phase equilibria, and economical, ecological and social aspects are addressed. This thesis contributes to the realization of ionic liquid/carbon dioxide processes.

Ionic liquids are salts with melting points close to room temperature. They are emerging as green solvents for chemical processes, because they combine good and tunable solubility properties with negligible vapor pressures and high thermal and (electro-) chemical stabilities. They are used as reaction media, where they enhance reaction rates and selectivities. It is possible to separate products from ionic liquids by extraction with supercritical carbon dioxide without detectable ionic liquid contamination, because the solubility of ionic liquids in carbon dioxide is negligibly low. Ionic liquid/carbon dioxide systems display the recently established miscibility windows phenomenon: carbon dioxide is able to force two or more immiscible phases to form one homogeneous phase at only moderate pressure increase in a narrow carbon dioxide mole fraction range. With this two-phase/single-phase transformation, it is possible to carry out the reaction in a homogeneous system, whereas the product can instantaneously be recovered from the biphasic system. High reaction and separation rates can be achieved compared with the conventional fully biphasic ionic liquid/carbon dioxide process.

The novel approach to combine reactions and separations using ionic liquids and carbon dioxide is applied to the enantioselective hydrogenation of methyl (*Z*)-α-acetamido-cinnamate in the 1-butyl-3-methylimidazolium tetrafluoroborate (ionic liquid) + carbon dioxide system. Operation conditions are determined on basis of the phase behavior of the model system. Although very high pressures (~50 MPa) were needed to dissolve all components in the ionic liquid phase, it was possible to carry out the homogeneously catalyzed reaction at reasonable pressures (~5 MPa) in a heterogeneous system in which all components except hydrogen were fully dissolved in the ionic liquid. Conversions and enantioselectivities were comparable to the conventional production process. The stability of the catalyst is however greatly improved.

The product N-acetyl-(*S*)-phenylalanine methyl ester can be separated from the ionic liquid using carbon dioxide either as co-solvent in extractions (in the low carbon dioxide

concentration regime), or as anti-solvent in precipitations (in the high carbon dioxide concentration regime). Because the ionic liquid has a negligible solubility in carbon dioxide, it is possible to extract pure product without any detectable amount of ionic liquid. It was demonstrated for the first time that a product could thus be separated from an ionic liquid by precipitation under influence of carbon dioxide. This effect is caused by the lower solubility of the product in ionic liquid/carbon dioxide mixtures compared to the solubility in the pure ionic liquid at atmospheric conditions. After precipitation the formed crystals can be washed using carbon dioxide to obtain a more pure product. Both separation methods work well and can reach a 100% recovery using a proper process lay-out.

The experimental determination of the conditions for reaction and separation in the new process set-up is very time-consuming and expensive. Therefore, an equation of state is developed that predicts the phase behavior of ionic liquid/carbon dioxide systems, which is based on the truncated Perturbed Chain Polar Statistical Associating Fluid Theory. This equation of state accounts explicitly for the dipolar interactions between ionic liquid molecules, the quadrupolar interactions between carbon dioxide molecules, and the Lewis acid-base type of interaction between the ionic liquid and the carbon dioxide molecules. Physically meaningful model pure component parameters for ionic liquids were estimated based on literature data. All experimental vapor-liquid equilibrium data are correlated with a single linearly temperature-dependent binary interaction parameter. The ability of the model to describe accurately carbon dioxide solubility in various 1-alkyl-3-methylimidazolium-based ionic liquids with different alkyl chain lengths and different anions at pressures from 0 MPa to 100 MPa and carbon dioxide fractions from 0 to 75 mole % is demonstrated.

Given the enormous variety of possible ionic liquids, there is a need to predict their properties, such as their thermal and (electro)chemical stabilities. In this thesis such a prediction method has been developed using quantum chemical calculations. This tool was used to predict the decomposition mechanisms and products of thermal and electrochemical breakdown reactions. The activation energies of the calculated thermal decomposition reactions corresponded well with the measured decomposition temperatures and may be used to predict the decomposition temperature of an ionic liquid before it is synthesized. The electrochemical window could be correlated to the calculated difference in energy level of Lowest Unoccupied Molecular Orbital (LUMO) of the cation and Highest Occupied Molecular Orbital (HOMO) of the anion. Moreover, the electrochemical decomposition reactions of several ionic liquids on the cathode limit were successfully predicted and verified by experiments.

The use of ionic liquids in combination with carbon dioxide in chemical processes leads to economical and environmental benefits compared to conventional production processes. Reductions in the use of catalyst and volatile organic solvents lead to lower costs for raw materials and lower waste disposal costs. No expensive purification steps are required to remove catalyst residues from the product. The energy costs for pressurizing the carbon dioxide in the ionic liquid/carbon dioxide process are lower than

Summary

_____

the energy costs for evaporating the solvent in the conventional process. When the ionic liquid/carbon dioxide process is for example applied to the production of 1600 ton/year Levodopa, a medicine against Parkinsonian disease, the energy consumption is reduced by 20,000 GJ per year and the waste generation is reduced by 4800 ton of methanol per year and 480 kg Rh-catalyst per year, resulting in a decrease in total operational costs of over 11 million euros per year.

From an economical and an environmental point of view, fast implementation of the new process-set up is desired. Suggestions for the fastest implementation are made based on the cyclic innovation model, which does not represent innovation by a linear chain, but by coupled 'circles of change' that connect science and business in a cyclic manner. The most important obstacles in the implementation of the ionic liquid/carbon dioxide production process are the successful life cycle management of current production plants, the linearity of current innovation thinking and a perceived high risk of adoption. According to the cyclic innovation model, these obstacles can be overcome when developments in all cycles occur in a parallel fashion and all involved actors collaborate in coupled networks.

Maaike C. Kroon

Samenvatting

Gecombineerde reacties en scheidingen met behulp van ionische vloeistoffen en koolstofdioxide

De chemische industrie staat onder druk om de enorme afvalproductie en energie-consumptie drastisch te verminderen. Bestaande oplossingen om de huidige process-industrie te verduurzamen zijn de vervanging van stoichiometrische reacties door katalytische alternatieven, de minimalisatie van oplosmiddelverliezen en de integratie van verschillende processtappen in één stap. Het hoofddoel van dit onderzoek is het ontwikkelen van een nieuwe procesmethode met behulp van ionische vloeistoffen en koolstofdioxide als gecombineerde reactie- en scheidingsmedia om de afvalproductie en het energieverbruik in de chemische industrie te reduceren. Knelpunten met betrekking tot reactie- en scheidingssnelheden, selectiviteiten, stabiliteiten, voorspellingen van thermodynamische evenwichten en economische, ecologische en sociale aspecten worden geadresseerd. Dit proefschrift draagt bij aan de realisatie van ionische vloeistof/koolstof-dioxide processen.

Ionische vloeistoffen zijn zouten met een smeltpunt rond de 25 ^{o}C. Ionische vloeistoffen staan in de belangstelling als alternatieve schone oplosmiddelen in de chemische industrie, omdat ze geen dampspanning hebben en daardoor niet tot emissies naar de atmosfeer kunnen leiden. Bovendien vertonen ionische vloeistoffen hoge oplosbaarheden voor allerlei chemicaliën, en hoge thermische en (electro-)chemische stabiliteiten. Ionische vloeistoffen worden gebruikt als reactiemedia, waar ze de reactiesnelheden en selectiviteiten verhogen. Het is mogelijk om producten van ionische vloeistoffen te scheiden door middel van extractie met superkritisch koolstofdioxide zonder meetbare verontreiniging met de ionische vloeistof, omdat ionische vloeistoffen niet oplossen in koolstofdioxide. Deze feiten vormen de basis van dit proefschrift, samen met de recente ontdekking van het 'miscibility windows' fenomeen: koolstofdioxide is in staat om twee of meer niet-mengbare fasen te forceren om één fase te vormen bij beperkte drukverhoging in een klein koolstofdioxide concentratiegebied. Door gebruik te maken van deze twee-fasen/één-fase transitie, is het mogelijk om een reactie in een homogeen systeem uit te voeren, terwijl de scheiding plaatsvindt in het twee-fasen systeem. Op deze manier worden hoge reactie- en scheidingssnelheden gehaald vergeleken met conventionele ionische vloeistof/koolstofdioxide processen, die geheel in het twee-fasen gebied plaatsvinden.

De nieuwe methode om reacties en scheidingen te combineren met behulp van ionische vloeistoffen en koolstofdioxide werd toegepast op de asymmetische hydrogenering van methyl-(*Z*)-α-acetamidocinnamaat in het systeem 1-butyl-3-methylimidazolium tetrafluoroboraat (ionische vloeistof) + koolstofdioxide. Op basis van het fasegedrag van het model systeem werden de werkcondities bepaald. Hoge drukken (~ 50 MPa) zijn nodig om alle componenten op te lossen in de ionische vloeistof. Daarom kan de homogeen-gekatalyseerde reactie beter plaatsvinden in een heterogeen systeem, waar alle

componenten behalve waterstof geheel in de ionische vloeistof zijn opgelost. De bereikte conversies en selectiviteiten zijn vergelijkbaar met het conventionele process. De katalysator kan worden hergebruikt zonder signifante deactivatie.

Het product N-acetyl-(S)-fenylalanine methylester kan van de ionische vloeistof worden afgescheiden door gebruik te maken van koolstofdioxide als 'co-solvent' in extracties of als 'anti-solvent' in precipitaties. Omdat ionische vloeistoffen niet oplossen in koolstofdioxide, werd zuiver product verkregen door middel van extractie. Ook werd aangetoond dat het mogelijk is om een product uit een ionische vloeistof te precipiteren onder invloed van koolstofdioxide. Dit effect wordt veroorzaakt door de lagere oplosbaarheid van het product in mengsels van ionische vloeistof en koolstofdioxide dan in zuivere ionische vloeistoffen. Na precipitatie werden de gevormde kristallen gewassen met koolstofdioxide, zodat een zuiver product wordt verkregen. Beide scheidings-methoden werken goed. Als het scheidingsproces goed is ontworpen, kan het product volledig worden teruggewonnen.

Het is erg tijdrovend om de werkcondities van het ionische vloeistof/koolstofdioxide proces experimenteel vast te stellen. Daarom is het verstandig om een model te ontwikkelen dat het fasegedrag van ionische vloeistof/koolstofdioxide systemen kan voorspellen. In dit proefschrift wordt het 'truncated Perturbed Chain Polar Statistical Associating Fluid Theory' model gebruikt om ionische vloeistof/koolstofdioxide systemen te modeleren. Deze statistisch mechanische toestandsvergelijking houdt rekening met de dipoolmomenten van de ionische vloeistof moleculen, de quadrupool momenten van de koolstofdioxide moleculen en de Lewis zuur-base interacties tussen de ionische vloeistof en de koolstofdioxide. De parameters voor de ionische vloeistof moleculen werden geschat op basis van microscopische gegevens voor ionische vloeistoffen uit de literatuur. Alleen de binaire interactie parameter werd gefit aan experimentele data van fasegedrag. Het model is in staat om het fasegedrag van verschillende ionische vloeistof + koolstofdioxide systemen goed te beschrijven over een drukbereik van 0 tot 100 MPa en een koolstofdioxide fractie bereik van 0 tot 75 mol%.

Door de enorme variëteit aan ionische vloeistoffen, is het noodzakelijk om hun eigenschappen te kunnen voorspellen. In dit proefschrift wordt een dergelijke rekenmethode op basis van quantumchemische berekeningen beschreven. Deze berekeningen worden gebruikt om de thermische en electrochemische decompositie-mechanismen en producten te kunnen voorspellen. De activeringsenergieën van de thermische decompositiereacties zijn een goede maat voor de experimenteel gemeten decompositietemperaturen. De electrochemische 'windows' kunnen worden gecorreleerd aan het berekende verschil in energieniveau tussen de laagste ongevulde electronenschil van het kation en de hoogste gevulde electronenschil van het anion. Op die manier kunnen decompositietemperaturen en electrochemische 'windows' worden geschat voor ionische vloeistoffen voordat ze gesynthetiseerd worden.

Het gebruik van ionische vloeistoffen in combinatie met koolstofdioxide in chemische processen leidt tot economische en ecologische voordelen vergeleken met conventionele

productieprocessen. Doordat minder afval wordt geproduceerd en er efficiënter wordt omgegaan met grondstoffen en energie, zijn de operationele kosten lager. Bovendien zijn er geen dure zuiveringsstappen nodig om het product zuiver in handen te krijgen. Bij toepassing van de nieuwe productiemethode op de productie van 1600 ton Levodopa (een medicijn tegen de ziekte van Parkinson) per jaar, kan de energieconsumptie worden gereduceerd met 20,000 GJ per jaar en de afvalproductie worden gereduceerd met 4800 ton methanol per jaar en 480 kg rhodium-katalysator per jaar. Dit resulteert in een besparing op de operationele kosten van ruim 11 miljoen euro per jaar.

Vanwege de enorme economische en ecologische voordelen, is een snelle industriële implementatie van de nieuwe productiemethode gebruikmakend van ionische vloeistoffen en koolstofdioxide gewenst. Een aantal suggesties om de nieuwe productiemethode zo snel mogelijk te implementeren wordt gedaan op basis van het cyclische innovatiemodel. De belangrijkste obstakels die implementatie van ionische vloeistoftechnologieën tegenhouden zijn de reeds gedane investeringen in bestaande productieplants, de lineariteit van het huidige innovatietraject, en het vermeende hoge risico door onbekendheid van de technologie. Volgens het cyclische innovatiemodel kunnen deze obstakels worden overwonnen wanneer innovatieve ontwikkelingen parallel plaatsvinden op verschillende plaatsen en niveaus (met onderlinge cyclische interactie), en wanneer alle betrokkenen met elkaar samenwerken in gekoppelde netwerken.

Maaike C. Kroon

Table of contents

1

Introduction

1

Introduction

Although the need for sustainable technology is widely recognized, many chemical processes are still energy-intensive and generate a lot of waste. Efforts to increase the resource-efficiency in chemical processing include the replacement of stoichiometric reactions by catalytic alternatives, the minimization of solvent losses and the integration of several unit operations into one process step. In this chapter different possibilities for increasing resource-efficiency are evaluated. Special attention is given to energy-intensive and waste-free processes that use ionic liquids and/or supercritical fluids as reaction and separation media. The chapter is concluded with an outline of this thesis.

1. Introduction

1.1 Problem definition

In the Western world, the chemical industry has matured and investments have stabilized. One reason is that the lifetime of production plants is much larger than anticipated due to careful maintenance. Another reason is that smart engineering has increased the capacities of existing plants beyond expectation. Therefore, many current production processes originated from twenty years ago and are not based on the latest state-of-the-art technology. These processes generally produce more waste than necessary and are energy-intensive.

Environmental concerns call for new technologies. The chemical industry, which uses 34% (= 155 EJ)[1] of the total world energy consumption, is under considerable pressure to replace many existing processes with new technologies aiming at a zero environmental footprint (zero emission, zero waste generation, use of renewable resources, zero energy consumption). This is especially true for the fine chemical and pharmaceutical industries, which use much energy[2] and generate a large amount of chemical waste[3] per kilogram net product (see table 1.1).

Table 1.1: World production volume[2], energy consumption[2] and waste generation[3] per specific product within various industry segments

Industry segment	Production (tons/annum)	Energy use (MJ) per kg product	Waste produced (kg) per kg product
Oil refining	10^6-10^9	0.5-10	<0.1
Bulk chemicals	10^4-10^7	5-30	0.1-5
Fine chemical industry	10^2-10^4	20-100	5-50
Pharmaceutical industry	10^1-10^3	50-200	25-100

If this issue is not addressed, the energy and waste problem will grow larger in the future, because the annual world energy consumption and waste generation are increasing strongly due to the growth of the world population and the increase in the standard of living in emerging economies (see figure 1.1).
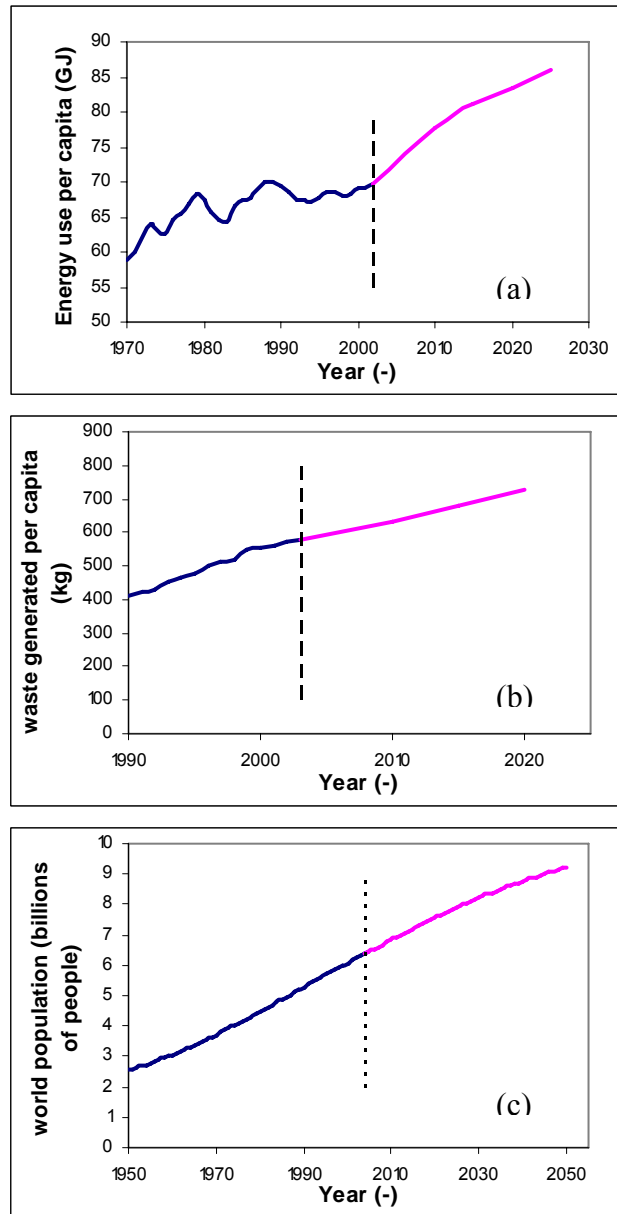
Figure 1.1: (a) World energy consumption per capita[1] (1970-2025), (b) non-recyclable EU municipal solid waste generation per capita[4] (1990-2015) and (c) world population[5] (1950-2050). Predictions are based on a 'business as usual' scenario for economic growth. The rise in total energy consumption and waste generation is much steeper than panels (a) and (b) depict, because of the multiplication by the increase in the world population (c).

According to Von Weizsäcker *et al*.[6], we could supply the needs of twice as many people using only half the resources, if only we would use available better technologies ('Factor 4'). Alternatively, we could increase the quality of life for twice as many people at half the present cost. Therefore, new sustainable technologies must be developed and existing better technologies must be implemented.

Anastas and Warner[7] have outlined twelve basic principles of green chemistry as a basis for judgements on sustainability:

1. Prevention (prevention of waste production instead of remediation of waste once formed)
2. Atom economy
3. Less hazardous chemicals
4. Design safer chemical products
5. Safer solvents & auxiliaries (with lower environmental impact)
6. Energy-efficient by design (energy consumption close to thermodynamically necessary energy)
7. Use of renewable feedstocks
8. Shorter synthesis (avoid derivatization)
9. Catalysis (more selective, less by-products)
10. Design for degradation
11. Real-time analysis for pollution prevention
12. Inherently safer chemistry for accident prevention

Green processes are therefore processes that are energy-efficient, minimize or preferably eliminate the formation of waste, avoid the use of toxic and/or hazardous solvents and reagents and, where possible, utilize renewable raw materials[8]. Green chemistry emphasizes primary pollution prevention instead of remediation. Most important is the minimization of waste generation and energy consumption by the chemical industry. This will not only lead to a cleaner environment, but also to a more cost-effective use of resources.

Today, new opportunities for increasing the resource-efficiency in chemical processing have emerged. These efforts include the replacement of stoichiometric reactions by catalytic alternatives, the minimization of solvent losses and the integration of several unit operations into one process step (see paragraph 1.2). Examples are the use of shape-selective catalysts (zeolites) in the butene to isobutene isomerization[9], the use of membrane reactors in the ethylene oxide production[10] and the use of reactive distillation for the methyl acetate production[11]. These processes combine reactions and separations into one process step and show a higher selectivity towards the main products. The result is less by-product generation (waste) and a lower energy requirement for purification.

However, despite more attention for sustainability, many chemical processes are still energy-intensive and generate a lot of waste. Commercialization of new technological breakthroughs is slow. Long implementation trajectories are a result of the current investment requirements, the perceived high risk of adoption of new technologies and the linearity of the steps in the innovation process. It is desirable to develop more sustainable technologies that significantly increase the resource-efficiency of a chemical process and to reduce the implementation time of such technologies.

1.2 Increasing resource-efficiency

1.2.1 Minimization of energy consumption

The energy consumption of the chemical process industry accounts for about one third of the total consumption by all the manufacturing industries. About 50% to 80% of this amount of energy is used for the separation or purification of chemicals. Most energy-intensive separation steps include distillation and drying by evaporation[12]. In recent decades there has been a significant increase in the energy-efficiency of these process steps by optimization. However, in several cases the limits on what can be done within economical restrictions on a unit operation scale have been reached. To maintain the trend of energy-efficiency increase, it will be necessary to integrate the different unit operations, such as reactions and separations, into one process step (= process intensification). This will lead to the development of new techniques and equipment that give substantial reductions in the energy use and waste production, the size of production equipment and the investment costs, resulting in more sustainable and safer technologies. Moreover, alternative separation methods instead of the energy-intensive distillation step have to be applied, such as membrane-based separations.

1.2.2 Minimization of waste generation

The total amount of non-hazardous waste generated by the chemical industry in the EU is 350 million ton/year[13], while the hazardous industrial waste generation in the EU is 62 million ton/year[13]. A major reason for this waste generation is that reactions are often performed with a stoichiometric amount of catalyst or carrier. Furthermore, solvent losses also substantially contribute to the waste generation (see table 1.2).

Table 1.2: Origins of industrial waste[8]

Origin	*Examples*
Stoichiometric waste	
• Brønsted acids and bases	Aromatic nitrations (H_2SO_4/HNO_3)
	Base promoted condensations (NaOH)
• Lewis acids	Friedel-Crafts acylation ($AlCl_3$, $ZnCl_2$, BF_3)
• Oxidants and reductants	Oxidation ($Na_2Cr_2O_7$, $KMnO_4$)
	Reduction ($LiAlH_4$, $NaBH_4$)
• Halogen replacements	Nucleophilic substitutions
Solvent losses	Air emissions
	Aqueous effluent

The key to waste minimization in chemical manufacture is the widespread substitution of classical stoichiometric syntheses by atom efficient, catalytic alternatives, consisting of fewer steps. Longevity and efficient recycling of the catalyst is a prerequisite for economically and environmentally attractive processes. An example of a classical versus a green atom-efficient reaction is shown in figure 1.2.

1.   Stoichiometric: atom-utilization = $\dfrac{108}{108+14+23+35.5} = 60\%$

2.   Catalytic: atom-utilization = 100%
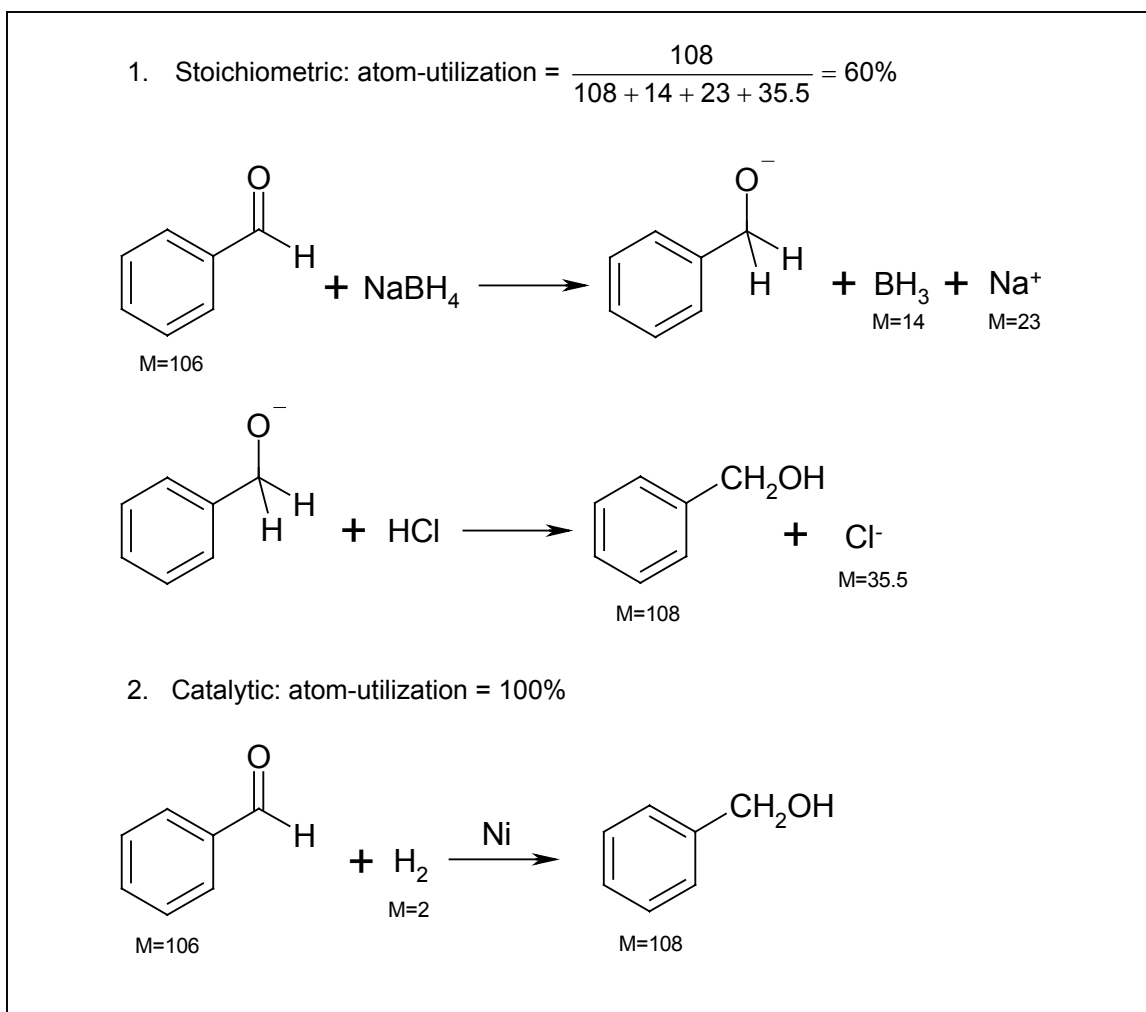
Figure 1.2: Classical (stoichiometric) versus green (catalytic atom-efficient) hydrogenation of benzaldehyde to benzyl alcohol

Solvent losses also contribute considerably to the formation of large amounts of waste. The use of large quantities of volatile organic solvents as liquid media for chemical reactions and extractions, with a current worldwide cost estimated at € 6,000,000,000 per year[14,15], is a major concern for today's chemical processing industry. The perceived effects of these solvents on human health, safety and the environment, combined with their volatility and flammability, is a strong incentive for minimizing their use, both for environmental and cost perspective. Minimizing solvent losses leads to avoiding the costs associated with disposal, legal liabilities and regulatory constraints. Therefore, the development of solvent-free processes as well as the development of environmentally benign new solvents, such as water and perfluorinated solvents (as used in biphasic systems), supercritical fluids and ambient temperature ionic liquids, has become a major issue.

1.3 Environmentally benign solvents

1.3.1 Solvent-free processes

Solvent-free processes are the best solution for minimizing solvent losses. Many reactions can be carried out without solvent when the reagents are liquids or when the mixture can be melted to produce a liquid. In this case the excess reagent serves as solvent. For example, the production of chlorinated natural rubber has been carried out in excess liquid chlorine in order to eliminate the need for the usual carbon tetrachloride as solvent, which is toxic and difficult to remove from the product, chlorinated rubber[8]. Solvent-free separation steps include mechanical extraction instead of extraction with an organic solvent.

However, it is not always possible to work without solvent. Sometimes solvents are necessary to dissolve solids, to lower the viscosity, to regulate temperatures, to recover compounds by means of extraction and crystallization, as reaction medium or for cleaning purposes[8]. In these cases less harmful solvents, which can easily be recovered, are desired.

1.3.2 Aqueous biphasic catalysis

Another solution to minimize and reduce the impact of solvent losses is the use of water as a green solvent in biphasic industrial transition metal catalyzed reactions. The reactants and products form an organic phase and the catalyst and ligand are dissolved in the water phase. The reactants can react in the aqueous phase by the formation of a complex with the catalyst/ligand system. The formed products are not water-soluble and return to the organic phase. In this way water and catalyst can easily be separated from the product and recycled, minimizing the solvent losses[2]. The low mutual solubility of water and organic product leads to a reduced product contamination. The high polarity of water may lead to different reactions.

The use of water as reaction medium is economically and environmentally attractive. In large parts of the world (for example in The Netherlands), water is abundantly available and inexpensive. Moreover it is non-flammable and non-toxic, odorless and colorless and environmentally friendly.

However, the application of water as a green solvent is still limited due to the low solubility of organic substrates in water, which often results in low reaction rates. Moreover, water is a protic coordinating solvent, so it can react with organometallic complexes. Therefore, water cannot be used as solvent for all catalytic reactions and often modifications of catalysts and ligands are necessary[16].

1.3.3 Fluorous biphasic catalysis

More recently, perfluorinated solvents have proven their utility for many thermal and catalytic reactions. The catalyst dissolves in the separate perfluorinated phase, which exists next to the organic reactant and product phase, and can therefore easily be recycled. The organic substrates have a higher solubility in perfluorinated solvents than in water, leading to higher reaction rates compared to aqueous biphasic systems. Nevertheless, specific ligands must be designed to dissolve the catalyst in the perfluorinated phase. Moreover, the fluorous solvents are greenhouse gases and thermal decomposition of these compounds yields toxic compounds, such as hydrogen fluoride. Finally, fluorous derivatives are often detected in the organic phase[8,16].

1.3.4 Supercritical carbon dioxide

Supercritical fluids, for example supercritical carbon dioxide, are also described as new solvents for organic and catalytic reactions. Carbon dioxide is non-toxic, non-flammable, relatively inert, abundant and inexpensive. In the supercritical region, the density of carbon dioxide and its solvent power can be varied by changing the temperature and pressure. Supercritical carbon dioxide has properties between those of gases and liquids. Diffusivity and mass transfer are better than in liquids, whereas the solubilities of many organic compounds are higher than in gases. The low critical temperature allows heat-sensitive materials to be processed without damage. The fact that not all chemical substances are soluble in supercritical carbon dioxide permits selective extraction. When the pressure is relieved after an extraction step, the carbon dioxide evaporates and pure product without any remaining carbon dioxide is obtained. Therefore, supercritical extraction is often used for foods and medicines, for which it eliminates the possibility of leaving toxic residues of organic solvents[17,18].

However, the use of carbon dioxide as green solvent has some limitations. It is not a very good solvent for many substances, especially large polar molecules. Moreover it is most commonly used as supercritical fluid (above its critical temperature of 31 °C and its critical pressure of 7.38 MPa). Therefore, carbon dioxide has to be used under pressure. This may lead to higher operating and equipment costs[16].

Supercritical carbon dioxide is not the only supercritical fluid that can be used, but it is among a few other supercritical solvents that offer the combination of the properties given. Unfortunately, many are toxic or flammable. Therefore, their use is rather limited.

1.3.5 Ambient temperature ionic liquids

During the last ten years, ambient temperature ionic liquids were recognized as a novel class of environmentally benign solvents[14,16,19]. Ambient temperature ionic liquids are molten salts that are liquid at room temperature. They are considered as green solvents, because they have negligible vapor pressure at room temperature[20]. Therefore, ionic liquids are easily recyclable and reusable. Their use as solvents for reactions and separations may offer a solution to both the solvent emission and the catalyst-recycling problem. In addition, ionic liquids can be adjusted in order to exhibit desired properties by the right choice of cation and anion[19]. In this way, they can be designed with low toxicity and high biodegradability (see paragraph 2.1.3).

The use of ionic liquids as combined reaction and separation media in the chemical industry may lead to a significant resource-efficiency increase. First of all, ionic liquids allow atom-efficient reactions to be carried out at high rates and selectivities, because they are able to dissolve a wide range of catalysts[21-23]. The fact that ionic liquids are non-volatile also makes them suitable solvents for energy-efficient separations and purifications. It is possible to extract organic compounds from ionic liquids with supercritical carbon dioxide without any contamination by the ionic liquid and without any solvent losses, because ionic liquids do not dissolve in carbon dioxide[24,25]. In this way, no energy-intensive distillation step is required.

Therefore, it is chosen to investigate a new method to combine reactions and separations using ionic liquids and supercritical carbon dioxide in this thesis. Although many data on ionic liquids are still unknown and the prices of ionic liquids high, the field of ionic liquids is currently one of the hottest research topics. Prices of ionic liquids are decreasing fast and the number of publications is increasing tremendously[26] (see figure 1.3). It is expected that new applications for ionic liquids will be found in the near future, and that more ionic liquids, in higher quantities and with lower prices and well-known properties, will be available.
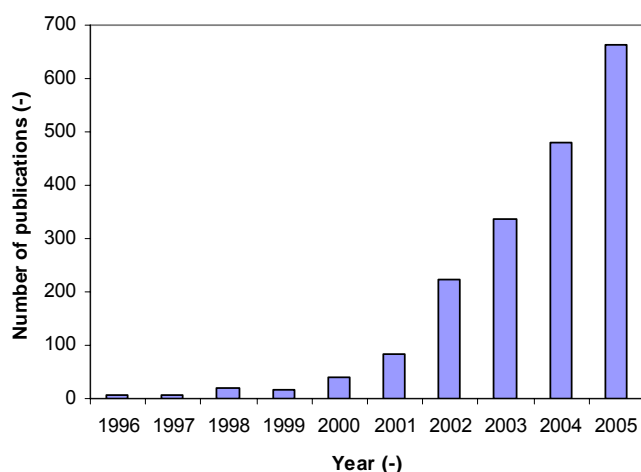
Figure 1.3: Number of publications on ionic liquids in 1996-2005

1.4 Scope of the thesis

This thesis aims at the resource-efficiency increase in the chemical industry by using ionic liquid and supercritical carbon dioxide as combined reaction and separation media. Therefore, a historical overview of the use of ionic liquids and supercritical carbon dioxide as solvents is presented in chapter 2. It is demonstrated that reactions and separations can be combined using ionic liquids and carbon dioxide, but so far these reactions and separations were always carried out in a biphasic system.

A new method to combine reactions and separations using ionic liquids and supercritical carbon dioxide is developed in chapter 3. It is found that carbon dioxide is able to force two or more immiscible phases to form one homogeneous phase at pressure increase, which is called 'miscibility switch' phenomenon[27-29]. With the two-phase/single-phase transformation, it is possible to carry out the reaction in a homogeneous system at high reaction rate, whereas the product is separated in the two-phase system of which one phase does not contain any ionic liquid.

The new process set-up is applied to a model system. In chapter 4 the phase behavior of the model system is investigated in order to find the conditions for reaction (homogeneous phase) and separation (biphasic system). Thereafter, these conditions are applied in the reaction step and the separation step in chapter 5. The kinetics of the reaction step and the efficiency of the separation step are measured. It is found that products can be removed from ionic liquids using carbon dioxide either as co-solvent in extractions or as anti-solvent in precipitations.

The experimental determination of the conditions for reaction and separation in the new process set-up is very time-consuming and expensive. Therefore, it is highly desirable to develop models that can predict the phase behavior of ionic liquid systems. In chapter 6 the phase behavior of ionic liquid + carbon dioxide systems is modeled with the truncated Perturbed Chain Polar Statistical Associating Fluid Theory (tPC-PSAFT) equation of state. In this model ionic liquids are considered to be neutral highly asymmetric ion pairs with a large dipole moment, which results in a better fit with experimental data compared to the situation in which ionic liquids are considered to be two separate charged species i.e., anion and cation.

There are limits to the operating conditions of the new process set-up. These limits are determined by the thermal stability and the electrochemical stability of ionic liquids. In chapter 7 the thermal stability is estimated using quantum chemical calculations. Not only is the maximum operating temperature below which no thermal degradation occurs predicted, but also the kinetics and the mechanism of the decomposition reaction are determined. Quantum chemical calculations are also used in chapter 8 to estimate the electrochemical stability of an ionic liquid, which is determined by the stability towards oxidation of the anion and the stability towards reduction of the cation.

An economical and environmental analysis of the new process set-up is presented in chapter 9. From both the economical and the environmental point of view, fast implementation of this new process set-up is desired. However, with a conventional plan of execution, the implementation of this new technology could take several decades. One important reason for this long implementation trajectory is that innovations are traditionally considered as linear chains of causal actions, where each stage requires a considerable amount of time. However, when actions take place simultaneously in all stages of the innovation process, the time between invention and implementation can be reduced dramatically. For a fast adoption of innovative technologies, the plan of execution should be based on an innovation model that considers the innovation process as coupled 'cycles of change', where developments take place in all cycles simultaneously[30,31]. Such an innovation model is described and subsequently applied to the commercialization of the ionic liquid technology in chapter 10.

Finally, in chapter 11 an outlook on the future potential of ionic liquids is presented. Other ways to combine reactions and separation using ionic liquids are described. Recommendations and challenges for future applications of ionic liquids are given.

1.5 References

1. Energy Information Administration, World energy consumption per capita 1970-2025, http://www.eia.doe.gov/
2. Worrell, E.; Phylipsen, D.; Einstein, D.; Martin, N. *Energy Use and Energy Intensity of the US Chemical Industry*; University of Berkeley: Berkeley (CA), USA, 2000.
3. Sheldon, R. A.; Organic Synthesis – Past, Present and Future, *Chem. & Ind.* **1992**, *(23)*, 903-906.
4. European Environment Agency, EU municipal solid waste generation per capita 1990-2015, http://www.eea.eu.int/
5. US Census Bureau Database, World population 1950-2050, http://www.census.gov/ipc/www/world.html
6. Von Weizsäcker, E. U.; Lovins, A. B.; Lovins, L. H. *Factor 4, Doubling Wealth, Halving Resource Use*; Earthscan: London, UK, 1997.
7. Anastas, P. T.; Warner, J. C. *Green Chemistry: Theory and Practice*; Oxford University Press: Oxford, UK, 1998.
8. Matlack, A. S. *Introduction to Green Chemistry*; Marcel Dekker, Inc.: New York (NY), USA, 2001.
9. Pellet, R. J.; O'Young, C. L.; Hazen, J.; Hadowanetz, A. E.; Browne, J. E.; Treated Bound Ferrierite Zeolites for Skeletal Isomerization of n-Olefins to Iso-Olefins, US Patent 5523510 (1996).
10. Al-Juaied, M. A.; Lafarga, D.; Varma, A.; Ethylene Epoxidation in a Catalytic Packed-Bed Membrane Reactor: Experiments and Model, *Chem. Eng. Sci.* **2001**, *56 (2)*, 395-402.
11. Huss, R. S.; Chen, F.; Malone, M. F.; Doherty, M. F.; Reactive Distillation for Methyl Acetate Production, *Computers Chem. Eng.* **2003**, *27 (12)*, 1855-1866.
12. Moulijn, J. A.; Makkee, M.; Van Diepen, A. E. *Chemical Process Technology*, John Wiley & Sons Ltd.: Chichester, UK, 2001.
13. Eurostat, Statistics on population, economics, industry, agriculture, trade, transport, science, technology, and environment of the EU countries, http://epp.eurostat.cec.eu.int/
14. Seddon, K. R.; Ionic Liquids for Clean Technology, *J. Chem. Tech. Biotechnol.* **1997**, *68 (4)*, 351-356.
15. Reichardt, C. *Solvents and solvent effects in organic chemistry*; 3rd Ed.; Wiley-VCH Verlag: Weinheim, Germany, 2003.
16. Olivier-Bourbigou, H.; Magna, L.; Ionic Liquids: Perspectives for Organic and Catalytic Reactions, *J. Mol. Catal. A* **2002**, *182-183*, 419-437.
17. Brunner, G.; Gas Extraction, Topics in Physical Chemistry Vol. 4, Springer: Darmstadt, Germany, 1994.
18. Beckman, E. J.; Supercritical and Near-Critical CO_2 in Green Chemical Synthesis and Processing, *J. Supercrit. Fluids* **2003**, *28 (2-3)*, 121-191.
19. Wasserscheid, P.; Welton, T., Eds. *Ionic Liquids in Synthesis*; Wiley-VHC Verlag: Weinheim, Germany, 2003.

20. Earle, M. J.; Esperança, J. M. S. S.; Gilea, M. A.; Lopes, J. N. C.; Rebelo, L. P. N.; Magee, J. W.; Seddon, K. R.; Widegren, J. A.; The Distillation and Volatility of Ionic Liquids, *Nature* **2006**, *439 (7078)*, 831-834.

21. Sheldon, R. A.; Catalytic Reactions in Ionic Liquids, *Chem. Commun.* **2001**, *(23)*, 2399-2407.

22. Jain, N.; Kumar, A.; Chauhan, S.; Chauhan, S. M. S.; Chemical and Biochemical Transformations in Ionic Liquids, *Tetrahedron* **2005**, *61 (5)*, 1015-1060.

23. Gordon, C. M.; New Developments in Catalysis using Ionic Liquids, *Appl. Catal. A* **2001**, *222 (1-2)*: 101-117.

24. Blanchard, L. A.; Hancu, D.; Beckman, E. J.; Brennecke, J. F.; Green Processing Using Ionic Liquids and CO_2, *Nature* **1999**, *399 (6731)*, 28-29.

25. Blanchard, L. A.; Brennecke, J. F.; Recovery of Organic Products from Ionic Liquids Using Supercritical Carbon Dioxide, *Ind. Eng. Chem. Res.* **2001**, *40 (1)*, 287-292.

26. Atkins, M. P.; Davey, P.; Fitzwater, G.; Rouher, O.; Seddon, K. R.; Swindall, J.; (QUILL), Ionic Liquids: A Map for Industrial Innovation, http://quill.qub.ac.uk/map/

27. Gauter, K.; Peters, C. J.; Scheidgen, A. L.; Schneider, G. M.; Cosolvency Effects, Miscibility Windows and Two-Phase LG Holes in Three-Phase LLG Surfaces in Ternary Systems: A Status Report, *Fluid Phase Equilib.* **2000**, *171 (1-2)*, 127-149.

28. Peters, C. J.; Gauter, K.; Occurrence of Holes in Ternary Fluid Multiphase Systems of Near-Critical Carbon Dioxide and Certain Solutes, *Chem. Rev.* **1999**, *99 (2)*, 419-431.

29. Kroon, M. C.; Florusse, L. J.; Shariati, A.; Gutkowski, K. E.; Van Spronsen, J.; Sheldon, R. A.; Witkamp, G. J.; Peters, C. J. On a Novel Class of Production Processes for the Chemical Industry, to be submitted for publication to *Nature* **2006**.

30. Berkhout, A. J. *The Dynamic Role of Knowledge in Innovation. An Integrated Framework of Cyclic Networks for the Assessment of Technological Change and Sustainable Growth*, Delft University Press: Delft, The Netherlands, 2000.

31. Berkhout, A. J.; Hartmann, D.; Van der Duin, P.; Ortt, R.; Innovating the Innovation Process, *Int. J. Technol. Manage.* **2006**, *34 (3-4)*, 390-404.

2

Background
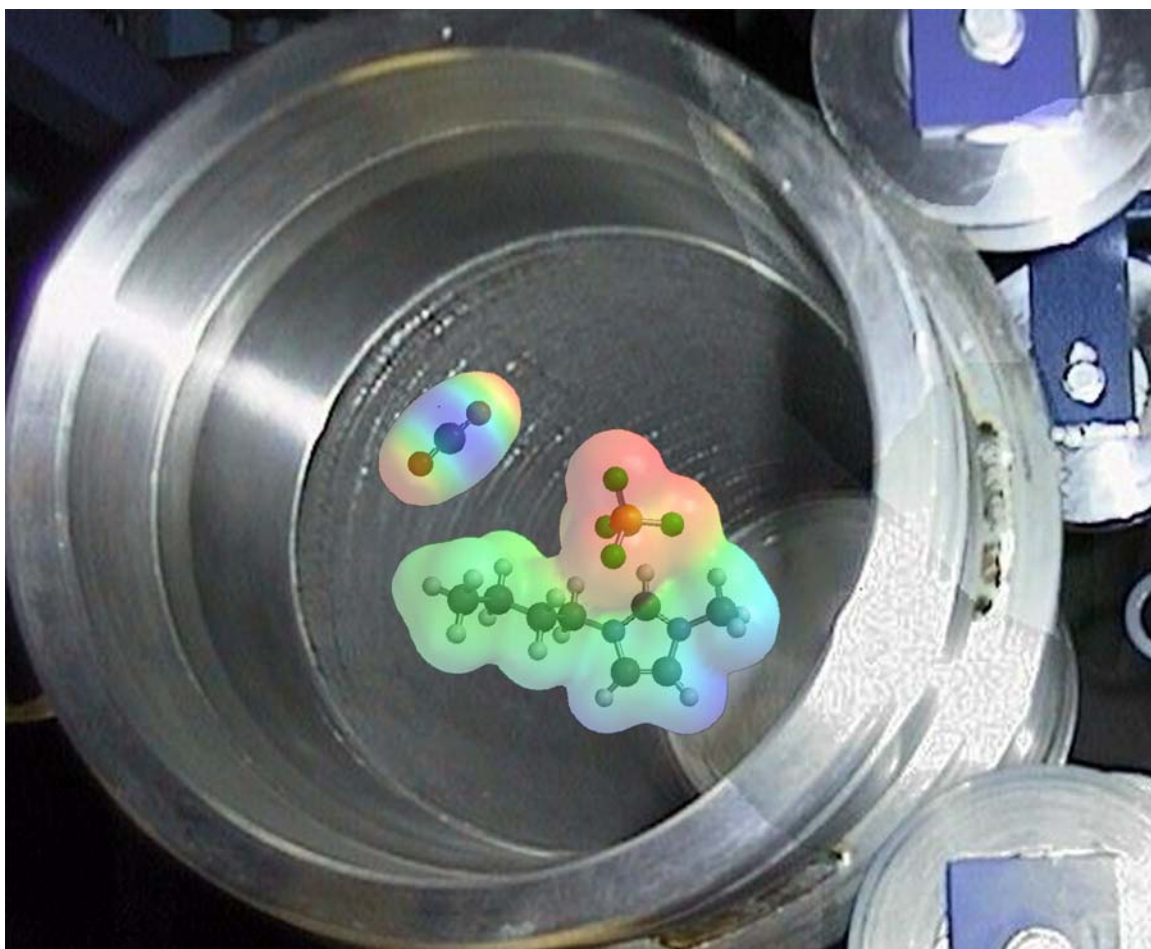
2

Background

Ionic liquids are emerging as green solvents for chemical processes, because they combine good and tunable solubility properties with negligible vapor pressures and high thermal and chemical stabilities. They are used as reaction media, where they may enhance reaction rates and selectivities. Supercritical carbon dioxide has been described as a green solvent for the extraction of hydrophobic compounds, because the solubility of apolar compounds is high and can be adjusted by varying the density of the carbon dioxide. Combining ionic liquids with carbon dioxide results in interesting phase behavior: supercritical carbon dioxide is highly soluble in ionic liquids, while the solubility of ionic liquids in supercritical carbon dioxide is negligibly low. Therefore, it is possible to remove an organic product from an ionic liquid by extraction with supercritical carbon dioxide without any ionic liquid contamination. Subsequently, this separation step is combined with homogeneously catalyzed reactions in ionic liquid/supercritical carbon dioxide biphasic solutions: The reactants are transported into the reactor using supercritical carbon dioxide as the mobile phase. In the reactor, the reactants partly dissolve in the ionic liquid phase, where the catalyzed reaction takes place. The products are continuously extracted with the supercritical carbon dioxide stream. The product and carbon dioxide are separated downstream by controlled density reduction. In this chapter, all previously reported processes using ionic liquid/carbon dioxide systems are summarized. These processes have the disadvantage of being biphasic, leading to low reaction and extraction rates.

2. Background

2.1 Introduction to ionic liquids

Ionic liquids are a unique class of salts with melting points at or below 100 ^{o}C. Some ionic liquids even melt below ambient temperature, in which case they can be called ambient temperature ionic liquids. Because ionic liquids are entirely composed of ions, they resemble high-temperature molten metallic salts, such as sodium chloride in the liquid state (at temperatures higher than 800 ^{o}C). However, ionic liquids contain at least one organic ion that is relatively large and asymmetric compared to a metallic ion. Therefore, the positively charged ions (cations) and the negatively charged ions (anions) of an ionic liquid can be kept so far apart that the attractive forces become small. Crystallization is thus hindered so that the resulting substance is a totally ionic (non-aqueous) liquid at room temperature[1,2].

2.1.1 History

The first ambient temperature ionic liquid reported is ethylammonium nitrate, having a melting point of 12 °C, and discovered in 1914 by Walden[3]. Modern ionic liquid research started in the late 1940s with the study of low melting eutectic mixtures of N-alkyl-pyridinium halides with aluminum chloride or aluminum bromide for the use as low-temperature, highly conductive electrolytes in batteries[4,5]. However, the reducible nature of the N-alkylpyridinium cation led to a search for more stable cations. Wilkes and co-workers[6,7] reported the first examples of ionic liquids based on dialkylimidazolium chloroaluminates in the early 1980s. These ionic liquids exhibit interesting chemical properties, such as superacidity[6]. They are also excellent non-volatile catalysts for Friedel-Crafts alkylation and acylation reactions[7]. Unfortunately, the chloroaluminate anions react with water under formation of hydrogen chloride, making these ionic liquids unstable in water and air[2]. This led to the search for water-stable anions, resulting in the discovery of tetrafluoroborate, hexafluorophosphate, nitrate, sulfate and acetate ionic liquids in 1992[8]. Since then, water-stable ionic liquids have been at the center of interest as novel environmentally benign solvents for various applications. The range of available anions and cations has expanded tremendously and new ionic liquids are continuously found. It is estimated that there are approximately one trillion (10^{18}) accessible room temperature ionic liquids[9]. Most common cations (with different functional groups R, which are usually alkyl chains) and anions are shown in figure 2.1.

Common cations:

Ammonium   Imidazolium   Pyrrolidinium

Pyridinium   Phosphonium   Guanidinium

Common anions:

Chloride: Cl^-
Methylsulfate: $CH_3OSO_3^-$
Triflate: $CF_3SO_3^-$
Trifluoroacetate: $CF_3CO_2^-$
Hexafluorophosphate: PF_6^-
Tetrafluoroborate: BF_4^-
Bis(trifluoromethanesulfonyl)imide: $N(CF_3SO_2)_2^-$
Dicyanamide: $N(CN)_2^-$
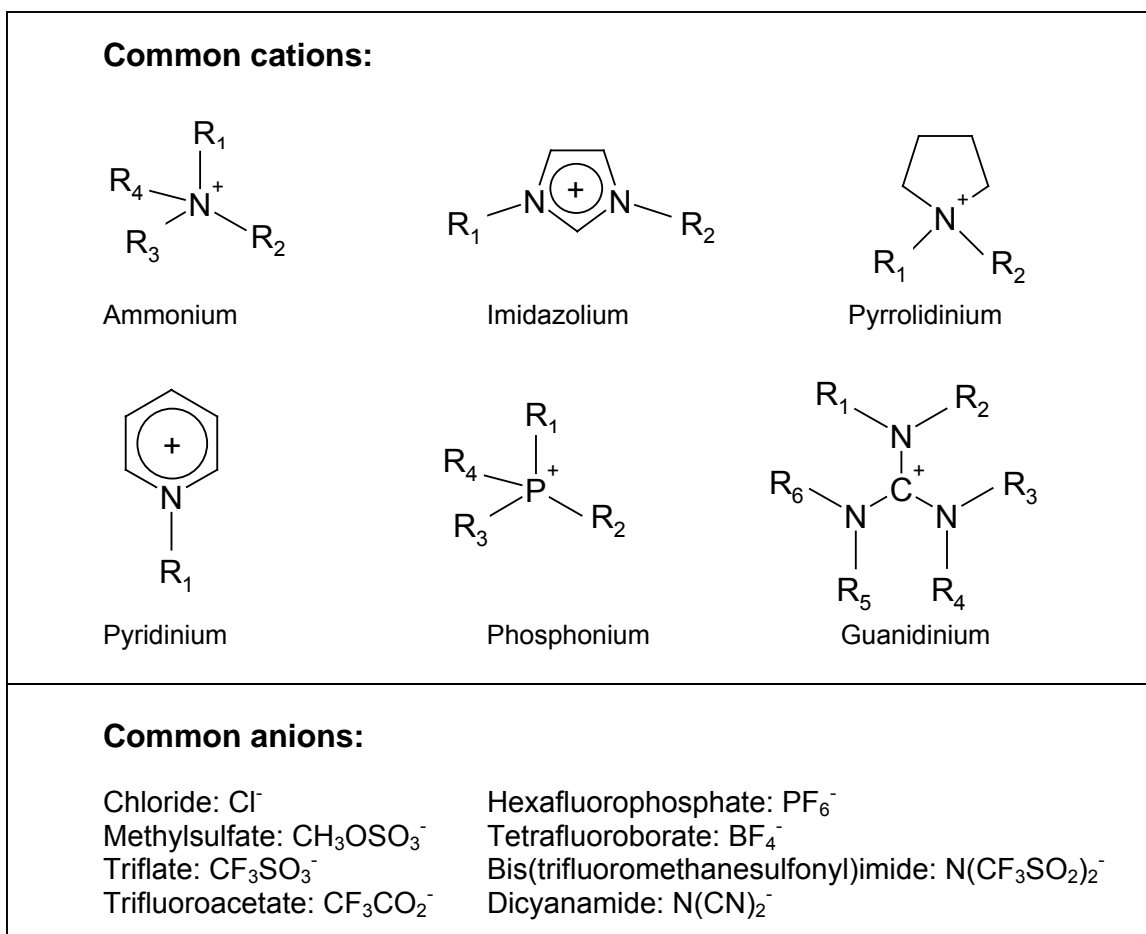
Figure 2.1: Most common cations and anions[10]

2.1.2 Properties of ionic liquids

The most important physical property of ionic liquids is that their vapor pressure is negligibly small at room temperature[11]. As a result, ionic liquids are odorless. They do not evaporate, even when exposed to vacuum, and most of them do not combust, even when exposed to an open flame. The fact that ionic liquids are non-volatile and non-flammable makes them safer and more environmentally benign solvents than the traditional volatile organic solvents[1]. Other properties of ionic liquids are inherent to salts in the liquid state and include the wide liquid temperature range allowing tremendous kinetic control in reactions, the good thermal stability, the high ionic conductivity and the wide electrochemical window representing the high electrochemical stability of ionic liquids against oxidation or reduction reactions[12]. Furthermore, ionic liquids have very good solvency power for both organic and inorganic materials, polar and non-polar, which makes them suitable for catalysis[13,14]. It is possible to tune the physical and chemical properties of ionic liquids by varying the nature of the anions and cations. In this way, ionic liquids can be made task-specific[1,2].

2.1.3 How green are ionic liquids?

Ionic liquids are regarded as environmentally benign replacements for volatile organic solvents due to their negligible vapor pressure. However, ionic liquids can have a hidden environmental cost. In a lot of synthesis routes halogen atoms are involved. Halogen materials in ionic liquids are undesirable, because of the low hydrolysis stability, the high toxicity, the low biodegradability and the high disposal cost[15,16]. For example, fluorinated anions such as PF_6^- and BF_4^- are sensitive to water and may release the corrosive and toxic hydrogen fluoride[2]. Moreover, the alkyl halides used in the syntheses of many ionic liquids are greenhouse gases and ozone-depleting materials[2]. Therefore, halogen-free ionic liquids have been developed, such as ionic liquids with alkyl sulfate, alkyl carbonate and alkyl sulfonate anions[15,16].

Low toxicity and biodegradability of the ionic liquid are required for safe use and environmental acceptable disposal. Although these data yet have to be determined for many ionic liquids, the lack of volatility greatly reduces any chance of exposure other than by direct physical contact with skin or by ingestion. Early studies show that it is possible to design ionic liquids that are non-toxic (by choice of cation and anion). Most investigated ionic liquids are irritating and have a toxicity comparable to common organic solvents[17]. From biological tests it appeared that the toxicity of ionic liquids is mainly determined by the type of cation: ionic liquids with short alkyl substituents in the cation usually have a lower toxicity[17,18]. It was also found that a number of ionic liquids is biodegradable, especially when an ester group is present in the alkyl side chain[16,18,19]. Recently, the first ionic liquids from bio-renewable sources were obtained[20].

Although ionic liquids might not be green in full context, they have the potential to make chemical processes more environmentally benign by reducing waste generation (eliminating solvent losses) and energy consumption (no energy-intensive solvent evaporation step). Due to their tunable properties, ionic liquids can be made 'green'.

2.1.4 Applications of ionic liquids

In first instance, ionic liquids were developed by electrochemists for use as low-temperature water-free electrolytes[2]. Compared to conventional mixed electrolyte systems, ionic liquid electrolytes have similar electrochemical windows and ionic conductivities, but are safer and possess lower toxicity and flammability[21]. Moreover, ionic liquids allow several metals conventionally obtained from high-temperature molten salts to be deposited at room temperature without corrosion problems[22,23]. Ionic liquid electrolytes can be applied in various electrochemical devices, such as battery systems[24,25], solar cells[26] and electrochemical capacitors[27-29].

During the last decade, ionic liquids were also found to be suitable solvents for chemical reactions, because they combine excellent thermal and chemical stabilities with good and tunable solubilities and catalytic properties[13,14]. Ionic liquids have been used as solvents

for nucleophilic[30,31] and electrophilic[31,32] reactions, including acidic catalyzed reactions, and reactions catalyzed by transition metal complexes[33,34]. Ionic liquids are also good media for bio-catalyzed reactions[35,36]. Especially the use of ionic liquids as solvents for transition metal catalysis is at the center of interest. Transition metal catalysts dissolve well in the ionic liquid, while many organic reactants and products only have very low solubility in ionic liquids. This gives rise to the possibility of a biphasic reaction procedure[35]: the catalyst is immobilized in the ionic liquid phase, and the organic starting materials and products are introduced and removed in a separate organic phase. Some reactant dissolves into the ionic liquid phase and undergoes a reaction, after which it returns to the organic layer and is removed via simple decantation (the organic phase has a lower density than the ionic liquid phase). The catalyst stays in the ionic liquid and can easily be reused (see figure 2.2). When the products are partially or totally miscible with the ionic liquid and sufficiently volatile, they can be easily separated from the ionic liquid by distillation (ionic liquids have negligible vapor pressure). Examples of transition metal catalyzed reactions in ionic liquids are hydrogenations, hydroformylations, oxidations, Heck coupling reactions and dimerization and oligomerization reactions[2,13,14,35-37]. It was demonstrated that the use of an ionic liquid often leads to higher reactivities and/or selectivities[2,35].
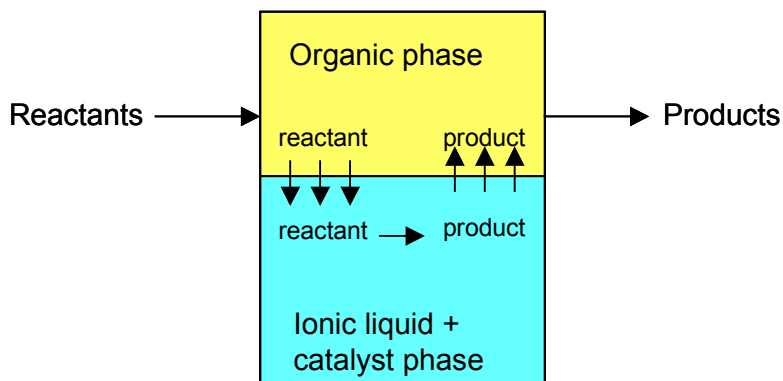
Figure 2.2: Process set-up for biphasic transition metal catalysis in ionic liquids[2,35]

Furthermore, ionic liquids can be used for separation and purification purposes[38]. Ionic liquids are able to selectively extract a specific compound out of a gas mixture or a liquid mixture[38-41]. An example of a gas extraction is the removal of carbon dioxide and hydrogen sulfide from sour natural gas using ionic liquids[39]. Examples of liquid extractions include the removal of organics from aqueous waste streams and the separation of aromatics from alkanes[40,41]. Recently, ionic liquids were applied in supported liquid membranes for separation purposes[42,43].

Other applications of ionic liquids include the usage as cleaning solvents, lubricants, heat-transfer fluids and storage media, for which they are suitable because of their solubility behavior, their high thermal stability, their large liquid temperature range and their wetting behavior[38].

Considerable progress towards commercialization of ionic liquids has recently been made. More types of ionic liquids become available from multiple vendors (Merck[10], Degussa[44], Cytec Industries[45]). Due to the expanding supply, prices of ionic liquids are decreasing (economies of scale)[10]. At the same time, more ionic liquids are demanded, because new industrial applications are found. Ionic liquids were for the first time commercially used in the BASIL® process from BASF[46]. The BASIL (Biphasic Acid Scavenging using Ionic Liquids) process uses N-methylimidazole to remove the acid that is formed in the production of alkoxyphenylphosphine, while at the same time producing an ionic liquid[46]. Another commercial application is the storage of arsine, boron trifluoride and phosphine in ionic liquids (GASGUARD® Sub-Atmospheric Systems), developed by Air Products[47]. Finally, various ionic liquid processes are available for licensing, such as the French Petroleum Institute's Difasol® process for the dimerization of small olefins[48].

2.2 Introduction to supercritical carbon dioxide

Carbon dioxide is a supercritical fluid at temperatures higher than 304.2 K (= 31.1 $^{\circ}$C) and pressures higher than 7.38 MPa (= 73.8 bar) and becomes solid at far greater pressures. Under these conditions the distinction between the gas phase and liquid phase is nonexistent, and carbon dioxide can only be described as a fluid. This can be explained by looking at the phase diagram of carbon dioxide (see figure 2.3). The boiling line separates the vapor and liquid region and ends in the critical point. At any point on the boiling line below its critical temperature and pressure, carbon dioxide exists as a liquid with vapor above it. As the temperature is raised, going along the boiling curve the liquid density falls due to expansion, whereas the gas density rises due the pressure increase. Eventually, at the critical point, the densities become identical and the distinction between liquid and gas disappears[49].
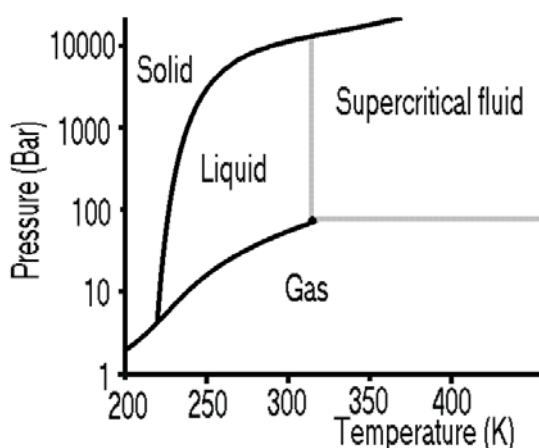
Figure 2.3: Phase diagram of carbon dioxide

Supercritical carbon dioxide has properties in between those of liquids and gases. It has the ability to diffuse through materials like a gas, and to dissolve organic compounds like a non-polar liquid (resembling hexane). Alkanes, aromatics, ketones and alcohols (up to a molecular weight of around 400 g/mol) dissolve in supercritical carbon dioxide, but polar molecules such as acids and most inorganic salts are insoluble. By adjusting the pressure of the supercritical carbon dioxide, the solvent properties can be adjusted to be more 'gas-like' (low solvency power) or 'liquid-like' (high solvency power), which makes it a highly tunable solvent (for this purpose also modifiers can be added). Because of these properties, supercritical carbon dioxide is a well-established solvent for use in extractions, such as the decaffeination of coffee and the extraction of hops, natural products, high value pharmaceutical precursors, essential oils, and environmental pollutants. Other emerging commercial technologies involving supercritical carbon dioxide include dry cleaning, dyeing of textiles, paint spraying and the use as environmentally benign solvent for various organic reactions, such as hydrogenations, hydroformylations, oxidations, biocatalytic reactions and polymerizations[50-55].

2.3 Reactions and separations in ionic liquids and supercritical carbon dioxide

Both ionic liquids and supercritical carbon dioxide have been described as alternative green solvents, but their properties are very different. Ionic liquids are non-volatile but highly polar compounds, whereas supercritical carbon dioxide is an apolar but highly volatile compound. The combination of these two solvents has some unique features. It has been discovered that supercritical carbon dioxide is highly soluble in ionic liquids, while the solubility of ionic liquids in supercritical carbon dioxide is negligibly low[56-58]. Therefore, supercritical carbon dioxide has been used to extract hydrophobic substances from ionic liquids without any contamination by the ionic liquid. Combined with the fact that ionic liquids are excellent reaction media for catalyzed reactions (good tunable solubility characteristics, high reactivity and high selectivity), this led to the development of chemical processes, where the reaction was carried out in the ionic liquid and the product was extracted afterwards with supercritical carbon dioxide[57,59,60]. An example of this chemical process set-up is the asymmetric hydrogenation of tiglic acid in the ionic liquid 1-butyl-3-methylimidazolium hexafluorophosphate ([bmim][PF_6]) with a dissolved chiral ruthenium catalyst with high conversion and enantioselectivity[59] (see figure 2.4). After the reaction, the product (*R*)-2-methylbutanoic acid was extracted from the ionic liquid with supercritical carbon dioxide giving clean separation of product and catalyst. The catalyst/ionic liquid solution was then reused repeatedly without significant loss of enantioselectivity or conversion. Disadvantages of this chemical process method are the low extraction rate due to mass transfer limitations at the liquid-vapor interface, and the fact that this process is operated batch-wise.
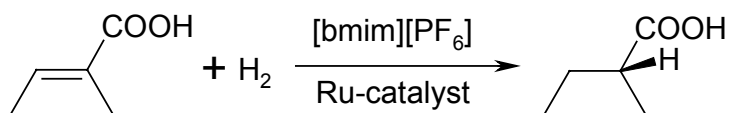
Figure 2.4: Asymmetric hydrogenation of tiglic acid in the ionic liquid 1-butyl-3-methylimidazolium hexafluorophosphate ([bmim][PF_6]), where the product is extracted afterwards with supercritical carbon dioxide[59]

It was found that continuous operation could be achieved when using ionic liquid/ supercritical carbon dioxide biphasic systems as combined reaction and separation media[61-76], where the CO_2 phase acts both as reactant and product reservoir (see figure 2.5) The reactants are transported into the reactor using supercritical carbon dioxide as the mobile phase. In the reactor, the reactants dissolve in the ionic liquid phase with immobilized catalyst, where the reaction takes place. The products are continuously extracted with the supercritical carbon dioxide stream. The product and carbon dioxide are separated downstream by controlled density reduction via pressure release or temperature increase. This method has been applied to hydrogenations[61,62], hydroformylations[63-66], dimerizations[67], (enzyme-catalyzed) esterifications[68-73], and the synthesis of cyclic carbonates (as CO_2 fixation method)[74-76].
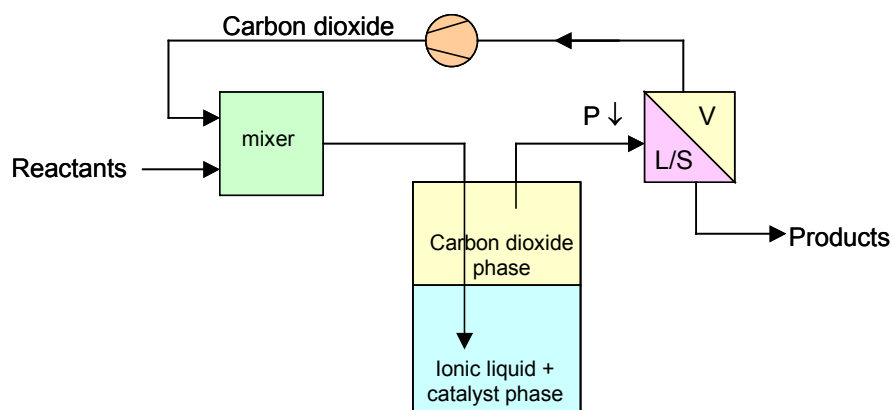
Figure 2.5: Continuous-flow operation in biphasic ionic liquid + supercritical carbon dioxide systems[61-76]

Liu *et al.*[61] applied the biphasic operation concept for the hydrogenation of alkenes (see figure 2.6). It was demonstrated that the rhodium catalyst was retained in the ionic liquid 1-butyl-3-methylimidazolium hexafluorophosphate, whereas the alkane products were selectively extracted with carbon dioxide. Also, enantioselective hydrogenations were carried out in biphasic ionic liquid/carbon dioxide media. For example, Solinas *et al.*[62] investigated the enantioselective hydrogenation of *N*-(1-phenylethylidene)alanine using a chiral iridium catalyst in various ionic liquid + carbon dioxide systems (see figure 2.7). It was found that the type of (anion of the) ionic liquid had a large effect on the enantioselectivity of the reaction. Moreover, the presence of carbon dioxide enhanced the solubility of hydrogen in the ionic liquid and therefore the reaction rate. Finally, the ionic liquid increased the stability of the catalyst.
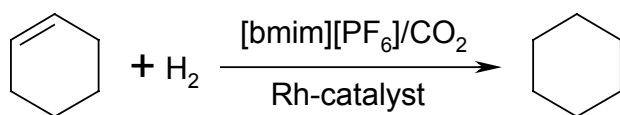
Figure 2.6: Hydrogenation of cyclohexene in the biphasic [bmim][PF$_6$] + CO$_2$ system[61]
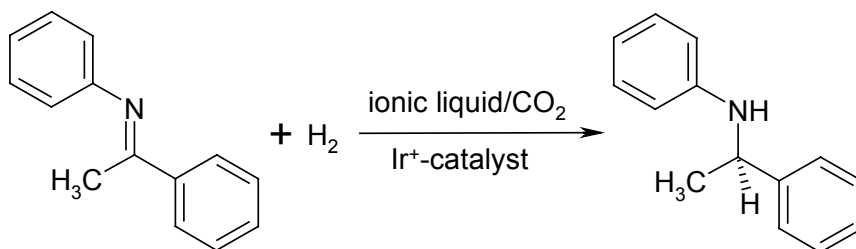
Figure 2.7: Enantioselective hydrogenation of N-(1-phenylethylidene)alanine in various biphasic ionic liquid + CO$_2$ systems[62]

Hydroformylations of alkenes were also carried out using the biphasic continuous operation method[63-66]. For example, the hydroformylation of 1-dodecene catalyzed by a rhodium complex was carried out in several ionic liquid + supercritical carbon dioxide systems[63] (see figure 2.8). The oxidation-sensitive rhodium catalyst was stabilized considerably by the ionic liquids. The nature of the ionic liquid had a large influence on the reaction rate. The 1-alkyl-3-methylimidazolium bis(trifluoromethylsulfonyl)imide ionic liquids with large alkyl chains gave the best activity. Moreover, the influence of the carbon dioxide on the reactivity and the selectivity to the linear aldehyde was investigated. In the absence of carbon dioxide, the reaction rate was higher, but the selectivity was lower. Carrying out the same reaction in the presence of supercritical carbon dioxide reduced the reaction rate, but increased the selectivity due to the lower reactant concentration by dilution. This contrasts the results of Solinas *et al.*[62], who found that the presence of carbon dioxide increased the reaction rate due to the higher hydrogen solubility. It can be concluded that for hydroformylations the dilution effect is larger than the increase in reactant solubility.
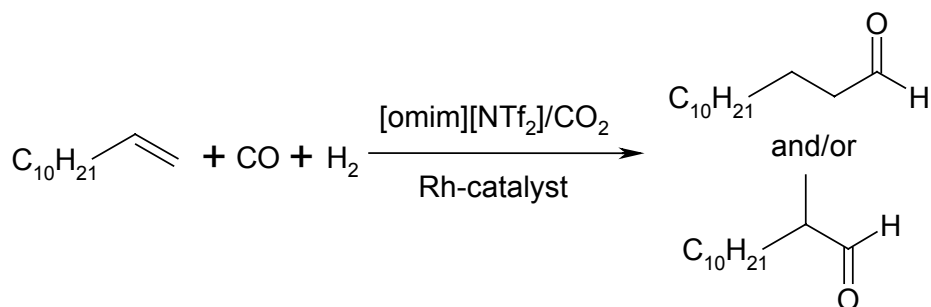
Figure 2.8: Hydroformylation of 1-dodecene in the biphasic 1-octyl-3-methylimidazolium bis(trifluoromethylsulfonyl)imide + carbon dioxide system[63]

Recently, hydroformylations were carried out in biphasic ionic liquid/supercritical carbon dioxide systems with carbon dioxide instead of carbon monoxide as carbon source[65,66]. In these cases, carbon dioxide is not only used as transport and extracting fluid, but it is also a reactant itself. An example is the biphasic hydroformylation of 1-hexene with carbon dioxide catalyzed by a ruthenium complex in the 1-butyl-3-methylimidazolium chloride + supercritical carbon dioxide system[66] (see figure 2.9). However, the reaction rate and selectivity were lower than in conventional hydroformylation processes.
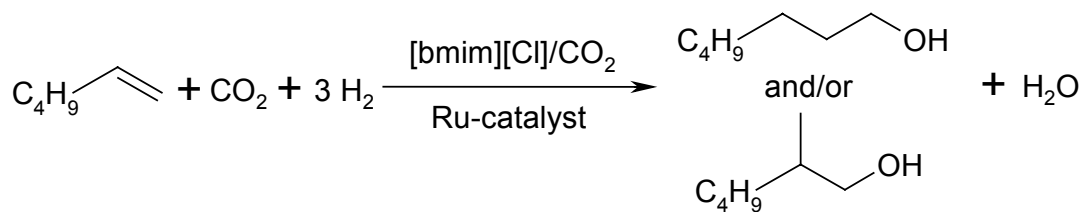
Figure 2.9: Hydroformylation/hydrogenation of 1-hexene with CO_2 as reactant in the biphasic [bmim][Cl] + CO_2 system[66]

Ballivet-Tkatchenko *et al.*[67] carried out the first carbon-carbon coupling reaction under ionic liquid/supercritical carbon dioxide biphasic conditions. They used the 1-butyl-3-methylimidazolium tetrafluoroborate ([bmim][BF$_4$]) + supercritical carbon dioxide system for the biphasic palladium-catalyzed dimerization of methyl acrylate (see figure 2.10). It was found that the selectivity to the tail-to-tail dimers was as high as under monophasic conditions, whereas the separation in the biphasic system was much easier. However, the methyl acrylate was much more soluble in carbon dioxide than the dimers, and high pressures were necessary to increase the extracting efficiency of the carbon dioxide to the dimer product.
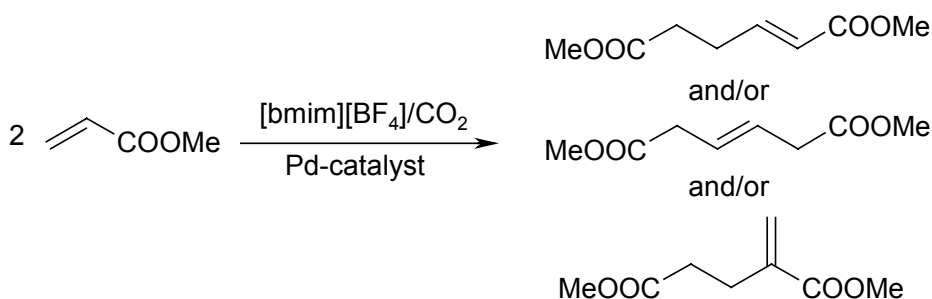
Figure 2.10: Dimerization of methyl acrylate in the biphasic [bmim][BF$_4$] + CO$_2$ system[67]

Another application of the continuous biphasic process set-up is the lipase-catalyzed enantioselective esterification of chiral secondary alcohols[68-72], resulting in the kinetic resolution of racemic alcohols. The racemic alcohol and the alkylating agent are transported into the reactor using supercritical carbon dioxide. In the reactor, one of the enantiomers is selectively esterified by the lipase in the ionic liquid. The mixture of products is continuously extracted with supercritical carbon dioxide. Ester and unreacted alcohol are separated downstream by carbon dioxide density reduction. An example is the transesterification of *rac*-1-phenylethanol with vinyl acetate, catalyzed by *Candida Antarctica* lipase B (CAL B)[69,70] (see figure 2.11). This reaction was carried out in several ionic liquid/carbon dioxide systems. It was found that all ionic liquids exhibited an exceptional ability to stabilize the enzyme, and that the ionic liquid 1-butyl-3-methyl-imidazolium bis(trifluoromethylsulfonyl)imide ([bmim][NTf$_2$]) gave the best results. It was also demonstrated that the enzyme could maintain its functionality under extreme denaturative conditions (up to 150 °C and 10 MPa) in a water-free environment[71].
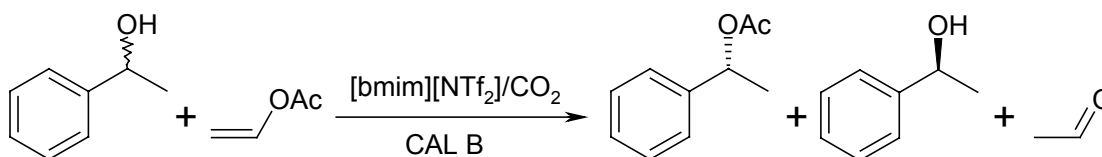
Figure 2.11: Lipase-catalyzed enantioselective transesterification of *rac*-1-phenylethanol with vinyl acetate in the biphasic [bmim][NTf$_2$] + CO$_2$ system, resulting in the production of (*R*)-1-phenylethyl acetate and (*S*)-1-phenylethanol[69,70]

Lozano *et al.*[72] investigated the influence of several lipases on the synthesis of chiral glycidyl esters from *rac*-glycidol in the biphasic 1-ethyl-3-methylimidazolium bis(trifluoromethylsulfonyl)imide ([emim][NTf₂]) + carbon dioxide system (see figure 2.12). (*R*)-Glycidyl esters were preferentially obtained by both *Candida Antarctica* lipase A (CAL A) and *Mucor Miehei* lipase (MML), while (*S*)-glycidyl ester synthesis was favored by *Candida Antarctica* lipase B (CAL B). The activities, stabilities and selectivities of all lipases were enhanced by the use of ionic liquid.
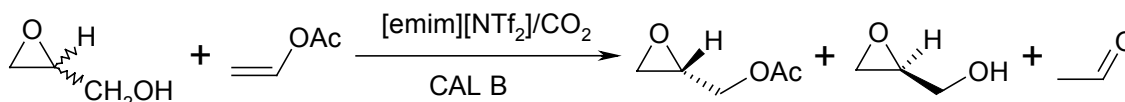
Figure 2.12: Lipase-catalyzed enantioselective transesterification of *rac*-glycidol with vinyl acetate in the biphasic [emim][NTf₂] + CO_2 system, resulting in the production of (*S*)-glycidyl ester and (*R*)-glycidol[72]

Esterifications in biphasic ionic liquid + carbon dioxide systems, in which the ionic liquid itself acts both as the solvent and the catalyst, have also been carried out. An example is the esterification of acetic acid and ethanol in the 1-butyl-3-methylimidazolium hydrogen sulfate/supercritical carbon dioxide system[73], where the presence of carbon dioxide enhanced the reaction rate, which is again in agreement with the results of Solinas *et al.*[62] (see figure 2.13).
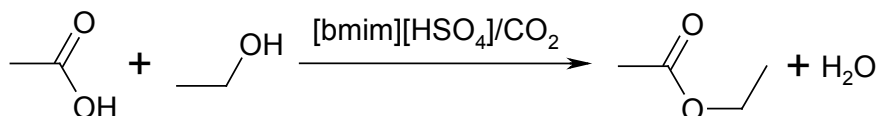
Figure 2.13: Esterification of acetate and ethanol in the biphasic [bmim][HSO₄] + CO_2 system[73]

Recently, the synthesis of cyclic carbonates via the coupling reaction of epoxides and carbon dioxide has attracted much attention as a way to convert carbon dioxide into industrially useful compounds (CO_2 fixation). Due to the high solubility of carbon dioxide in ionic liquids, this reaction was also carried out in different ionic liquid/supercritical carbon dioxide systems[74-76]. For example, the cycloaddition of carbon dioxide and propylene oxide has been performed in the biphasic 1-butyl-3-methylimidazolium tetrachloroindate ([bmim][InCl₄]) + supercritical carbon dioxide system, where the ionic liquid acts both as solvent and catalyst[76] (see figure 2.14). Compared to the conventional phosgene-free processes for the synthesis of cyclic carbonates, the selectivity and stability of the biphasic ionic liquid/supercritical carbon dioxide process are higher, and it is easier to separate the product from the catalyst.
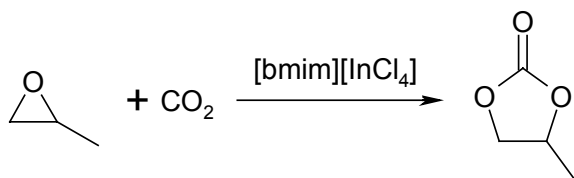
Figure 2.14: Cycloaddition of carbon dioxide and propylene oxide in the biphasic [bmim][InCl₄] + CO₂ system[76]

So far, all reported processes using ionic liquid/supercritical carbon dioxide systems are biphasic. Advantages of the biphasic operation are the ease of separation of product and catalyst, the enhanced stability and selectivity of the catalyst by the ionic liquid, and (in most cases) the increased reaction rate by adding supercritical carbon dioxide as compared to the biphasic operation without CO_2. However, the reported reaction rates in these *biphasic* systems are low compared to conventional catalytic *single-phase* processes, as a result of mass transfer limitations and low reactant solubilities. For example, the rhodium-catalyzed hydrogenation of cyclohexene to cyclohexane in the *biphasic* [hmim][PF₆] + CO_2 system proceeds with 96% conversion in 3 hours at 50 °C, 48 bar hydrogen pressure and a total pressure of 207 bar[61], whereas the same hydrogenation can take place as *single-phase* process with 100% conversion in 3 hours at 25°C and under 2 bar hydrogen pressure[77]. Moreover, mass transfer limitations also lead to low separation rates.

In order to achieve high reaction rates, it is highly desirable to create a homogeneous liquid phase during reaction. In addition, instantaneous demixing into two phases, where the product is recovered from the phase that does not contain any ionic liquid, is desirable for a fast separation. In the next chapter, a novel process that combines such features is presented, based on the recently discovered phenomenon of miscibility windows, which was proven to be generally applicable for ternary systems including those with ionic liquids involved. Using this phenomenon, it is possible to control the homogeneity/ biphasicity of the system by altering only, and to a very limited extent, one simple variable such as the CO_2 pressure or equivalently the CO_2-concentration. Combined with the characteristics of ionic liquids, the novel principle is the basis for performing reactions and separations with minimum waste generation, no use of volatile organic solvents, very pure products, and easy recycling of the ionic liquid, catalyst and carbon dioxide. This revolutionary process set-up is applicable to many reactions performed in the fine chemical and pharmaceutical industry.

2.4 References

1. Earle, M. J.; Seddon, K. R.; Ionic Liquids. Green Solvents for the Future, *Pure Appl. Chem.* **2000**, *72 (7)*, 1391-1398.
2. Wasserscheid, P.; Welton, T., Eds. *Ionic Liquids in Synthesis*; Wiley-VCH Verlag: Weinheim, Germany, 2003.
3. Walden, P.; Molecular Weights and Electrical Conductivity of Several Fused Salts, *Bull. Acad. Sci. (St. Petersburg)* **1914**, 405-422.
4. Wier, T. P., Jr.; Hurley, F. H.; Electrodeposition of Aluminum, US Patent 2446349 (1948).
5. Gale, R. J.; Gilbert, B.; Osteryoung, R. A.; Raman Spectra of Molten Aluminum Chloride: 1-Butylpyridinium Chloride Systems at Ambient Temperatures, *Inorg. Chem.* **1978**, *17 (10)*, 2728-2729.
6. Wilkes, J. S.; Levisky, J. A.; Wilson, R. A.; Hussey, C. L.; Dialkylimidazolium Chloroaluminate Melts: A New Class of Room-Temperature Ionic Liquids for Electrochemistry, Spectroscopy and Synthesis, *Inorg. Chem.* **1982**, *21 (3)*, 1263-1264.
7. Boon, J. A.; Levisky, J. A.; Pflug, J. L.; Wilkes, J. S.; Friedel-Crafts Reactions in Ambient-Temperature Molten Salts, *J. Org. Chem.* **1986**, *51 (4)*, 480-483.
8. Wilkes, J. S.; Zaworotko, M. J.; Air and Water Stable 1-Ethyl-3-methylimidazolium Based Ionic Liquids, *J. Chem. Soc., Chem. Commun.* **1992**, *(13)*, 965-967.
9. Holbrey, J. D.; Seddon, K. R.; Ionic Liquids, *Clean Products & Processes* **1999**, *1 (4)*, 223-236.
10. Ionic Liquids Database Merck, Ionic Liquids: New Materials for New Applications, http://ildb.merck.de/ionicliquids/en/startpage.htm
11. Earle, M. J.; Esperança, J. M. S. S.; Gilea, M. A.; Lopes, J. N. C.; Rebelo, L. P. N.; Magee, J. W.; Seddon, K. R.; Widegren, J. A.; The Distillation and Volatility of Ionic Liquids, *Nature* **2006**, *439 (7078)*, 831-834.
12. Buzzeo, M. C.; Evans, R. G.; Compton, R. G.; Non-Haloaluminate Room Temperature Ionic Liquids in Electrochemistry – A Review, *Chem. Phys. Chem.* **2004**, *5 (8)*, 1106-1120.
13. Olivier-Bourbigou, H.; Magna, L.; Ionic Liquids: Perspectives for Organic and Catalytic Reactions, *J. Mol. Catal. A* **2002**, *182-183*, 419-437.
14. Welton, T.; Ionic Liquids in Catalysis, *Coord. Chem. Rev.* **2004**, *248 (21-24)*, 2459-2477.
15. Holbrey, J. D.; Reichert, W. M.; Swatloski, R. P.; Broker, G. A.; Pitner, W. R.; Seddon, K. R.; Rogers, R. D.; Efficient, Halide Free Synthesis of New, Lost Cost Ionic Liquids: 1,3-Dialkylimidazolium Salts Containing Methyl- and Ethyl-Sulfate Anions, *Green Chem.* **2002**, *4 (5)*, 407-413.
16. Garcia, M. T.; Gathergood, N.; Scammells, P. J.; Biodegradable Ionic Liquids. Part II. Effect of the Anion and Toxicity, *Green Chem.* **2005**, *7 (1)*, 9-14.
17. Docherty, K. M.; Kulpa, C. F., Jr.; Toxicity and Antimicrobial Activity of Imidazolium and Pyridinium Ionic Liquids, *Green Chem.* **2005**, *7 (4)*, 185-189.

18. Gathergood, N.; Garcia, M. T.; Scammells, P. J.; Biodegradable Ionic Liquids. Part I. Concept, Preliminary Targets and Evaluation, *Green Chem.* **2004**, *6 (3)*, 166-175.
19. Gathergood, N.; Scammells, P. J.; Garcia, M. T.; Biodegradable Ionic Liquids. Part III. The First Readily Biodegradable Ionic Liquids, *Green Chem.* **2006**, *8 (2)*, 156-160.
20. Handy, S. T.; Okello, M.; Dickenson, G.; Solvents from Bio-renewable Sources: Ionic Liquids Based on Fructose, *Org. Lett.* **2003**, *5 (14)*, 2513-2515.
21. Hagiwara, R.; Ito, Y.; Room Temperature Ionic Liquids of Alkylimidazolium Cations and Fluoroanions, *J. Fluorine Chem.* **2000**, *105 (2)*, 221-227.
22. Freyland, W.; Zell, C. A.; Zein El Abedin, S.; Endres, F.; Nanoscale Electro-deposition of Metals and Semiconductors from Ionic Liquids, *Electrochim. Acta* **2003**, *48 (20-22)*, 3053-3061.
23. Liao, Q.; Pitner, W. R.; Stewart, G.; Hussey, C. L.; Stafford, G. R.; Electro-deposition of Aluminum from the Aluminum Chloride – 1-Methyl-3-ethyl-imidazolium Chloride Room Temperature Molten Salt + Benzene, *J. Electrochem. Soc.* **1997**, *144 (3)*, 936-943.
24. Lee, S. Y.; Yong, H. H.; Lee, Y. J.; Kim, S. K.; Ahn, S.; Two-Cation Competition in Ionic Liquid-Modified Electrolytes for Lithium Ion Batteries, *J. Phys. Chem. B* **2005**, *109 (28)*, 13663-13667.
25. Sakaebe, H.; Matsumoto, H.; *N*-Methyl-*N*-propylpiperidinium bis(trifluoro-methanesulfonyl)imide (PP13-TFSI) – Novel Electrolyte Base for Li Battery, *Electrochem. Commun.* **2003**, *5 (7)*, 594-598.
26. Kuang, D.; Wang, P.; Ito, S.; Zakeeruddin, S. M.; Grätzel, M.; Stable Mesoscopic Dye-Sensitized Solar Cells Based on Tetracyanoborate Ionic Liquid Electrolyte, *J. Am. Chem. Soc.* **2006**, *128 (24)*, 7732-7733.
27. McEwen, A. B.; Ngo, H. L.; LeCompte, K.; Goldman, J. L.; Electrochemical Properties of Imidazolium Salt Electrolytes for Electrochemical Capacitor Applications, *J. Electrochem. Soc.* **1999**, *146 (5)*, 1687-1695.
28. Ue, M.; Takeda, M.; Toriumi, A.; Kominato, A.; Hagiwara, R.; Ito, Y.; Application of Low-Viscosity Ionic Liquid to the Electrolyte of Double-Layer Capacitors, *J. Electrochem. Soc.* **2003**, *150 (4)*, A499-A502.
29. Sato, T.; Masuda, G.; Takagi, K.; Electrochemical Properties of Novel Ionic Liquids for Electric Double Layer Capacitor Applications, *Electrochim. Acta* **2004**, *49 (21)*, 3603-3611.
30. D'Anna, F.; Frenna, V.; Noto, R.; Pace, V.; Spinelli, D.; Can the Absence of Solvation of Neutral Reagents by Ionic Liquids Be Responsible for the High Reactivity in Base-Assisted Intramolecular Nucleophilic Substitutions in These Solvents, *J. Org. Chem.* **2005**, *70 (7)*, 2828-2831.
31. Chiappe, C.; Pieraccini, D.; Ionic Liquids: Solvent Properties and Organic Reactivity, *J. Phys. Org. Chem.* **2005**, *18 (4)*, 275-297.
32. Ross, J.; Xiao, J.; Friedel-Crafts Acylation Reactions Using Metal Triflates in Ionic Liquid, *Green Chem.* **2002**, *4 (2)*, 129-133.
33. Wasserscheid, P.; Keim, W.; Ionic Liquids – New Solutions for Transition Metal Catalysis, *Angew. Chem., Int. Ed.* **2000**, *39 (21)*, 3772-3789.

34. Dyson, P. J.; Transition Metal Chemistry in Ionic Liquids, *Transition Metal Chem.* **2002**, *27 (4)*, 353-358.
35. Sheldon, R. A.; Lau, R. M.; Sorgedrager, M. J.; Van Rantwijk, F.; Seddon, K. R.; Biocatalysis in Ionic Liquids, *Green Chem.* **2002**, *4 (2)*, 147-151.
36. Jain, N.; Kumar, A.; Chauhan, S.; Chauhan, S. M. S.; Chemical and Biochemical Transformations in Ionic Liquids, *Tetrahedron* **2005**, *61 (5)*, 1015-1060.
37. Muzart, J.; Ionic Liquids as Solvents for Catalyzed Oxidations of Organic Compounds, *Adv. Synth. Catal.* **2006**, *348 (3)*, 275-295.
38. Brennecke, J. F.; Maginn, E. J.; Ionic Liquids: Innovative Fluids for Chemical Processing, *AIChE J.* **2001**, *47 (11)*, 2384-2389.
39. Anthony, J. L.; Aki, S. N. V. K.; Maginn, E. J.; Brennecke, J. F.; Feasibility of Using Ionic Liquids for Carbon Dioxide Capture, *Int. J. Environ. Technol. Manage.* **2004**, *4 (1-2)*, 105-115.
40. Huddleston, J. G.; Willauer, H. D.; Swatloski, R. P.; Visser, A. E.; Rogers, R. D.; Room Temperature Ionic Liquids as Novel Media for Clean Liquid-Liquid Extraction, *Chem. Commun.* **1998**, *(16)*, 1765-1766.
41. Zhao, H.; Xia, S.; Ma, P.; Use of Ionic Liquids as Green Solvents for Extractions, *J. Chem. Technol. Biotechnol.* **2005**, *80 (10)*, 1089-1096.
42. Fortunato, R.; Afonso, C. A. M.; Reis, M. A. M.; Crespo, J. G.; Supported Liquid Membranes Using Ionic Liquids: Study of Stability and Transport Mechanisms, *J. Membrane Sci.* **2004**, *242 (1-2)*, 197-209.
43. Matsumoto, M.; Inomoto, Y.; Kondo, K.; Selective Separation of Aromatic Hydrocarbons Through Supported Liquid Membranes Based on Ionic Liquids, *J. Membrane Sci.* **2005**, *246 (1)*, 77-81.
44. Degussa, Product information on Ionic Liquids, http://productkaleidoscope.degussa.com/productkaleidoscope/en/productkaleidoscope.html
45. Cytec Industries, Cytec's Phosphine and Phosphorus Specialties (Ionic Liquids), http://www.cytec.com/business/Phosphine/Applications/IonicLiquids.shtm
46. BASF, BASIL Process (Biphasic Acid Scavenging using Ionic Liquids), http://www.basf.com/corporate/051004_ionic.htm
47. Air Products, GASGUARD Sub-Atmospheric Systems (SAS), http://www.airproducts.com/NR/rdonlyres/ 9D919AAD-DE4F-4614-B3C4-E923C6BF786E/ 0/ GasguardSAS.pdf
48. Chauvin, Y.; Olivier, H.; Wyrvalski, C. N.; Simon, L. C.; De Souza, R. F.; Oligomerization of n-Butenes Catalyzed by Nickel Complexes Dissolved in Organochloroaluminate Ionic Liquids, *J. Catal.* **1997**, *165 (2)*, 275-278.
49. Poling, B. E.; Prausnitz, J. M.; O'Connell, J. P. *The Properties of Gases and Liquids,* 5th ed., McGraw-Hill: New York (NY), USA, 2001.
50. Beckman, E. J.; Supercritical and Near-Critical CO_2 in Green Chemical Synthesis and Processing, *J. Supercrit. Fluids* **2003**, *28 (2-3)*, 121-191.
51. Jessop, P. G.; Leitner, W., Eds. *Chemical Synthesis Using Supercritical Fluids*; Wiley-VCH Verlag: Weinheim, Germany, 1999.
52. Leitner, W.; Supercritical Carbon Dioxide as a Green Reaction Medium for Catalysis, *Acc. Chem. Res.* **2002**, *35 (9)*, 746-756.

53. Kemmere, M. F.; Meyer, T., Eds. *Supercritical Carbon Dioxide in Polymer Reaction Engineering*; Wiley-VCH Verlag: Weinheim, Germany, 2005.

54. Sheldon, R. A.; Green Solvents for Sustainable Organic Synthesis: State of the Art, *Green Chem.* **2005**, *7 (5)*, 267-278.

55. Eckert, C. A.; Liotta, C. L.; Bush, D.; Brown, J. S.; Hallett, J. P.; Sustainable Reactions in Tunable Solvents, *J. Phys. Chem. B* **2004**, *108 (47)*, 18108-18118.

56. Blanchard, L. A.; Hancu, D.; Beckman, E. J.; Brennecke, J. F.; Green Processing Using Ionic Liquids and CO_2, *Nature* **1999**, *399 (6731)*, 28-29.

57. Blanchard, L. A.; Brennecke, J. F.; Recovery of Organic Products from Ionic Liquids Using Supercritical Carbon Dioxide, *Ind. Eng. Chem. Res.* **2001**, *40 (1)*, 287-292.

58. Blanchard, L. A.; Gu, Z.; Brennecke, J. F.; High-Pressure Phase Behavior of Ionic Liquid/ CO_2 Systems, *J. Phys. Chem. B* **2001**, *105 (12)*, 2437-2444.

59. Brown, R. A.; Pollet, P.; McKoon, E.; Eckert, C. A.; Liotta, C. L.; Jessop, P. G.; Asymmetric Hydrogenation and Catalyst Recycling Using Ionic Liquid and Supercritical Carbon Dioxide, *J. Am. Chem. Soc.* **2001**, *123 (6)*, 1254-1255.

60. Dzyuba, S. V.; Bartsch, R. A.; Recent Advances in Applications of Room Temperature Ionic Liquid/Supercritical CO_2 Systems, *Angew. Chem., Int. Ed.* **2003**, *42 (2)*, 148-150.

61. Liu, F.; Abrams, M. B.; Baker, R. T.; Tumas, W.; Phase-Separable Catalysis Using Room Temperature Ionic Liquids and Supercritical Carbon Dioxide, *Chem. Commun.* **2001**, *(5)*, 433-434.

62. Solinas, M.; Pfaltz, A.; Cozzi, P. G.; Leitner, W.; Enantioselective Hydrogenation of Imines in Ionic Liquid/Carbon Dioxide Media, *J. Am. Chem. Soc.* **2004**, *126 (49)*, 16142-16147.

63. Webb, P. B.; Sellin, M. F.; Kunene, T. E.; Williamson, S.; Slawin, A. M. Z.; Cole-Hamilton, D. J.; Continuous-Flow Hydroformylation of Alkenes in Supercritical Fluid – Ionic Liquid Biphasic Systems, *J. Am. Chem. Soc.* **2003**, *125 (50)*, 15577-15588.

64. Bronger, R. P. J.; Silva, S. M.; Kamer, P. C. J.; Van Leeuwen, P. W. N. M.; A Novel Dicationic Phenoxaphosphino-Modified Xantphos-Type Ligand: A Ligand for Highly Active and Selective, Biphasic, Rhodium Catalyzed Hydroformylation in Ionic Liquids, *Dalton Trans.* **2004**, *(10)*, 1590-1596.

65. Tominaga, K.; An Environmentally Friendly Hydroformylation using Carbon Dioxide as a Reactant Catalyzed by Immobilized Ru-Complex in Ionic Liquids, *Catal. Today* **2006**, *115 (1-4)*, 70-72.

66. Tominaga, K.; Sasaki, Y.; Biphasic Hydroformylation of 1-Hexene with Carbon Dioxide Catalyzed by Ruthenium Complex in Ionic Liquids, *Chem. Lett.* **2004**, *33 (1)*, 14-15.

67. Ballivet-Tkatchenko, D.; Picquet, M.; Solinas, M.; Franciò, G.; Wasserscheid, P.; Leitner, W.; Acrylate Dimerization under Ionic Liquid – Supercritical Carbon Dioxide Conditions, *Green Chem.* **2003**, *5 (2)*, 232-235.

68. Reetz, M. T.; Wiesenhöfer, W.; Franciò, G.; Leitner, W.; Biocatalysis in Ionic Liquids: Batchwise and Continuous Flow Processes using Supercritical Carbon Dioxide as the Mobile Phase, *Chem. Commun.* **2002**, *(9)*, 992-993.

69. Reetz, M. T.; Wiesenhöfer, W.; Franciò, G.; Leitner, W.; Continuous Flow Enzymatic Kinetic Resolution and Enantiomer Separation using Ionic Liquid/Supercritical Carbon Dioxide Media, *Adv. Synth. Catal.* **2003**, *345 (11)*, 1221-1228.

70. Lozano, P.; De Diego, T.; Carrié, D.; Vaultier, M.; Iborra, J. L.; Continuous Green Biocatalytic Processes Using Ionic Liquids and Supercritical Carbon Dioxide, *Chem. Commun.* **2002**, *(7)*, 692-693.

71. Lozano, P.; De Diego, T.; Carrié, D.; Vaultier, M.; Iborra, J. L.; Lipase Catalysis in Ionic Liquids and Supercritical Carbon Dioxide at 150 °C, *Biotechnol. Prog.* **2003**, *19 (2)*, 380-382.

72. Lozano, P.; De Diego, T.; Carrié, D.; Vaultier, M.; Iborra, J. L.; Synthesis of Glycidyl Esters Catalyzed by Lipases in Ionic Liquids and Supercritical Carbon Dioxide, *J. Mol. Catal. A* **2004**, *214 (1)*, 113-119.

73. Zhang, Z.; Wu, W.; Han, B.; Jiang, T.; Wang, B.; Liu, Z.; Phase Separation of the Reaction System Induced by CO_2 and Conversion Enhancement for the Esterification of Acetic Acid with Ethanol in Ionic Liquid, *J. Phys. Chem. B* **2005**, *109 (33)*, 16176-16179.

74. Xiao, L. F.; Li, F. W.; Peng, J. J.; Xia, C. G.; Immobilized Ionic Liquid/Zinc Chloride: Heterogeneous Catalyst for Synthesis of Cyclic Carbonates from Carbon Dioxide and Epoxides, *J. Mol. Catal. A* **2006**, *253 (1-2)*, 265-269.

75. Gu, Y.; Shi, F.; Deng, Y.; Ionic Liquid as an Efficient Promoting Medium for Fixation of CO_2: Clean Synthesis of α-Methylene Cyclic Carbonates from CO_2 and Propargyl Alcohols Catalyzed by Metal Salts under Mild Conditions, *J. Org. Chem.* **2004**, *69 (2)*, 391-394.

76. Kim, Y. J.; Varma, R. S.; Tetrahaloindate(III)-Based Ionic Liquids in the Coupling Reaction of Carbon Dioxide and Epoxides to Generate Cyclic Carbonates: H-Bonding and Mechanistic Studies, *J. Org. Chem.* **2005**, *70 (20)*, 7882-7891.

77. Boudart, M.; Sajkowski, D. J.; Catalytic Hydrogenation of Cyclohexene: Liquid-Phase Reaction on Rhodium, *Faraday Discuss.* **1991**, *92*, 57-67.

3

A Novel Approach to Combine Reactions and Separations Using Ionic Liquids and Supercritical Carbon Dioxide

3
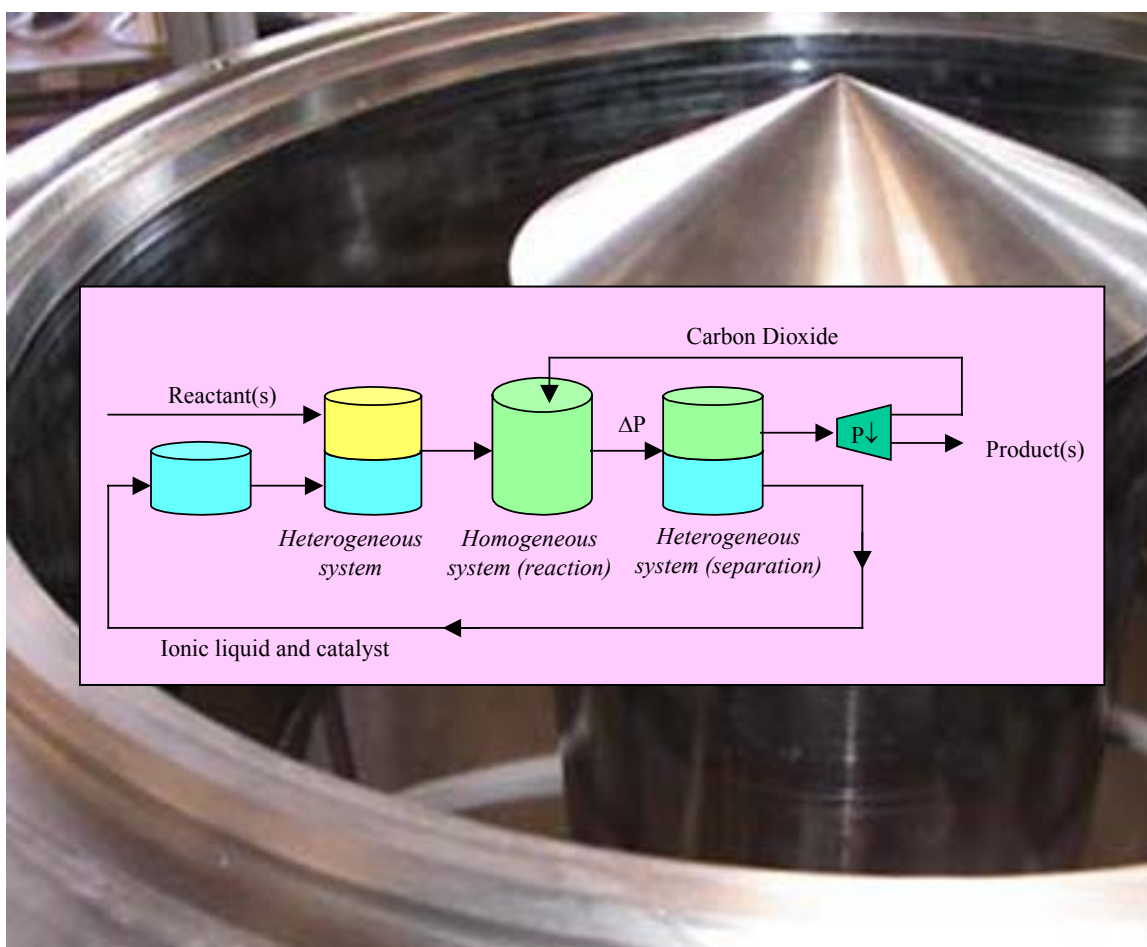
A Novel Approach to Combine Reactions and Separation Using Ionic Liquids and Supercritical Carbon Dioxide

A new and general type of process for the chemical industry is presented using ionic liquids and supercritical carbon dioxide as combined reaction and separation media. In this process the carbon dioxide pressure controls the miscibility of reactants, products, catalyst and ionic liquid, enabling fast atom-efficient reactions in a homogenous phase as well as instantaneous product recovery in a biphasic system. High reaction and separation rates can be achieved compared with the conventional fully biphasic alternative.

3. A Novel Approach to Combine Reactions and Separations using Ionic Liquids and Supercritical Carbon Dioxide

3.1 Introduction

Previously reported processes using ionic liquids and supercritical carbon dioxide have been presented in chapter 2. All these processes have the disadvantage of being biphasic. This results in low reaction and separation rates due to mass transfer limitations[1-4]. Especially in reactions in which one of the reactants is a gas with very low solubility in the ionic liquid, the reaction rate can be rather low[4]. Examples include hydrogenations, hydroformylations and oxidations, where the reaction rate is low due to the low solubility of hydrogen and oxygen in ionic liquids. Previously, it was found that adding carbon dioxide could increase the solubility of gases in ionic liquids[5,6]. It was also found that carbon dioxide could induce ternary[7-10] and quaternary[11-13] ionic liquid systems to undergo a 'two-phase' – 'three-phase' – 'two-phase' transition as the pressure of carbon dioxide was increased (see figure 3.1). However, a fully homogeneous phase has never been reached previously.
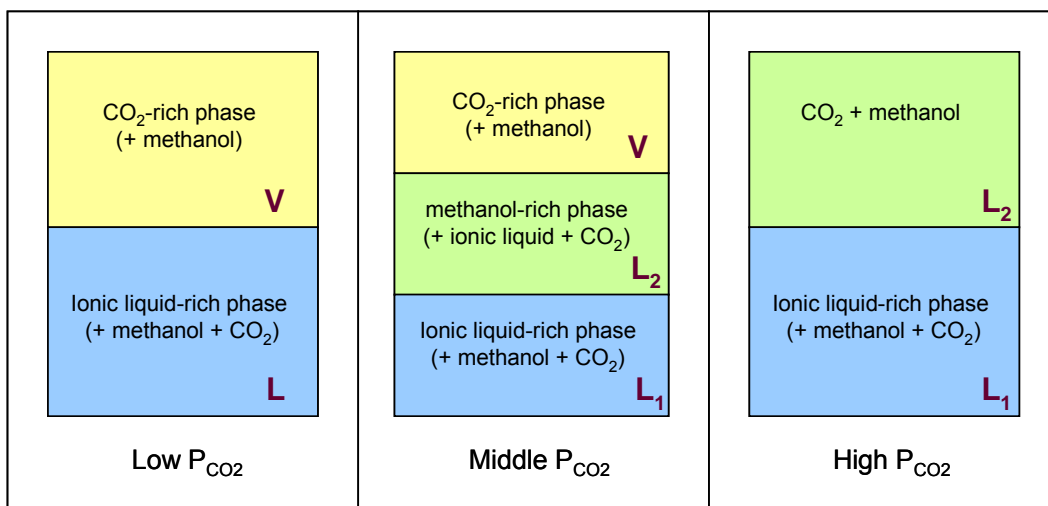
Figure 3.1: Carbon dioxide induced 'two-phase' – 'three-phase' – 'two-phase' transition in the ternary [bmim][PF_6] + methanol + CO_2 system[7]

In this chapter a novel approach to combine reactions and separations using ionic liquids and supercritical carbon dioxide is presented. In the novel process set-up, the reaction takes place at high rates in a homogeneous system, whereas separation is achieved by instantaneous demixing into two phases, where the product is recovered from the phase that does not contain any ionic liquid. The novel process is based on the recently established phenomenon of miscibility windows[14,15].

3.2 Miscibility windows

From experimental and theoretical work[14,15], the generally valid conclusion was drawn that in ternary inhomogeneous systems of the nature 'carbon dioxide' + 'liquid (1)' + 'liquid (2)/solid' with limited miscibility of both condensed phases, pressurization of the system with carbon dioxide will force the heterogeneous two-phase system to form a homogeneous one-liquid phase system. In reverse, at pressure relief the homogeneous liquid phase will phase split again into a liquid-liquid two-phase system. This means that the homogeneity of the reacting phase is fully controlled by varying the carbon dioxide pressure (or equivalently, the carbon dioxide concentration). The fundamental basis for this complex phase behavior was proven for many ternary systems of the kind 'carbon dioxide' + 'liquid (1)' (n-alkane) + 'liquid (2)' (1-alkanol), and the physical background could be ascribed to co-solvency effects[15]. From equations of state this behavior could also be predicted[16].

In this chapter it is demonstrated that the principle of miscibility windows also holds for ternary carbon dioxide systems with an ionic liquid as one of the condensed phases[17,18]. For a number of selected ternary systems of the nature 'carbon dioxide' + 'ionic liquid' + 'alkanol', the complex phase behavior was investigated experimentally using the Cailletet apparatus (a detailed description of this experimental set-up can be found in paragraph 4.3.1). Low-molecular weight alkanols were chosen to clearly demonstrate the basic principle in fluid phase behavior without the inference of the occurrence of a solid phase. It should be emphasized that presence of a solid phase will not affect the basic features at all.

Figure 3.2 summarizes the miscibility windows phenomenon for the ternary system 'CO_2' + '[hmim][BF_4]' + '2-propanol', where [hmim][BF_4] (1-hexyl-3-methylimidazolium tetrafluoroborate) is the selected ionic liquid (the preparation can be found in paragraph 4.2.1) and 2-propanol the selected alkanol[17]. In all graphs both liquids have the same mixing ratio i.e., ratio 2-propanol:[hmim][BF_4] = 20:1, while the mole fraction of carbon dioxide in the system only increases from 0.5209 up to 0.6023. The first graph (*a*) at the lowest CO_2 mole fraction shows that the homogeneous liquid phase region L is surrounded by three two-phase regions: two $L_1 + L_2$ regions and one region L + V. Also two narrow three-phase regions $L_1 + L_2 + V$ are present. As can be seen from the second graph (*b*), already a slight increase of the mole fraction of CO_2 causes the two two-phase regions $L_1 + L_2$ to approach each other, which means a narrowing of the temperature window for the occurrence of a homogeneous one-phase region L. This shift continues with increasing CO_2 mole fraction in the third graph (*c*), and as shown in this graph, the homogeneous L region is completely surrounded by the two-phase region $L_1 + L_2$, while at the same time the homogeneous L region also shifts rapidly to higher pressures. The vertical double arrow in graph (*c*) shows how in the real process the CO_2-pressure controls the occurrence of a homogeneous phase L (region where the reaction takes place) or a two-phase system $L_1 + L_2$ (region suitable for product separation). The fourth graph (*d*) at a mole fraction of CO_2 of 0.6023 shows that in the given temperature and pressure window, there is no homogeneous one-phase region anymore[17].
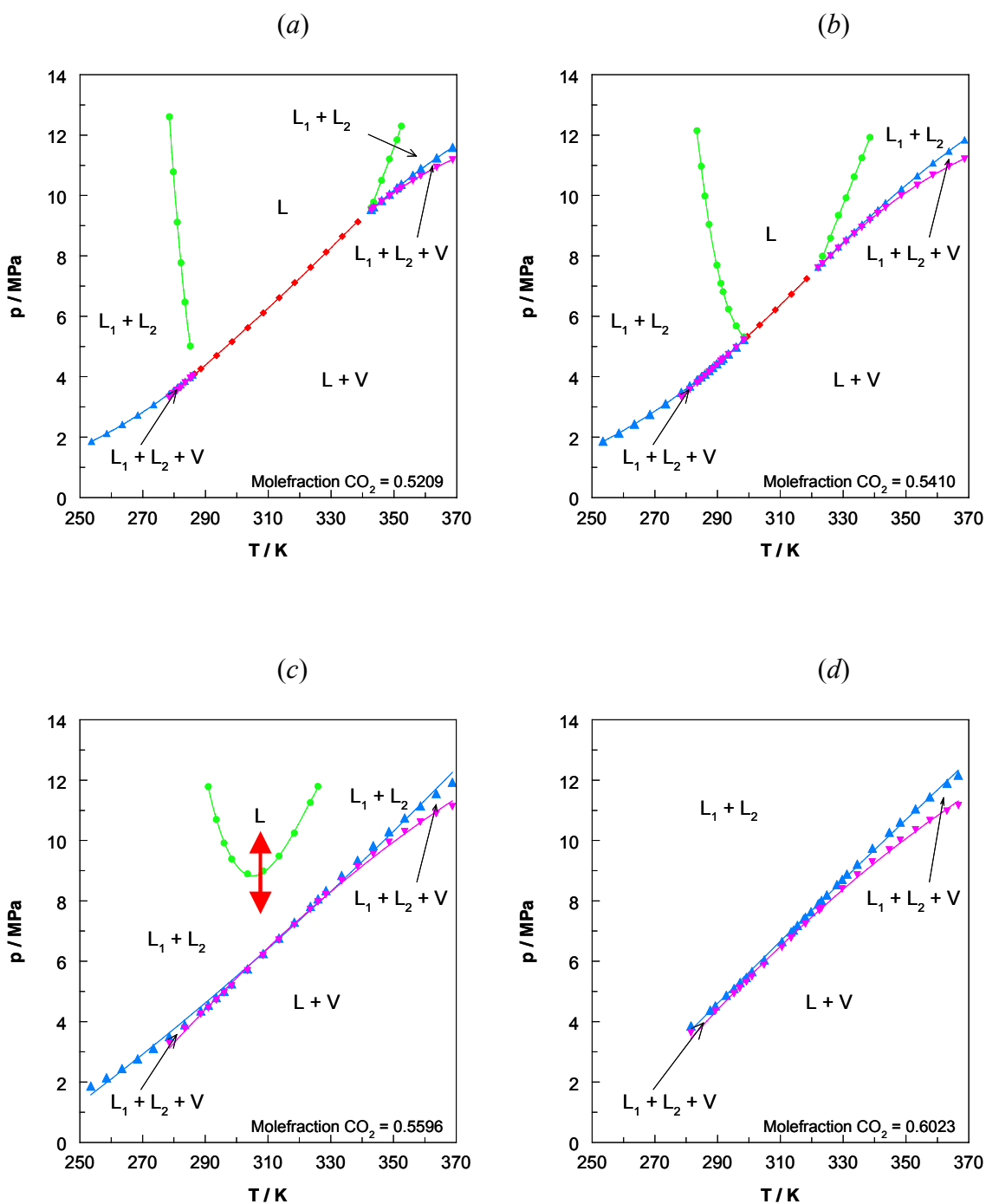
Figure 3.2: Fluid Phase Behavior of the Ternary System 'CO$_2$' + '[hmim][BF$_4$]' + '2-propanol' (Mixing ratio 2-propanol:[hmim][BF$_4$] = 20:1): the dots represent experimental measurements, whereas the lines are second-order polynomial trendlines. The vertical double arrow in the third graph (c) shows how CO$_2$-pressure controls the occurrence of a homogeneous phase (region where the reaction takes place) or a two-phase system (region suitable for product separation)[17].

Similar fluid phase behavior was found in the ternary systems 'CO$_2$' + '[hmim][BF$_4$]' + 'methanol'[18].

According to Gauter *et al.*[15], a homogeneous one-phase region always has to be present in ternary or even multi-component carbon dioxide systems, though its exact location in terms of temperature and pressure depends on the nature of the molecules present in the system and the composition of the mixture. Similar constraints hold for the case an ionic liquid is present in the mixture.

It is clear from the sequence of graphs of figure 3.2 that the conditions where the homogeneous one-phase region is bounded by an L$_1$ + L$_2$ region at slightly lower pressures (as in figure 3.2c) may be hard to locate. Its location is rather sensitive to the carbon dioxide mole fraction, because it occurs in a relatively narrow range of the mole fractions of carbon dioxide (here at 56 mole%). This also explains that in earlier efforts to combine reactions and separations using ionic liquids and supercritical carbon dioxide, the role of carbon dioxide was limited to the application as an extraction fluid at high carbon dioxide concentrations, leaving the single-phase region at lower carbon dioxide concentrations undiscovered.

3.3 Novel process set-up

The now thermodynamically understood phenomenon of miscibility windows (carbon dioxide-induced 'single-phase'/'two-phase' transition, see figure 3.3) allows us to design a completely new class of integrated processes to combine reactions and separations[19,20].
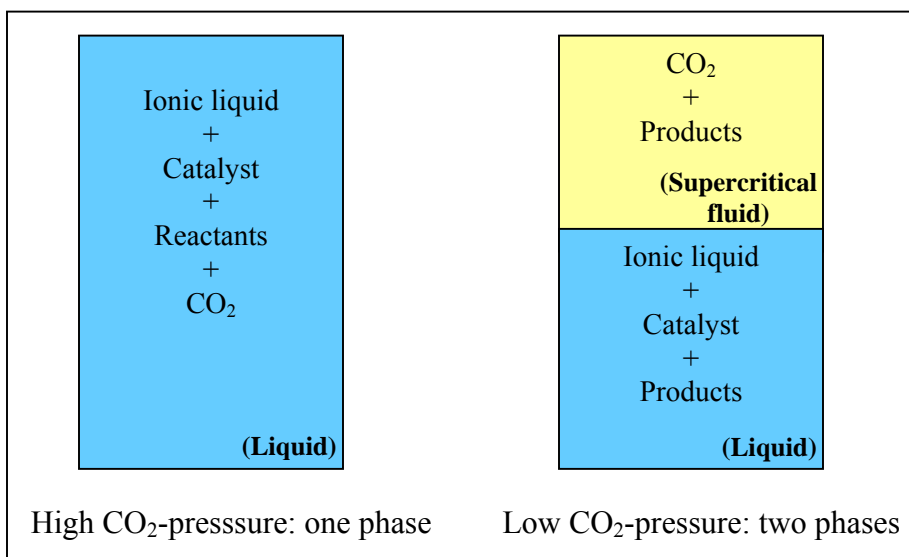
Figure 3.3: Miscibility switch phenomenon: at high carbon dioxide pressures a homogeneous liquid phase is formed, whereas at lower carbon dioxide pressures two immiscible phases are present[19,20]

The atom-efficient reaction is carried out in the homogeneous system, where the reactants as well as the catalyst dissolve in the ionic liquid[19,20]. The advantage of using an ionic liquid as reaction medium is that the immobilized catalyst is stabilized by the ionic liquid against oxidation, resulting in a longer lifetime of the catalyst without the need of regeneration. The advantage of adding carbon dioxide to the reaction mixture is that the solubility of many reactants is increased (higher concentrations) and/or that reactants, which are normally immiscible with pure ionic liquid, can dissolve in ionic liquid + carbon dioxide mixtures (= co-solvency effect). Therefore, it is possible to bring all components in high concentrations into one homogeneous phase. In this homogeneous system, the reaction takes place without any mass transfer limitations, which results in a high reaction rate. Moreover, the addition of carbon dioxide to the reaction mixture leads to a lower viscosity of the reaction system and a higher diffusion rate of the reactants, resulting in a further increase in reaction rate. The ionic liquid hardly expands when carbon dioxide is dissolved, because the carbon dioxide molecules occupy the cavities in the ionic liquid phase[21]. Therefore, the reaction volume can be kept small, leading to a small equipment size.

The separation is carried out in the biphasic system[19,20]. Application of the miscibility switch (pressure release) results in the instantaneous formation of a second phase out of the homogeneous liquid system (spinodal demixing). The light phase consists of supercritical carbon dioxide with dissolved products (and reactants in case of incomplete conversion), but does not contain any ionic liquid, because carbon dioxide cannot dissolve ionic liquid[22,23]. The heavy phase consists of ionic liquid with dissolved catalyst and some remaining products (and some remaining reactants in case of incomplete conversion). These phases can be separated from each other, and the pressure of the light phase is further decreased, leading to precipitation of the product (as a liquid or as a solid) out of the carbon dioxide. In this way, pure product is obtained without any detectable ionic liquid or catalyst (and no reactants when the reaction is complete). The catalyst remains in the ionic liquid phase and can be easily recycled, without negatively affecting the activity and enantioselectivity. Also, the carbon dioxide can be recompressed and reused The essential advantage of using instantaneous demixing instead of conventional extraction with carbon dioxide is the higher rate of product separation from the ionic liquid (no diffusion limitations). Another advantage of the novel process set-up is that the energy-consumption is low. Energy is only required for recompressing the carbon dioxide, but no energy-intensive distillation step is needed. Compared to the conventional separation processes, the energy consumption in the novel process set-up can be decreased by 50-80% (see chapter 9).

Finally, it should be noted that the use of ionic liquids and carbon dioxide as combined reaction and separation media is safe for health and environment. Ionic liquids cannot evaporate. Therefore, they cannot lead to emissions into the atmosphere. Moreover, ionic liquids cannot be inhaled and most of them are non-flammable. Also, carbon dioxide is non-flammable and non-toxic.

The novel process set-up in which reactions and separations are combined using ionic liquids and supercritical carbon dioxide as solvents is schematically shown in figure 3.4. An international patent application for this process set-up has been submitted[19]. It is the first time that a process is described using an ionic liquid and a carbon dioxide induced switch between a fully homogeneous phase and a two-phase system. The catalysis and extraction using supercritical fluids (CESS) process described previously also switches between a fully homnogeneous phase and a two-phase system, but does not make use of any ionic liquid[24]. In the next chapter, the novel process set-up will be applied to a model system. Since the principle of miscibility windows is a general phenomenon, it is likely that the new process set-up is applicable to many industrial processes. Therefore, the new process set-up using ionic liquids and supercritical carbon dioxide offers the potential to replace conventional processes with higher reaction and separation rates, but at the same time with lower energy consumption, a higher quality product and safer working conditions.
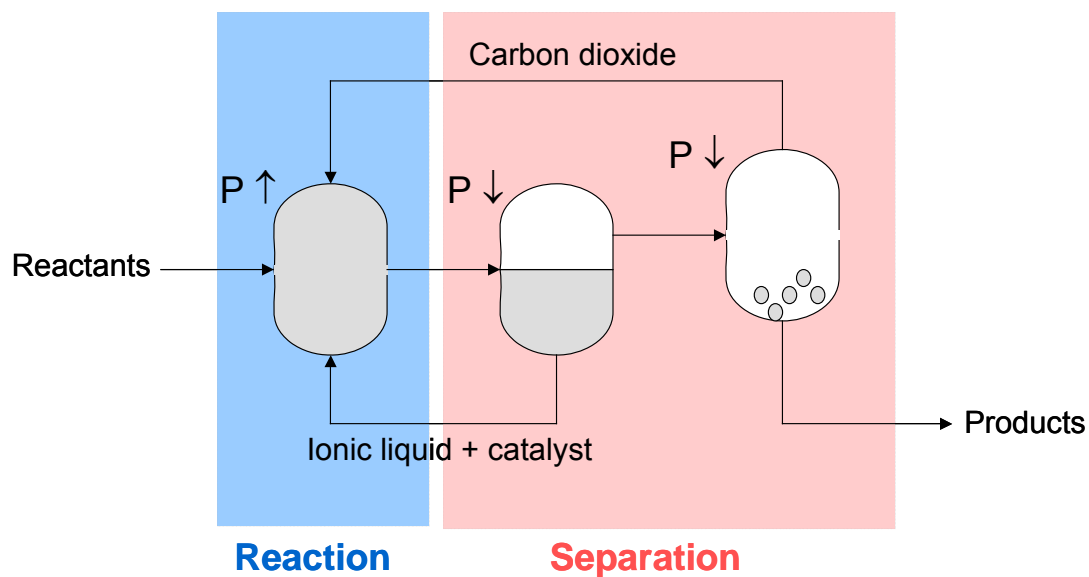
Figure 3.4: Novel process set-up. At high pressure the reaction is carried out in a homogeneous phase (complete conversion is assumed). The product is separated from the ionic liquid in the biphasic system that is formed at lower CO_2 pressure. Finally, the product is separated from the CO_2 by further pressure release.

3.4 References

1. Webb, P. B.; Sellin, M. F.; Kunene, T. E.; Williamson, S.; Slawin, A. M. Z.; Cole-Hamilton, D. J.; Continuous-Flow Hydroformylation of Alkenes in Supercritical Fluid – Ionic Liquid Biphasic Systems, *J. Am. Chem. Soc.* **2003**, *125 (50)*, 15577-15588.
2. Liu, F.; Abrams, M. B.; Baker, R. T.; Tumas, W.; Phase-Separable Catalysis Using Room Temperature Ionic Liquids and Supercritical Carbon Dioxide, *Chem. Commun.* **2001**, *(5)*, 433-434.
3. Bronger, R. P. J.; Silva, S. M.; Kamer, P. C. J.; Van Leeuwen, P. W. N. M.; A Novel Dicationic Phenoxaphosphino-Modified Xantphos-Type Ligand: A Ligand for Highly Active and Selective, Biphasic, Rhodium Catalyzed Hydroformylation in Ionic Liquids, *Dalton Trans.* **2004**, *(10)*, 1590-1596.
4. Dzyuba, S. V.; Bartsch, R. A.; Recent Advances in Applications of Room Temperature Ionic Liquid/Supercritical CO_2 Systems, *Angew. Chem., Int. Ed.* **2003**, *42 (2)*, 148-150.
5. Solinas, M.; Pfaltz, A.; Cozzi, P. G.; Leitner, W.; Enantioselective Hydrogenation of Imines in Ionic Liquid/Carbon Dioxide Media, *J. Am. Chem. Soc.* **2004**, *126 (49)*, 16142-16147.
6. Hert, D. G.; Anderson, J. L.; Aki, S. N. V. K.; Brennecke, J. F.; Enhancement of Oxygen and Methane Solubility in 1-Hexyl-3-methylimidazolium bis(trifluoro-methylsulfonyl)imide using Carbon Dioxide, *Chem. Commun.* **2005**, *(20)*, 2603-2605.
7. Scurto, A. M.; Aki, S. N. V. K.; Brennecke, J. F.; CO_2 as a Separation Switch for Ionic Liquid/Organic Mixtures, *J. Am. Chem. Soc.* **2002**, *124 (35)*, 10276-10277.
8. Aki, S. N. V. K.; Scurto, A. M.; Brennecke, J. F.; Ternary Phase Behavior of Ionic Liquid – Organic – CO_2 Systems, *Ind. Eng. Chem. Res.* **2006**, ASAP Web Release Date: 9 Feb 2006.
9. Liu, Z.; Wu, W.; Han, B.; Dong, Z.; Zhao, G.; Wang, J.; Jiang, T.; Yang, G.; Study of the Phase Behaviors, Viscosities, and Thermodynamic Properties of CO_2/[C_4mim][PF_6]/Methanol System at Elevated Pressures, *Chem. Eur. J.* **2003**, *9 (16)*, 3897-3903.
10. Zhang, Z.; Wu, W.; Gao, H.; Han, B.; Wang, B.; Huang, Y.; Tri-Phase Behavior of Ionic Liquid – Water – CO_2 System at Elevated Pressures, *Phys. Chem. Chem. Phys.* **2004**, *6 (21)*, 5051-5055.
11. Najdanovic-Visak, V.; Serbanovic, A.; Esperança, J. M. S. S.; Guedes, H. J. R.; Rebelo, L. P. N.; Nunes Da Ponte, M.; Supercritical Carbon Dioxide-Induced Phase Changes in Ionic Liquid, Water and Ethanol Mixture Solutions: Application to Biphasic Catalysis, *Chem. Phys. Chem.* **2003**, *4 (5)*, 520-522.
12. Najdanovic-Visak, V.; Rebelo, L. P. N.; Nunes Da Ponte, M.; Liquid-Liquid Behavior of Ionic Liquid – 1-Butanol – Water and High Pressure CO_2-Induced Phase Changes, *Green Chem.* **2005**, *7 (6)*, 443-450.
13. Zhang, Z.; Wu, W.; Han, B.; Jiang, T.; Wang, B.; Liu, Z.; Phase Separation of the Reaction System Induced by CO_2 and Conversion Enhancement for the

Esterification of Acetic Acid with Ethanol in Ionic Liquid, *J. Phys. Chem. B* **2005**, *109 (33)*, 16176-16179.

14. Peters, C. J.; Gauter, K.; Occurrence of Holes in Ternary Fluid Multiphase Systems of Near-Critical Carbon Dioxide and Certain Solutes, *Chem. Rev.* **1999**, *99 (2)*, 419-431.

15. Gauter, K.; Peters, C. J.; Scheidgen, A. L.; Schneider, G. M.; Cosolvency Effects, Miscibility Windows and Two-Phase LG Holes in Three-Phase LLG Surfaces in Ternary Systems: A Status Report, *Fluid Phase Equilib.* **2000**, *171 (1-2)*, 127-149.

16. Gauter, K.; Heidemann, R. A.; Peters, C. J.; Modeling of Fluid Multiphase Equilibria in Ternary Systems of Carbon Dioxide as the Near-Critical Solvent and Two Low-Volatile Solutes, *Fluid Phase Equilib.* **1999**, *158-160*, 133-141.

17. Florusse, L. J.; E. Domingo Force; Peters, C. J.; Fluid Phase Equilibria in the Ternary System Carbon Dioxide + Iso-propanol + 1-Hexyl-3-methylimidazolium Tetrafluoroborate ([bmim][BF$_4$]), to be submitted for publication to *Fluid Phase Equilibria* **2006**.

18. Florusse, L. J.; Peters, C. J.; Fluid Phase Equilibria in the Ternary System Carbon Dioxide + Methanol + 1-Hexyl-3-methylimidazolium Tetrafluoroborate ([bmim][BF$_4$]), to be submitted for publication to *J. Supercrit. Fluids* **2006**.

19. Kroon, M. C.; Shariati, A.; Florusse, L. J.; Peters, C. J.; Van Spronsen, J.; Witkamp, G. J.; Sheldon, R. A.; Gutkowski, K. E.; Process for Carrying Out a Chemical Reaction, International Patent WO 2006/088348 A1 (2006).

20. Kroon, M. C.; Florusse, L. J.; Shariati, A.; Gutkowski, K. E.; Van Spronsen, J.; Sheldon, R. A.; Witkamp, G. J.; Peters, C. J. On a Novel Class of Production Processes for the Chemical Industry, to be submitted for publication to *Nature* **2006**.

21. Huang, X.; Margulis, C. J.; Li, Y.; Berne, B. J.; Why is the Partial Molar Volume of CO$_2$ so Small when Dissolved in a Room Temperature Ionic Liquid? Structure and Dynamics of CO$_2$ Dissolved in [bmim$^+$][PF$_6^-$], *J. Am. Chem. Soc.* **2005**, *127 (50)*, 17842-17851.

22. Blanchard, L. A.; Hancu, D.; Beckman, E. J.; Brennecke, J. F.; Green Processing Using Ionic Liquids and CO$_2$, *Nature* **1999**, *399 (6731)*, 28-29.

23. Blanchard, L. A.; Brennecke, J. F.; Recovery of Organic Products from Ionic Liquids Using Supercritical Carbon Dioxide, *Ind. Eng. Chem. Res.* **2001**, *40 (1)*, 287-292.

24. Franciò, G.; Leitner, W.; Highly Regio- and Enantio-Selective Rhodium-Catalysed Asymmetric Hydroformylation Without Organic Solvents, *Chem. Commun.* **1999**, *(17)*, 1663-1664.

4

Experimental Determination of the Operation Conditions

4

Experimental Determination of the Operation Conditions

Experiments are performed to apply the novel approach from chapter 3 to the asymmetric hydrogenation of methyl (Z)-α-acetamidocinnamate in the 1-butyl-3-methylimidazolium tetrafluoroborate + carbon dioxide system. In order to determine the operation conditions, the phase behavior of this model system is investigated. First, the phase behavior of the binary system consisting of ionic liquid + carbon dioxide is studied experimentally. Carbon dioxide has a high solubility in ionic liquid at lower pressures, but the bubble point pressures sharply increase at higher pressures. Therefore, the binary ionic liquid + carbon dioxide system shows type-III phase behavior according to the classification of Scott and Van Konynenburg. Second, the influences of adding reactants, product and catalyst on this phase behavior are measured. At low carbon dioxide concentrations, the solubilities of the reactants in the ionic liquid + carbon dioxide system are higher than the solubilities of the reactants in pure ionic liquid (carbon dioxide works as co-solvent and addition of carbon dioxide increases the solubility of the reactants in ionic liquid). However, carbon dioxide at high concentrations starts to work as anti-solvent, which means that at high carbon dioxide concentrations the solubilities of the reactants in the ionic liquid + carbon dioxide system are lower than the solubilities of the reactants in pure ionic liquid. Finally, operation conditions for carrying out the reaction and separation are determined on basis of the phase behavior of the model system.

4. Experimental Determination of the Operation Conditions

4.1 The model system

To demonstrate the novel miscibility window concept, the asymmetric hydrogenation of methyl (*Z*)-α-acetamidocinnamate is chosen as a model reaction (see figure 4.1). This reaction yields N-acetyl-(*S*)-phenylalanine methyl ester, and is carried out in the combined 1-butyl-3-methylimidazolium tetrafluoroborate (ionic liquid) + carbon dioxide system.
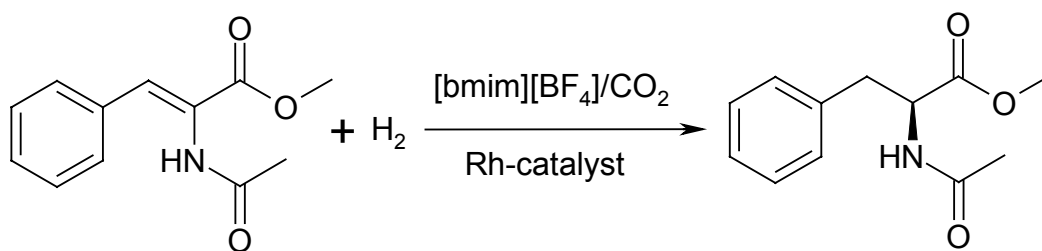
Figure 4.1: Model reaction: asymmetric hydrogenation of methyl (*Z*)-α-acetamidocinnamate in the [bmim][BF$_4$] + CO$_2$ system

The reaction is catalyzed by (-)-1,2-bis((2*R*,5*R*)-2,5-dimethylphospholano)benzene (cyclooctadiene)rhodium(I) tetrafluoroborate (Rh-MeDuPHOS, see figure 4.2).
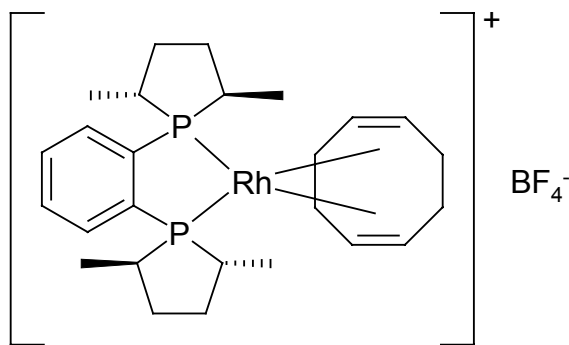
Figure 4.2: Rh-MeDuPHOS catalyst

This reaction is related to the most important step in the industrial manufacture of levodopa (*L*-dopa), an anti-parkinsonian drug (dopamine precursor).

The asymmetric hydrogenation of methyl (*Z*)-α-acetamidocinnamate was carried out for the first time in 1993 by Burk *et al.*[1] They used methanol as the solvent. Later on, also dichloromethane and ethyl acetate were used as solvents[2]. The conversions and enantioselectivities were high due to the use of the efficient chiral complex Rh-MeDuPHOS as homogeneous catalyst, but the rather expensive Rh-MeDuPHOS was very sensitive to oxidation. Hence, an inert atmosphere was required for its preparation and handling. Furthermore, the separation and recovery of the chiral complex from reagents and products was difficult.

Possible solutions to these drawbacks have focused on the engineering of chiral heterogenized catalysts. Heterogenization of chiral complexes by immobilization in various organic and inorganic supports has been successful, but leaching and stability of the complex still remain severe problems. Another approach was the use of two-phase systems, in which the phase of preference of the complex differs from that of the substrate, but only limited success has been achieved. In most cases, the activity and enantioselectivity of the chiral complexes were lower than those of the corresponding homogeneous system as a result of mass transfer limitations[3,4].

In 2001, the model reaction was carried out for the first time in ionic liquids, such as 1-butyl-3-methylimidazolium hexafluorophosphate ([bmim][PF$_6$])[5] and 1-butyl-3-methyl-imidazolium tetrafluoroborate ([bmim][BF$_4$])[6]. These ionic liquids are not only good hosts for immobilization of the chiral catalyst, but they also protect the complex from the attack by atmospheric oxygen. For example, [bmim][BF$_4$] provides extra stability to the air-sensitive chiral catalyst Rh-MeDuPHOS in the asymmetric hydrogenation of enamides[7]. Moreover, the immobilization of the catalyst in the ionic liquid phase allows easy recycling, without negatively affecting the activity and enantioselectivity[5,6]. However, the tetrafluoroborate and hexafluorophosphate ionic liquids are not water stable (formation of hydrogen fluoride, especially at high temperatures[8]), and moisture-free operation is required.

Despite the advantages of using ionic liquids as medium for the model reaction, the low solubility of hydrogen and the high viscosity of the ionic liquid still remain important drawbacks. Higher reaction rates, conversions and enantioselectivities can be reached when the availability of hydrogen is increased in the ionic liquid phase[6,9]. Therefore, significant efforts will have to be made to increase interfacial area and enhance mass transfer, and/or high-pressure operation will be required. Furthermore, co-solvents such as *iso*-propanol are always needed to increase the solubility of hydrogen and to lower the viscosity of the ionic liquid phase[5]. The use of co-solvents, which are often volatile organic solvents, leads to the need of an additional recovery step and a higher environmental impact.

This problem can be overcome when carbon dioxide is used as co-solvent. Carbon dioxide also lowers the viscosity of the ionic liquid and increases the solubility of hydrogen, leading to higher reaction rates, but does not suffer from the disadvantages mentioned above. Carbon dioxide is an alternative 'green' solvent. Moreover, carbon

dioxide can force all components into one phase, in which the reaction is carried out, whereas a biphasic system can be reached by changing the carbon dioxide pressure, where the product is separated from the phase that does not contain any ionic liquid (phenomenon of miscibility windows, see chapter 3). In this novel approach the model reaction can be simultaneously combined with the separation step, leading to considerable process intensification.

It is not possible to carry out the model reaction in only carbon dioxide as solvent (no ionic liquid), since the catalyst is not soluble in supercritical carbon dioxide and is therefore inactive[10,11].

In table 4.1 the conversion data and enantioselectivities of the model reaction in different solvents are shown. Enantioselectivities are expressed as enantiomeric excess (ee%), equal to $(R-S)/(R+S)\cdot 100\%$, where R and S are the concentrations of the two enantiomers, respectively.

Table 4.1: Conversion data of model reaction in literature[1,2,5,6,9]

Solvent	Conversion (%)	Time (h)	ee (%)	Substrate/ Rh-ratio (mole/mole)	T (^{0}C)	P_{H2} (bar)	Ref.
MeOH	100	1	98	2000	20	2	1
CH_2Cl_2	100	3	95	20	20	1	2
CH_2Cl_2	100	0.67	95	200	20	5	2
CH_2Cl_2	100	2	95	1000	20	15	2
CH_2Cl_2	81	16	95	6666	20	5	2
EtOAc	100	2	95	20	20	1	2
EtOAc	100	0.07	97	110	20	60	2
THF	100	12	93	20	20	1	2
Acetone	100	12	92	20	20	1	2
[bmim][PF_6]/i-PrOH	7	24	66	100	25	5	6
[bmim][PF_6]/i-PrOH	26	24	81	100	25	50	6
[bmim][PF_6]/i-PrOH	41	24	90	100	25	100	6
[bmim][PF_6]/i-PrOH	83	0.33	96	NA	25	2	5
[bmim][BF_4]/i-PrOH	73	24	93	100	25	50	6
i-PrOH	99	24	94	100	25	50	6
$scCO_2$	0	18	-	520	40	14	10

4.2 Preparation of the components of the model system

The model system consists of six components:

- 1-butyl-3-methylimidazolium tetrafluoroborate (solvent)
- carbon dioxide (solvent)
- methyl (*Z*)-α-acetamidocinnamate (reactant)
- hydrogen (reactant)
- N-acetyl-(*S*)-phenylalanine methyl ester (product)
- (-)-1,2-bis((2*R*,5*R*)-2,5-dimethylphospholano)benzene(cyclooctadiene)rhodium(I) tetrafluoroborate (catalyst)

Only the carbon dioxide and the hydrogen were bought (see table 4.2); the other components were synthesized (with the help of J. van Spronsen from the section Process Equipment and C. Simons from the section Biocatalysis and Organic Chemistry at the Delft University of Technology).

Table 4.2: Supplied components

Component	Purity (%)	Supplier
Carbon dioxide	99.95	Air Products
Hydrogen	99.9990	HoekLoos

4.2.1 Preparation of 1-butyl-3-methylimidazolium tetrafluoroborate

The ionic liquid 1-butyl-3-methylimidazolium tetrafluoroborate ([bmim][BF$_4$]) was prepared by a reaction of 1-methylimidazole and 1-chlorobutane yielding 1-butyl-3-methylimidazolium chloride ([bmim][Cl]) followed by ion exchange with sodium tetrafluoroborate in the solvent dichloromethane[8]. The two-steps preparation is shown in figure 4.3. All starting materials were bought from Sigma-Aldrich with purities over 99.5%.
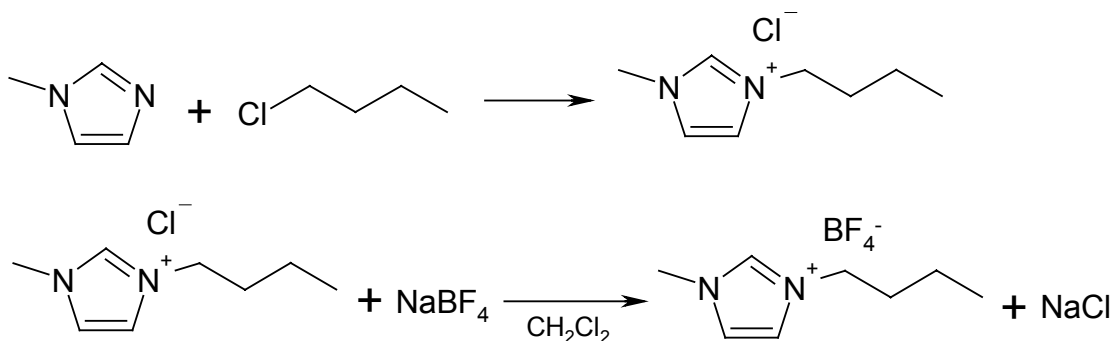
Figure 4.3: Preparation of 1-butyl-3-methylimidazolium tetrafluoroborate

Step 1:

The salt 1-butyl-3-methylimidazolium chloride was prepared by reaction of 628.3 g (7.652 mole) 1-methyl-imidazole and an excess of 837.6 g (9.048 mole) 1-chlorobutane in a 2 l round-bottomed flask fitted with a reflux condenser by heating and stirring at 80 °C for 5 days under a nitrogen atmosphere[12]. The excess of 1-chlorobutane was removed by rotary evaporation yielding 1314.6 g (7.526 mole) of 1-butyl-3-methylimidazolium chloride (conversion = 98.4 %) as a yellow-orange viscous liquid. The experimental set-up is shown in figure 4.4.

Figure 4.4: Experimental set-up for the preparation of [bmim][Cl] from 1-methylimidazole and 1-chlorobutane

Step 2:

The chloride ion was exchanged for the tetrafluoroborate ion by dissolving 1314.6 g (7.526 mole) 1-butyl-3-methylimidazolium chloride in 6.0 l dichloromethane, adding an excess of 879.8 g (8.013 mole) of sodium tetrafluoroborate crystals and stirring the mixture for 20 h at room temperature[12]. The mixture was filtered to remove the formed sodium chloride crystals. The solvent dichloromethane was evaporated by rotary evaporation yielding 1677.1 g (7.420 mole) of 1-butyl-3-methyl-imidazolium tetrafluoroborate (conversion = 98.6 %) as a yellow-orange liquid. The experimental set-up is shown in figure 4.5.

Figure 4.5: Experimental set-up for the preparation of [bmim][BF$_4$] from [bmim][Cl] and sodium tetrafluoroborate

The purity of the resulting ionic liquid was measured to be >99.5% using boron analysis (ICP-AES): 4.76 ± 0.10 mol% boron (theoretical amount is 4.78 mol%) and NMR analysis[12]: ^{1}H NMR (300.2 MHz, CDCl$_3$, TMS): δ0.93 (t, 3H), 1.34 (m, 2H), 1.86 (m, 2H), 3.95 (s, 3H), 4.20 (t, 2H), 7.47 (s, 2H), 8.71 (s, 1H). The amount of chloride in the ionic liquid was measured with ion chromatography and was 60 ppm. The largest impurity was fluoride, with an amount of 230 ppm. Prior to use, the [bmim][BF$_4$] was dried under vacuum conditions at room temperature for several days. The water content of the dried ionic liquid was measured using Karl-Fischer moisture analysis and was 30 ppm.

Table 4.3: Equipment used for analyzing the purity of the ionic liquid

Equipment	Description	
Nuclear magnetic resonance (NMR)	Company	Varian
	Type	Unity Inova 300 s
Inductively coupled plasma atomic emission spectroscopy (ICP-AES)	Company	Spectro
	Type	Spectroflame
Ion chromatography	Company	Dionex
	Type	DX-120
Karl-Fischer moisture analysis	Company	Metrohm
	Type	756 KF Coulometer

From literature it is known that 1-butyl-3-methylimidazolium tetrafluoroborate should be colorless[8]. However, the produced ionic liquid had a yellow-orange color, which is due to colored impurities. The chemical nature of the colored impurities in ionic liquids is still not very clear, but it is probably a mixture of traces of compounds originating from the starting materials, oxidation products, and thermal degradation products of the starting materials[8]. It was impossible to detect the trace amounts of colored impurities by analytical techniques. Decolorization was achieved by silica gel column chromatography separation with dichloromethane as the mobile phase (column diameter: 6 cm; column height: 50 cm; thickness of silica layer: 10 cm), where the colored components show less interaction with the mobile phase and remain in the silica bed.

4.2.2 Preparation of methyl (Z)-α-acetamidocinnamate

The reactant methyl (Z)-α-acetamidocinnamate was prepared with a purity of over 99.5% by esterification of the corresponding acid with methyl iodide (purchased from Sigma-Aldrich and Fluka with >99.5% purity), where the formed hydrogen iodide was removed by reaction with potassium carbonate[13] (see figure 4.6). 20.5 g (0.10 mole) of α-acetamidocinnamic acid was dissolved in 600 ml acetone and 27.6 g (0.20 mole) of potassium carbonate was slowly added. This mixture was refluxed at 56 °C and 28.4 g (0.20 mole) of methyl iodide was slowly added. The solution was boiled under reflux overnight, during which a white precipitate (potassium iodide) formed. The precipitate was removed by filtration and the filtrate was dried. The resulting solid was re-dissolved in water and the water layer was extracted with dichloromethane (three times). The organic layer was dried with sodium sulfate and the solvent was removed. The residue was re-crystallized from ethyl acetate/hexane[14]. Eventually, 18.7 g (0.085 mole) of methyl (Z)-α-acetamidocinnamate was obtained (conversion = 85%). The purity was measured using NMR analysis[15]: ^{1}H NMR (300.2 MHz, CDCl$_3$, TMS): δ1.61 (s, 1H), 2.14 (s, 3H), 3.85 (s, 3H), 7.38 (m, 6H).
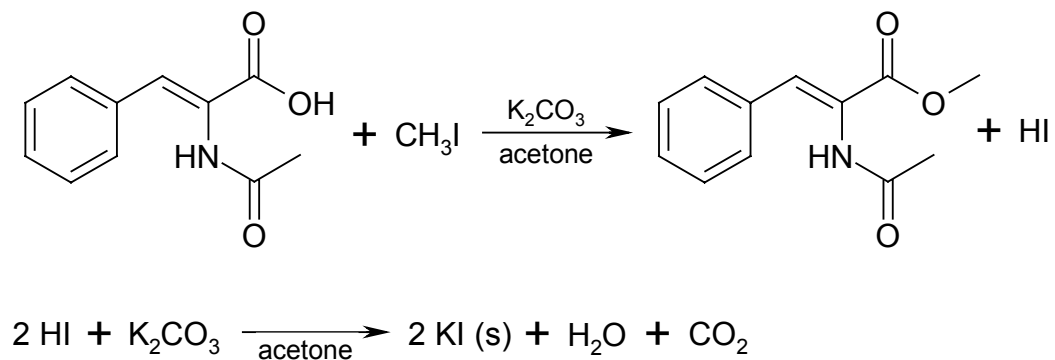
Figure 4.6: Preparation of methyl (Z)-α-acetamidocinnamate[13]

4.2.3 Preparation of N-acetyl-(S)-phenylalanine methyl ester

The product N-acetyl-(S)-phenylalanine methyl ester was prepared with a purity of over 99.5% by a reaction of the corresponding acid with thionyl chloride (purchased from Sigma-Aldrich with >99.5% purity), followed by esterification with methanol[13] (see figure 4.7). N-acetyl-(S)-phenylalanine (98.0 g, 0.473 mole) was dissolved in methanol (430 ml) and this solution was cooled to 0 ^{0}C. Thereafter a small excess of thionyl chloride (65.6 g, 0.551 mole) was slowly added. The mixture was stirred for an additional 4 h after which all volatiles were removed by evaporation. The residue was taken up in 100 ml water, which was three times extracted with 50 ml dichloromethane. The organic layer was dried with sodium sulfate and evaporated to dryness. A yield of solid crystals of N-acetyl-(S)-phenylalanine methyl ester as high as 99.5% was reached (104.1 g, 0.471 mole). The purity was analysed using NMR analysis[15]: ^{1}H NMR (300.2 MHz, CDCl$_3$, TMS): δ1.93 (s, 3H), 3.06 (m, 2H), 3.67 (s, 3H), 4.84 (q, 1H), 6.66 (d, 1H), 7.18 (m, 5H).
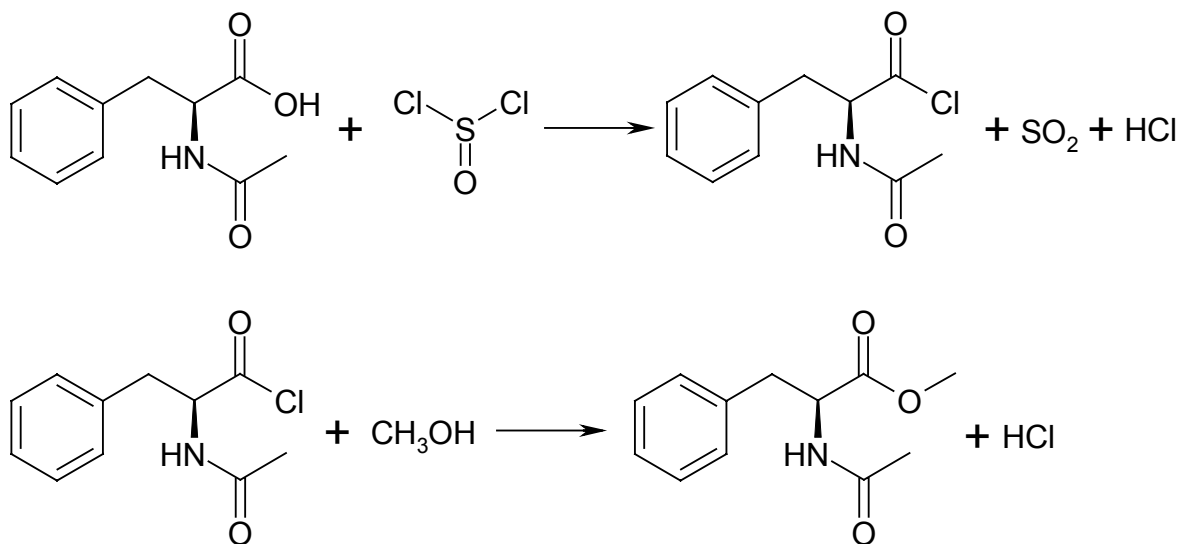
Figure 4.7: Preparation of N-acetyl-(S)-phenylalanine methyl ester[13]

4.2.4 Preparation of (-)-1,2-bis((2R,5R)-2,5-dimethylphospholano)benzene(cycloocta-diene)rhodium(I) tetrafluoroborate

The Rh-MeDuPHOS catalyst was prepared with a purity of over 99.0 % as previously described[1]. The starting material (2R,5R)-dihydroxyhexane was converted to the corresponding cyclic sulfate by reaction with thionyl chloride followed by oxidation. The cyclic sulfate was isolated with a yield of 90% as colorless crystalline solid by precipitation out of hexane. Thereafter the cyclic sulfate was subjected to treatment with 1,2-(diphosphino)benzene at room temperature, yielding the ligand 1,2-bis-((2R,5R)-

dimethylphospholano)benzene. The ligand was purified by recrystallization in hexane. Finally the catalyst precursor [(cyclo-octadiene)$_2$Rh]$^+$BF$_4^-$ was reacted with the ligand in tetrahydofuran as solvent at room temperature, yielding the catalyst complex (-)-1,2-bis((2R,5R)-2,5-dimethylphospholano)benzene(cyclooctadiene)rhodium(I) tetrafluoroborate. The total synthesis of the catalyst complex is shown in figure 4.8.
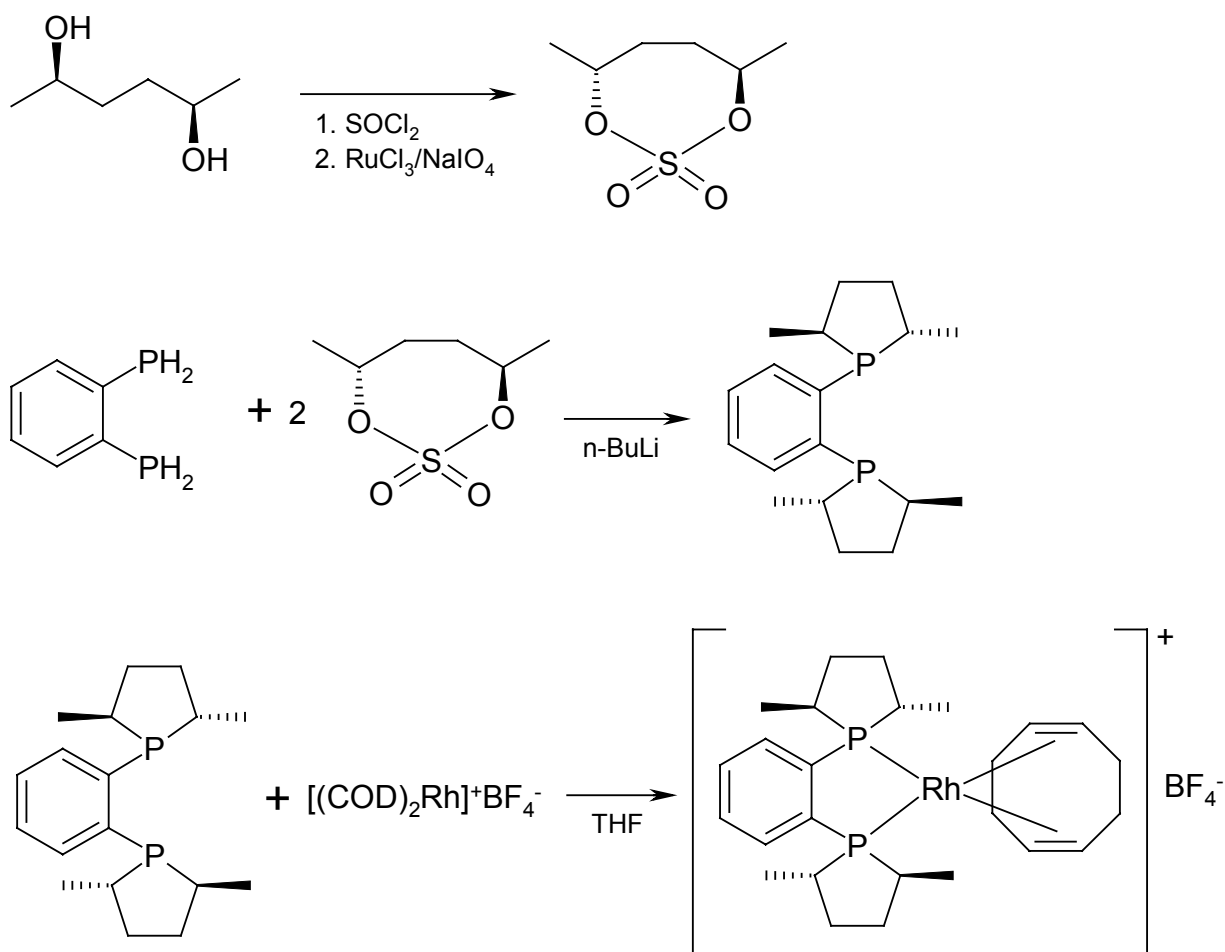
Figure 4.8: Synthesis of the Rh-MeDuPHOS catalyst[1]

4.3 Phase behavior of the ionic liquid + carbon dioxide system

In order to find the conditions for carrying out the model reaction (homogeneous system) and separation (biphasic system), the phase behavior of the model system is investigated. First, the phase behavior of the binary system consisting of supercritical carbon dioxide and the ionic liquid 1-butyl-3-methylimidazolium tetrafluoroborate is discussed experimentally in this paragraph[16] and compared to other ionic liquid + carbon dioxide phase behavior data in literature[17-30]. Thereafter, in the next paragraph the influences of the reactants, product and catalyst on this phase behavior are measured and operation conditions are determined[31].

4.3.1 Experimental

The measurement of the phase behavior of the [bmim][BF$_4$] + carbon dioxide system involves bubble point pressure measurements at different temperatures and compositions. The solubility of carbon dioxide in [bmim][BF$_4$] at the lower end of the concentrations ($x_{CO2} \leq 0.4825$) was determined using the Cailletet apparatus. The Cailletet equipment allows measurement of phase equilibria within a pressure range from 0.1 – 15 MPa and temperatures from 255 – 470 K, depending on the heat-transferring fluid used. The solubility of carbon dioxide in [bmim][BF$_4$] at the higher end of the concentrations ($x_{CO2} > 0.4825$) was determined in a windowed autoclave, because of the higher equilibrium pressures (higher than the 15 MPa pressure limit of the Cailletet apparatus). The windowed autoclave allows measurement of phase equilibria at pressures from 0.2 – 100 MPa and temperatures from 240 – 360 K. On the front cover of this chapter a picture of the Cailletet apparatus is shown. The windowed autoclave equipment is shown in figure 4.9.

Figure 4.9: The windowed autoclave equipment

Both the Cailletet apparatus and the windowed autoclave work according to the same operation principle: at any desired temperature, the pressure is varied for a sample of constant overall composition until a phase change is observed visually. The essential part of both pieces of equipment is a Pyrex glass tube, which serves as equilibrium cell. For the Cailletet apparatus, this glass tube is called Cailletet tube (see figure 4.10). The difference between the Cailletet apparatus and the windowed autoclave is the type of pressure containment. For the Cailletet apparatus the glass tube itself is the high-pressure vessel. In case of windowed autoclaves, the glass vessel is contained in the autoclave from stainless steel and surrounded by pressurized water.

Figure 4.10: The Cailletet tube

Figure 4.11 gives a schematic representation of the Cailletet apparatus. A sample with fixed composition is resided in the top of the Cailletet tube and sealed by a mercury column. The pressure is generated by pressing hydraulic oil into the system with a screw type hand pump, which causes the level of the mercury column in the capillary tube to rise and to create the desired pressure in the top. A dead-weight pressure gauge is used to measure the pressure. The temperature of the sample is kept constant by circulating thermostat liquid through a thermostat jacket surrounding the Cailletet tube. The temperature is measured with a platinum resistance thermometer in the heat jacket near the top of the sample tube. Homogeneous mixing of the sample is realized by moving a steel ball with two moving magnets.

1: Thermometer	7: Tripod	13: Raw pressure gauge
2: Magnetic stirrer	8: Thermostat fluid overflow	14: Handle to in- or decrease
3: Cailletet tube	9: Thermostat fluid outlet	pressure
4: Thermostat jacket	10: Metal stirring ball	15: Metal weights of different sizes
5: Rubber seal	11: Thermostat fluid inlet	16: Spinning metal stick with exactly
6: Metal casing	12: Mercury overflow	known cross section area
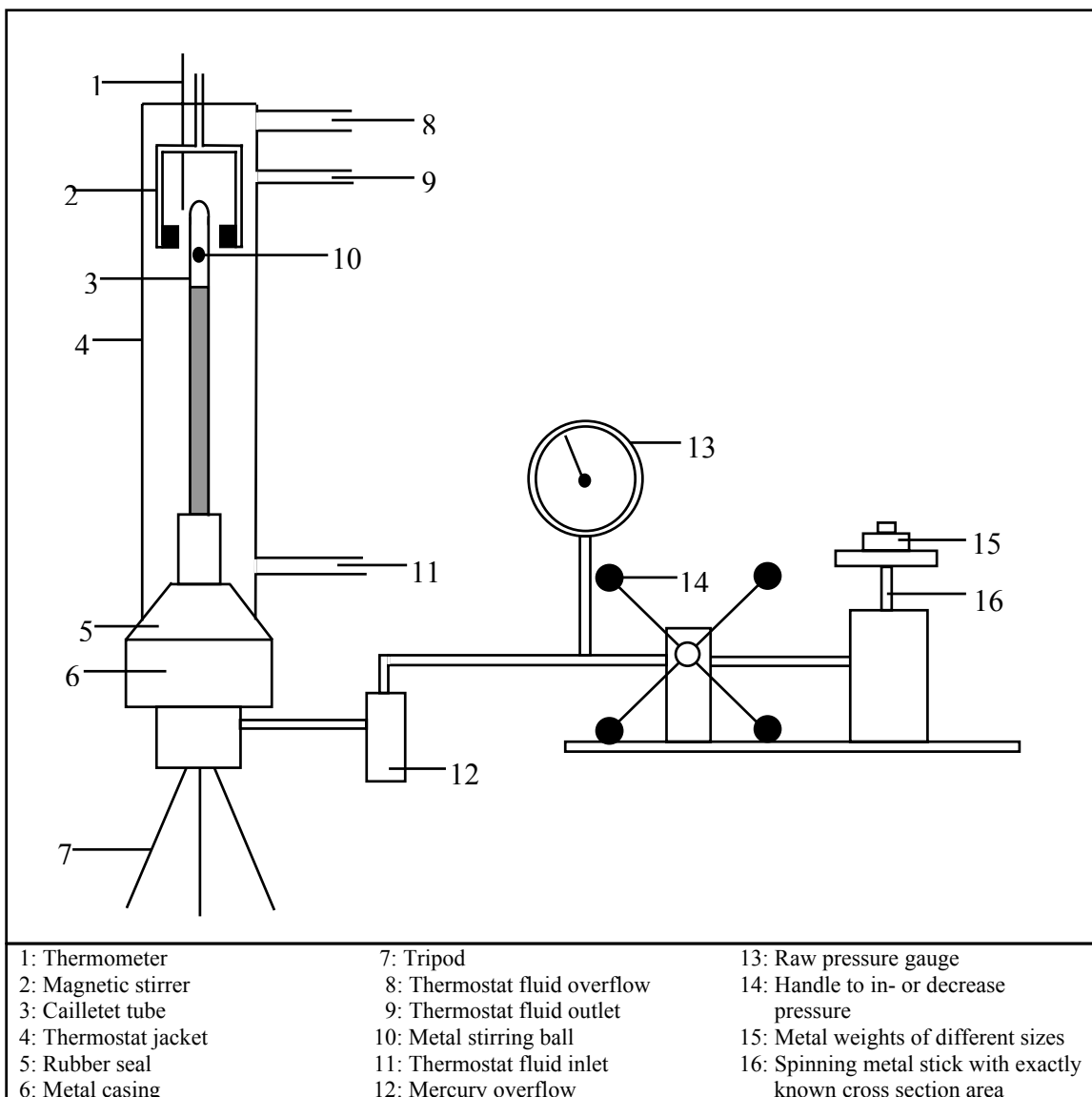
Figure 4.11: Schematic representation of the Cailletet apparatus

The temperature measurements in the Cailletet apparatus have an uncertainty of 0.01 K, which is the error in the reading of the thermometer. The temperature measurements in the windowed autoclave have an uncertainty of ±0.05 K, due to the temperature fluctuations in the water bath. The uncertainty of the pressure measurements is ±0.0025 MPa for the Cailletet apparatus and ±0.04% for the windowed autoclave.

The samples were prepared according to the synthetic method: First a well-defined amount of ionic liquid was put into the tube. Thereafter the capillary tube was connected to a vessel with calibrated volume in a gas-rack (see figure 4.12). This vessel can be filled with gas from a gas reservoir (CO_2) or may be evacuated (vacuum pump). After de-

aeration of the ionic liquid, mercury is used to seal the carbon dioxide in the calibrated volume vessel and to press the carbon dioxide and mercury into the capillary tube. The amount of moles of carbon dioxide in the calibrated vessel can be calculated from an appropriate p-V-T relation (ideal gas law). The uncertainty in compositions of the samples is ±0.005 in mole fraction.

Section I:	This section is used to refill the amount of mercury in the filling equipment.
Section II:	The Cailletet or autoclave tubes are attached to this part during the filling.
Section III:	Vacuum measuring device (top of the picture).
Section IV & V:	Pressure measuring by reading the difference between atmospheric pressure and the system pressure in mm mercury.
Section VI:	Gas dosing part: four different connections connected to four different gasses.
Section VII:	High-pressure nitrogen mostly used to push the mercury into the tube.
Section VIII:	Main vacuum pump.

Figure 4.12: Schematic representation of the gas-rack

The measurement of phase equilibria with both the Cailletet apparatus and the windowed autoclave is based on visual observation of the phases and their transitions. The temperature is kept constant at a certain value and the pressure is adjusted until it reaches the equilibrium value. For measuring the solubility of carbon dioxide in ionic liquids, this means that one increases the pressure in the vapor/liquid system until the last bubble of vapor disappears (bubble point measurement).

4.3.2 Results and discussion

The solubility of carbon dioxide in 1-butyl-3-methylimidazolium tetrafluoroborate was measured using the Cailletet apparatus and the windowed autoclave. This solubility is dependent on temperature and pressure. For systems with a fixed composition of carbon dioxide and ionic liquid, the bubble point pressures were measured as a function of temperature. The results are shown in figure 4.13.
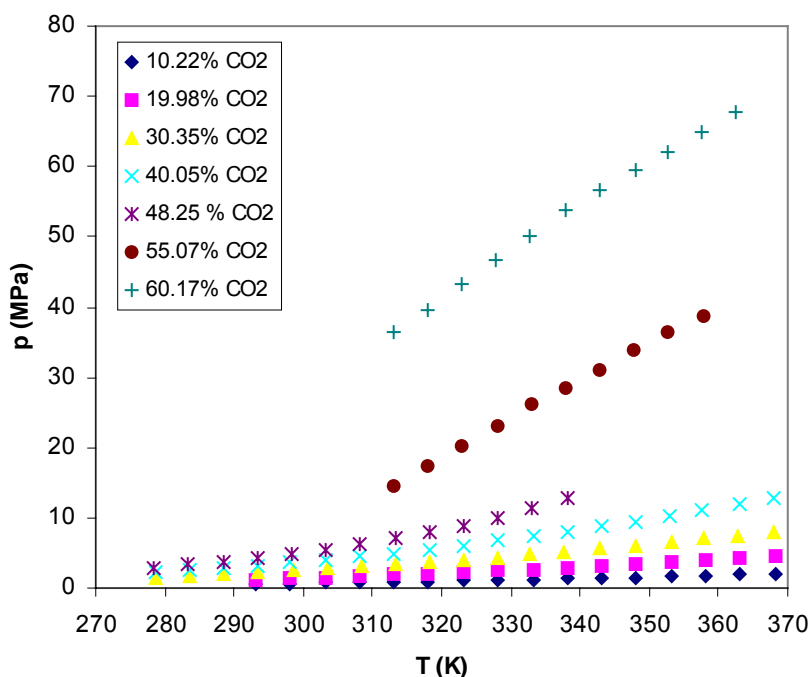
Figure 4.13: Experimentally determined isopleths for several concentrations of carbon dioxide (mole%) in the CO_2 + [bmim][BF$_4$] system

From figure 4.13, it is clear that bubble-point pressures increase when higher temperatures are used at fixed compositions. This means that the solubility of carbon dioxide in the ionic liquid decreases at higher temperatures. This is mostly the common trend for the solubility of gases in liquids.

When the mole fraction of carbon dioxide is increased isothermally, the bubble point pressures increase dramatically. This can be seen from a *p-x* diagram in which the bubble point pressure is plotted against the mole fraction of carbon dioxide at fixed temperature. Figure 4.14 shows the phase behavior of CO_2 + [bmim][BF$_4$] at 320 K and 330 K. From this figure it can also be noticed that the solubility of carbon dioxide in the ionic liquid decreases with an isobaric increase in temperature and the effect of temperature on the carbon dioxide solubility is larger at higher mole fractions of carbon dioxide.
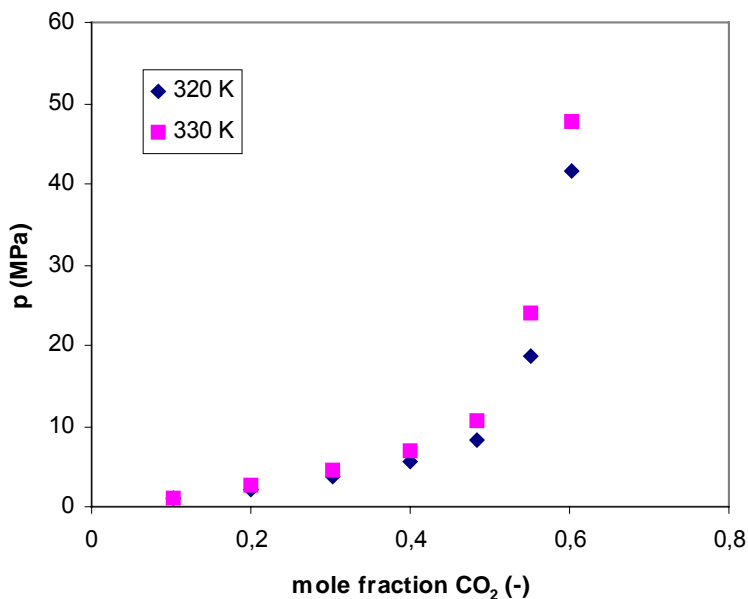
Figure 4.14: Isotherms at 320 K and 330 K of the system CO_2 + [bmim][BF_4]

The phase behavior of the system CO_2 + [bmim][BF_4] is unusual: carbon dioxide dissolves well in 1-butyl-3-methylimidazolium tetrafluoroborate at lower pressures, while the bubble point pressures sharply increase at high mole fractions of carbon dioxide. A system, in which large amounts of carbon dioxide dissolve in the liquid phase at low pressures, should generally have a simple two-phase envelope with a mixture critical point at moderate pressures[17]. However, instead of having a critical point at moderate pressures, its two-phase boundary extends almost vertically to very high pressures. This remarkable behavior has been noticed more often for carbon dioxide + ionic liquid systems[18-30]. Shariati *et al.*[29] concluded that these carbon dioxide + ionic liquid systems show Type-III fluid phase behavior according to the classification of Scott and Van Konynenburg[32,33]. They discovered the occurrence of a three-phase locus L_1L_2V close to the location of the LV line of pure carbon dioxide, and a critical endpoint of the nature $(L_1=V) + L_2$ close to the critical point of pure carbon dioxide. According to the classification of fluid-phase behavior of Scott and Van Konynenburg, this system could have Type III, Type IV, or Type V fluid-phase behavior. However, because no binary CO_2 systems are known to show Type V behavior in the literature, and because the occurrence of a Type IV system is rare, the system binary ionic liquid + carbon dioxide most likely has Type III fluid-phase behavior.
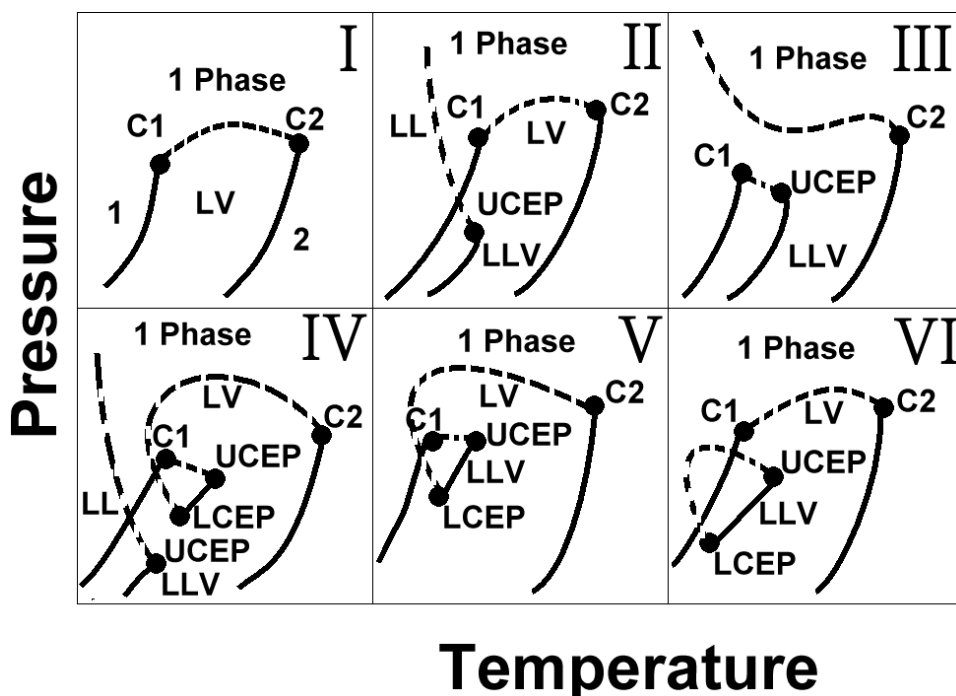
Figure 4.15: Classification of the liquid-vapor phase behavior of binary systems according to Scott and Van Konynenburg[34]. C = critical point; L = liquid; V = vapor; UCEP = upper critical end point; LCEP = lower critical end point.

The remarkable phase behavior of ionic liquid + carbon dioxide systems has been related to the large difference in polarity between the highly polar ionic liquid and the less polar carbon dioxide (carbon dioxide has no dipole moment, only a quadrupole moment). Generally, binary mixtures of solvents and volatile components with same high polarity have critical lines at much lower temperatures and pressures due to the stronger molecular interactions compared to binary systems of the same solvent with a less polar volatile molecule[35]. For example, when the strongly polar fluoroform (with a dipole moment of 1.65 $D^{[36]}$) instead of carbon dioxide is used as volatile compound in combination with ionic liquid, the system indeed shows the expected closed phase envelope, including the occurrence of a critical point, as a result of the stronger molecular interactions between fluoroform and ionic liquid[37].

The phase behavior of the binary system [bmim][BF_4] + CO_2 is compared to previously measured phase behavior data of other ionic liquid + carbon dioxide systems. Figure 4.16 compares the p-x diagram at 330 K of the system [bmim][BF_4] + CO_2 with the systems 1-hexyl-3-methylimidazolium tetrafluoroborate ([hmim][BF_4]) + CO_2[28] and 1-methyl-3-octylimidazolium tetrafluoroborate ([omim][BF_4]) + CO_2[30] in order to investigate the effect of the alkyl chain length of the cation. From figure 4.16 it can be concluded that a larger alkyl group leads to lower bubble point pressures and, therefore, to higher solubilities of carbon dioxide in the imidazolium-based ionic liquid. The higher solubility

of carbon dioxide in ionic liquids with larger alkyl groups can be related to their lower polarity and their lower density as a result of the bulkier alkyl groups.
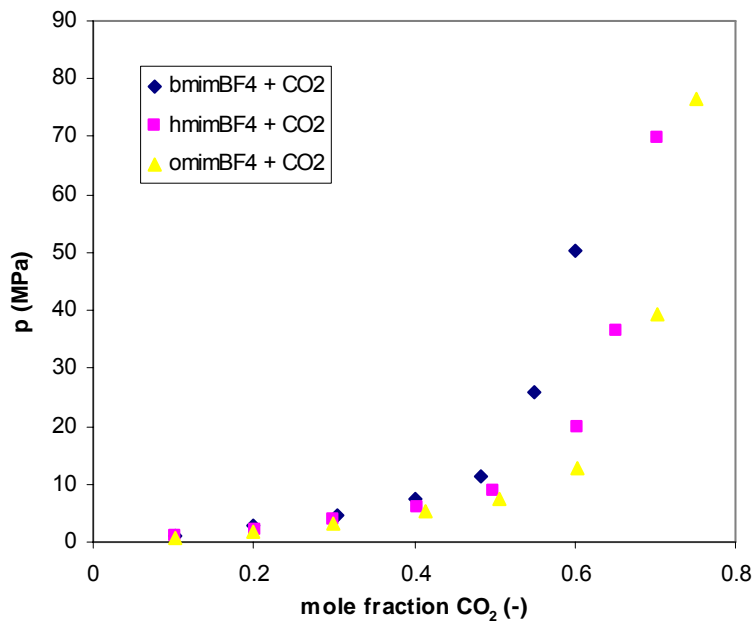
Figure 4.16: Comparison of the isotherms at 330 K for the binary systems [bmim][BF$_4$] + CO$_2$, [hmim][BF$_4$] + CO$_2$[28] and [omim][BF$_4$] + CO$_2$[30]

4.4 Phase behavior of the model system

After measuring the phase behavior of the binary ionic liquid + carbon dioxide system, the effects of the reactants, product and catalyst on this phase behavior were determined[31,38-40].

4.4.1 Effect of methyl (Z)-α-acetamidocinnamate on the ionic liquid/carbon dioxide system

The effect of the reactant methyl (Z)-α-acetamidocinnamate (MAAC) on the ionic liquid + carbon dioxide system was measured with the Cailletet apparatus[38]. Therefore, solutions of MAAC in ionic liquid in different concentrations were prepared and put into the Cailletet tube. The highest concentration used was 5.8 mole% of MAAC in ionic liquid (72.5 g/l), because this is the maximum solubility at room temperature and atmospheric pressure[38]. The carbon dioxide was added using the gas-rack and the new bubble point pressures were measured. The results of the effect of MAAC on the ionic liquid/carbon dioxide system are plotted in figures 4.17 to 4.19.
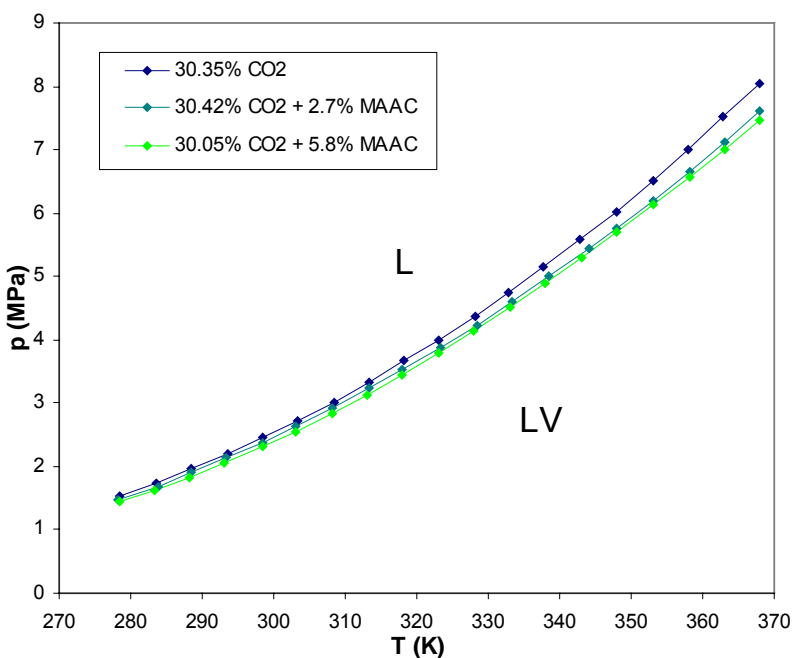
Figure 4.17: Experimentally determined isopleths for several concentrations of MAAC (mole%) in the system CO_2 + [bmim][BF_4] (30/70 mole%) + MAAC[38]
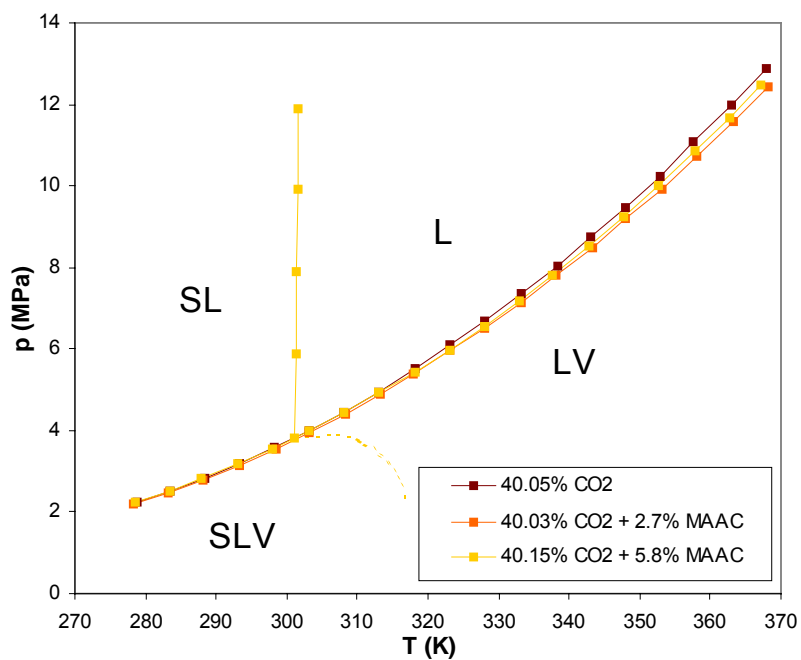
Figure 4.18: Experimentally determined isopleths for several concentrations of MAAC (mole%) in the system CO_2 + [bmim][BF_4] (40/60 mole%) + MAAC (dotted line is not measured)[38]
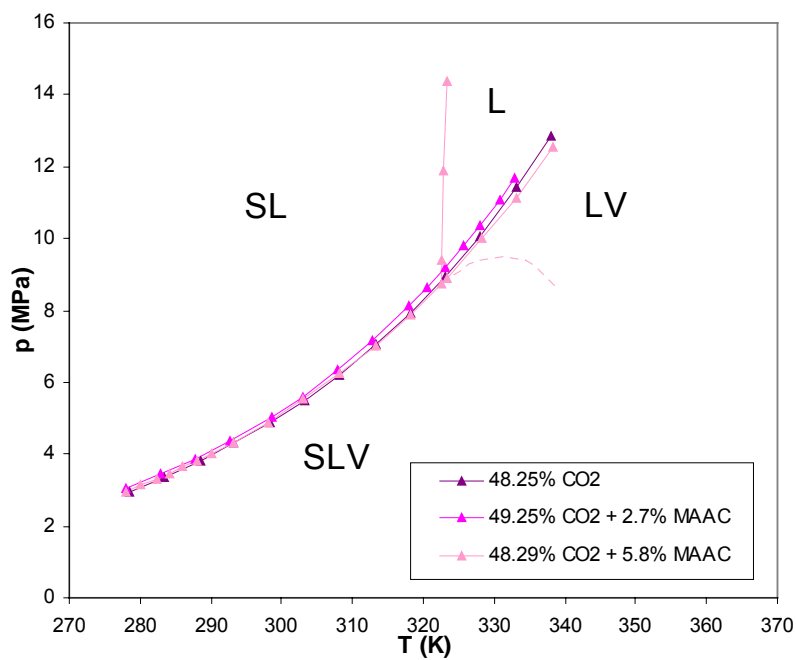
Figure 4.19: Experimentally determined isopleths for several concentrations of MAAC (mole%) in the system CO_2 + [bmim][BF_4] (50/50 mole%) + MAAC (dotted line is not measured)[38]

From figures 4.17 to 4.19 it can be concluded that carbon dioxide at low concentrations slightly works as co-solvent, since the equilibrium pressures of the ternary system with MAAC are lower than the equilibrium pressures in the binary system (see figure 4.17). Therefore, at low carbon dioxide concentrations, the solubility of MAAC in the ionic liquid/carbon dioxide system is higher than the solubility of MAAC in pure ionic liquid (adding carbon dioxide increases the solubility of the reactant in ionic liquid). However, it can immediately be seen that carbon dioxide at high concentrations starts to work as anti-solvent (figures 4.18 and 4.19). The MAAC precipitates out at low temperatures and high concentrations of carbon dioxide, because at high carbon dioxide concentrations the solubility of MAAC in the ionic liquid/carbon dioxide system is lower than the solubility of MAAC in pure ionic liquid. This is in agreement with the theoretical results from chapter 3, where a homogeneous phase could be reached at lower carbon dioxide concentrations, but where two phases (ionic liquid phase and organic reactant phase) were present at high carbon dioxide concentrations.

4.4.2. Effect of hydrogen on the ionic liquid/carbon dioxide system

The effect of the reactant hydrogen on the ionic liquid + carbon dioxide system was measured in the windowed autoclave equipment by V. A. Toussaint[39]. The bubble point pressures of the ternary ionic liquid + carbon dioxide + hydrogen system are plotted in figure 4.20 and compared to the binary ionic liquid + carbon dioxide system and the binary ionic liquid + hydrogen system.
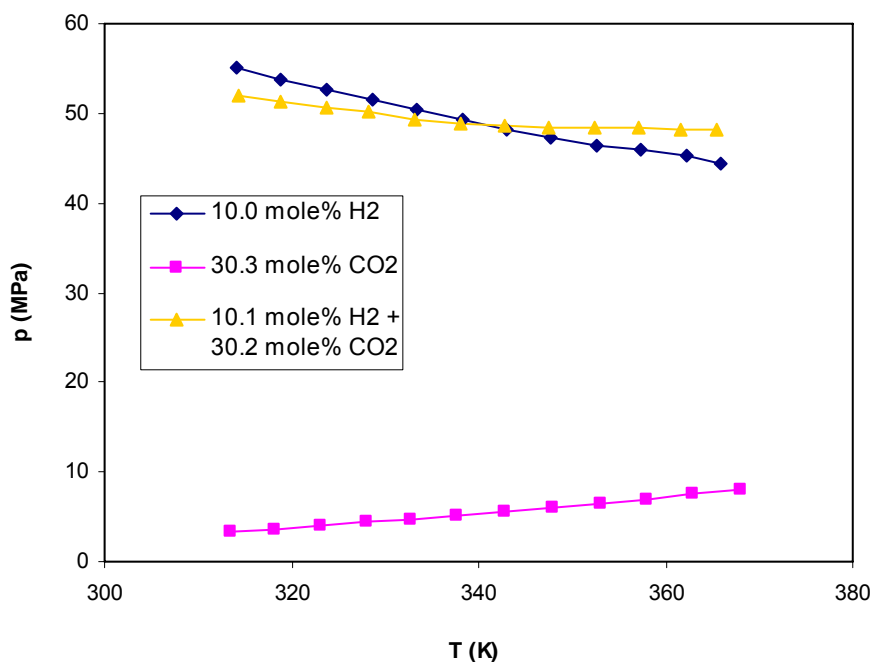
Figure 4.20: Experimentally determined isopleths of the systems: a) CO_2 + [bmim][BF$_4$]; b) H_2 + [bmim][BF$_4$]; c) CO_2 + H_2 + [bmim][BF$_4$][39]

From figure 4.20 it can be seen that hydrogen has a completely different solubility behavior in ionic liquid compared to carbon dioxide. The solubility of hydrogen is much lower and increases with increasing temperature, whereas the solubility of carbon dioxide is high but decreases with increasing temperature. Moreover, the effect of hydrogen on the ionic liquid + carbon dioxide system is interesting: it can be noticed that carbon dioxide works as co-solvent at low temperatures, since the bubble point pressures of the ionic liquid + hydrogen system are reduced in the presence of carbon dioxide. Thus, at low temperatures, adding carbon dioxide increases the solubility of hydrogen in the ionic liquid. However, at high temperatures, the carbon dioxide works as anti-solvent, because in this regime the solubility of hydrogen in the ionic liquid + carbon dioxide system is lower than the solubility of hydrogen in pure ionic liquid. Again, a two-regime system where carbon dioxide either works as co-solvent (where the homogeneous system can be reached) or as anti-solvent is found.

Pressing hydrogen into the [bmim][BF_4] ionic liquid requires high pressures. If one wants to reach a homogeneous phase of all components of the model system (with 10 mole% of the hydrogen reactant), pressures as high as 50 MPa are needed for carrying out the model reaction at room temperature. The presence of carbon dioxide increases the hydrogen solubility in ionic liquid and lowers the necessary pressure for reaching the homogeneous phase with 5 MPa. It was also found that the presence of the catalyst increases the hydrogen solubility in the ionic liquid, resulting in a further decrease in pressure needed (~ 4 MPa, see figure 4.21)[39]. This could be expected, since the catalyst is a hydrogenation catalyst that forms complexes with hydrogen. Therefore, the catalyst attracts the hydrogen into the ionic liquid phase.
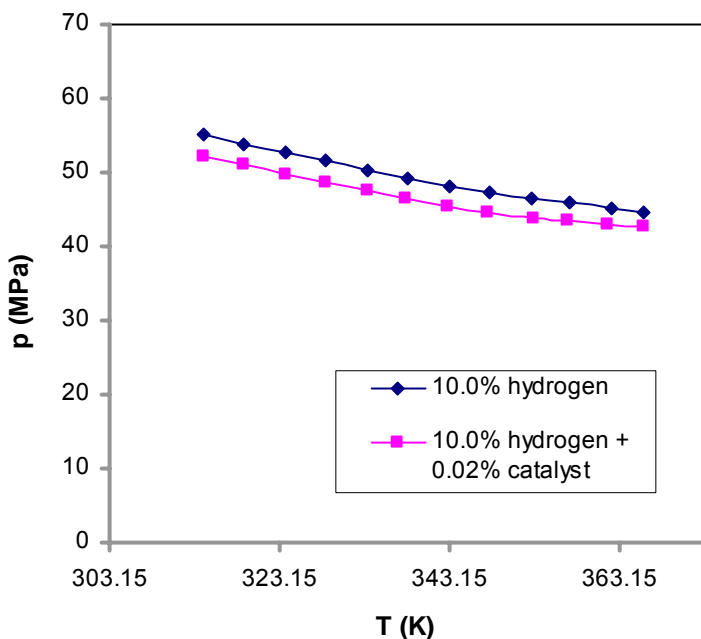
Figure 4.21: Experimentally determined isopleths for the effect of catalyst on hydrogen solubility in the system [bmim][BF_4] + H_2 (90:10 mole%)[39]

However, even when carbon dioxide and catalyst are added, the pressure for reaching a homogeneous phase is still high, resulting in high costs for equipment and pressurization. Two options for carrying out the reaction at lower pressures are suggested. Firstly, the reaction can be carried out in a homogeneous system at lower pressures when the hydrogen concentration is reduced (see figure 4.22), but this unfortunately leads to lower reaction rates. Secondly, instead of reaching a homogeneous system (which unfortunately required too high pressures for the model system) the reaction can be carried out in a heterogeneous system, where all components except hydrogen are fully dissolved in the ionic liquid, which also results in a lower reaction rate.
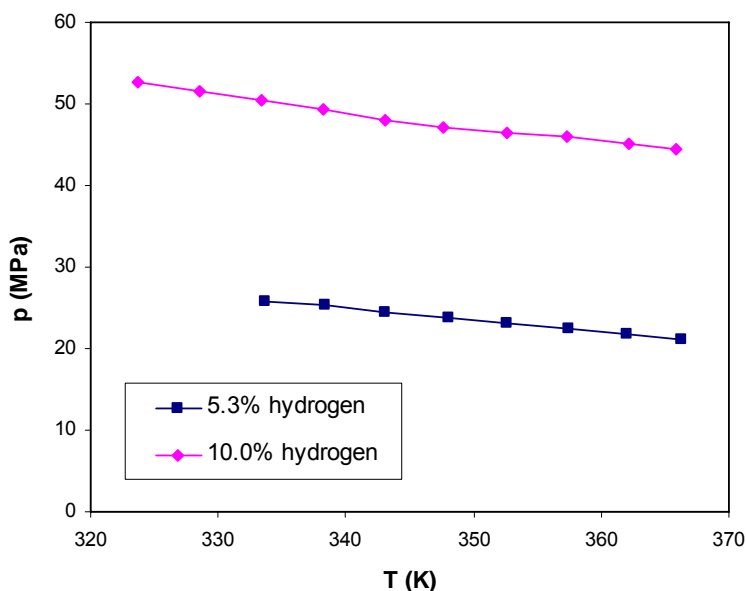
Figure 4.22: Experimentally determined isopleths for several concentrations of hydrogen (mole%) in the hydrogen + [bmim][BF$_4$] system[39]

4.4.3 Effect of N-acetyl-(S)-phenylalanine methyl ester on the ionic liquid/carbon dioxide system

Finally, the effect of the product N-acetyl-(S)-phenylalanine methyl ester (APAM) on the ionic liquid + carbon dioxide system was measured with the Cailletet apparatus[38]. The results of the effect of APAM on the ionic liquid + carbon dioxide system are plotted in figure 4.23. From this figure it can be seen that the effect of N-acetyl-(S)-phenylalanine methyl ester on the ionic liquid/carbon dioxide system is only very small. Carbon dioxide has almost no influence on the solubility of APAM in the ionic liquid at measured concentrations. It was also found that the solubility of APAM in pure ionic liquid at room temperature and atmospheric pressure is very high (36 mole% of APAM in ionic liquid = 667 g/l), so APAM will always be miscible with ionic liquid, and never be the limiting factor in finding the homogeneous phase.
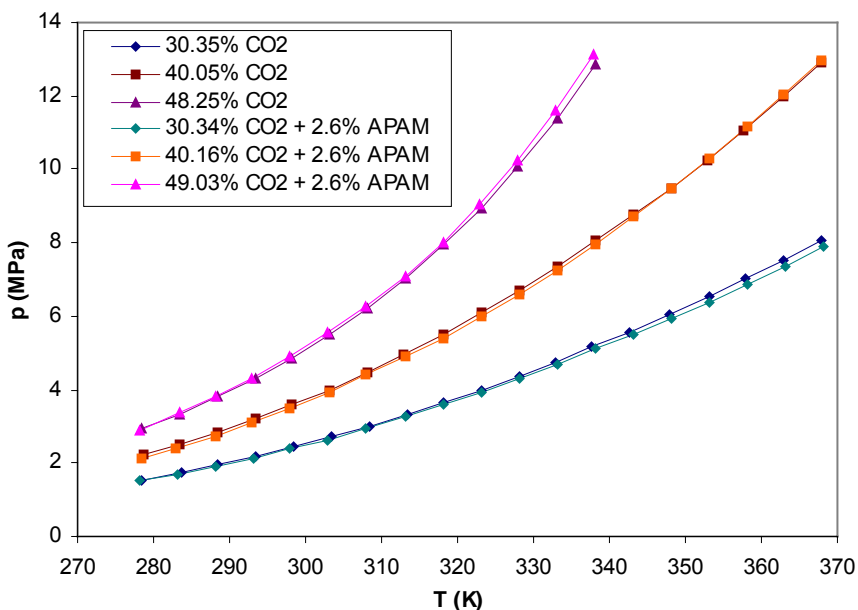
Figure 4.23: Experimentally determined isopleths for several concentrations of carbon dioxide (mole%) in the system CO_2 + [bmim][BF_4] + APAM

4.4.4 Operation conditions of the model system

The idea is to carry out the reaction in the homogeneous regime. The low solubility of hydrogen in the ionic liquid 1-butyl-3-methylimidazolium tetrafluoroborate is the limiting factor in reaching a homogeneous phase. Adding carbon dioxide and catalyst enhances the solubility of hydrogen in ionic liquid, as long as the temperature is below 340 K (see figure 4.20). At this temperature, the pressure required to dissolve the reactant methyl (Z)-α-acetamidocinnamate using carbon dioxide as co-solvent (carbon dioxide increases the reactant solubility in the low concentration regime (< 30 mole%)) is only 5 MPa (see figure 4.17). However, the pressure required to dissolve all hydrogen (substrate concentration of 10 mole%) in the ionic liquid phase is as high as 50 MPa. Due to equipment limitations, it was chosen to carry out the reaction at lower pressures. This can be done either by decreasing the hydrogen concentration, or by decreasing the overall pressure, resulting in a heterogeneous system in which all components except hydrogen are fully dissolved in the ionic liquid. Because the experiments described in chapter 3 were carried out at a later point in time than the results from this chapter (there was no proof of reaching a homogeneous phase in all ternary ionic liquid + carbon dioxide + organic reactant systems yet), the choice for the second option was made in this thesis. At room temperature and 5 MPa, the reactant MAAC, the catalyst and the co-solvent carbon dioxide were completely dissolved in the ionic liquid (where the homogeneously catalyzed reaction took place), but the reactant hydrogen was only partly dissolved. In later research ionic liquids showing higher hydrogen solubility were found, such as the 1-

ethyl-3-methylimidazolium bis(trifluoromethylsulfonyl)imide ionic liquid[40]. Using this ionic liquid, the homogeneous phase for carrying out the model reaction could indeed be reached at reasonable pressures[40].

The separation step is carried out in the biphasic system, where the carbon dioxide and the product are only partly dissolved in the ionic liquid phase. Therefore, higher concentrations of carbon dioxide are necessary. However, at higher concentrations (> 50 mole%), carbon dioxide works as anti-solvent at low temperatures and pressures (see figure 4.19). But for the separation of the product from the ionic liquid, the carbon dioxide should act as co-solvent that can dissolve the product and recover it from the ionic liquid phase. Therefore, higher temperatures (>320 K) and pressures (>8 MPa) are required for the separation (see figure 4.19). The occurrence of the miscibility windows phenomenon between reaction and separation conditions is the result of the change in the carbon dioxide concentration.

4.5 References

1. Burk, M. J.; Feaster, J. E.; Nugent, W. A.; Harlow, R. L.; Preparation and Use of C2-Symmetric Bis(phospholanes): Production of α-Amino Acid Derivatives via Highly Enantioselective Hydrogenation Reactions, *J. Am. Chem. Soc.* **1993**, *115 (22)*, 10125-10138.
2. Van Den Berg, M.; Minnaard, A. J.; Haak, R. M.; Leeman, M.; Schudde, E. P.; Meetsma, A.; Feringa, B. L.; De Vries, A. H. M.; Maljaars, C. E. P.; Willans, C. E.; Hyett, D.; Boogers, J. A. F.; Henderickx, H. J. W.; De Vries, J. G.; Monodentate Phosphoramidites: A Breakthrough in Rhodium-Catalyzed Asymmetric Hydrogenation of Olefins, *Adv. Synth. Catal.* **2003**, *345 (1-2)*, 308-323.
3. Blaser, H. U.; Heterogeneous Catalysis for Fine Chemicals Production, *Catal. Today* **2000**, *60 (3-4)*, 161-165.
4. De Rege, F. M.; Morita, D. K.; Ott, K. C.; Tumas, W.; Broene, R. D.; Non-Covalent Immobilization of Homogeneous Cationic Chiral Rhodium-Phosphine Catalysts on Silica Surfaces, *Chem. Commun.* **2000**, *(18)*, 1797-1798.
5. Guernik, S.; Wolfson, A.; Herskowitz, M.; Greenspoon, N.; Geresh, S.; A Novel System Consisting of Rh-DuPHOS and Ionic Liquid for Asymmetric Hydrogenations, *Chem. Commun.* **2001**, *(22)*, 2314-2315.
6. Berger, A.; De Souza, R. F.; Delgado, M. R.; Dupont, J.; Ionic Liquid-Phase Asymmetric Catalytic Hydrogenation: Hydrogen Concentration Effects on Enantioselectivity, *Tetrahedron Asymm.* **2001**, *12 (13)*, 1825-1828.
7. Lee, S.; Zhang, Y. J.; Piao, J. Y.; Yoon, H.; Song, C. E.; Choi, J. H.; Hong, J.; Catalytic Asymmetric Hydrogenation in a Room Temperature Ionic Liquid Using Chiral Rh-Complex of Ionic Liquid Grafted 1,4-Bisphosphine Ligand, *Chem. Commun.* **2003**, *(20)*, 2624-2625.
8. Wasserscheid, P.; Welton, T., Eds. *Ionic Liquids in Synthesis*; Wiley-VHC Verlag: Weinheim, Germany, 2003.
9. Dyson, P. J.; Laurenczy, G.; Ohlin, A.; Vallance, J.; Welton, T.; Determination of Hydrogen Concentration in Ionic Liquids and the Effect (or Lack of) on Rates of Hydrogenation, *Chem. Commun.* **2003**, *(19)*, 2418-2419.
10. Van Den Broeke, J.; *Highly Fluorous Tetraarylborate Anions; Versatile Counterions for Homogeneous Catalysis in Novel Reaction Media*, University of Utrecht: Utrecht, The Netherlands, 2001.
11. Jessop, P. G.; Ikariya, T.; Noyori, R.; Homogeneous Catalysis in Supercritical Fluids, *Chem. Rev.* **1999**, *99 (2)*, 475-494.
12. Huddleston, J. G.; Willauer, H. D.; Swatloski, R. P.; Visser, A. E.; Rogers, R. D.; Room Temperature Ionic Liquids as Novel Media for Clean Liquid-Liquid Extraction, *Chem. Commun.* **1998**, *(16)*, 1765-1766.
13. Gladiali, S.; Pinna, L.; Asymmetric Hydroformylation of N-Acyl-1-aminoacrylic Acid Derivatives by Rhodium/Chiral Diphosphine Catalysts, *Tetrahedron Asymm.* **1991**, *2 (7)*, 623-632.

14. Smallridge, A. J.; Trewhella, M. A.; Wang, Z.; The Enzyme-Catalyzed Stereoselective Transesterification of Phenylalanine Derivatives in Supercritical Carbon Dioxide, *Aust. J. Chem.* **2002**, *55 (4)*, 259-262.

15. Glaser, R.; Geresh, S.; Twaik, M.; Benoiton, N. L.; Structural Requirements in Chiral Diphosphine-Rhodium Complexes-XII: Asymmetric Homogeneous Hydrogenation of Z-α-N-Methylacetamidocinnamic Acid and Methyl Ester Catalyzed by Rhodium(I) Complexes of DIOP and its Carbocyclic Analogues, *Tetrahedron* **1978**, *34 (24)*, 3617-3621.

16. Kroon, M. C.; Shariati, A.; Costantini, M.; Van Spronsen, J.; Witkamp, G. J.; Sheldon, R. A.; Peters, C. J.; High-Pressure Phase Behavior of Systems with Ionic Liquids: Part V. The Binary System Carbon Dioxide + 1-Butyl-3-methyl-imidazolium Tetrafluoroborate, *J. Chem. Eng. Data* **2005**, *50 (1)*, 173-176.

17. Blanchard, L. A.; Gu, Z.; Brennecke, J. F.; High-Pressure Phase Behavior of Ionic Liquid/CO_2 Systems, *J. Phys. Chem. B* **2001**, *105 (12)*, 2437-2444.

18. Anthony, J. L.; Anderson, J. L.; Maginn, E. J.; Brennecke, J. F.; Anion Effects on Gas Solubilities in Ionic Liquids, *J Phys. Chem. B* **2005**, *109 (13)*, 6366-6374.

19. Aki, S. N. V. K.; Mellein, B. R.; Saurer, E. M.; Brennecke, J. F.; High-Pressure Phase Behavior of Carbon Dioxide with Imidazolium-Based Ionic Liquids, *J. Phys. Chem. B* **2004**, *108 (52)*, 20355-20365.

20. Husson-Borg, P.; Majer, V.; Costa Gomes, M. F.; Solubilities of Oxygen and Carbon Dioxide in Butyl Methyl Imidazolium Tetrafluoroborate as a Function of Temperature and at Pressures Close to Atmospheric Pressure, *J. Chem. Eng. Data* **2003**, *48 (3)*, 480-485.

21. Kamps, A. P. S.; Tuma, D.; Xia, J.; Maurer, G.; Solubility of CO_2 in the Ionic Liquid [bmim][PF_6], *J. Chem. Eng. Data* **2003**, *48 (3)*, 746-749.

22. Camper, D.; Scovazzo, P.; Koval, C.; Noble, R.; Gas Solubilities in Room Temperature Ionic Liquids, *Ind. Eng. Chem. Res.* **2004**, *43 (12)*, 3049-3054.

23. Shiflett, M. B.; Yokozeki, A.; Solubilities and Diffusivities of Carbon Dioxide in Ionic Liquids: [bmim][PF_6] and [bmim][BF_4], *Ind. Eng. Chem. Res.* **2005**, *44 (12)*, 4453-4464.

24. Baltus, R. E.; Culbertson, B. H.; Dai, S.; Luo, H.; DePaoli, D. W.; Low-Pressure Solubility of Carbon Dioxide in Room-Temperature Ionic Liquids Measured with a Quartz Crystal Microbalance, *J. Phys. Chem. B* **2004**, *108 (2)*, 721-727.

25. Kim, Y. S.; Choi, W. Y.; Jang, J. H.; Yoo, K. P.; Lee, C. S.; Solubility Measurement and Prediction of Carbon Dioxide in Ionic Liquids, *Fluid Phase Equilib.* **2005**, *228-229*, 439-445.

26. Shariati, A.; Peters, C. J.; High-Pressure Phase Behavior of Systems with Ionic Liquids: II. The Binary System Carbon Dioxide + 1-Ethyl-3-methylimidazolium Hexafluorophosphate, *J. Supercrit. Fluids* **2004**, *29 (1-2)*, 43-48.

27. Shariati, A.; Peters, C. J.; High-Pressure Phase Behavior of Systems with Ionic Liquids: Part III. The Binary System Carbon Dioxide + 1-Hexyl-3-methyl-imidazolium Hexafluorophosphate, *J. Supercrit. Fluids* **2004**, *30 (2)*, 139-144.

28. Constantini, M.; Toussaint, V. A.; Shariati, A.; Peters, C. J.; Kikic, I.; High-Pressure Phase Behavior of Systems with Ionic Liquids: Part IV. Binary System

Carbon Dioxide + 1-Hexyl-3-methylimidazolium Tetrafluoroborate, *J. Chem Eng. Data*, **2005**, *50 (1)*, 52-55.

29. Shariati, A.; Gutkowski, K.; Peters, C. J.; Comparison of the Phase Behavior of Some Selected Binary Systems with Ionic Liquids, *AIChE J.* **2005**, *51 (5)*, 1532-1540.

30. Shariati, A.; Peters, C. J.; High-Pressure Phase Equilibria of Systems with Ionic Liquids, *J. Supercrit. Fluids* **2005**, *34 (2)*, 171-182.

31. Shariati, A.; Simons, C.; Sheldon, R. A.; Witkamp, G. J.; Peters, C. J.; Enantio-selective Catalytic Hydrogenation of Methyl α-acetamidocinnamate in [bmim][BF$_4$], submitted for publication to *Green Chem.* **2006**.

32. Scott, R. L.; Van Konynenburg, P. H.; Static Properties of Solutions: Van der Waals and Related Models for Hydrocarbon Mixtures, *Discuss. Faraday Soc.* **1970**, *49*, 87-97.

33. Van Konynenburg, P. H.; Scott, R. L.; Critical Lines and Phase Equilibriums in Binary Van der Waals Mixtures, *Phil. Trans. R. Chem. Soc. London, Series A* **1980**, *298 (1442)*, 495-540.

34. Prausnitz, J. M.; Lichtenthaler, R. N.; Gomes De Azevedo, E. *Molecular Thermodynamics of Fluid-Phase Equilibria*, 3rd ed.; Prentice Hall: Upper Saddle River (NJ), USA, 1999.

35. Levelt Sengers, J. M. H.; Solubility near the Solvent's Critical Point, *J. Supercrit. Fluids* **1991**, *4 (4)*, 215-222.

36. Lide, D. R., Ed. *Handbook of Chemistry and Physics*, 78th ed.; CRC Press: New York (NY), USA, 1997.

37. Shariati, A.; Peters, C. J.; High-Pressure Phase Behavior of Systems with Ionic Liquids: Measurements and Modeling of the Binary System Fluoroform + 1-Ethyl-3-methylimidazolium Hexafluorophosphate, *J. Supercrit. Fluids* **2003**, *25 (2)*, 109-117.

38. Kroon, M. C.; Toussaint, V. A.; Shariati, A.; Florusse, L. J.; Witkamp, G. J.; Peters, C. J.; Fluid Phase Equilibria of Ternary Systems with Ionic Liquids, Carbon Dioxide and Some Organic Compounds of Pharmaceutical Interest, to be submitted to *J. Chem. Eng. Data* **2006**.

39. Toussaint, V. A.; Florusse, L. J.; Peters, C. J.; High-Pressure Phase Behavior of Systems with Ionic Liquids. Part VI: Phase Behavior of Various Systems Selected from the Components Carbon Dioxide, Hydrogen, the Hydrogenation Catalyst ((R,R)-MeDuPHOS)Rh(COD)BF$_4$ and 1-Butyl-3-methylimidazolium Tetrafluoro-borate, to be submitted for publication to *Fluid Phase Equilibria* **2006**.

40. Schilderman, A. M.; Raeissi, S.; Peters, C. J.; Solubility of Carbon Dioxide in the Ionic Liquid 1-Ethyl-3-methylimidazolium Bis(trifluoromethylsulfonyl)imide, submitted for publication to *Fluid Phase Equilibria* **2006**.

5

Experimental Investigation of Reaction and Separation

5

Experimental Investigation of Reaction and Separation

The ionic liquid 1-butyl-3-methylimidazolium tetrafluoroborate is a good solvent for the asymmetric hydrogenation of methyl (Z)-α-acetamidocinnamate. Higher concentrations of hydrogen lead to higher conversions, but lower enantioselectivities. Adding carbon dioxide enhances the enantioselectivity, but it only enhances the conversion at low concentrations. When larger amounts of carbon dioxide are used, the conversion is decreased due to the dilution effect. The catalyst can be reused without losing its activity and selectivity. The product N-acetyl-(S)-phenylalanine methyl ester can be separated from the ionic liquid by using either carbon dioxide as co-solvent in extractions, or as anti-solvent in precipitations. For extraction of the product, the solubility of the product in carbon dioxide should be sufficiently high. This solubility is 1.78 g/kg at 12.0 MPa and 323 K, whereas the ionic liquid has a negligible solubility in carbon dioxide. Therefore, the extracted product does not contain any detectible amount of ionic liquid. The product can also be precipitated out of the ionic liquid phase using carbon dioxide. This effect is caused by the lower solubility of the product in ionic liquid/carbon dioxide mixtures compared to the solubility in the pure ionic liquid at atmospheric conditions (650 g/l). For example, the solubility of the product in ionic liquid + carbon dioxide (1:1.34 g/g) at 313 K and 18.0 MPa is only 162 g/l. After precipitation the formed crystals can be displaced using carbon dioxide to obtain a purer product.

5. Experimental Investigation of Reaction and Separation

5.1 The reaction

Ionic liquids have been used as solvents for homogeneously catalyzed chiral reactions, where the catalyst is immobilized in the ionic liquid phase[1-6]. The product is then extracted by another solvent, such as supercritical carbon dioxide, in which the ionic liquid and the catalyst do not dissolve[2-7]. The catalyst can easily be recycled without losing its activity, because ionic liquids stabilize the catalyst against oxidation[4].

In this paragraph, the homogeneously Rh-catalyzed asymmetric hydrogenation of methyl (*Z*)-α-acetamidocinnamate (MAAC) in the 1-butyl-3-methylimidazolium tetrafluoro-borate ([bmim][BF_4]) + carbon dioxide system is described, applying the conditions determined in the previous chapter (T = 298 K, p = 5 MPa, x_{CO2} < 30 mole%)[8]. The effects of temperature, pressure and concentrations of hydrogen and carbon dioxide on the reaction rate and enantioselectivity are investigated[8]. Finally, the recyclability of the catalyst is studied[8].

5.1.1 Experimental

The reaction experiments were carried out by A. Shariati and C. Simons in a 160 ml Parr autoclave at room temperature[8] (which is 293 K in The Netherlands). First, a solution of 20 g/l MAAC and 0.146 g/l Rh-MeDuPHOS catalyst in [bmim][BF_4] was prepared under nitrogen in a glove box. Next, 50 ml of this solution was transferred into the autoclave. The autoclave was then closed and the hydrogen and carbon dioxide were added until the desired pressure in the autoclave was reached. During 24 hours the reaction took place in the autoclave under continuous stirring (600 rpm). At the end of the reaction experiment, the remaining pressure was released and the ionic liquid solution was analyzed in order to determine the conversion and enantioselectivity. Therefore, a sample of the ionic liquid solution was extracted with methyl *tert*-butyl ether (MTBE), which dissolves both the reactant MAAC and the product N-acetyl-(*S*)-phenylalanine methyl ester (APAM), but is immiscible with the ionic liquid. The conversion of the extracted sample was determined with gas chromatography (Varian Chrompack CP-1301 GC column) and ^{1}H NMR analysis (Varian Unity, INOVA 300, Varian VXR-400 S). The enantiomeric excesses (ee%) of the samples were determined by chiral high performance liquid chromatography (chiral HPLC) using a Chiralcel OD column with 2-propanol/hexane (10:90) as eluent.

The uncertainty in temperature is ±2 K, which is due to temperature fluctuations in the building. The uncertainty of the pressure in the autoclave is ±0.1 MPa. The measured conversions and enantioselectivities have an uncertainty of ±0.5%.

5.1.2 Results and discussion

First, the homogeneously catalyzed chiral model reaction was carried out in the ionic liquid phase at room temperature without adding any carbon dioxide[8]. These results serve as a reference for investigating the effect of adding carbon dioxide on the conversion and enantioselectivity of the model reaction. The results are shown in table 5.1. It can be noticed that the conversion increases and the enantioselectivity decreases with increasing hydrogen pressure. This was expected, because an increased hydrogen pressure leads to a higher hydrogen concentration in the ionic liquid phase, and thus to higher reaction rates, whereas higher hydrogen concentrations also result in less controlled hydrogenation reactions, and thus to lower selectivities[2,3]. The homogeneous reaction in the ionic liquid phase had quite high conversion and enantioselectivity at 20 bar, comparable to the conventional reaction in methanol[9] (see paragraph 4.1 and table 5.2). However, at 5 bar, no conversion was detected[8]. This indicates the absence of sufficient hydrogen in the ionic liquid phase at low pressures.

Table 5.1: Asymmetric hydrogenation of MAAC in [bmim][BF$_4$], catalyzed by chiral Rh-catalyst (c_{MAAC} = 20 g/l, c_{cat} = 0.146 g/l) at room temperature (reaction time = 24 h)

Entry	Solvent	P_{H2} (bar)	P_{CO2} (bar)	Conv (%)	Ee (%)
1	[bmim][BF$_4$]	5	0	0	--
2	[bmim][BF$_4$]	20	0	94.2	91.9
3	[bmim][BF$_4$]	50	0	100	56.2

Table 5.2: Conventional asymmetric hydrogenation of MAAC in methanol, catalyzed by chiral Rh-catalyst (c_{MAAC} = 20 g/l, c_{cat} = 0.146 g/l) at room temperature (reaction time = 24 h)[8,9]

Entry	Solvent	P_{H2} (bar)	P_{CO2} (bar)	Conv (%)	Ee (%)
4	methanol	5	0	100	94.1
5	methanol	20	0	100	90.0
6	methanol	50	0	100	85.8

In order to study the effect of adding carbon dioxide on the conversion and enantioselectivity of the model reaction, carbon dioxide was added to the system at different pressures[8]. The results are shown in table 5.3. It was observed that at lower pressures of carbon dioxide and hydrogen (p_{H2} = 5 bar), the conversion increases. However, the conversion drops dramatically at higher carbon dioxide pressures. This is in agreement with the results from chapter 3 and 4, where carbon dioxide worked as co-solvent at lower concentrations (resulting in an increase in the solubility of hydrogen in the ionic liquid), whereas the carbon dioxide worked as anti-solvent at higher concentrations (in this regime the solubility of hydrogen in the ionic liquid + carbon dioxide system is lower than the solubility of hydrogen in pure ionic liquid). Another reason of the increase in reaction conversion at lower carbon dioxide concentrations is the decreased viscosity of the ionic liquid phase as a result of carbon dioxide dissolution,

making it easier for the hydrogen to dissolve in the ionic liquid phase[4-6]. A second reason for the decrease in hydrogen concentration in the ionic liquid phase at higher carbon dioxide concentrations is the dilution effect[10] (adding carbon dioxide decreases the overall hydrogen concentration).

From table 5.3 it can also be noticed that adding carbon dioxide increases the enantioselectivity of the reaction. This can be easily explained by the dilution effect: adding carbon dioxide results in lower overall hydrogen concentrations, which leads to well-controlled hydrogenation reactions with higher enantioselectivities[10].

Table 5.3: Effect of adding carbon dioxide on the asymmetric hydrogenation of MAAC in [bmim][BF$_4$], catalyzed by chiral Rh-catalyst (c_{MAAC} = 20 g/l, c_{cat} = 0.146 g/l) at room temperature (reaction time = 24 h)

Entry	Solvent	P_{H2} (bar)	P_{CO2} (bar)	P_{total} (bar)	x_{H2} (-)	x_{CO2} (-)	Conv (%)	Ee (%)
7	[bmim][BF$_4$]	5	35	40	0.13	0.87	10.0	69.7
8	[bmim][BF$_4$]	20	35	55	0.36	0.64	25.8	90.8
9	[bmim][BF$_4$]	20	5	25	0.80	0.20	61.0	81.8
10	[bmim][BF$_4$]	40	20	60	0.67	0.33	95.2	79.4
11	[bmim][BF$_4$]	50	10	60	0.83	0.17	100	71.2
3	[bmim][BF$_4$]	50	0	50	1.00	0.00	100	56.2

Plots of the conversion and enantioselectivity as a function of the carbon dioxide pressure ratios (P_{CO2}/P_{total}) and hydrogen pressure ratios (P_{H2}/P_{total}) with P_{total} = 50-60 bar (entries 8, 10, 11 and 3 from table 5.3) show some interesting results (see figures 5.1 and 5.2). The carbon dioxide and hydrogen pressure ratios are representative of the carbon dioxide and hydrogen concentrations in the ionic liquid phase, respectively. As shown in figure 5.1, by increasing the carbon dioxide pressure ratio (and thus decreasing the hydrogen pressure ratio), the conversion decreases while the enantioselectivity increases as a result of the dilution effect.

From the reaction experiments can be concluded that adding carbon dioxide enhances the enantioselectivity, but it only enhances the reaction rate at low concentrations. However, at lower concentrations the overall reaction rate is too low for practical application. At higher concentrations of carbon dioxide, the reaction rate is decreased due to the dilution effect. Therefore, although evidence of co-solvency behavior in the model system at low carbon dioxide concentrations is found, the best reaction results are obtained without adding carbon dioxide, or with adding only low concentrations of carbon dioxide (to increase the enantioselectivity) when using higher pressures of hydrogen.
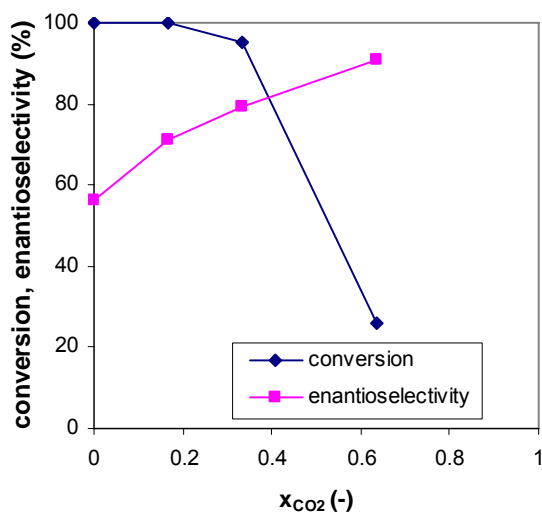
Figure 5.1: Conversion and enantioselectivity of the asymmetric hydrogenation of MAAC in [bmim][BF$_4$] versus CO$_2$ pressure ratio (P$_{total}$ = 50-60 bar)
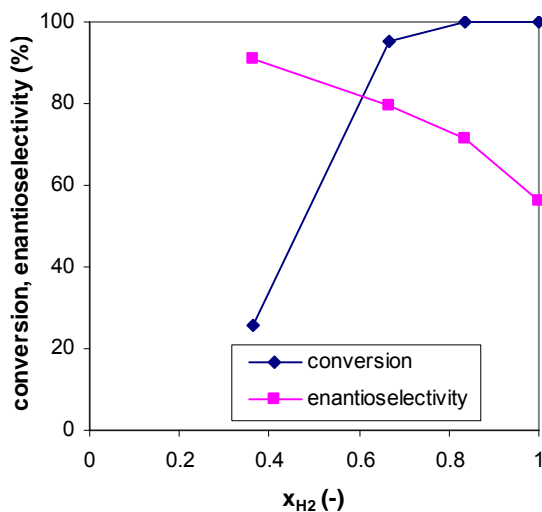
Figure 5.2: Conversion and enantioselectivity of the asymmetric hydrogenation of MAAC in [bmim][BF$_4$] versus H$_2$ pressure ratio (P$_{total}$ = 50-60 bar)

The effect of temperature was also investigated and shown in table 5.4. As expected, a higher temperature results in higher conversions, but lower enantioselectivities[8].

Table 5.4: Effect of temperature on the asymmetric hydrogenation of MAAC in [bmim][BF$_4$], catalyzed by Rh-catalyst (c$_{MAAC}$ = 20 g/l, c$_{cat}$ = 0.146 g/l, reaction time = 24 h)

Entry	Solvent	P$_{H2}$ (bar)	P$_{CO2}$ (bar)	T (^{o}C)	Conv (%)	Ee (%)
2	[bmim][BF$_4$]	20	0	25	94.2	91.9
12	[bmim][BF$_4$]	20	0	50	100	77.8

Finally, A. Shariati performed biphasic hydrogenation reactions in the [bmim][BF$_4$] + methyl *tert*-butyl ether (MTBE) system to study the recyclability of the chiral Rh-MeDuPHOS catalyst[8]. The ionic liquid and MTBE act as the immobilizer of the catalyst and the solvent for the reactant and the product, respectively. The results for three subsequent cycles are shown in table 5.5. Figure 5.3 shows the results graphically. These experiments show that it is indeed possible to reuse the catalyst a number of times with high conversion and selectivity (without any loss in the conversion and only a slight drop in the selectivity)[4], although it is impossible to detect any catalyst decay in the 100% conversion range.

Table 5.5: Three subsequent cycles of the asymmetric hydrogenation of MAAC in [bmim][BF$_4$]/MTBE, catalyzed by the same Rh-catalyst (c_{MAC} = 20 g/l, c_{cat} = 0.146 g/l) at room temperature (reaction time = 24 h)

Entry	Solvent	P_{H2} (bar)	P_{CO2} (bar)	Conv (%)	Ee (%)
13a	[bmim][BF$_4$]/MTBE	20	0	100	91.4
13b	[bmim][BF$_4$]/MTBE	20	0	100	88.5
13c	[bmim][BF$_4$]/MTBE	20	0	100	88.4
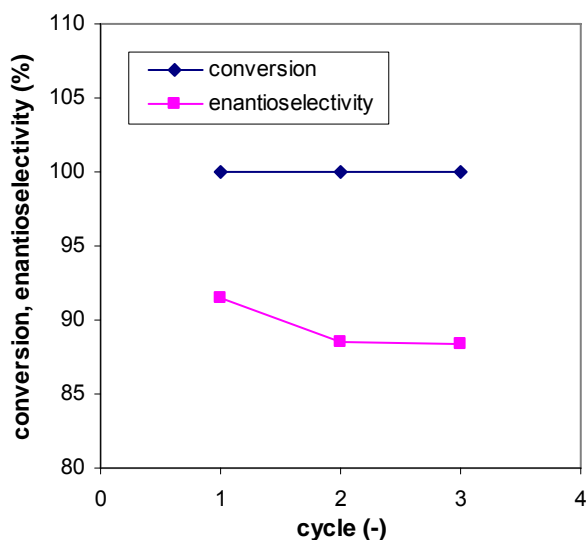
Figure 5.3: Conversion and enantioselectivity of the asymmetric hydrogenation of MAAC in [bmim][BF$_4$]/MTBE during three cycles of using the Rh-MeDuPHOS catalyst

In chapter 9 an economical and ecological comparison of the model reaction in the ionic liquid/carbon dioxide system with the conventional reaction is made.

5.2 The separation

When ionic liquids are used as reaction media, the recovery of products from ionic liquids can be difficult. Only when the product is immiscible with the ionic liquid, and the catalyst highly prefers the ionic liquid phase, then the product can be easily separated by means of decantation[11]. However, if the product and ionic liquid show partial mutual solubility, the separation is much more complicated. Distillation or evaporation is an option for solute recovery, due to the lack of any measurable ionic liquid vapor pressure, but distillation is only suited for the recovery of volatile and thermally stable products[12]. Another option to recover products from ionic liquids is extraction[13]. However, the possibility of cross-contamination between the phases presents a problem. Also, the partitioning of the solute between the phases limits the extent of solute extraction. Finally, an additional product recovery from the extractant can lead to further problems.

A solution to these problems is the use of supercritical carbon dioxide as co-solvent for product extractions or as anti-solvent for product precipitations from ionic liquids. It was shown that it is possible to extract a solute from an ionic liquid using supercritical carbon dioxide without any detectable contamination by the ionic liquid[7]. However, precipitation of products from ionic liquids using supercritical carbon dioxide as anti-solvent has never been reported in literature yet. It was believed that precipitation of products from ionic liquids using supercritical carbon dioxide is impossible, because the ionic liquids do not expand significantly when carbon dioxide is dissolved[7]. Therefore, the influence of dissolving carbon dioxide on the solubility of the product was considered to be low. In this chapter it is shown for the first time that it is possible to recover products from ionic liquids using carbon dioxide as anti-solvent in precipitations[14].

In paragraph 5.3, the recovery of the product N-acetyl-(*S*)-phenylalanine methyl ester (APAM) from the ionic liquid 1-butyl-3-methylimidazolium tetrafluoroborate ([bmim][BF$_4$]) using carbon dioxide as co-solvent in extractions is investigated[14]. In chapter 4 it was found that carbon dioxide works as co-solvent at lower concentrations (x_{CO2} < 50 mole%, T = 320 K, p = 8 MPa). Therefore, these were applied in the extraction step.

The recovery of APAM from [bmim][BF$_4$] using carbon dioxide as anti-solvent in precipitations is investigated in paragraph 5.4[14]. From chapter 4 it can be concluded that carbon dioxide acts as anti-solvent at higher carbon dioxide concentrations (x_{CO2} > 50 mole%, T < 320 K, p > 8 MPa). These conditions are applied to separate the product from the ionic liquid by precipitation.

5.3 The extraction

5.3.1 Experimental

The solubility of the product N-acetyl-(*S*)-phenylalanine methyl ester (APAM) and the reactant methyl (*Z*)-α-acetaminocinnamate (MAAC) in supercritical carbon dioxide at different conditions was measured in the following way: at the bottom of an autoclave a well-defined amount of solid APAM (resp. MAAC) was placed in a small holder. Carbon dioxide at the desired temperature was pumped into the autoclave until the desired pressure was reached. With a flow meter the amount of entering carbon dioxide was measured. The autoclave with APAM and carbon dioxide was closed and kept at fixed temperature by a heat jacket. The carbon dioxide was stirred in order to enhance mass transport of APAM from the solid phase into the carbon dioxide phase. After waiting until equilibrium was reached (30 minutes), the pressure was released and the autoclave was opened. Any APAM which would have been precipitated during expansion would have settled on the wall of the autoclave and only to a very limited extent on the sample holder. However, no visible afterprecipitation could be detected. The amount of APAM that was still left in the autoclave was measured. The dissolved amount was calculated from the difference between the initial and final amount of solid APAM in the autoclave.

In the extraction process step a solution of APAM in ionic liquid with known concentration was put into the autoclave (10.0 g APAM in 163.5 ml [bmim][BF$_4$] = 61.2 g/l). Carbon dioxide was continuously pumped through the autoclave during 30 minutes, while keeping the vessel at a temperature of 323 K and a pressure of 12.0 MPa. The amount of carbon dioxide that was pumped through the autoclave was measured using a flow meter (5.595 kg CO$_2$ in 30 minutes). After leaving the autoclave, the carbon dioxide entered an expansion vessel in which the pressure was relieved and the product precipitated due to the negligible solubility at ambient pressure. After extraction (extraction time = 30 minutes), the pump was turned off and the pressure in the autoclave was relieved. The concentration of APAM in ionic liquid after extraction was measured using High Performance Liquid Chromatography (HPLC) from Waters, type Waters 510 HPLC pump & Waters Symmetry C$_{18}$-column. The purity of the precipitated APAM was determined using Inductively Coupled Plasma Atomic Emission Spectroscopy (ICP-AES) from Spectro, type Spectroflame.

The autoclave used allows extractions using carbon dioxide within a pressure range from 0.1 to 20 MPa and temperatures from 255 to 470 K, depending on the heat-transferring fluid in the heat jacket. The uncertainty in temperature is ±0.5 K, which is due to temperature fluctuations of the heating bath. The uncertainty of the pressure in the autoclave is ±0.05 MPa. The uncertainty of the solubility measurements in the extraction experiments is ±1%. The concentrations of APAM in ionic liquid before and after separation were measured using HPLC and have an uncertainty of ±0.5%.

5.3.2 Results and discussion

When the solubility of APAM in supercritical carbon dioxide is sufficiently high, APAM can be extracted from [bmim][BF$_4$] by carbon dioxide. The solubility of APAM in carbon dioxide as function of carbon dioxide density was measured by determining the difference in weight of APAM before and after exposure to a well-defined amount of carbon dioxide at certain conditions[14]. In table 5.6 the solubility of APAM in carbon dioxide at different temperatures and pressures is shown. In figure 5.4 the solubility of APAM in carbon dioxide is plotted against the carbon dioxide-density.

Table 5.6: Solubility of APAM in carbon dioxide at different conditions

T/K	p/MPa	ρ_{CO2}/kg$\cdot$m^{-3}	c^*/g$\cdot$kg^{-1}
303	8.0	701.72	0.207
303	10.0	771.50	0.329
303	12.0	808.93	0.457
313	8.0	277.90	0.150
313	10.0	628.61	0.798
313	12.0	717.76	1.412
323	8.0	219.18	0.142
323	10.0	384.33	0.628
323	12.0	584.71	1.781
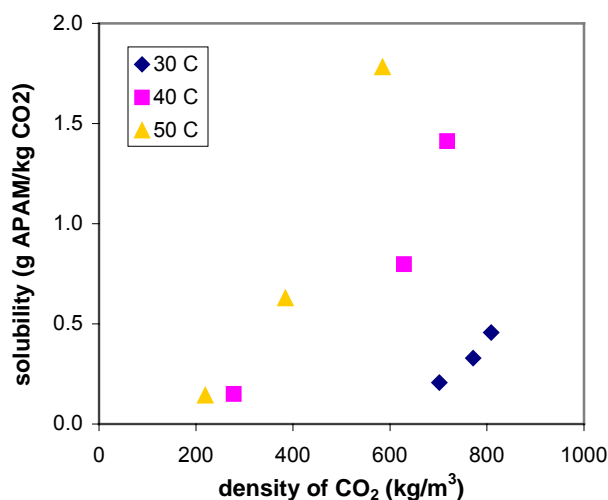
Figure 5.4: Solubility of APAM in carbon dioxide

Figure 5.4 shows that it is possible to extract APAM from the ionic liquid phase using carbon dioxide, because APAM is soluble in carbon dioxide (typically in the order of a few grams per kg CO_2). Moreover, the solubility of APAM in carbon dioxide increases when higher temperatures are used at fixed carbon dioxide-density and when the density is increased (by increasing the pressure) at fixed temperature. This is a common trend for the solubility of solutes in supercritical carbon dioxide.

The solubility of the reactant MAAC in carbon dioxide was also measured[14]. In table 5.7 the solubility of MAAC in carbon dioxide at different temperatures and pressures is shown. In figure 5.5 the solubility of MAAC in carbon dioxide is plotted against the carbon dioxide-density. The solubility of APAM in carbon dioxide is compared to the solubility of MAAC in carbon dioxide. At the same conditions the solubility of MAAC in carbon dioxide is fives times lower than the solubility of APAM in carbon dioxide (see figure 5.6). Therefore, a selectivity towards extraction of the product exists when reaction and extraction are carried out simultaneously.

Table 5.7: Solubility of MAAC in carbon dioxide at different conditions

T/K	p/MPa	ρ_{CO_2}/kg·m^{-3}	c^*/g·kg^{-1}
303	12.0	808.93	0.084
313	12.0	717.76	0.254
323	8.0	219.18	0.045
323	10.0	384.33	0.135
323	12.0	584.71	0.390
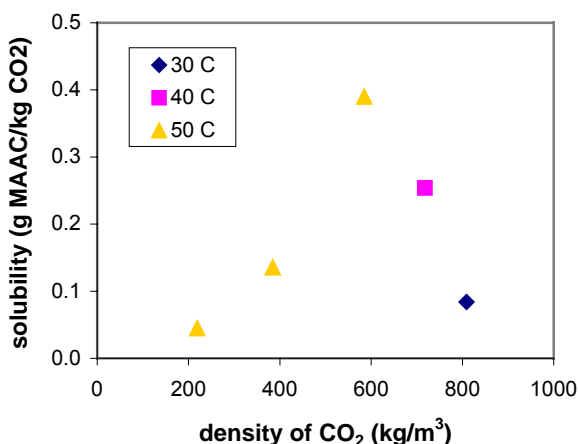
Figure 5.5: Solubility of MAAC in carbon dioxide
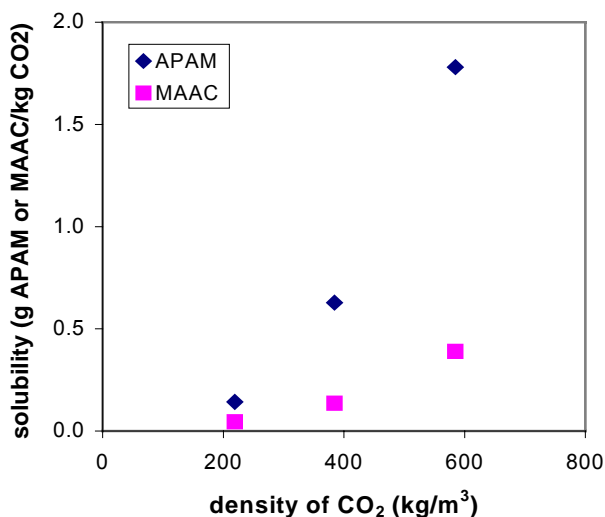
Figure 5.6: Comparison of solubility of APAM and MAAC in carbon dioxide at 50 °C

Thereafter, the extraction process was carried out[14]. APAM was extracted from the ionic liquid [bmim][BF_4] using supercritical carbon dioxide at 12.0 MPa and 323 K. A solution of 10.0 g APAM in 163.5 ml [bmim][BF_4] (61.2 g/l) was extracted with 5.595 kg CO_2 during 30 minutes (flow rate = 0.187 kg CO_2 per min). After extraction, the concentration of APAM in [bmim][BF_4] was only 10.1 g/l (= 1.7 g per 163.5 ml [bmim][BF_4]). The amount of dissolved APAM in carbon dioxide is thus 10.0 - 1.7 = 8.3 g in 5.595 kg CO_2 (1.48 g/kg, recovery = 83%), which is lower than the solubility in CO_2 (1.78 g/kg). This can be due to mass transfer limitations during the real extraction process. The precipitated APAM contains no detectable [bmim][BF_4] (measured via boron analysis with ICP-AES), indicating that the solubility of ionic liquid in carbon dioxide is lower than 10^{-5} mole fraction. Therefore, pure product can be recovered without ionic liquid contamination.

5.4 The precipitation

5.4.1 Experimental

The solubility of APAM in ionic liquid at atmospheric conditions was measured by dissolving APAM into the ionic liquid under continuous stirring until saturation was reached.

The solubility data of APAM in mixtures of [bmim][BF$_4$] + CO$_2$ were determined by adding supercritical carbon dioxide to a mixture of [bmim][BF$_4$] and APAM in an autoclave, waiting until the precipitation stops and measuring the amount of APAM that is still dissolved in the [bmim][BF$_4$] + CO$_2$ mixture after precipitation: a solution of [bmim][BF$_4$] with APAM with known concentration (76.3 g APAM in 171.4 ml [bmim][BF$_4$] = 445 g/l) was put into an autoclave vessel with a filter on the bottom. Carbon dioxide, after heating to the desired temperature (313 K), was pumped into the autoclave until the desired pressure was reached (18.0 MPa). With a flow meter the amount of entered carbon dioxide was measured (278 g). The autoclave was closed and kept at fixed temperature by a heating jacket. The mixture in the autoclave was stirred for 30 minutes. Thereafter, the valve at the bottom of the autoclave was opened and at the same time, more carbon dioxide was pressed into the autoclave to keep the pressure at constant level. In this way the liquid phase was pushed through the filter at the bottom of the autoclave and recovered, but the formed precipitate could not pass through the filter. At the moment that no liquid left the autoclave anymore, the carbon dioxide pump was turned off and the pressure in the autoclave was relieved. The concentration of APAM in the filtrate was measured with HPLC to determine the solubility of APAM in a mixture of [bmim][BF$_4$] + CO$_2$. The crystal form of the precipitated APAM was analyzed using Scanning Electron Microscopy (SEM) from Jeol, type JSM-5400.

The autoclave used is the same as the one used for extraction. The concentrations of APAM in ionic liquid before and after separation were measured using HPLC and have an uncertainty of ±0.5%. The overall uncertainty in the whole precipitation experiment is therefore ±1%.

5.4.2 Results and discussion

The product APAM can only be precipitated out of the ionic liquid phase using carbon dioxide when the solubility of APAM in pure ionic liquid is higher than the solubility in an ionic liquid + carbon dioxide mixture. In that case supersaturation can be created by adding carbon dioxide. The solubility of APAM in [bmim][BF$_4$] is 650 g/l at ambient conditions, whereas the solubility of APAM in ionic liquid + carbon dioxide (1:1.34 kg/kg) at 313 K and 18.0 MPa is 162 g/l. Therefore, in principle it is possible to precipitate 650-162 = 488 g out of 1 liter ionic liquid (single step recovery = 75%).

The product APAM was precipitated out of a solution with an initial APAM concentration in [bmim][BF$_4$] of 445 g/l (76.3 g APAM per 171.4 ml (=207.4 g) ionic liquid) using 278 g CO$_2$. The amount of remaining APAM in ionic liquid is 162 g/l (=27.8 g in 171.4 ml). The amount of precipitated APAM is 76.3 − 27.8 = 48.5 g (recovery = 64%). This is the first time that a product is precipitated from an ionic liquid using carbon dioxide[14]. So far, only one more article on the precipitation of products from ionic liquids using carbon dioxide was found[15]. In that work, Saurer *et al.*[15] were able to precipitate salts from ionic liquid/organic mixtures, where the concentration of ionic liquid was very low.

From the fact that it is possible to precipitate products out of ionic liquids it can be concluded that it is not the expansion of the fluid that determines whether a product can be precipitated or not. Rather, the interaction between the molecules determines solubility behavior.

After precipitation the formed crystals can be washed using carbon dioxide to obtain the product. However, it is difficult to remove all ionic liquid from the APAM by washing with carbon dioxide, because the carbon dioxide can only push the ionic liquid away and not strip it away, since the ionic liquid doesn't have any vapor pressure. This issue needs to be addressed in future research. The product APAM was obtained as crystals in the form of small needles (see figure 5.7).

The solubility of the starting material MAAC under precipitation conditions was not investigated. Since the separation step is carried out after the reaction step, and in principle a conversion of 100% can be reached in the reaction step[8], it is assumed that the desired product APAM will not be contaminated with the starting material MAAC.
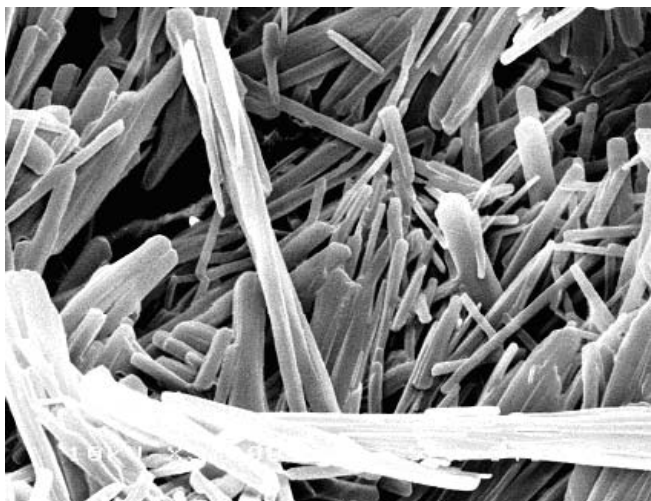
Figure 5.7: SEM-image of the precipitated APAM (5000x magnified, 10 kV)

In conclusion, carbon dioxide can be used to separate the product APAM from the ionic liquid [bmim][BF$_4$] in the co-solvency regime (extraction) or in the anti-solvent regime (precipitation). Both methods work well. In a real process, the recovery can reach 100% with a proper process lay-out. However, in this work only the pressure and temperature were optimized for high product recovery. The experiments were not optimized for carbon dioxide flow rate and duration of the experiments. Therefore, a recovery of 100% is not reached in this work. Although the separation methods were only tested on the recovery of APAM from [bmim][BF$_4$], it is believed that both methods are generally applicable for the recovery of other solutes from ionic liquids, since for each solute an optimized ionic liquid may be designed.

5.5 References

1. Berthod, M.; Joerger, J. M.; Mignani, G.; Vaultier, M.; Lemaire, M.; Enantioselective Catalytic Asymmetric Hydrogenation of Ethyl Acetoacetate in Room Temperature Ionic Liquids, *Tetrahedron Asymm.* **2004**, *15 (14)*, 2219-2221.
2. Berger, A.; De Souza, R. F.; Delgado, M. R.; Dupont, J.; Ionic Liquid-Phase Asymmetric Catalytic Hydrogenation: Hydrogen Concentration Effects on Enantioselectivity, *Tetrahedron Asymm.* **2001**, *12 (13)*, 1825-1828.
3. Guernik, S.; Wolfson, A.; Herskowitz, M.; Greenspoon, N.; Geresh, S.; A Novel System Consisting of Rh-DuPHOS and Ionic Liquid for Asymmetric Hydrogenations, *Chem. Commun.* **2001**, *(22)*, 2314-2315.
4. Brown, R. A.; Pollet, P.; McKoon, E.; Eckert, C. A.; Liotta, C. L.; Jessop, P. G.; Asymmetric Hydrogenation and Catalyst Recycling Using Ionic Liquid and Supercritical Carbon Dioxide, *J. Am. Chem. Soc.* **2001**, *123 (6)*, 1254-1255.
5. Jessop, P. G.; Stanely, R. R.; Brown, R. A.; Eckert, C. A.; Liotta, C. L.; Ngo, T. T.; Pollet, P.; Neoteric Solvents for Asymmetric Hydrogenation: Supercritical Fluids, Ionic Liquids, and Expanded Ionic Liquids, *Green Chem.* **2003**, *5 (2)*, 123-128.
6. Solinas, M.; Pfaltz, A.; Cozzi, P. G.; Leitner, W.; Enantioselective Hydrogenation of Imines in Ionic Liquid/Carbon Dioxide Media, *J. Am. Chem. Soc.* **2004**, *126 (49)*, 16142-16147.
7. Blanchard, L. A.; Brennecke, J. F.; Recovery of Organic Products from Ionic Liquids Using Supercritical Carbon Dioxide, *Ind. Eng. Chem. Res.* **2001**, *40 (1)*, 287-292.
8. Shariati, A.; Simons, C.; Sheldon, R. A.; Witkamp, G. J.; Peters, C. J.; Enantio-selective Catalytic Hydrogenation of Methyl α-acetamidocinnamate in [bmim][BF$_4$], submitted for publication to *Green Chem.* **2006**.
9. Burk, M. J.; Feaster, J. E.; Nugent, W. A.; Harlow, R. L.; Preparation and Use of C2-Symmetric Bis(phospholanes): Production of α-Amino Acid Derivatives via Highly Enantioselective Hydrogenation Reactions, *J. Am. Chem. Soc.* **1993**, *115 (22)*, 10125-10138.
10. Webb, P. B.; Sellin, M. F.; Kunene, T. E.; Williamson, S.; Slawin, A. M. Z.; Cole-Hamilton, D. J.; Continuous-Flow Hydroformylation of Alkenes in Supercritical Fluid – Ionic Liquid Biphasic Systems, *J. Am. Chem. Soc.* **2003**, *125 (50)*, 15577-15588.
11. Earle, M. J.; Seddon, K. R.; Ionic Liquids. Green Solvents for the Future, *Pure Appl. Chem.* **2000**, *72 (7)*, 1391-1398.
12. Zhao, D.; Wu, M.; Kou, Y.; Min, E.; Ionic Liquids: Applications in Catalysis, *Catal. Today* **2002**, *74 (1-2)*, 157-189.
13. Huddleston, J. G.; Willauer, H. D.; Swatloski, R. P.; Visser, A. E.; Rogers, R. D.; Room Temperature Ionic Liquids as Novel Media for Clean Liquid-Liquid Extraction, *Chem. Commun.* **1998**, *(16)*, 1765-1766.
14. Kroon, M. C.; Van Spronsen, J.; Peters, C. J.; Sheldon, R. A.; Witkamp, G. J.; Recovery of Pure Products from Ionic Liquids Using Supercritical Carbon

Dioxide as a Co-solvent in Extractions or as a Anti-solvent in Precipitations, *Green Chem.* **2006**, *8 (3)*, 246-249.

15. Saurer, E. M.; Aki, S. N. V. K.; Brennecke, J. F.; Removal of Ammonium Bromide, Ammonium Chloride, and Zinc Acetate from Ionic Liquid/Organic Mixtures Using Carbon Dioxide, *Green Chem.* **2006**, *8 (2)*, 141-143.

6

Modeling of the Phase Behavior of Ionic Liquid/Carbon Dioxide Systems with the tPC-PSAFT Equation of State

6

Modeling of the Phase Behavior of Ionic Liquid/Carbon Dioxide Systems with the tPC-PSAFT Equation of State

An equation of state has been developed to predict accurately the phase behavior of ionic liquid/carbon dioxide systems based on the truncated Perturbed Chain Polar Statistical Associating Fluid Theory (tPC-PSAFT) equation of state. This equation of state accounts explicitly for the dipolar interactions between ionic liquid molecules, the quadrupolar interactions between carbon dioxide molecules, and the Lewis acid-base type of interaction between the ionic liquid and the carbon dioxide molecules. Physically meaningful model pure component parameters for ionic liquids are estimated based on literature data. All experimental vapor-liquid equilibrium data are correlated with a single linearly temperature-dependent binary interaction parameter. The ability of the model to describe accurately carbon dioxide solubility in various 1-alkyl-3-methylimidazolium-based ionic liquids with different alkyl chain lengths and different anions at pressures from 0 MPa to 100 MPa and carbon dioxide fractions from 0 mole % to 75 mole % is demonstrated. In all cases, good agreement with experimental data is obtained.

6. Modeling of the Phase Behavior of Ionic Liquid + Carbon Dioxide Systems with the tPC-PSAFT Equation of State

6.1 Introduction

In the previous chapters a new process set-up to combine reactions and separations using ionic liquids and supercritical carbon dioxide has been described[1]. Operation conditions have been determined on basis of the phase behavior of ionic liquid + carbon dioxide systems[2,3]. Further development of the new process set-up requires more data on vapor-liquid equilibria of mixtures of ionic liquids and carbon dioxide. Although experimental data on carbon dioxide solubility in ionic liquids are available in literature[3-16], more data are needed for process design, and their experimental determination is often difficult, time-consuming and expensive. Therefore, it is highly desirable to develop predictive methods for estimating the carbon dioxide solubility in ionic liquids over a wide range of conditions. This also leads to a better understanding of the solubility behavior of ionic liquids.

Different approaches were proposed for modeling the phase behavior of ionic liquid + carbon dioxide systems. At the molecular level, carbon dioxide solubilities in ionic liquids were predicted using Monte Carlo simulation techniques[17-19]. Molecular simulation allows elucidation of microscopic phenomena that control macroscopic physical properties. In this respect, molecular dynamics simulation was used to investigate the solvation dynamics of carbon dioxide in ionic liquids, and it was shown that carbon dioxide occupies the cavities in the ionic liquid phase[20,21]. At a more coarse-grained level, Lee[22] and Carda-Broch et al.[23] used a linear solvation energy relationship in solute parameters in order to analyze the carbon dioxide solvation in ionic liquids. The irregular ionic lattice model was applied to predict carbon dioxide solubility in ionic liquids by Ally et al.[24] Furthermore, Scovazzo et al.[25] used regular solution theory for this purpose.

Equations of state have been also used for modeling the ionic liquid phase behavior in carbon dioxide and other solvents. All of these efforts have been restricted to low and medium pressure. Applications to ionic liquid + carbon dioxide mixtures close to or above 100 MPa are non-existent. Shiflett et al.[26] used the Redlich-Kwong equation of state for modeling of the carbon dioxide solubility in 1-butyl-3-methylimidazolium tetrafluoroborate ([bmim][BF$_4$]) and 1-butyl-3-methylimidazolium hexafluorophosphate ([bmim][PF$_6$]) at pressures under 2 MPa (vapor-liquid equilibrium). However, at higher pressures this equation of state cannot accurately predict the phase behavior of ionic liquid + carbon dioxide systems. Shariati et al.[27] used the Peng-Robinson equation of state in order to model the phase behavior of the 1-ethyl-3-methylimidazolium hexafluorophosphate ([emim][PF$_6$]) + fluoroform binary system (vapor-liquid equilibrium), but also this equation of state was not able to accurately describe the completely different phase behavior of [emim][PF$_6$] + carbon dioxide[27]. Furthermore,

binary ionic liquid + water systems (liquid-liquid equilibrium) have been modeled using the NRTL equation of state[28] and excess Gibbs energy methods[29]. Ternary ionic liquid + alcohol + alkane systems have been modeled using the UNIQUAC equation of state[30].

In this chapter an equation of state is developed in order to accurately predict the phase behavior of imidazolium-based ionic liquid + carbon dioxide systems up to high pressures (100 MPa)[31]. In order to obtain a model capable to capture accurately both the low and the high-pressure phase behavior, a statistical mechanics-based equation of state is used that accounts explicitly for the microscopic characteristics of ionic liquids and carbon dioxide. The cation and the anion of the ionic liquid form an ion pair in the melt due to Coulomb interactions that keep them closely associated, even in systems diluted with carbon dioxide[32-34]. Therefore, ionic liquid molecules are considered to be highly asymmetric neutral ion pairs with a dipole moment as a result of the charge distribution over the ion pair[35,36]. Moreover, carbon dioxide molecules have a quadrupole moment[37]. The equation of state proposed here should therefore take the polar interactions between the ionic liquid molecules and the carbon dioxide molecules explicitly into account. Also, evidence of a strong association between the carbon dioxide and the anion of the ionic liquid was found[38]. Kazarian *et al.*[39] found that this association is probably the result of a Lewis acid-base interaction between the carbon dioxide and the anions of the ionic liquids, where the carbon dioxide acts as a Lewis acid and the anions act as Lewis bases. Huang *et al.*[21] claim that this association is due to the strong charge-quadrupole moment interaction between carbon dioxide and the anions. In all cases, this association should also be accounted for in the equation of state.

A model suitable for the purposes outlined above is rooted to the Statistical Associating Fluid Theory (SAFT)[40-43], which is based on Wertheim's first-order Thermodynamic Perturbation Theory (TPT1)[44-47]. The original SAFT equation of state uses a chain of hard spheres with short-range directional forces accounting for hydrogen bonding (association) as reference fluid, and treats the dispersive interactions as a perturbation to the reference fluid. However, the SAFT equation of state accounts for the chainlike shape of the molecules only in the repulsive contribution. In one of the most successful modifications, the Perturbed Chain-SAFT (PC-SAFT), the chain-length dependence of the dispersive interactions is also accounted for, resulting in a more accurate model for chain molecules[48].

Several groups have extended the SAFT equation of state and the PC-SAFT equation of state in order to incorporate multipolar interactions, where the long-ranged multipolar forces (together with the dispersive forces) were considered as a perturbation over the short-range forces that almost exclusively determine the structure of the fluid[49-58]. Most of these different approaches use a simple Padé approximant[59,60] for the *u*-expansion for multipolar interactions. Differences between these modifications include the second and third order terms in the Padé approximant and the number of additional pure-component parameters for the polar term. For example, Gross[56] developed a new term for dipolar and quadrupolar interactions, where the model constants were adjusted to molecular simulation data, without the need of an additional polar interactions parameter. Jog *et*

al.[50,51] developed expressions for dipole-dipole interactions and for quadrupole-quadrupole interactions based on the work of Larsen *et al.*[60] They introduced a new adjustable parameter i.e., the fraction of dipolar segments (or quadrupolar segments) per chain. On the basis of the work of Larsen *et al.*,[60] Karakatsani *et al.*[57,58] developed an extended PC-SAFT model for polar interactions, namely the PC-Polar SAFT (PC-PSAFT) equation of state. The PC-PSAFT model is an accurate but rather complex model for real mixture calculations. For this purpose, a truncated version of the model was proposed, known as tPC-PSAFT[58], which uses an effective polar diameter as adjustable parameter in order to extend the range of dipolar and quadrupolar interactions beyond the first coordination shell of the polar molecule. Next to dipole-dipole and quadrupole-quadrupole interactions, cross-polar interactions and polarizability effects are also taken into account by both PC-PSAFT and tPC-PSAFT models[57,58].

In this work, modeling of the phase behavior of imidazolium-based ionic liquid + carbon dioxide systems is based on tPC-PSAFT equation of state[58]. It is the first attempt to accurately predict the solubility of carbon dioxide in ionic liquids at high pressures up to 100 MPa.

6.2 Model description

In the PC-SAFT equation of state, the reference fluid is the hard chain fluid, whereas the perturbation accounts for association effects and dispersion interactions. The essence of PC-SAFT is that the residual Helmholtz free energy per mole (a^{res}) is given by a sum of contributions arising from hard sphere (a^{hs}), chain formation (a^{chain}), association (a^{assoc}), and dispersion (a^{disp}) interactions. In the tPC-PSAFT equation of state, the model is extended in order to incorporate multipolar interactions. Therefore, an additional perturbation term is added to account for multipolar interactions, a^{polar}, which includes dipole-dipole interactions, quadrupole-quadrupole interactions, and cross dipole-quadrupole interactions:

$$\frac{a^{res}(T,\rho)}{RT} = \frac{a(T,\rho)}{RT} - \frac{a^{ideal}(T,\rho)}{RT} =$$

$$= \frac{a^{hs}(T,\rho)}{RT} + \frac{a^{chain}(T,\rho)}{RT} + \frac{a^{disp}(T,\rho)}{RT} + \frac{a^{assoc}(T,\rho)}{RT} + \frac{a^{polar}(T,\rho)}{RT} \tag{6.1}$$

where T and ρ are the temperature and the molar density of the system, respectively, and R is the universal gas constant. The residual Helmholtz free energy is the difference between the real Helmholtz free energy of the fluid, a, and the Helmholtz free energy for an ideal gas, a^{ideal}, at the same T and ρ. All other thermodynamic properties (pressure, chemical potential, etc.) are calculated from the Helmholtz free energy of the fluid using standard thermodynamic relations[61].

The hard-sphere term in equation (6.1) is given by the Carnahan-Starling expression[62]:

$$\frac{a^{hs}}{RT} = m \frac{4\eta - 3\eta^2}{(1-\eta)^2} \tag{6.2}$$

In this equation, m is the number of spherical segments per molecule and η, the reduced density (segment packing fraction), is:

$$\eta = \tau \rho m v^o \tag{6.3}$$

where $\tau = \pi/6 \cdot \sqrt{2} = 0.74078$ and v^o is the temperature-dependent segment molar volume of the fluid, which can be calculated from the temperature-independent volume of the fluid, v^{oo}, in the following way[63]:

$$v^o = v^{oo} \left(1 - C \exp\left(-\frac{3u}{kT} \right) \right)^3 \tag{6.4}$$

where u/k is the dispersive energy parameter per segment and $C = 0.12$ for all components except hydrogen[42].

The hard-sphere term contains three pure-component parameters: the number of segments m, the temperature-independent segment volume v^{oo} and the dispersion energy per segment u/k. Sometimes, the segment diameter σ rather than the segment volume v^{oo} is selected as pure-component parameter, which can be calculated from the following expression:

$$v^{oo} = \left(\frac{\pi N_A}{6\tau}\right)\sigma^3$$

(6.5)

where N_A is Avogadro's number.

For the chain term in equation (6.1) the following expression is used[42]:

$$\frac{a^{chain}}{RT} = (1-m)\ln\left(\frac{2-\eta}{2(1-\eta)^3}\right)$$

(6.6)

This equation follows from Wertheim's TPT for association[41], where association bonds are replaced by covalent, chain-forming bonds. It can be noticed that this term contains the same three pure-component parameters as those used for calculating the hard-sphere contribution. No additional parameter is necessary to account for chain connectivity.

The dispersion contribution to the Helmholtz free energy in equation (6.1) is given by[48]:

$$\frac{a^{disp}}{RT} = -2\pi\rho I_1(\eta,m)m^2\frac{u}{kT}\sigma^3 - \pi\rho m C_1 I_2(\eta,m)m^2\left(\frac{u}{kT}\right)^2\sigma^3$$

(6.7)

where C_1 is the following compressibility expression:

$$C_1 = \left(1 + m\frac{8\eta - 2\eta^2}{(1-\eta)^4} + (1-m)\frac{20\eta - 27\eta^2 + 12\eta^3 - 2\eta^4}{[(1-\eta)(2-\eta)]^2}\right)^{-1}$$

(6.8)

The integrals in the dispersion term are given by the following series expansions:

$$I_1(\eta,m) = \sum_{i=0}^{6} a_i(m)\eta^i$$

(6.9)

$$I_2(\eta,m) = \sum_{i=0}^{6} b_i(m)\eta^i$$

(6.10)

where the coefficients a_i and b_i are functions of the chain length m and the universal coefficients a_{ji} and b_{ji} (given by Gross $et\ al.$[48]):

$$a_i(m) = a_{0i} + \frac{m-1}{m}a_{1i} + \frac{m-1}{m}\frac{m-2}{m}a_{2i} \tag{6.11}$$

$$b_i(m) = b_{0i} + \frac{m-1}{m}b_{1i} + \frac{m-1}{m}\frac{m-2}{m}b_{2i} \tag{6.12}$$

Also for the dispersion term the same three pure-component parameters are used, and no additional pure-component parameter is required.

The association term in equation (6.1) is obtained from Wertheim's TPT for association[41]:

$$\frac{a^{assoc}}{RT} = \sum_{A=1}^{M}\left(\ln X^A - \frac{X^A}{2}\right) + \frac{M}{2} \tag{6.13}$$

where M is the number of association sites per molecule, and X^A is the mole fraction of molecules not bonded at specific interaction site A. The summation is over all association sites on the molecule. The non-bonded fraction X^A is calculated from:

$$X^A = \frac{1}{1 + \sum_{B=1}^{M}\rho X^B \Delta^{AB}} \tag{6.14}$$

where the summation is over all different types of sites, and Δ^{AB} is the association strength, given by:

$$\Delta^{AB} = \sqrt{2}v^{oo}\frac{2-\eta}{2(1-\eta)^3}\left[\exp\left(\frac{\varepsilon^{AB}}{kT}\right) - 1\right]\kappa^{AB} \tag{6.15}$$

In the association term, two new association parameters are introduced: the association energy ε^{AB}, and the association volume κ^{AB}. In the mixtures considered in this work, molecules do not self-associate but they cross-associate. Carbon dioxide is considered to have one association site A^+ (acting as a Lewis acid) while the ionic liquid is considered to have one association site B^- (acting as a Lewis base). Consequently, equation (6.14) results to a set of two equations with two unknowns (X^A and X^B) that can be solved analytically[64]. Because no numerical approach was involved, the computational time was considerably reduced compared to the general case of associating mixtures.

The polar term of PC-PSAFT is based on the work of Larsen et al.[60] and has the form of a simple Padé approximant for the Helmholtz free energy[59,60]:

$$\frac{a^{polar}}{RT} = m \frac{a_2^{polar}}{1 - a_3^{polar}/a_2^{polar}} \tag{6.16}$$

where the first order perturbation term vanishes[65], and a_2^{polar} and a_3^{polar} are the second and third order perturbation polar terms, respectively. The third order term consists of a two-body term ($a_{3,2}^{polar}$) and a three-body term ($a_{3,3}^{polar}$), which both make a significant contribution to the Helmholtz free energy[59,66]:

$$\frac{a_3^{polar}}{RT} = \frac{a_{3,2}^{polar}}{RT} + \frac{a_{3,3}^{polar}}{RT} \tag{6.17}$$

Larsen et al.[60] developed accurate expressions for the multipole terms of equation (6.17) for a hard sphere fluid. These expressions contain double and triple spatial integrals over the reference fluid that are approximated by third and fifth order density polynomials. In PC-PSAFT, Karakatsani et al.[57,58] extended these expressions to chain fluids, both pure components and mixtures. Furthermore, in truncated PC-PSAFT (tPC-PSAFT)[58], the model was simplified considerably by approximating the double and triple integrals with their first order terms of the corresponding density polynomials. In tPC-PSAFT, an effective polar interaction diameter, σ_p, is introduced. This parameter specifies the transition between the first coordination shell where the short-range repulsion and hydrogen bonding interactions dominate and the region beyond this first coordination shell where longer-ranged electrostatic polar interactions prevail[67]. The effective polar diameter for various polar compounds (water, methanol, acetone, carbon dioxide) has been reported previously[68,69]. In this work, the effective polar interactions diameter is a model parameter.

As a result, the following expressions are used for the polar interactions[58]:

$$\frac{a_2^{polar}}{RT} = -\left(\frac{u}{kT}\right)^2 \eta \left[\frac{4}{3} \frac{\tilde{\mu}^4}{(\sigma_p/\sigma)^3} + \frac{12}{5} \frac{\tilde{\mu}^2 \tilde{Q}^2}{(\sigma_p/\sigma)^5} + \frac{12}{5} \frac{\tilde{Q}^4}{(\sigma_p/\sigma)^7} \right] \tag{6.18}$$

$$\frac{a_{3,2}^{polar}}{RT} = \left(\frac{u}{kT}\right)^3 \eta \tilde{Q}^2 \left[\frac{6}{5} \frac{\tilde{\mu}^4}{(\sigma_p/\sigma)^8} + \frac{144}{175} \frac{\tilde{\mu}^2 \tilde{Q}^2}{(\sigma_p/\sigma)^{10}} + \frac{72}{245} \frac{\tilde{Q}^4}{(\sigma_p/\sigma)^{12}} \right] \tag{6.19}$$

$$\frac{a_{3,3}^{polar}}{RT} = \left(\frac{u}{kT}\right)^3 \eta^2 \left[\frac{10}{9} \frac{\tilde{\mu}^6}{(\sigma_p/\sigma)^3} + \frac{159}{125} \frac{\tilde{\mu}^4 \tilde{Q}^2}{(\sigma_p/\sigma)^5} + \frac{689}{1000} \frac{\tilde{\mu}^2 \tilde{Q}^4}{(\sigma_p/\sigma)^7} + \frac{243}{800} \frac{\tilde{Q}^6}{(\sigma_p/\sigma)^9} \right] \tag{6.20}$$

where:

$$\tilde{\mu} = 85.12 \frac{\mu/m}{\sqrt{(u/k)\sigma^3}} \tag{6.21}$$

$$\tilde{Q} = 85.12 \frac{Q/m}{\sqrt{(u/k)\sigma^5}} \tag{6.22}$$

and μ is the dipole moment of the fluid in D and Q is its quadrupole moment in DÅ.

The tPC-PSAFT equation of state is extended straightforwardly to mixtures using standard mixing rules. For the dispersion term the following mixing rules are used:

$$m = \sum_i x_i m_i \tag{6.23}$$

$$m^2 \frac{u}{k} \sigma^3 = \sum_i \sum_j x_i x_j m_i m_j \left(\frac{u_{ij}}{kT}\right) \sigma_{ij}^3 \tag{6.24}$$

$$m^2 \left(\frac{u}{kT}\right)^2 \sigma^3 = \sum_i \sum_j x_i x_j m_i m_j \left(\frac{u_{ij}}{kT}\right)^2 \sigma_{ij}^3 \tag{6.25}$$

with:

$$\sigma_{ij} = \frac{1}{2}(\sigma_i + \sigma_j) \tag{6.26}$$

$$\frac{u_{ij}}{k} = \left(\frac{u_{ii}}{k}\frac{u_{jj}}{k}\right)^{1/2}(1 - k_{ij}) \tag{6.27}$$

where x_i is the mole fraction of component i, and k_{ij} is the adjustable binary interactions parameter that accounts for the non-ideality of the mixture.

The mixing rules for the two-body polar terms (a_2^{polar} and $a_{3,2}^{polar}$) are:

$$\tilde{\mu} = \frac{\sum_i \sum_j x_i x_j m_i m_j \tilde{\mu}_{ij}}{\left(\sum_i x_i m_i\right)^2} \tag{6.28}$$

$$\tilde{Q} = \frac{\sum_i \sum_j x_i x_j m_i m_j \tilde{Q}_{ij}}{\left(\sum_i x_i m_i\right)^2} \tag{6.29}$$

with:

$$\tilde{\mu}_{ij} = \sqrt{\tilde{\mu}_i \tilde{\mu}_j} \tag{6.30}$$

$$\tilde{Q}_{ij} = \sqrt{\tilde{Q}_i \tilde{Q}_j} \tag{6.31}$$

Finally, for the three-body polar term ($a_{3,3}^{polar}$) the following mixing rules are proposed:

$$\tilde{\mu} = \frac{\sum_i \sum_j \sum_k x_i x_j x_k m_i m_j m_k \tilde{\mu}_{ijk}}{\left(\sum_i x_i m_i\right)^3} \tag{6.32}$$

$$\tilde{Q} = \frac{\sum_i \sum_j \sum_k x_i x_j x_k m_i m_j m_k \tilde{Q}_{ijk}}{\left(\sum_i x_i m_i\right)^3} \tag{6.33}$$

$$\tilde{\Lambda} = \left(\tilde{\mu}^2 \tilde{Q}\right)^{1/3} = \frac{\sum_i \sum_j \sum_k x_i x_j x_k m_i m_j m_k \tilde{\Lambda}_{ijk}}{\left(\sum_i x_i m_i\right)^3} \tag{6.34}$$

$$\tilde{\Gamma} = \left(\tilde{\mu} \tilde{Q}^2\right)^{1/3} = \frac{\sum_i \sum_j \sum_k x_i x_j x_k m_i m_j m_k \tilde{\Gamma}_{ijk}}{\left(\sum_i x_i m_i\right)^3} \tag{6.35}$$

with:

$$\tilde{\mu}_{ijk} = \left(\tilde{\mu}_i \tilde{\mu}_j \tilde{\mu}_k\right)^{1/3} \tag{6.36}$$

$$\tilde{Q}_{ijk} = \left(\tilde{Q}_i \tilde{Q}_j \tilde{Q}_k\right)^{1/3} \tag{6.37}$$

$$\tilde{\Lambda}_{ijk} = \left(\tilde{\mu}_i \tilde{\mu}_j \tilde{Q}_k \right)^{1/3} \tag{6.38}$$

$$\tilde{\Gamma}_{ijk} = \left(\tilde{\mu}_i \tilde{Q}_j \tilde{Q}_k \right)^{1/3} \tag{6.39}$$

6.3 Parameter estimation

The tPC-PSAFT equation of state contains six pure-component parameters: three parameters for nonassociating nonpolar compounds (i.e., the segment number m, the temperature-independent segment volume v^{oo}, and the segment dispersive energy parameter u/k), two additional parameters for association (i.e., the association energy ε^{AB}, and the association volume κ^{AB}) and one additional parameter for polar interactions (i.e., the effective polar interactions diameter σ_p). For nonpolar compounds, the tPC-PSAFT equation of state reduces to the original PC-SAFT equation of state.

In this chapter, the tPC-PSAFT equation of state is used to model the phase behavior of ionic liquid + carbon dioxide systems[31]. The ionic liquids that are modeled are 1-ethyl-3-methylimidazolium hexafluorophosphate ([emim][PF$_6$]), 1-butyl-3-methylimidazolium hexafluorophosphate ([bmim][PF$_6$]), 1-hexyl-3-methylimidazolium hexafluorophosphate ([hmim][PF$_6$]), 1-butyl-3-methylimidazolium tetrafluoroborate ([bmim][BF$_4$]), 1-hexyl-3-methyl-imidazolium tetrafluoroborate ([hmim][BF$_4$]) and 1-octyl-3-methylimidazolium tetrafluoroborate ([omim][BF$_4$]). In Figure 6.1, a schematic representation of these ionic liquids is shown. For carbon dioxide the PC-SAFT and tPC-PSAFT pure component parameters can be found in literature[48,56,58]. However, the tPC-PSAFT parameters for ionic liquids were unknown and had to be estimated.

$$BF_4^- \qquad\qquad\qquad PF_6^-$$
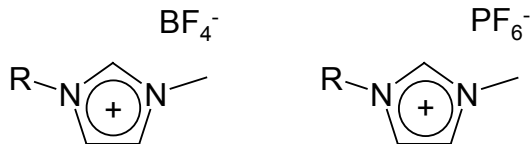
Figure 6.1: Structures of the 1-alkyl-3-methylimidazolium tetrafluoroborate and 1-alkyl-3-methyl-imidazolium hexafluorophosphate ionic liquids (R = ethyl, butyl, hexyl, octyl,…)

Physically meaningful pure-component parameters for ionic liquids (ion pairs) were estimated based on ionic liquid experimental thermodynamic data (density, enthalpy and entropy of dissolution of carbon dioxide) and physicochemical data (size, polarizability, number of electrons) for the constituent ions (cation and anion)[31]. The following protocol was used for this purpose. For the anions [BF$_4^-$] and [PF$_6^-$], the size and shape parameters were available in literature[70]. The dispersive energy parameter for the anions was calculated using the Mavroyannis and Stephen equation[71]:

$$\left(\frac{u}{k}\right)_{anion} = 356\frac{\alpha_{anion}^{3/2}n_{anion}^{1/2}}{r_{anion}^{6}} \qquad\qquad (6.40)$$

where α is the polarizability of the anion, n is the number of electrons of the anion, and r is the radius of the anion. The values of α, n and r for [BF$_4$$^-$] and [PF$_6$$^-$] were also found in literature[72].

For the size, shape and energy parameters of the cations [emim$^+$], [bmim$^+$], [hmim$^+$] and [omim$^+$], the PC-SAFT values for ethylbenzene, butylbenzene, hexylbenzene and octylbenzene, respectively, were used [48].

In Table 6.1 the values for the three nonassociating nonpolar parameters for both anions and cations are presented.

Table 6.1: tPC-PSAFT parameters for various anions and cations

Compound	M_w (g/mol)	m (-)	v^{oo} (ml/mol)	α ($\mathring{A}^3$)	n (-)	r ($\mathring{A}$)	u/k (K)
[BF$_4$$^-$]	86.80	1.00	28.91	4.41	42	2.25	162.9
[PF$_6$$^-$]	144.96	1.00	40.95	7.32	70	2.53	223.8
[emim$^+$]	111.17	3.0990	23.31	-	-	-	285.0
[bmim$^+$]	139.22	3.7662	24.72	-	-	-	285.0
[hmim$^+$]	167.28	4.4334	26.14	-	-	-	285.0
[omim$^+$]	195.33	5.1006	27.55	-	-	-	285.0

The size, shape and energy parameters for the pure total ionic liquids were calculated using standard combining rules:

$$(u/k)_{ionic\_liquid} = \sqrt{(u/k)_{anion}(u/k)_{cation}} \tag{6.41}$$

$$v^{oo}_{ionic\_liquid} = \frac{m_{anion}v^{oo}_{anion} + m_{cation}v^{oo}_{cation}}{m_{ionic\_liquid}} \tag{6.42}$$

where m_{ionic_liquid} was fitted to ionic liquid density data at 20°C and 25°C[35], with an absolute average deviation (AAD%) of smaller than $5 \cdot 10^{-3}$ %.

The polar nature of ionic liquids makes them suitable for solvents in a wide range of chemical processes. Unfortunately, the dipole moment of the ionic liquids examined here is not known experimentally. However, the polarity of various imidazolium-based ionic liquids has been measured by Carmichael et al.[36] using solvatochromic methods and more recently by Wakai et al.[73] using dielectric spectroscopy and shown to be comparable to the polarity of lower to medium alcohols. Other experimental measurements for ionic liquid mixtures have resulted to similar conclusions that ionic liquids behave as moderately polar organic solvents[74]. Although ionic liquids are larger than lower alcohols, the distance between the positive charge (hydrogen on the C2-position of the cation) and negative charge (fluoride on the anion) within an ionic pair is only 1.914Å[75]. This distance is slightly larger than the distance between the charges in

___

lower alcohols. Based on the above arguments, it is reasonable to assume that ionic liquids have the same dipole moment (μ = 1.70 D) and effective polar interactions parameter (σ_p = 1.4 σ) as methanol[70].

The association parameters for the Lewis acid-base association between the carbon dioxide (Lewis acid) and the anion of the ionic liquid (Lewis base) were estimated from literature data[38] for the enthalpy and entropy of dissolution of carbon dioxide in ionic liquid using the expressions[76]:

$$\frac{\varepsilon^{AB}}{k} \approx -\Delta H^{dissol} \tag{6.43}$$

$$\kappa^{AB} \approx \exp\left(\frac{\Delta S^{dissol}}{R}\right) \tag{6.44}$$

The resulting values for the energy of association and the volume of association are ε^{AB}/k = 2200 K, and κ^{AB} = 0.0017 (-), respectively. For comparison, for 1-alcohols larger than 1-butanol ε^{AB}/k is 2500 – 2700 K and κ^{AB} = 0.0010 – 0.0013 (-)[57].

In Table 6.2 the tPC-PSAFT pure component parameters for carbon dioxide and ionic liquids are presented. All parameters proposed have a clear physical value. For the homologous series of ionic liquids with increasing alkyl chain, it is also ensured that the parameters vary smoothly with molecular weight (m, v^{oo}, σ_p) or are constant (u/k, ε^{AB}, κ^{AB}). For example, in Figure 6.2 the total volume of the ionic liquid equal to $m \cdot v^{oo}$ is plotted against the molecular weight of the ionic liquid. As can be seen from this graph, a linear dependence holds, which means that extension to other alkylmethylimidazolium ionic liquids with different alkyl chain length is straightforward.

Table 6.2: tPC-PSAFT pure-component parameters for carbon dioxide and various ionic liquids. For the cross-association between carbon dioxide and ionic liquid, it is ε^{AB}/k = 2200 K and κ = 0.0017 (-).

Compound	M_w	Nonassociating Parameters					
	(g/mol)	m	v^{oo}	u/k	μ	Q	σ_p
		(-)	(ml/mol)	(K)	(D)	(DÅ)	(Å)
CO_2	44.01	1.911	9.90	157.92	0.00	4.3	2.974
[emim$^+$][PF$_6^-$]	256.13	3.521	27.61	252.57	1.70	0.00	5.625
[bmim$^+$][PF$_6^-$]	284.18	4.235	28.13	252.57	1.70	0.00	5.660
[hmim$^+$][PF$_6^-$]	312.24	4.834	28.86	252.57	1.70	0.00	5.709
[omim$^+$][PF$_6^-$]	340.29	5.451	29.75	252.57	1.70	0.00	5.767
[emim$^+$][BF$_4^-$]	197.97	3.300	24.67	215.47	1.70	0.00	5.418
[bmim$^+$][BF$_4^-$]	226.02	3.862	25.60	215.47	1.70	0.00	5.485
[hmim$^+$][BF$_4^-$]	254.08	4.417	26.65	215.47	1.70	0.00	5.559
[omim$^+$][BF$_4^-$]	282.13	4.973	27.77	215.47	1.70	0.00	5.636
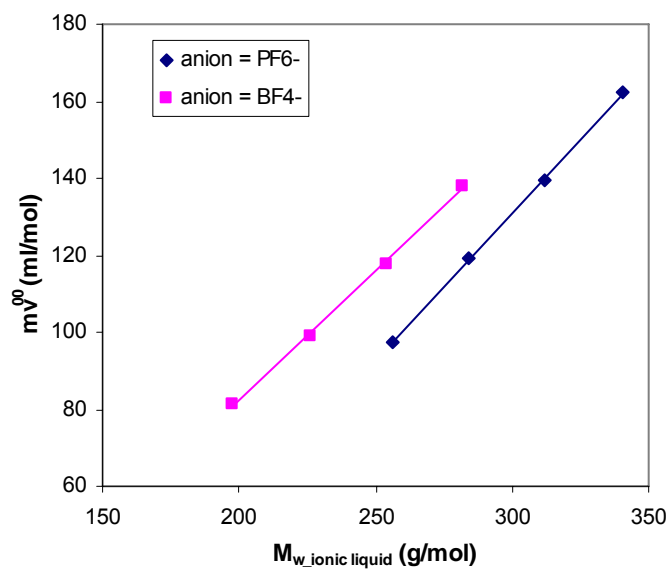
Figure 6.2: Total volume of the ionic liquid (= m·v^{oo}) against the molecular weight of the ionic liquid

6.4 Results and discussion

The phase behavior of several alkylmethylimidazolium ionic liquid + carbon dioxide systems is modeled using the tPC-PSAFT equation of state and the parameters estimated in the previous section[31]. Only the temperature-dependent binary interaction parameter k_{ij} is adjusted in order to fit the model to experimental vapor-liquid equilibrium data.

In Figure 6.3, the bubble-point pressures versus the carbon dioxide mole fraction for different binary carbon dioxide + ionic liquid (anion = PF_6^-) systems are shown at 333.15 K. Good agreement between experimental data[12,13,16] and the model is observed. It is particularly encouraging that tPC-PSAFT predicts a nearly infinite bubble point pressure slope at a specific maximum concentration of carbon dioxide beyond which increasing the external pressure hardly increases the carbon dioxide solubility in ionic liquid, which is in agreement with experiments[3,12-16]. According to Huang *et al.*[21], the reason for this sharp pressure increase at a certain maximum carbon dioxide concentration is that at this point all cavities in the ionic liquid phase are occupied by carbon dioxide, so that further insertion of carbon dioxide would require "breaking" the cohesive structure of the ionic liquid. Similarly good agreement between experiment and model was obtained for other temperatures between 313.15 K and 353.15 K.

Figure 6.3: Experimental data[12,13,16] and tPC-PSAFT equation of state correlation for the bubble-point pressures of different ionic liquid (anion = PF_6^-) + carbon dioxide systems at 333.15 K

A temperature-independent binary interaction parameter was not able to describe the phase behavior accurately over the entire temperature range. A reason for this could be that the association energy is based on a constant enthalpy of dissolution, whereas in reality the enthalpy of dissolution changes with temperature ($\Delta H \sim RT$). Therefore, when a constant binary interaction parameter is used, the pressure is underpredicted at higher temperatures and overpredicted at lower temperatures. In order to take the temperature-dependence of the enthalpy of dissolution into account, the binary interaction parameter k_{ij} was allowed to vary with temperature. In Table 6.3 the values for the binary interaction parameter at different temperatures are presented and in Figures 6.4 and 6.5 the dependence of the binary interaction parameter on temperature and molecular weight are shown.

Table 6.3: Binary interaction parameter for different ionic liquid (anion = PF_6^-) + carbon dioxide mixtures

T (K)	Binary interaction parameter k_{ij} (-)		
	[emim][PF_6] + CO_2	[bmim][PF_6] + CO_2	[hmim][PF_6] + CO_2
313.15	0.2027	0.1745	0.1570
323.15	0.2077	0.1794	0.1623
333.15	0.2127	0.1846	0.1675
343.15	0.2184	0.1902	0.1726
353.15	0.2237	0.1954	0.1780

Figure 6.4: Dependence of the binary interaction parameter on temperature for different ionic liquid (anion = PF_6^-) + carbon dioxide systems

Figure 6.5: Dependence of the binary interaction parameter on molecular weight (alkyl chain length) of ionic liquid (anion = PF_6^-) for different temperatures

The binary interaction parameter increases linearly with temperature and decreases asymptotically with molecular weight. Thus, the lowest k_{ij}-values are observed for the ionic liquid + carbon dioxide mixtures where the alkyl chain is the longest (highest molecular weight) and the temperature is the lowest. This is expected because the deviation from ideal mixing becomes larger at higher temperatures (above the critical point of carbon dioxide) when the density difference between carbon dioxide and ionic liquid increases. Moreover, in small ionic liquids the non-ideal behavior of the imidazolium-ring and anion are dominating, whereas in large ionic liquids the long alkyl chains (similar to ideal-behaving alkanes) predominate. In later research, also other groups found the need of a linearly temperature-dependent adjustable parameter for the modeling of ionic liquid systems[77].

The same approach was used to correlate the bubble-point pressures for carbon dioxide + ionic liquid system where the anion is BF_4^-. Again, the binary interaction parameter was allowed to vary with temperature. The results at 333.15 K are shown in Figure 6.6. Similar plots were obtained for other temperatures between 313.15 K and 353.15 K. As can be seen from this figure, the agreement with experimental data[3,14,15] is good. A similar trend as before is observed for the binary interaction parameter as a function of temperature and of molecular weight (see table 6.4 and figures 6.7 and 6.8). However, the temperature-dependence of the binary interaction parameter for the $[BF_4^-]$ - ionic liquids is larger than the temperature-dependence for the $[PF_6^-]$ - ionic liquids.
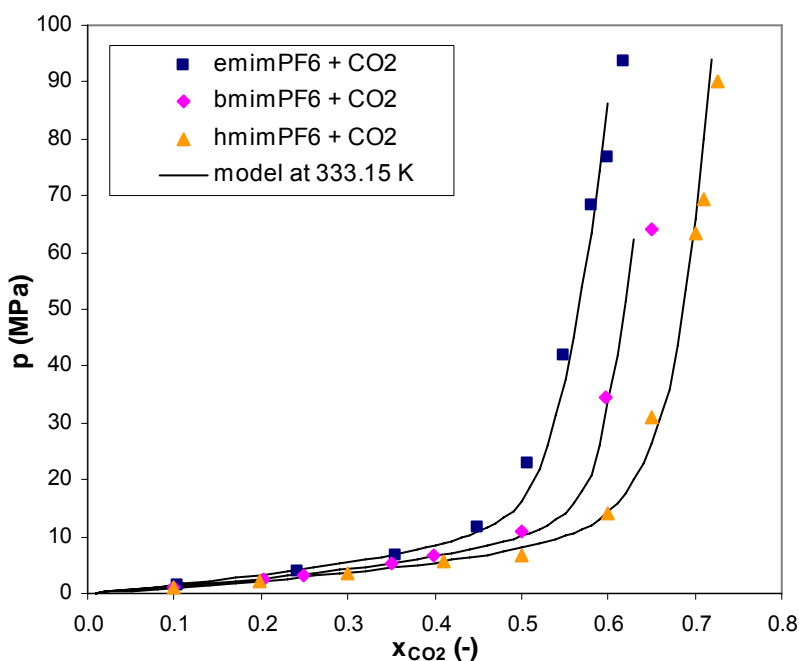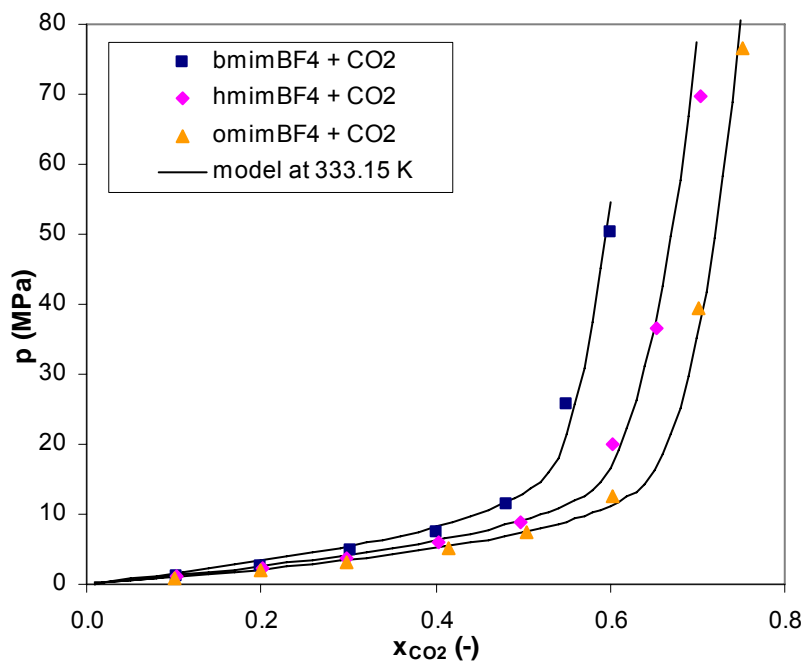
Figure 6.6: Experimental data[3,14,15] and tPC-PSAFT equation of state correlation for the bubble-point pressures of different ionic liquid (anion = BF_4^-) + carbon dioxide systems at 333.15 K

Table 6.4: Binary interaction parameter for different ionic liquid (anion = BF_4^-) + carbon dioxide mixtures

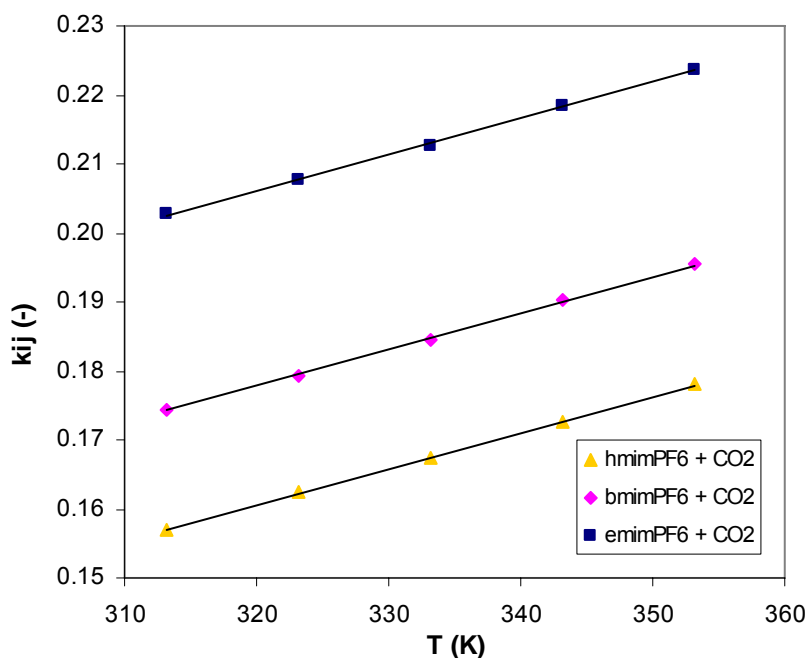| T (K)	Binary interaction parameter k_{ij} (-)		
	[bmim][BF_4] + CO_2	[hmim][BF_4] + CO_2	[omim][BF_4] + CO_2
313.15	0.2144	0.1856	0.1673
323.15	0.2252	0.1948	0.1763
333.15	0.2343	0.2043	0.1854
343.15	0.2433	0.2145	0.1948
353.15	0.2536	0.2237	0.2043
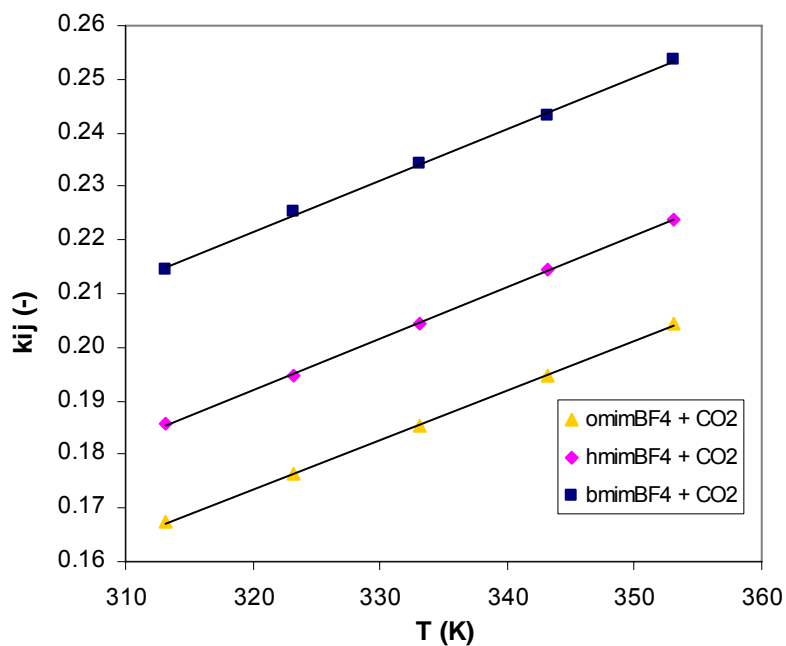
Figure 6.7: Dependence of the binary interaction parameter on temperature for different ionic liquid (anion = BF_4^-) + carbon dioxide systems
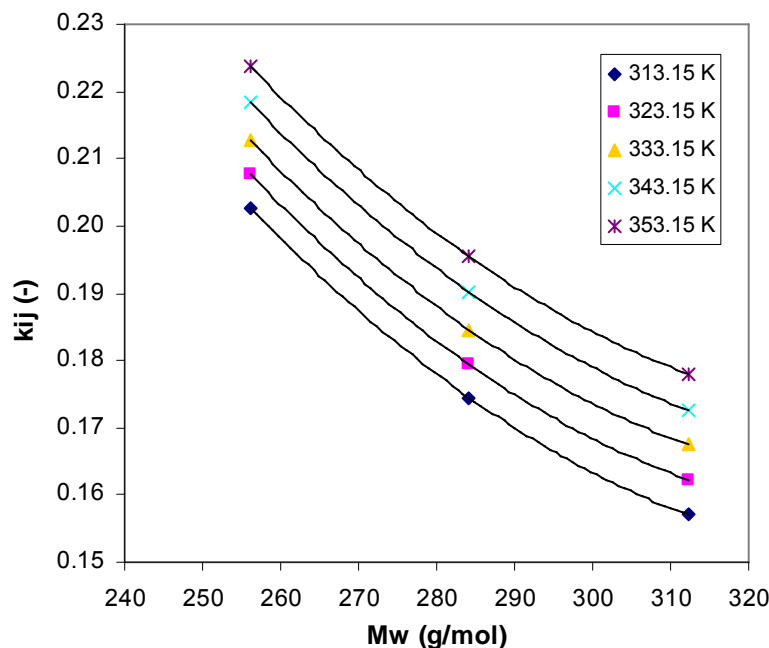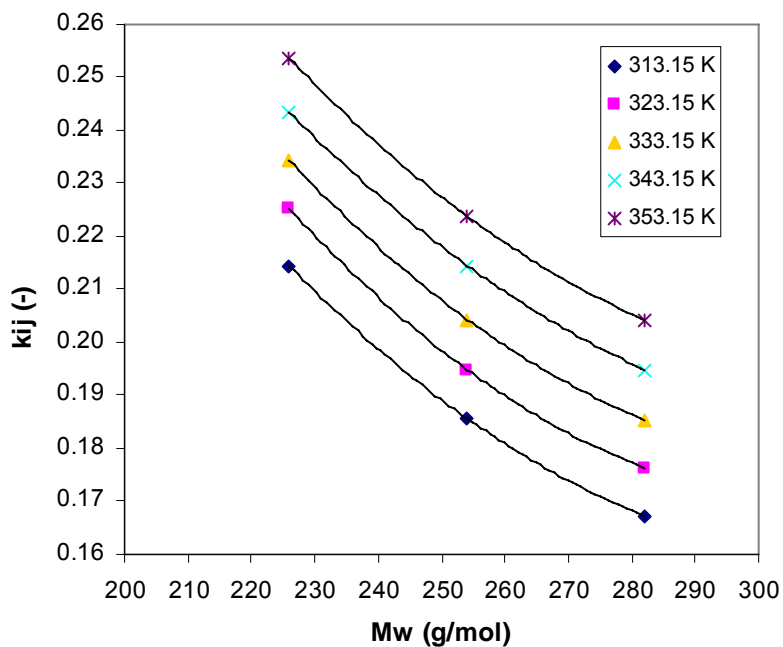

Figure 6.8: Dependence of the binary interaction parameter on molecular weight (alkyl chain length) of ionic liquid (anion = BF_4^-) for different temperatures

_____

In bubble point calculations with an equation of state, the composition of the vapor phase is calculated also. These have never been measured because it was assumed that ionic liquids have negligible vapor pressure. In Figure 6.9, the entire p,x,y-diagram for [bmim][[PF$_6$] + CO$_2$ mixture at 353.15 K is shown. It can be seen that the solubility of carbon dioxide in ionic liquid (liquid phase) is high, whereas the solubility of ionic liquid in the vapor phase is very low (especially for pressures under 10 MPa), which is in agreement with experimental observations of negligible solubility of ionic liquids in carbon dioxide[78-80]. However, at pressures higher than 10 MPa, the model predicts that some ionic liquid will be present in the supercritical carbon dioxide phase. Similar predictions were obtained for the other temperatures and the other mixtures examined.
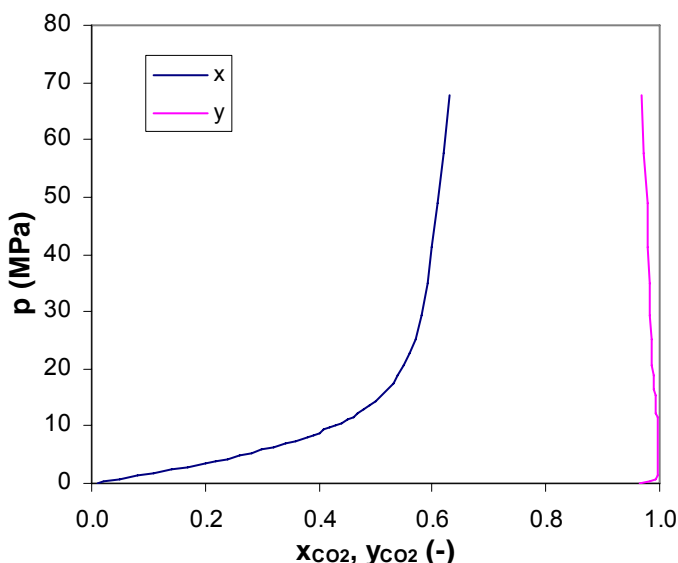
Figure 6.9: P, x, y – diagram of the [bmim][PF$_6$] + CO$_2$ system at 353.15 K

In the tPC-PSAFT model, it is assumed that the cation and anion of the ionic liquid form a neutral ion pair, which has a dipole moment due to the charge distribution. In order to see whether this assumption is appropriate, ionic liquids were also modeled as two separate charged species i.e., anion and cation, that only partially associate to form ion pairs. The anions are small and symmetric and have a negative charge. The cations are represented as chains, where the positive charge is present on only one segment of the chain and the other segments are charge-free. The negatively changed anion and the positively charged segment of the cation show electrostatic Coulomb interactions. The cations and anions partly associate due to ion pair formation, where it is assumed that an associated ion pair is a neutral molecule that does not show any electrostatic or polar interactions.

Under these assumptions the tPC-PSAFT equation of state is changed. The polar term only accounts for the interactions between the carbon dioxide molecules (and no longer

for the interactions between the ionic liquid molecules), but an extra term accounting for the charge-charge interactions between the cation and the anion is added. This term is represented by the mean spherical approximation (MSA) model of Blum and Høye[81,82] for ions of different size in a continuous medium with specified dielectric constant (non-restricted primitive model). It is assumed that the charge of the cation is located on the imidazole-ring and therefore the continuous medium surrounding the charged segments consists of alkyl side chains (with a dielectric constant of the corresponding alkane) and carbon dioxide. Finally, the association term no longer accounts for the Lewis acid-base interaction between the carbon dioxide and the anions, but for the ion pair formation between the anion and the cation of the ionic liquid.

Using this modified equation of state with the same three non-associating non-polar pure component parameters, the same polar parameter for carbon dioxide, adding the charge parameters ($q = -1.6022 \cdot 10^{-19}$ C for the anions, $q = +1.6022 \cdot 10^{-19}$ C for the cations) and using an adjustable temperature-dependent association parameter (fitted to experimental vapor-liquid equilibrium data), the phase behavior of the system [hmim][BF$_4$] + CO$_2$ was modeled again. Figure 6.10 compares the modified model with the original tPC-PSAFT model. It is concluded that the original tPC-PSAFT equation of state better predicts the experimental data than the modified model. Therefore, the assumption that ionic liquid molecules are totally associated (so that cation and anion always form ion pairs) seems to be appropriate. This was also confirmed by Klamt[83], who was only able to obtain vapor pressures near the measured values assuming complete association of the ions (ion pair formation) instead of separate ions using COSMOtherm®. Otherwise, the predicted vapor pressure would be about 10^{10} less than measured!
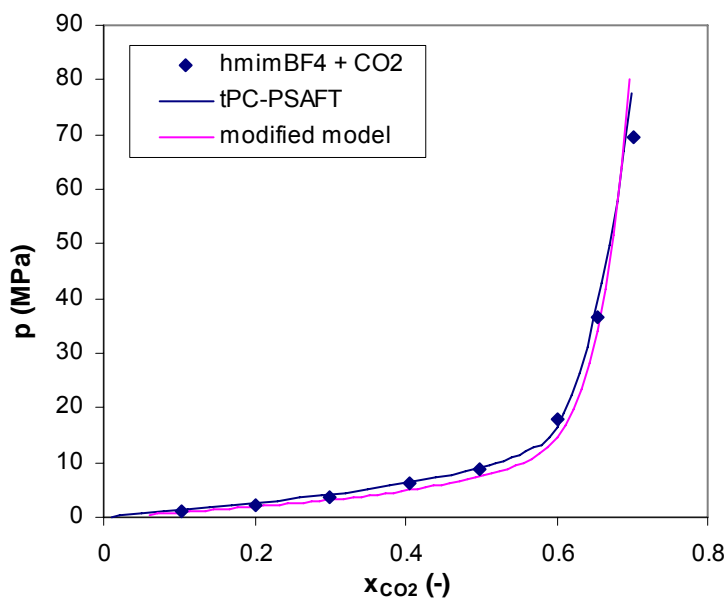
Figure 6.10: Comparison of the tPC-PSAFT model (complete association of the cation and anion) and the modified model (partly association of the cation and anion) for the prediction of the bubble-point pressures of the [hmim][BF$_4$] + CO$_2$ system at 333.15 K

6.5 Conclusions

The tPC-PSAFT equation of state is able to model the phase behavior of several imidazolium-based ionic liquid + carbon dioxide systems, where the dipolar interactions between the ionic liquid molecules, the quadrupolar interactions between the carbon dioxide molecules, and the Lewis acid – base association between the ionic liquid molecules and the carbon dioxide molecules are explicitly taken into account. Physically meaningful pure-component parameters were estimated on the basis of literature data and by using standard combining rules. The sole parameter that was fitted to experimental vapor-liquid equilibrium data was the binary interaction parameter. This binary interaction parameter increases linearly with temperature. The best agreement with experimental data and the lowest binary interaction parameter values were observed for ionic liquid + carbon dioxide mixtures where the alkyl chain was the longest and the temperature was the lowest. The assumption that ionic liquid molecules are present as ion pairs results in a better fit with experimental data compared to the situation in which ionic liquids are considered to be two separate charged species i.e., anion and cation.

6.6 List of symbols

Table 6.5: Roman symbols

Symbol	Quantity	Unit
a	molar Helmholtz free energy	$[\text{J}\cdot\text{mol}^{-1}]$
a_i	coefficient in equation 6.9	[-]
a^{assoc}	association contribution to molar Helmholtz free energy	$[\text{J}\cdot\text{mol}^{-1}]$
a^{chain}	chain formation contribution to molar Helmholtz free energy	$[\text{J}\cdot\text{mol}^{-1}]$
a^{disp}	dispersion contribution to molar Helmholtz free energy	$[\text{J}\cdot\text{mol}^{-1}]$
a^{hs}	hard sphere contribution to molar Helmholtz free energy	$[\text{J}\cdot\text{mol}^{-1}]$
a^{ideal}	molar Helmholtz free energy of ideal gas	$[\text{J}\cdot\text{mol}^{-1}]$
a^{polar}	multipolar contribution to molar Helmholtz free energy	$[\text{J}\cdot\text{mol}^{-1}]$
a^{res}	residual molar Helmholtz free energy	$[\text{J}\cdot\text{mol}^{-1}]$
b_i	coefficient in equation 6.10	[-]
C	constant with value 0.12 for all components except H_2	[-]
C_1	compressibility factor in equation 6.7	[-]
I_1	integral in equation 6.7	[-]
I_2	integral in equation 6.7	[-]
k	Boltzmann constant	$[\text{J}\cdot\text{K}^{-1}]$
k_{ij}	binary interactions parameter	[-]
m	segment number	[-]
M	number of association sites per molecule	[-]
M_w	molecular weight	$[\text{g}\cdot\text{mol}^{-1}]$
n	number of electrons	[-]
N_A	Avogadro's number	$[\text{mol}^{-1}]$
p	pressure	[Pa]
Q	quadrupole moment	[DÅ]
r	radius	[m]
R	universal gas constant	$[\text{J}\cdot\text{mol}^{-1}\cdot\text{K}^{-1}]$
T	temperature	[K]
u	segment dispersive energy	[J]
v^o	temperature-dependent segment molar volume	$[\text{m}^3\cdot\text{mol}^{-1}]$
v^{oo}	temperature-independent segment molar volume	$[\text{m}^3\cdot\text{mol}^{-1}]$
x_i	mole fraction of component i	[-]
X^A	mole fraction of molecules not bonded at site A	[-]

Table 6.6: Greek symbols

Symbol	Quantity	Unit
α	polarizability	$[\text{Å}^3]$
Δ^{AB}	association strength between site A and site B	$[\text{m}^3\cdot\text{mol}^{-1}]$
ΔH^{dissol}	enthalpy of dissolution	$[\text{J}\cdot\text{mol}^{-1}]$
ΔS^{dissol}	entropy of dissolution	$[\text{J}\cdot\text{mol}^{-1}\cdot\text{K}^{-1}]$

Continuation of table 6.6: Greek symbols

Symbol	Quantity	Unit
ε^{AB}	association energy	[J]
η	reduced density/segment packing fraction	[-]
κ^{AB}	association volume	[-]
μ	dipole moment	[D]
ρ	molar density	[mol·m^{-3}]
σ	segment diameter	[m]
σ_p	effective polar interaction diameter	[m]
τ	constant with value $\pi/6 \cdot \sqrt{2}$ $(= 0.74078)$	[-]

6.7 References

1. Kroon, M. C.; Florusse, L. J.; Shariati, A.; Gutkowski, K. E.; Van Spronsen, J.; Sheldon, R. A.; Witkamp, G. J.; Peters, C. J. On a Novel Class of Production Processes for the Chemical Industry, to be submitted for publication to *Nature* **2006**.

2. Shariati, A.; Simons, C.; Sheldon, R. A.; Witkamp, G. J.; Peters, C. J.; Enantio-selective Catalytic Hydrogenation of Methyl α-acetamidocinnamate in [bmim][BF$_4$], submitted for publication to *Green Chem.* **2006**.

3. Kroon, M. C.; Shariati, A.; Costantini, M.; Van Spronsen, J.; Witkamp, G. J.; Sheldon, R. A.; Peters, C. J.; High-Pressure Phase Behavior of Systems with Ionic Liquids: Part V. The Binary System Carbon Dioxide + 1-Butyl-3-methyl-imidazolium Tetrafluoroborate, *J. Chem. Eng. Data* **2005**, *50 (1)*, 173-176.

4. Husson-Borg, P.; Majer, V.; Costa Gomes, M. F.; Solubilities of Oxygen and Carbon Dioxide in Butyl Methyl Imidazolium Tetrafluoroborate as a Function of Temperature and at Pressures Close to Atmospheric Pressure, *J. Chem. Eng. Data* **2003**, *48 (3)*, 480-485.

5. Kamps, A. P. S.; Tuma, D.; Xia, J.; Maurer, G.; Solubility of CO$_2$ in the Ionic Liquid [bmim][PF$_6$], *J. Chem. Eng. Data* **2003**, *48 (3)*, 746-749.

6. Camper, D.; Scovazzo, P.; Koval, C.; Noble, R.; Gas Solubilities in Room Temperature Ionic Liquids, *Ind. Eng. Chem. Res.* **2004**, *43 (12)*, 3049-3054.

7. Aki, S. N. V. K.; Mellein, B. R.; Saurer, E. M.; Brennecke, J. F.; High-Pressure Phase Behavior of Carbon Dioxide with Imidazolium-Based Ionic Liquids, *J. Phys. Chem. B* **2004**, *108 (52)*, 20355-20365.

8. Anthony, J. L.; Anderson, J. L.; Maginn, E. J.; Brennecke, J. F.; Anion Effects on Gas Solubilities in Ionic Liquids, *J Phys. Chem. B* **2005**, *109 (13)*, 6366-6374.

9. Shiflett, M. B.; Yokozeki, A.; Solubilities and Diffusivities of Carbon Dioxide in Ionic Liquids: [bmim][PF$_6$] and [bmim][BF$_4$], *Ind. Eng. Chem. Res.* **2005**, *44 (12)*, 4453-4464.

10. Baltus, R. E.; Culbertson, B. H.; Dai, S.; Luo, H.; DePaoli, D. W.; Low-Pressure Solubility of Carbon Dioxide in Room-Temperature Ionic Liquids Measured with a Quartz Crystal Microbalance, *J. Phys. Chem. B* **2004**, *108 (2)*, 721-727.

11. Kim, Y. S.; Choi, W. Y.; Jang, J. H.; Yoo, K. P.; Lee, C. S.; Solubility Measurement and Prediction of Carbon Dioxide in Ionic Liquids, *Fluid Phase Equilib.* **2005**, *228-229*, 439-445.

12. Shariati, A.; Peters, C. J.; High-Pressure Phase Behavior of Systems with Ionic Liquids: II. The Binary System Carbon Dioxide + 1-Ethyl-3-methylimidazolium Hexafluorophosphate, *J. Supercrit. Fluids* **2004**, *29 (1-2)*, 43-48.

13. Shariati, A.; Peters, C. J.; High-Pressure Phase Behavior of Systems with Ionic Liquids: Part III. The Binary System Carbon Dioxide + 1-Hexyl-3-methyl-imidazolium Hexafluorophosphate, *J. Supercrit. Fluids* **2004**, *30 (2)*, 139-144.

14. Constantini, M.; Toussaint, V. A.; Shariati, A.; Peters, C. J.; Kikic, I.; High-Pressure Phase Behavior of Systems with Ionic Liquids: Part IV. Binary System Carbon Dioxide + 1-Hexyl-3-methylimidazolium Tetrafluoroborate, *J. Chem Eng. Data*, **2005**, *50 (1)*, 52-55.

15. Shariati, A.; Gutkowski, K.; Peters, C. J.; Comparison of the Phase Behavior of Some Selected Binary Systems with Ionic Liquids, *AIChE J.* **2005**, *51 (5)*, 1532-1540.

16. Shariati, A.; Peters, C. J.; High-Pressure Phase Equilibria of Systems with Ionic Liquids, *J. Supercrit. Fluids* **2005**, *34 (2)*, 171-182.

17. Shah, J. K.; Maginn, E. J.; Monte Carlo Simulations of Gas Solubility in the Ionic Liquid 1-n-Butyl-3-methylimidazolium Hexafluorophosphate, *J. Phys. Chem. B* **2005**, *109 (20)*, 10395-10405.

18. Urukova, I.; Vorholz, J.; Maurer, G.; Solubility of CO_2, CO and H_2 in the Ionic Liquid [bmim][PF_6] from Monte Carlo Simulations, *J. Phys. Chem. B* **2005**, *109 (24)*, 12154-12159.

19. Shah, J. K.; Maginn, E. J.; A Monte Carlo Simulation Study of the Ionic Liquid 1-n-Butyl-3-methylimidazolium Hexafluorophosphate: Liquid Structure, Volumetric Properties and Infinite Dilution Solution Thermodynamics of CO_2, *Fluid Phase Equilib.* **2004**, *222-223*, 195-203.

20. Shim, Y.; Choi, M. Y.; Kim, H. J.; A Molecular Dynamics Computer Simulation Study of Room-Temperature Ionic Liquids. 1. Equilibrium Solvation Structure and Free Energies, *J. Chem. Phys.* **2005**, *122 (4)*, 044510/1-044510/12.

21. Huang, X.; Margulis, C. J.; Li, Y.; Berne, B. J.; Why is the Partial Molar Volume of CO_2 So Small When Dissolved in a Room Temperature Ionic Liquid? Structure and Dynamics of CO_2 Dissolved in [$Bmim^+$][PF_6^-], *J. Am. Chem. Soc.* **2005**, *127 (50)*, 17842-17851.

22. Lee, S. B.; Analysis of Solvation in Ionic Liquids Using a New Linear Solvation Energy Relationship, *J. Chem. Technol. Biotechnol.* **2005**, *80 (2)*, 133-137.

23. Carda-Broch, S.; Berthod, A.; Armstrong, D. W.; Solvent Properties of the 1-Butyl-3-methylimidazolium Hexafluorophosphate Ionic Liquid, *Anal. Bioanal. Chem.* **2003**, *375 (2)*, 191-199.

24. Ally, M. R.; Braunstein, J.; Baltus, R. E.; Dai, S.; DePaoli, D. W.; Simonson, J. M.; Irregular Ionic Lattice Model for Gas Solubilities in Ionic Liquids, *Ind. Eng. Chem. Res.* **2004**, *43 (5)*, 1296-1301.

25. Scovazzo, P.; Camper, D.; Kieft, J.; Poshusta, J.; Koval, C.; Noble, R.; Regular Solution Theory and CO_2 Gas Solubility in Room-Temperature Ionic Liquids, *Ind. Eng. Chem. Res.* **2004**, *43 (21)*, 6855-6860.

26. Shiflett, M. B.; Yokozeki, A.; Solubilities and Diffusivities of Carbon Dioxide in Ionic Liquids: [bmim][PF_6] and [bmim][BF_4], *Ind. Eng. Chem. Res.* **2005**, *44 (12)*, 4453-4464.

27. Shariati, A.; Peters, C. J.; High-Pressure Phase Behavior of Systems with Ionic Liquids: Measurements and Modeling of the Binary System Fluoroform + 1-Ethyl-3-methylimidazolium Hexafluorophosphate, *J. Supercrit. Fluids* **2003**, *25 (2)*, 109-117.

28. Belvèze, L. S.; Brennecke, J. F.; Stadtherr, M. A.; Modeling of Activity Coefficients of Aqueous Solutions of Quaternary Ammonium Salts with the Eletrolyte-NRTL Equation, *Ind. Eng. Chem. Res.* **2004**, *43 (3)*, 815-825.

29. Rebelo, L. P. N.; Najdanovic-Visak, V.; Visak, Z. P.; Nunes da Ponte, M.; Szydlowski, J.; Cerdeiriña, C. A.; Troncoso, J.; Romaní, L.; Esperança, J. M. S.

_____

S.; Guedes, H. J. R.; De Sousa, H. C.; A Detailed Thermodynamic Analysis of [C$_4$mim][BF$_4$] + Water as a Case Study to Model Ionic Liquid Aqueous Solutions, *Green. Chem.* **2004**, *6 (8)*, 369-381.

30. Banerjee, T.; Singh, M. K.; Kumar Sahoo, R.; Khanna, A.; Volume, Surface and UNIQUAC Interaction Parameters for Imidazolium Based Ionic Liquids via Polarizable Continuum Model, *Fluid Phase Equilib.* **2005**, *234 (1-2)*, 64-76.

31. Kroon, M. C.; Karakatsani, E. K.; Economou, I. G.; Witkamp, G. J.; Peters, C. J.; Modeling of the Carbon Dioxide Solubility in Imidazolium-Based Ionic Liquids with the PC-PSAFT Equation of State, *J. Phys. Chem. B* **2006**, *110 (18)*, 9262-9269.

32. Katsyuba, S. A.; Dyson, P. J.; Vandyukova, E. E.; Chernova, A. V.; Vidiš, A.; Molecular Structure, Vibrational Spectra, and Hydrogen Bonding of the Ionic Liquid 1-Ethyl-3-methyl-1H-imidazolium Tetrafluoroborate, *Helvetica Chim. Acta* **2004**, *87 (10)*, 2556-2565.

33. Anthony, J. H.; Mertens, D.; Breitenschein, T.; Dölle, A.; Wasserscheid, P.; Carper, W. R.; Molecular Structure, Reorientation Dynamics, and Intermolecular Interactions in the Neat Ionic Liquid 1-Butyl-3-methylimidazolium Hexafluoro-phosphate, *Pure Appl. Chem.* **2004**, *76 (1)*, 255-261.

34. Paulechka, Y. U.; Kabo, G. J.; Blokhin, A. V.; Vydrov, O. A.; Magee, J. M.; Frenkel, M.; Thermodynamic Properties of 1-Butyl-3-methylimidazolium Hexafluorophosphate in the Ideal Gas State, *J. Chem. Eng. Data* **2003**, *48 (3)*, 457-462.

35. Wasserscheid, P.; Welton, T., Eds. *Ionic Liquids in Synthesis*; Wiley-VHC Verlag: Weinheim, Germany, 2003.

36. Carmichael, A. J.; Seddon, K. R.; Polarity Study of Some 1-Alkyl-3-methylimidazolium Ambient-Temperature Ionic Liquids with the Solvatochromic Dye, Nile Red, *J. Phys. Org. Chem.* **2000**, *13 (10)*, 591-595.

37. Buckingham, A. D.; Disch, R. L.; The Quadrupole Moment of the Carbon Dioxide Molecule, *Proc. Roy. Soc. (London) Ser. A* **1963**, *273 (1353)*, 275-289.

38. Cadena, C.; Anthony, J. L.; Shah, J. K.; Morrow, T. I.; Brennecke, J. F.; Maginn, E. J.; Why is CO$_2$ So Soluble in Imidazolium-Based Ionic Liquids?, *J. Am. Chem. Soc.* **2004**, *126 (16)*, 5300-5308.

39. Kazarian, S. G.; Briscoe, B. J.; Welton, T.; Combining Ionic Liquids and Supercritical Fluids: in situ ATR-IR Study of CO$_2$ Dissolved in Two Ionic Liquids at High Pressures, *Chem. Commun.* **2000**, *(20)*, 2047-2048.

40. Chapman, W. G.; Gubbins, K. E.; Jackson, G.; Radosz, M.; SAFT: Equation of State Solution Model for Associating Fluids, *Fluid Phase Equilib.* **1989**, *52*, 31-38.

41. Chapman, W. G.; Gubbins, K. E.; Jackson, G.; Radosz, M.; New Reference Equation of State for Associating Liquids, *Ind. Eng. Chem. Res.* **1990**, *29 (8)*, 1709-1721.

42. Huang, S. H.; Radosz, M.; Equation of State for Small, Large, Polydisperse, and Associating Molecules, *Ind. Eng. Chem. Res.* **1990**, *29 (11)*, 2284-2294.

43. Huang, S. H.; Radosz, M.; Equation of State for Small, Large, Polydisperse, and Associating Molecules: Extension to Fluid Mixtures, *Ind. Eng. Chem. Res.* **1991**, *30 (8)*, 1994-2005.

44. Wertheim, M. S.; Fluids with Highly Directional Attractive Forces. I. Statistical Thermodynamics, *J. Stat. Phys.* **1984**, *35 (1-2)*, 19-34.

45. Wertheim, M. S.; Fluids with Highly Directional Attractive Forces. II. Thermodynamic Perturbation Theory and Integral Equations, *J. Stat. Phys.* **1984**, *35 (1-2)*, 35-47.

46. Wertheim, M. S.; Fluids with Highly Directional Attractive Forces. III. Multiple Attraction Sites, *J. Stat. Phys.* **1986**, *42 (3-4)*, 459-476.

47. Wertheim, M. S.; Fluids with Highly Directional Attractive Forces. IV. Equilibrium Polymerization, *J. Stat. Phys.* **1986**, *42 (3-4)*, 477-492.

48. Gross, J.; Sadowski, G.; Perturbed-Chain SAFT: An Equation of State Based on a Perturbation Theory for Chain Molecules, *Ind. Eng. Chem. Res.* **2001**, *40 (4)*, 1244-1260.

49. Walsh, J. M.; Guedes, H. J. R.; Gubbins K. E.; Physical Theory for Fluids of Small Associating Molecules, *J Phys Chem.* **1992**, *96 (26)*, 10995-11004.

50. Jog, P. K.; Chapman, W. G.; Application of Wertheim's Thermodynamic Perturbation Theory to Dipolar Hard Sphere Chains, *Mol. Phys.* **1999**, *97 (3)*, 307-319.

51. Jog, P.; Sauer, S. G.; Blaesing, J.; Chapman, W. G.; Application of Dipolar Chain Theory to the Phase Behavior of Polar Fluids and Mixtures, *Ind. Eng. Chem. Res.* **2001**, *40 (21)*, 4641-4648.

52. Sauer, S. G.; Chapman, W. G.; A Parametric Study of Dipolar Chain Theory with Applications to Ketone Mixtures, *Ind. Eng. Chem. Res.* **2003**, *42 (22)*, 5687-5696.

53. Chapman, W. G.; Sauer, S. G.; Ting, D.; Ghosh, A.; Phase Behavior Applications of SAFT Based Equations of State – From Associating Fluids to Polydisperse, Polar Copolymers, *Fluid Phase Equilib.* **2004**, *217 (2)*, 137-143.

54. Tumakaka, F.; Sadowski, G.; Application of the Perturbed-Chain SAFT Equation of State to Polar Systems, *Fluid Phase Equilib.* **2004**, *217 (2)*, 233-239.

55. Tumakaka, F.; Gross, J.; Sadowski, G.; Thermodynamic Modeling of Complex Systems Using PC-SAFT, *Fluid Phase Equilib.* **2005**, *228-229*, 89-98.

56. Gross, J.; An Equation of State Contribution for Polar Components: Quadrupolar Molecules, *AIChE J.* **2005**, *51 (9)*, 2556-2568.

57. Karakatsani, E. K.; Spyriouni, T.; Economou, I. G.; Extended Statistical Associating Fluid Theory (SAFT) Equations of State for Dipolar Fluids, *AIChE J.* **2005**, *51 (8)*, 2328-2342.

58. Karakatsani, E. K.; Economou, I. G.; Perturbed Chain-Statistical Associating Fluid Theory Extended to Dipolar and Quadrupolar Molecular Fluids, *J. Phys. Chem. B* **2006**, *110 (18)*, 9252-9261.

59. Stell G.; Rasaiah, J. C.; Narang, H.; Thermodynamic Perturbation Theory for Simple Polar Fluids. II. *Mol Phys.* **1974**, *27 (5)*, 1393-1414.

60. Larsen, B.; Rasaiah, J. C.; Stell, G.; Thermodynamic Perturbation Theory for Multipolar and Ionic Liquids, *Mol. Phys.* **1977**, *33 (4)*, 987-1027.

61. Prausnitz, J. M.; Lichtenthaler, R. N.; Gomes De Azevedo, E. *Molecular Thermodynamics of Fluid-Phase Equilibria*, 3rd ed.; Prentice Hall: Upper Saddle River (NJ), USA, 1999.

62. Carnahan, N. F.; Starling, K. E.; Equation of State for Nonattracting Rigid Spheres, *J Chem. Phys.* **1969**, *51 (2)*, 635-636.

63. Chen, S. S.; Kreglewski, A.; Applications of the Augmented van der Waals Theory of Fluids. I. Pure Fluids, *Ber. Bunsen-Ges. Phys. Chem.* **1977**, *81 (10)*, 1048-1052.

64. Kraska, T.; Analytic and Fast Numerical Solutions and Approximations for Cross-Association Models within Statistical Association Fluid Theory, *Ind. Eng. Chem. Res.* **1998**, *37 (12)*, 4889-4892.

65. Vega, C.; A Perturbation Theory of Hard Quadrupolar Fluids, *Mol. Phys.* **1992**, *75 (2)*, 427-442.

66. Rasaiah, J. C.; Stell. G.; Three-Body Free-Energy Terms and Effective Potentials in Polar Fluids and Ionic Solutions, *Chem. Phys. Lett.* **1974**, *25 (4)*, 519-522.

67. Nezbeda, I.; Structure of Water: Short-Ranged Versus Long-Ranged Forces, *Czech. J. Phys.* **1998**, *48 (1)*, 117-122.

68. Kolafa, J.; Nezbeda, I.; Effect of Short and Long Range Forces on the Structure of Water. II. Orientational Ordering and the Dielectric Constant, *Mol. Phys.* **2000**, *98 (19)*, 1505-1520.

69. Kettler, M.; Nezbeda, I.; Chialvo, A.A.; Cummings, P.T.; Effect of the Range of Interactions on the Properties of Fluids. Phase Equilibria in Pure Carbon Dioxide, Acetone, Methanol, and Water, *J. Phys. Chem. B* **2002**, *106 (30)*, 7537-7546.

70. McEwen, A. B.; Ngo, H. L.; LeCompte, K.; Goldman, J. L.; Electrochemical Properties of Imidazolium Salt Electrolytes for Electrochemical Capacitor Applications, *J. Electrochem. Soc.* **1999**, *146 (5)*, 1687-1695.

71. Mavroyannis, C.; Stephen, M. J.; Dispersion Forces, *Mol. Phys.* **1962**, *5 (6)*, 629-638.

72. Lide, D.R., Ed. *Handbook of Chemistry and Physics*, 78th ed.; CRC Press: New York (NY), USA, 1997.

73. Wakai, C.; Oleinikova, A.; Ott, M.; Weingärtner, H.; How Polar Are Ionic Liquids? Determination of the Static Dielectric Constant of an Imidazolium-Based Ionic Liquid by Microwave Dielectric Spectroscopy, *J. Phys. Chem. B* **2005,** *109 (36),* 17028-17030.

74. Znamenskiy, V.; Kobrak, M. N.; Molecular Dynamics Study of Polarity in Room-Temperature Ionic Liquids, *J. Phys. Chem. B* **2004,** *108 (3),* 1072-1079.

75. Meng, Z.; Dölle, A.; Carper, W. R.; Gas Phase Model of an Ionic Liquid: Semi-Empirical and Ab Initio Bonding and Molecular Structure, *J. Mol. Structure (Theochem)* **2002**, *585 (1-3)*, 119-128.

76. Wolbach, J. P.; Sandler, S. I.; Using Molecular Orbital Calculations to Describe the Phase Behavior of Cross-Associating Mixtures, *Ind. Eng. Chem. Res.* **1998**, *37 (8)*, 2917-2928.

77. Crosthwaite, J. M.; Muldoon, M. J.; Aki, S. N. V. K.; Maginn, E. J.; Brennecke, J. F.; Liquid Phase Behavior of Ionic Liquids with Alcohols: Experimental Studies and Modeling, *J. Phys. Chem. B* **2006**, *110 (18)*, 9354-9361.

---

78. Blanchard, L. A.; Hancu, D.; Beckman, E. J.; Brennecke, J. F.; Green Processing Using Ionic Liquids and CO_2, *Nature* **1999**, *399 (6731)*, 28-29.

79. Blanchard, L. A.; Brennecke, J. F.; Recovery of Organic Products from Ionic Liquids Using Supercritical Carbon Dioxide, *Ind. Eng. Chem. Res.* **2001**, *40 (1)*, 287-292.

80. Blanchard, L. A.; Gu, Z.; Brennecke, J. F.; High-Pressure Phase Behavior of Ionic Liquid/ CO_2 Systems, *J. Phys. Chem. B* **2001**, *105 (12)*, 2437-2444.

81. Blum, L.; Høye, J. S.; Mean Spherical Model for Asymmetric Electrolytes. 2. Thermodynamic Properties and the Pair Correlation Function, *J. Phys. Chem.* **1977**, *81 (13)*, 1311-1316.

82. Li, X. S.; Lu, J. F.; Li, Y. G.; Study on Ionic Surfactant Solutions by SAFT Equation Incorporated with MSA, *Fluid Phase Equilib.* **2000**, *168 (1)*, 107-123.

83. Klamt, A.; Cosmotherm_Edu: A Tool for Turning Molecular Thermodynamics Into a Vivid Experience, Proceedings of Thermo International 2006: Boulder (CO), USA, July 2006.

7

Limits to Operation Conditions: Thermal Stability of Ionic Liquids

7
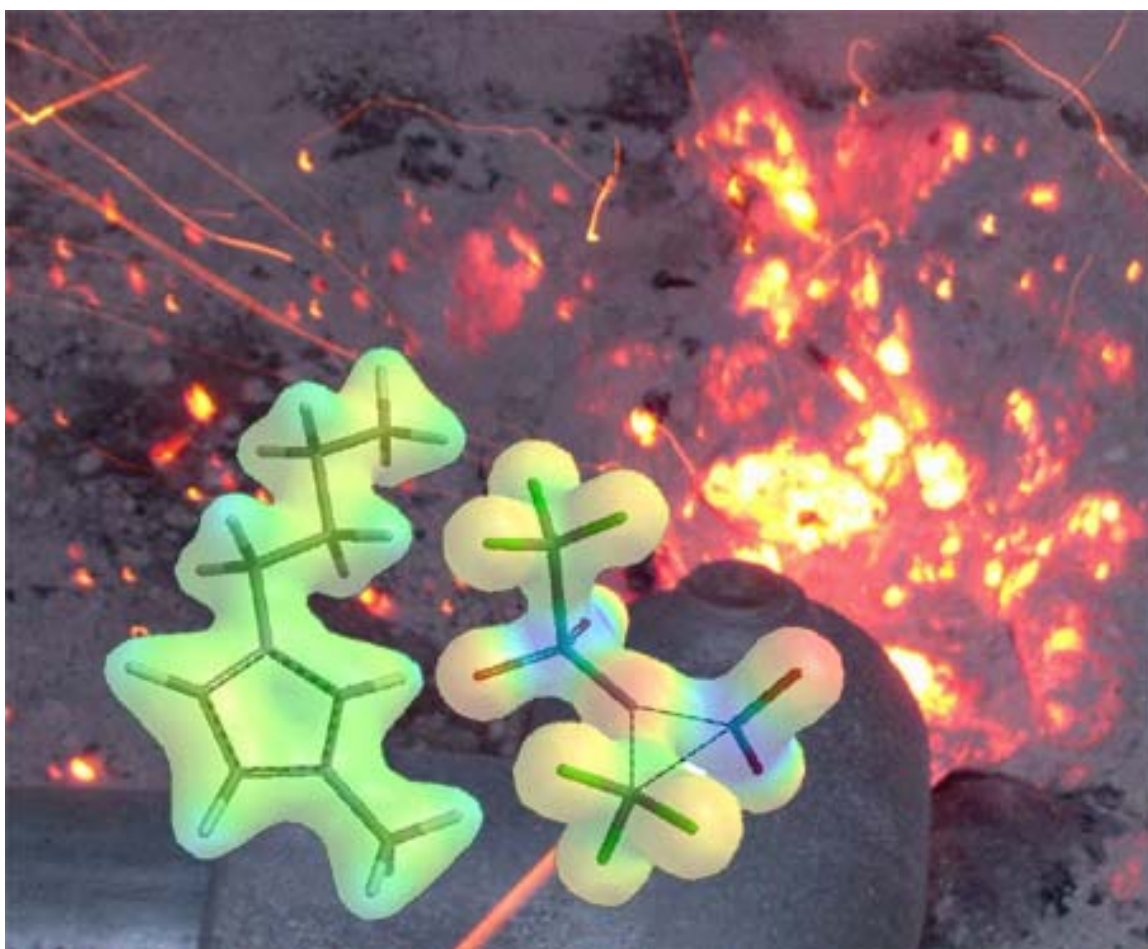
Limits to Operation Conditions: Thermal Stability of Ionic Liquids

The long-term thermal stability of ionic liquids is of utmost importance for their industrial application. Although the thermal decomposition temperatures of various ionic liquids have been measured previously, experimental data on the thermal decomposition mechanisms and kinetics are scarce. It is desirable to develop quantitative chemical tools that can predict thermal decomposition mechanisms and temperatures (kinetics) of ionic liquids. In this chapter ab initio quantum chemical calculations (DFT-B3LYP) have been used to predict thermal decomposition mechanisms, temperatures and the activation energies of the thermal breakdown reactions. These quantum chemical calculations proved to be an excellent method to predict the thermal stability of various ionic liquids.

7. Limits to Operation Conditions: Thermal Stability of Ionic Liquids

7.1 Introduction

In the previous chapters, a new process set-up for combining reactions and separations using ionic liquids and supercritical carbon dioxide has been described. For every chemical process, limits of operation are defined by the stability of the chemicals and the equipment specifications. Because the new process set-up requires prolonged operation at elevated temperatures, it is essential to know the long-term stability of ionic liquids.

The thermal stability of an ionic liquid is manifested by the height of the thermal decomposition temperature and has been extensively studied for a variety of ionic liquids using thermogravimetric analysis (TGA) at a single linear heating rate (10 to 20 ^{o}C/min)[1-13]. It was found that the decomposition temperature strongly depends on the ionic liquid structure. Ionic liquids with poorly proton-abstracting anions, such as the bis(trifluoro-methylsulfonyl)imide anion, are the most stable to high-temperature decomposition ($T^{decomp} \approx 420$ ^{o}C), whereas ionic liquids with nucleophilic and highly proton-abstracting anions, such as halides, decompose at much lower temperatures. ($T^{decomp} \approx 270$ ^{o}C)[1-8]. The decomposition temperature of ionic liquids also depends on the type of cation. For example, the imidazolium-based ionic liquids appear to have a better thermal stability than the pyridinium-based and tetraalkylammonium-based ionic liquids[1,9-11]. Methyl substitution on the 2-position of the imidazolium-cation enhances the thermal stability due to the removal of the acidic hydrogen[2,7,11,12]. The alkyl chain length of the alkyl group on the cation does not have a large effect on the thermal stability of the ionic liquids[13]. Finally, it was found that the conditions of measurement (atmosphere, pan composition) have some impact on the thermal stability of the ionic liquid[1]. For example, imidazolium-based hexafluorophosphate ionic liquids decompose at lower temperatures in the presence of an air atmosphere and an aluminum pan, compared to a nitrogen atmosphere and an alumina pan.

In literature, mostly overestimated long-term thermal stabilities are reported, which are calculated from TGA-measurements by intersection of a straight baseline (in the low-temperature region without weight-loss) with the tangent of the weight versus temperature (in the high-temperature decomposition region)[14]. An example of such a TGA-curve can be found in figure 7.1. From figure 7.1 it can be seen that the decomposition already starts far below the onset temperature (~100 ^{o}C). Moreover, the sample is heated fast and extremely brief compared to long-term operation, leading to the overestimation of the temperature at which decomposition starts (T_{start} in figure 7.1)[14-17]. For a better understanding of the thermal decomposition of ionic liquids, more detailed information on the decomposition mechanism and kinetics is needed.

_____
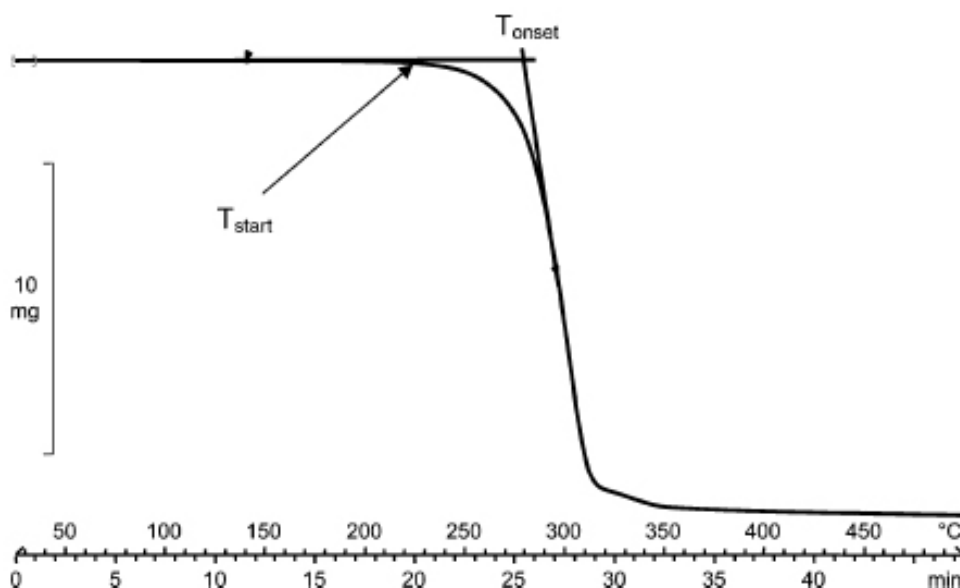
Figure 7.1: Characteristic decomposition curve determined by TGA, indicating the start and onset temperatures[2]

So far, only a few attempts were made to analyze the thermal decomposition mechanism, the decomposition kinetics and the decomposition products of ionic liquids. Chan *et al.*[18] found that 1-ethyl-3-methylimidazolium halide ionic liquids decompose by an attack of the highly nucleophilic halide on the primary alkyl group (S_N2 reaction), with 1-ethylimidazole and methyl halide as the main products[19]. Therefore, imidazolium-based ionic liquids decompose at lower temperatures in the presence of nucleophiles[20]. It was argued that branched alkyl groups are attacked by the halide via an S_N1 reaction, leading to lower decomposition temperatures[7]. Baranyai *et al.*[17] investigated the thermal decomposition mechanism of 1,3-dialkylimidazolium bis(trifluoromethylsulfonyl)imide ionic liquids, and suggested degradation of the anion as possible thermal decomposition pathway, but the anion degradation products were not detected. Wooster *et al.*[21] found that pyrrolidinium ionic liquids decompose under formation of *N*-alkyl pyrrolidine. Furthermore, it was found that bis(trifluoromethylsulfonyl) imide ionic liquids undergo exothermic decomposition, whereas halide ionic liquids decompose endothermically[1]. Kinetics of the thermal decomposition of 1-butyl-2,3-dimethylimidazolium tetrafluoroborate were measured by Fox *et al.*[16]

The thermal decomposition mechanism and kinetics of most ionic liquids are still unknown. A first reason is that the number of ionic liquids is very large. Moreover, it is impossible to measure the thermal decomposition mechanism and kinetics of all ionic liquids, because the synthesis of a large variety of ionic liquids is cumbersome and measurements are time-consuming and expensive. A tool to predict thermal decomposition properties of ionic liquids on basis of their structure is desired. This tool should not only calculate a maximum operating temperature below which no thermal

_____

degradation occurs, but also indicate how rapidly an ionic liquid decomposes at a specific temperature (kinetics) and predict which decomposition products are formed (mechanism). So far, such a tool is non-existent.

In this chapter quantum chemical calculations will be used to develop a tool that predicts the thermal stability of ionic liquids[22]. This chapter aims to use the quantum chemical calculations (density functional theory, B3LYP) only as a predictive tool for the decomposition reactions of ionic liquids, and not to provide the highest accurate chemical structures of the ionic liquids using the most advanced quantum chemical theory. The thermal breakdown phenomena, including the type of thermal decomposition reactions and products that are formed under high temperatures, as well as the thermal decomposition temperatures and kinetics of a variety of ionic liquids, are predicted[21]. Moreover, the obtained mechanistic information gives insight into the reactivity of ionic liquids with certain chemical compounds, such as the reactor construction material or the solute that is distilled from an ionic liquid. Finally, the height of the decomposition temperature determines whether an ionic liquid itself can be distilled albeit at very high temperatures and very low pressures, where ionic liquids have a measurable vapor pressure[23]. All these issues are particularly important for the selection of a suitable ionic liquid for a specific high-temperature application.

_____

7.2 Experimental

All quantum chemical calculations were carried out using the Spartan '04 molecular modeling suite of programs[24]. First, the ionic liquid structures were fully geometry-optimized using the semi-empirical PM3 method. This method aims to find a solution to the Schrödinger equation by drastic simplications and uses parameters derived from experimental data (PM3 parameterization) as compensation[25]. Next to the equilibrium geometries, also the transition state geometries of the thermal decomposition reactions (the minimization of the maximum energy in all possible reaction pathways) were calculated with the PM3 method. Thereafter, all PM3 structures were used as input for full optimization using Density Functional Theory calculations at the B3LYP level. This quantum chemical model uses an empirical estimate of the electron density (in this case the Becke-style three-parameter functional of Lee, Yang and Par = B3LYP) to account for the correlation of electron motion in the Schrödinger equation[25]. As basis set, the 6-31 G[**] basis set is chosen[25]. This is a Gaussian-type split-valence basis set that uses more basis functions to describe valence orbitals than core orbitals, since the valence orbitals are more affected by the molecular environment. In the 6-31G[**] basis set, the core orbital is made of 6 Gaussians and the valence orbital is described by two orbitals – one made of 3 Gaussians and one made of a single Gaussian. The two asterisks indicate that two polarization functions (= additional basis functions of higher angular momentum than the ground state) are added, one on non-hydrogen atoms and one on hydrogen atoms, in order to account for the fact that not all basis functions are atom-centered[25]. The B3LYP energies were used to calculate the activation energies of the decomposition reactions.

7.3 Results and discussion

In this chapter, the thermal decomposition mechanism and temperatures of several ionic liquids are predicted using quantum chemical calculations at the B3LYP level. The structures and total energies of the ionic liquids and the transitions states of the thermal decomposition reactions are calculated. The total energies are used to calculate the activation energy $\Delta E^{\ddagger}$ of the thermal decomposition reaction:

$$\Delta E^{\ddagger} = E_{transition\ state} - E_{reactant\ 1} - E_{reactant\ 2} - \ldots \tag{7.1}$$

In principle, it is possible to predict the kinetics of the decomposition reaction from the activation energy $\Delta E^{\ddagger}$. The simplest estimate for the reaction rate constant k_r of the thermal decomposition reaction is:

$$k_r = \left(\frac{k_B T}{h}\right)\exp\left(-\frac{\Delta E^{\ddagger}}{RT}\right) \tag{7.2}$$

wherein thermodynamic contributions are neglected, and k_B and h are the Boltzmann and Planck constants, respectively. A better prediction of the kinetics can be obtained using a more sophisticated quantum chemical approach for the pre-exponential factor. This will make the computational effort considerably larger, and thus make the application as a fast tool for pre-optimization less attractive. It will be shown that B3LYP calculations are sufficient to predict the thermal decomposition mechanism and temperature of ionic liquids, taking into account that previously measured experimental decomposition temperatures are not highly accurate due to their sensitivity to impurities.

First, the effect of the anion of the ionic liquid on the thermal decomposition mechanism and kinetics is investigated. Using quantum chemical calculations, the ionic liquids with highly nucleophilic anions, such as halides, were found to be thermally decomposing by dealkylation of the cation via an s_N2 reaction of the most easy accessible alkyl group, which is in agreement with experimental results[18]. For example, the ionic liquid 1-butyl-3-methylimidazolium chloride ([bmim][Cl]) decomposes into methyl chloride and 1-butylimidazole ($\Delta E^{\ddagger} = 127$ kJ/mol), which is favored over the formation of butyl chloride and 1-methylimidazole ($\Delta E^{\ddagger} = 136$ kJ/mol). This was also found in experiments[19]. Figure 7.2 schematically shows the thermal decomposition mechanism of [bmim][Cl] and figure 7.3 shows the corresponding calculated transition state geometry.
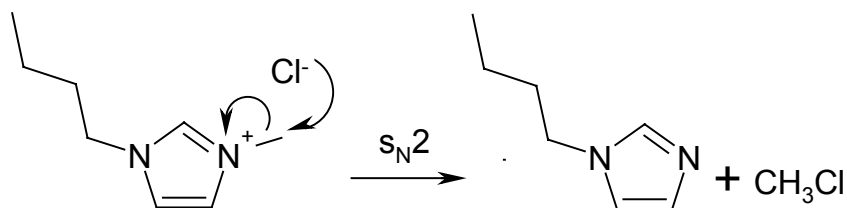
Figure 7.2: Thermal decomposition of [bmim][Cl] into methyl chloride and 1-butylimidazole ($\Delta E^{\ddagger}$ = 127 kJ/mol)
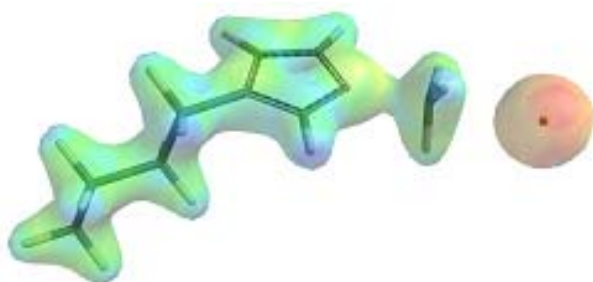
Figure 7.3: Transition state geometry (via $s_N 2$) of the thermal breakdown of [bmim][Cl] into methyl chloride and 1-butylimidazole (surface = electron density of 0.08 e/au^3; property = electrostatic potential). The electron density is high at the red positions (large negative values of the potential) and low at the blue positions (large positive values of the potential).

For the decomposition of the ionic liquids 1-butyl-3-methylimidazolium hexa-fluorophosphate ([bmim][PF$_6$]) and 1-butyl-3-methylimidazolium tetrafluoroborate ([bmim][BF$_4$]), two decomposition mechanisms seem to be possible. The first route involves the transfer of the proton on the C2-position to the anion, resulting in the formation of a 1-butyl-3-methylimidazolium carbene, hydrogen fluoride and PF$_5$ or BF$_3$ (see figure 7.4). The carbene is not stable, but reacts via an addition reaction with the double bond of a second ionic liquid molecule. The proton transfer step is an endothermic reaction that does not show any transition state. The energy barrier for this reaction is calculated from the difference in energy level of the products and reactants and is very high. For example, the energy barrier for the decomposition of [bmim][PF$_6$] via this route is as high as 313 kJ/mol, which is close to the upper limit of 347 kJ/mol for the breaking of carbon-carbon bonds in cracking reactions. Therefore, a decomposition mechanism with a smaller activation energy is more likely to occur.
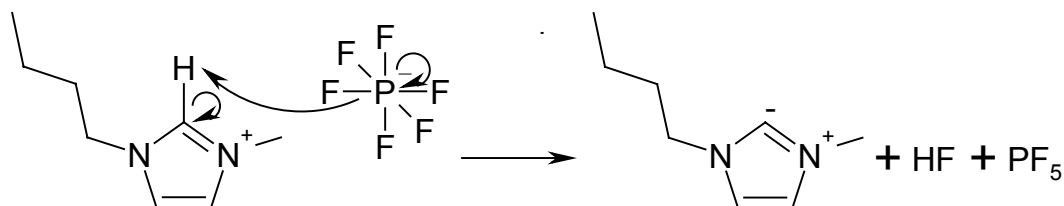
Figure 7.4: Thermal decomposition of [bmim][PF$_6$] into a 1-butyl-3-methylimidazolium carbene, HF and PF$_5$ ($\Delta E^{\ddagger}$ = 313 kJ/mol)

_____

The second possible route is the formation of 1-butylimidazole, methyl fluoride and PF_5 or BF_3 via an s_N2-mechanism (see figures 7.5 and 7.6), which is favored over the formation of 1-methylimidazole and butyl fluoride (see decomposition of [bmim][Cl]). The activation barrier of the thermal decomposition of [bmim][PF_6] via this route is only 213 kJ/mol, so this decomposition mechanism is favored. Also, for [bmim][BF_4] the second route is preferred ($\Delta E^{\ddagger}$ 195 kJ/mol) over the first route.
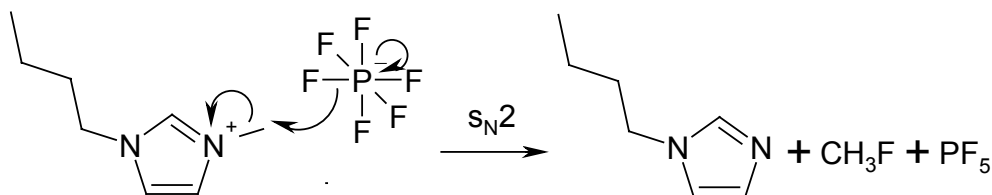
Figure 7.5: Thermal decomposition of [bmim][PF_6] into 1-butylimidazole, methyl fluoride and PF_5 ($\Delta E^{\ddagger}$ = 213 kJ/mol)
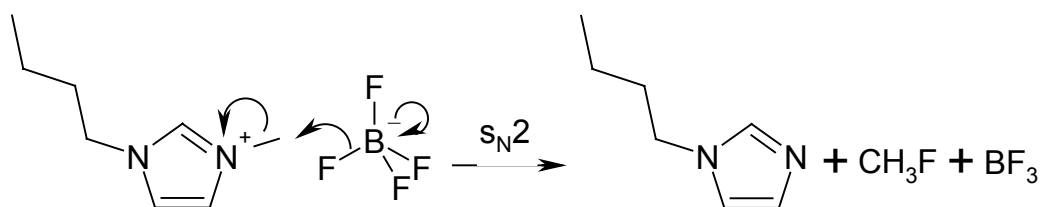
Figure 7.6: Thermal decomposition of [bmim][BF_4] into 1-butylimidazole, methyl fluoride and BF_3 ($\Delta E^{\ddagger}$ = 195 kJ/mol)

The transition state geometries of the decomposition of [bmim][PF_6] and [bmim][BF_4] via the second route are shown in figures 7.7 and 7.8, respectively.
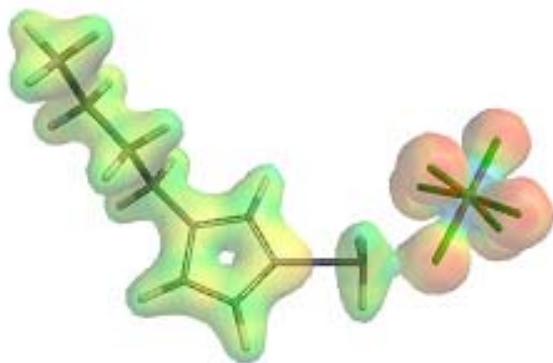
Figure 7.7: Transition state geometry (via s_N2) of the thermal breakdown of [bmim][PF_6] into 1-butylimidazole, methyl fluoride and PF_5 (surface = electron density of 0.08 e/au^3; property = electrostatic potential). The electron density is high at the red positions (large negative values of the potential) and low at the blue positions (large positive values of the potential).

_____
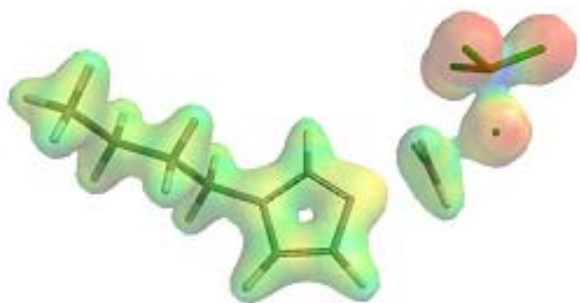
Figure 7.8: Transition state geometry (via s_N2) of the thermal breakdown of [bmim][BF$_4$] into 1-butylimidazole, methyl fluoride and BF$_3$ (surface = electron density of 0.08 e/au^3; property = electrostatic potential). The electron density is high at the red positions (large negative values of the potential) and low at the blue positions (large positive values of the potential).

It can be concluded that thermal degradation of [bmim][PF$_6$] and [bmim][BF$_4$] in the absence of water does not lead to the formation of hydrogen fluoride. However, when water is added to the system (or present as impurity in the ionic liquid), the methyl fluoride will react with water under the formation of methanol and hydrogen fluoride. This can be the reason for the experimental observation that hydrogen fluoride is formed in [bmim][PF$_6$] and [bmim][BF$_4$] ionic liquids at higher temperatures[1]. Finally, it can be concluded that [bmim][PF$_6$] and [bmim][BF$_4$] have a better thermal stability (higher activation energy) than [bmim][Cl], which is in accordance with experiments[8].

Dicyanamide ionic liquids also decompose via an s_N2 dealkylation. For example, the ionic liquid 1-butyl-3-methylimidazolium dicyanamide ([bmim][N(CN)$_2$]) decomposes into 1-butylimidazole and methylated dicyanamide ($\Delta E^{\ddagger} = 160$ kJ/mol), which is favored over the formation of 1-methylimidazole and butylated dicyanamide. Figure 7.9 schematically shows the thermal decomposition mechanism of [bmim][Cl] and in figure 7.10 the corresponding calculated transition state geometry is demonstrated. It can be noticed that [bmim][N(CN)$_2$] has a thermal stability higher than [bmim][Cl], but lower than [bmim][BF$_4$] and [bmim][PF$_6$], which is in agreement with experimental results[2].
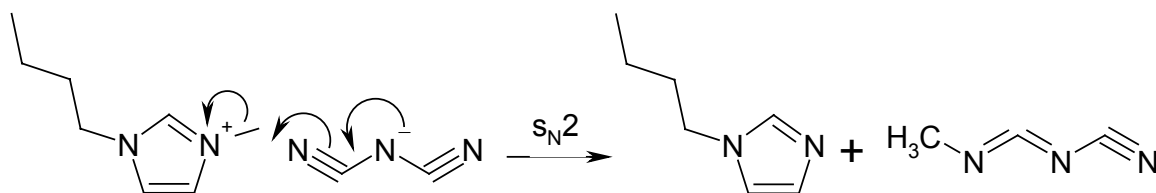
Figure 7.9: Thermal decomposition of [bmim][N(CN)$_2$] into butylimidazole and methylated dicyanamide ($\Delta E^{\ddagger} = 160$ kJ/mol)

_____

Figure 7.10: Transition state geometry (via s$_N$2) of the thermal breakdown of [bmim][N(CN)$_2$] into butylimidazole and methylated dicyanamide (surface = electron density of 0.08 e/au^3; property = electrostatic potential). The electron density is high at the red positions (large negative values of the potential) and low at the blue positions (large positive values of the potential).

Ionic liquids that contain non-nucleophilic anions, such as the bis(trifluoro-methylsulfonyl)imide anion, cannot decompose via dealkylation or proton transfer. According to the quantum chemical calculations, the lowest activation barrier reaction for the thermal breakdown of 1-butyl-3-methylimidazolium bis(trifluoromethylsulfonyl) imide ([bmim][NTf$_2$]) is the degradation of the anion by sulfur dioxide release (the cation stays intact, see figure 7.11 and 7.12). This is in agreement with the results from Baranyai et al.[17], that suggest degradation of the anion as possible thermal decomposition pathway. The activation energy of this thermal decomposition is 255 kJ/mol, from which it can be concluded that [bmim][NTf$_2$] is a more thermally stable ionic liquid than [bmim][Cl], [bmim][BF$_4$], [bmim][PF$_6$] and [bmim][N(CN)$_2$]. This was also found in experiments[2,3,8].
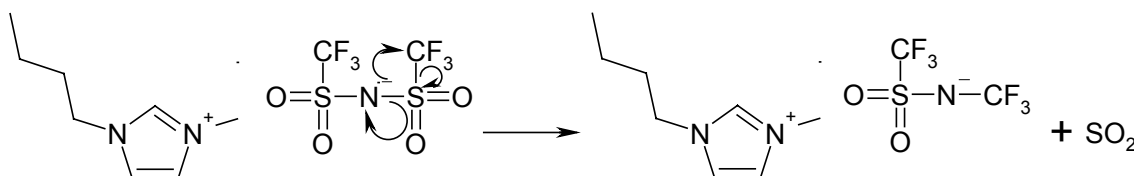
Figure 7.11: Thermal decomposition of [bmim][NTf$_2$] by sulfur dioxide release ($\Delta E^{\ddagger}$ = 255 kJ/mol)
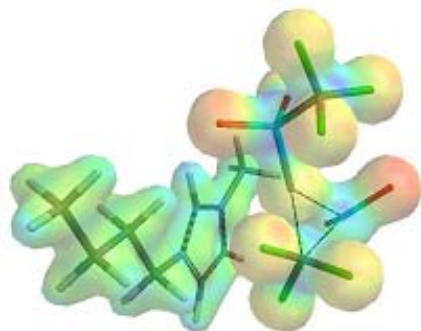
Figure 7.12: Transition state geometry of the thermal breakdown of [bmim][NTf$_2$] by sulfur dioxide release (surface = electron density of 0.08 e/au^3; property = electrostatic potential). The electron density is high at the red positions (large negative values of the potential) and low at the blue positions (large positive values of the potential).

_____

Because only the anion of [bmim][NTf$_2$] is degrading (the cation stays intact), the quantum chemical calculations were repeated for the anion only. Using this simplification, an activation energy of 260 kJ/mol was found, which is in close agreement with the 255 kJ/mol for the calculation in which the cation is included. Therefore, the anion approximation, which requires less computational effort, gives a reasonable estimate for the thermal decomposition of bis(trifluoromethylsulfonyl)imide ionic liquids.

In table 7.1 an overview of the calculated activation energies and the experimentally determined thermal decomposition temperatures of several 1-butyl-3-methylimidazolium ionic liquids with different anions is given. From Figure 7.13 it can be seen that the correlation is excellent with a correlation coefficient of 0.99. Therefore, the quantum chemical calculations are able to predict the thermal stability of these ionic liquids very well.

Table 7.1: Calculated activation energies (this work) and experimentally determined thermal decomposition temperatures (from literature) for the thermal degradation of several 1-butyl-3-methylimidazolium ionic liquids with different anion

Ionic liquid	$\Delta E^{\ddagger}$ (kJ/mol)	T_{decomp} (^{o}C)	Ref.
[bmim][Cl]	127	254	3
[bmim][N(CN)$_2$]	160	300	2
[bmim][BF$_4$]	195	361	2
[bmim][PF$_6$]	213	370	12
[bmim][NTf$_2$]	255	427	13
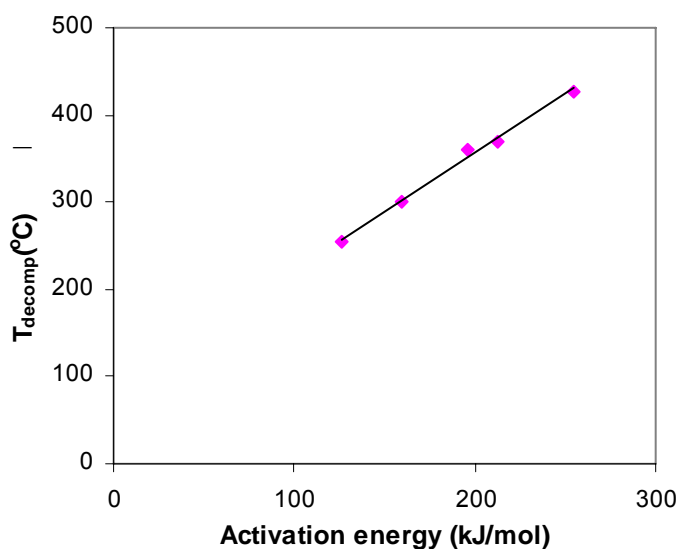
Figure 7.13: Plot of the calculated activation energy (B3LYP method) of the most likely thermal degradation reaction versus the experimentally determined thermal decomposition temperature of the ionic liquid[2,3,12,13]. The correlation coefficient is 0.99.

However, using the simplest estimate for k_r (equation 7.2) the quantum chemical calculations predict that ionic liquids degrade at much lower temperatures (~100 ^{o}C) than the experimentally TGA-determined thermal decomposition temperatures indicate. For example, the first order rate constant of the thermal degradation reaction of [bmim][BF$_4$] ($\Delta E^{\ddagger}$ = 195 kJ/mol) at a temperature of 265 ^{o}C (= 538 K) is 1.0·10^{-6} s^{-1} (equation 7.2), resulting in 0.1% conversion in 1000 seconds. This means that significant decomposition takes place well below the experimentally TGA-determined thermal decomposition temperature of 361 ^{o}C[6]. Reason is that the TGA-measured onset decomposition temperatures are calculated by intersection of a straight baseline with the tangent of the weight versus temperature, so that some decomposition occurs at temperatures lower than this onset decomposition temperature, which was also previously found by other groups[14-17] (see paragraph 7.1).

Next, the effect of the chain length of the cation of the ionic liquid on the thermal decomposition temperature is investigated. Therefore, the activation energies of the thermal breakdown reactions of several 1-alkyl-3-methylimidazolium chloride ionic liquids with different alkyl chain groups (ethyl, propyl, butyl, hexyl and octyl) were calculated. The results are shown in table 7.2. As can be seen from table 7.2, the effect of the alkyl chain length on the thermal decomposition temperature is very small, which is in agreement with experimental results[1-3,13]. In all cases, the formation of methyl chloride and alkylimidazole via an s$_N$2-mechanism (see figure 7.2) was preferred over the formation of alkyl chloride and methylimidazole, because the activation energy was always ~10 kJ/mol lower. This was also found in experiments[19].

Table 7.2: Calculated activation barriers (this work) and experimentally determined thermal decomposition temperatures (from literature) for the thermal degradation of several 1-alkyl-3-methylimidazolium chloride ionic liquids with different alkyl chain length

Ionic liquid	$\Delta E^{\ddagger}$ (kJ/mol)	T_{decomp} (^{o}C)	Ref.
[emim][Cl]	126	261	1
[pmim][Cl]	125	261	1
[bmim][Cl]	127	254	3
[hmim][Cl]	128	253	3
[omim][Cl]	128	254	3

Finally, the effect of the type of cation on the thermal decomposition mechanism and kinetics has been investigated. Therefore, the thermal degradation reactions of several tetrafluoroborate ionic liquids with different cation are predicted. Using quantum chemical calculations, pyridinium-based ionic liquids were found to be thermally decomposing by dealkylation of the cation via an s$_N$2 reaction. For example, the ionic liquid 1-butylpyridinium tetrafluoroborate ([bpy][BF$_4$]) decomposes into pyridine, butyl fluoride and BF$_3$ ($\Delta E^{\ddagger}$ = 134 kJ/mol). Figure 7.14 schematically shows the thermal decomposition mechanism of [bpy][BF$_4$] and figure 7.15 shows the corresponding calculated transition state geometry. Although the thermal decomposition temperature of

_____

[bpy][BF$_4$] is unknown, it was previously found that pyridinium-based ionic liquids are less stable than imidazolium-based ionic liquids[9,11], which is in agreement with the lower calculated activation energy for the thermal decomposition of [bpy][BF$_4$] ($\Delta E^{\ddagger} =$ 134 kJ/mol) compared to [bmim][BF$_4$] ($\Delta E^{\ddagger} = 195$ kJ/mol).
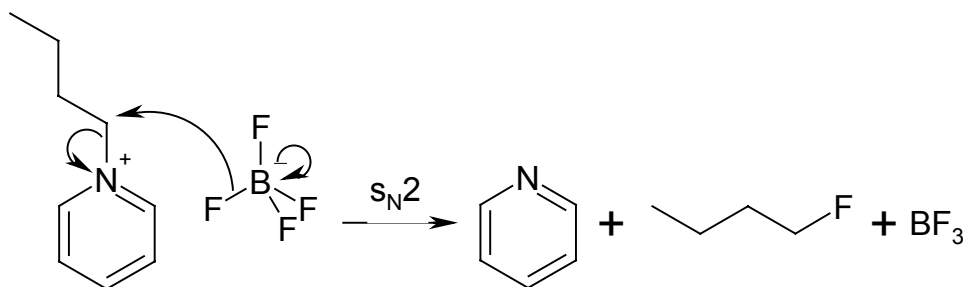
Figure 7.14: Thermal decomposition of [bpy][BF$_4$] into pyridine, butyl fluoride and BF$_3$ ($\Delta E^{\ddagger} = 134$ kJ/mol)
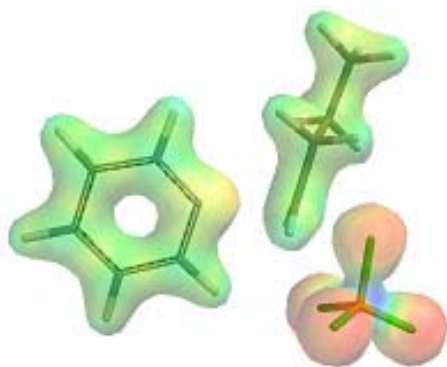
Figure 7.15: Transition state geometry (via s$_N$2) of the thermal breakdown of [bpy][BF$_4$] into pyridine, butyl fluoride and BF$_3$ (surface = electron density of 0.08 e/au^3; property = electrostatic potential). The electron density is high at the red positions (large negative values of the potential) and low at the blue positions (large positive values of the potential).

Dialkylpyrrolidinium-based ionic liquids also decompose via an s$_N$2 dealkylation reaction. For example, the ionic liquid 1,1-butylmethylpyrrolidinium tetrafluoroborate ([bmpyrrol][BF$_4$]) decomposes into 1-butylpyrrolidine, methyl fluoride and BF$_3$ ($\Delta E^{\ddagger} =$ 144 kJ/mol), which is favored over the formation of 1-methylpyrrolidine, butyl fluoride and BF$_3$, the formation of 1-methylpyrrolidine, butene and HBF$_4$ (E2-elimination), and the formation of a tertiary amine as a result of a ring opening reaction. This is in agreement with the results of Wooster _et al._[21] In figure 7.16 the thermal decomposition mechanism is presented, and figure 7.17 shows the calculated transition state geometry. It can be noticed that [bmpyrrol][BF$_4$] has a higher thermal stability than [bpy][BF$_4$], but a lower thermal stability than [bmim][BF$_4$], which is in agreement with the experimental observation that pyrrolidinium-based ionic liquids are more stable than pyridinium-based ionic liquids, but less stable than imidazolium-based ionic liquids[10,11].

_____
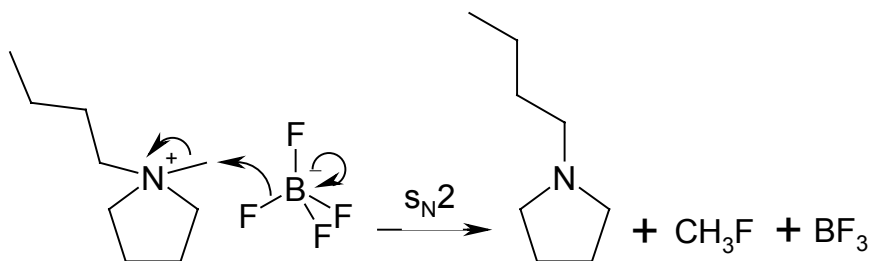
Figure 7.16: Thermal decomposition of [bmpyrrol][BF$_4$] into 1-butylpyrrolidine, methyl fluoride and BF$_3$ ($\Delta E^{\ddagger}$ = 144 kJ/mol)
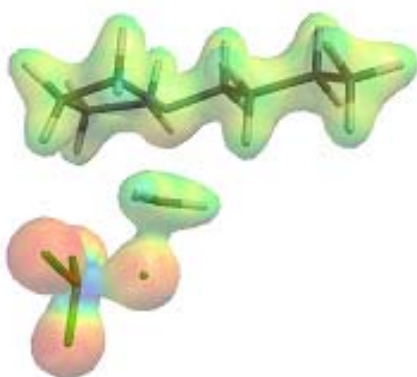
Figure 7.17: Transition state geometry (via s$_N$2) of the thermal breakdown of [bmpyrrol][BF$_4$] into 1-butylpyrrolidine, methyl fluoride and BF$_3$ (surface = electron density of 0.08 e/au^3; property = electrostatic potential). The electron density is high at the red positions (large negative values of the potential) and low at the blue positions (large positive values of the potential).

Imidazolium-based ionic liquids that are substituted with a methyl group on the C2-position were experimentally found to be more thermally stable due to the removal of the acidic hydrogen[2,7,11,12]. However, using quantum chemical calculations it was found that the ionic liquid 1-butyl-2,3-dimethylimidazolium tetrafluoroborate ([bdmim][BF$_4$]) does not decompose at the C2-position, but via a dealkylation reaction at one of the nitrogen atoms, resulting in the formation of 1-butyl-2-methylimidazole, methyl fluoride and BF$_3$ (similar to the decomposition of [bmim][BF$_4$], see figure 7.6). In fact, the activation energy of the thermal decomposition reaction of 1-butyl-2,3-dimethylimidazolium tetrafluoroborate ([bdmim][BF$_4$]) is even lower ($\Delta E^{\ddagger}$ = 182 kJ/mol) than that of [bmim][BF$_4$] ($\Delta E^{\ddagger}$ = 195 kJ/mol). Therefore, a lower thermal stability of [bdmim][BF$_4$] compared to [bmim][BF$_4$] is expected according to the quantum chemical calculations. The reason for the experimental observation that [bdmim][BF$_4$] actually decomposes at higher temperatures is most likely the result of the presence of water in the ionic liquid, which is generally present as an impurity. When the acidic hydrogen on C2-position is replaced by a methyl group, the acid-catalyzed reaction of water with methyl fluoride (leading to the formation of hydrogen fluoride) will proceed slower, thus resulting in a more stable ionic liquid. However, [bdmim][BF$_4$] will decompose faster than [bmim][BF$_4$] when no water is present in the ionic liquids.

_____

Finally, the thermal decomposition mechanism and activation energy of tetraalkylammonium and tetraalkylphosphonium ionic liquids was investigated. It was found that both types of ionic liquids decompose into the trialkyl-form via an s_N2-mechanism that is energetically favored over an E2-elimination reaction. For example, the ionic liquid tetraethylammonium tetrafluoroborate ([N2222][BF$_4$]) decomposes into triethylamine, ethyl fluoride and BF$_3$ ($\Delta E^{\ddagger}$ = 151 kJ/mol), which is shown in figures 7.18 and 7.19. In the same way, the ionic liquid tetraethylphosphonium tetrafluoroborate ([P2222][BF$_4$]) decomposes into triethylphosphine, ethyl fluoride and BF$_3$ ($\Delta E^{\ddagger}$ = 204 kJ/mol). It can be concluded that the ammonium-based ionic liquid has a lower stability than imidazolium-based ionic liquids, whereas the phosphonium-based ionic liquid has a higher stability. This was also found in experiments[10,11].
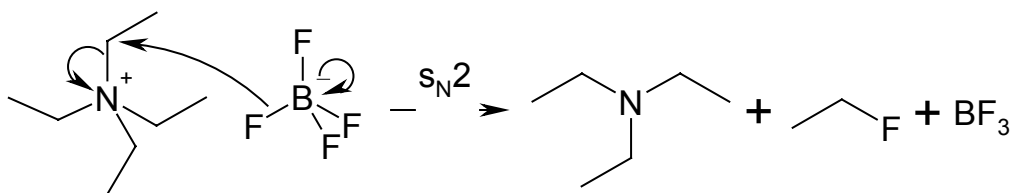
Figure 7.18: Thermal decomposition of [N2222][BF$_4$] into triethylamine, ethyl fluoride and BF$_3$ ($\Delta E^{\ddagger}$ = 151 kJ/mol)
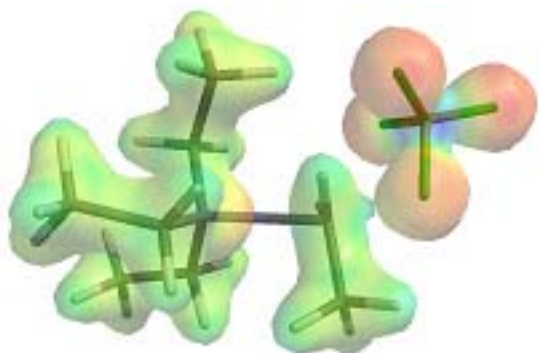
Figure 7.19: Transition state geometry (via s_N2) of the thermal breakdown of [N2222][BF$_4$] into triethylamine, ethyl fluoride and BF$_3$ (surface = electron density of 0.08 e/au^3; property = electrostatic potential). The electron density is high at the red positions (large negative values of the potential) and low at the blue positions (large positive values of the potential).

An overview of the calculated activation energies of several tetrafluoroborate ionic liquids with different cations can be found in table 7.3. Although the TGA-determined thermal decomposition temperatures of these ionic liquids are unknown, the trend in thermal stability is also observed in experiments[1,9-11], except for the experimentally-determined higher stability of [bdmim][BF$_4$] compared to [bmim][BF$_4$], which has been related to the reaction of [bmim][BF$_4$] with water.

Table 7.3: Calculated activation barriers for the thermal degradation of several tetrafluoroborate ionic liquids with different cation

Ionic liquid	$\Delta E^{\ddagger}$ (kJ/mole)
[bpy][BF$_4$]	134
[bmpyrrol][BF$_4$]	144
[N2222][BF$_4$]	151
[bdmim][BF$_4$]	182
[bmim][BF$_4$]	195
[P2222][BF$_4$]	204

_____

7.4 Conclusions

Quantum chemical calculations are an excellent tool to predict the thermal stability of ionic liquids. The effects of anion, cation and alkyl chain length on the thermal decomposition mechanism and kinetics can be investigated and correlated with experimental results. Using quantum chemical calculations it is possible to find the most probable decomposition mechanism, as well as the activation energy of the decomposition reaction. The calculated activation energy corresponds well with the measured decomposition temperature and may be used to predict the decomposition temperature of an ionic liquid before it is synthesized.

7.5 References

1. Ngo, H. L.; LeCompte, K.; Hargens, L.; McEwen, A. B.; Thermal Properties of Imidazolium Ionic Liquids, *Thermochim. Acta* **2000**, *357-358*, 97-102.
2. Fredlake, C. P.; Crosthwaite, J. M.; Hert, D. G.; Aki, S. N. V. K.; Brennecke, J. F.; Thermophysical Properties of Imidazolium-Based Ionic Liquids, *J. Chem. Eng. Data* **2004**, *49 (4)*, 954-964.
3. Huddleston, J. G.; Visser, A. E.; Reichert, W. M.; Willauer, H. D.; Broker, G. A.; Rogers, R. D.; Characterization and Comparison of Hydrophilic and Hydrophobic Room Temperature Ionic Liquids Incorporating the Imidazolium Cation, *Green Chem.* **2001**, *3 (4)*, 156-164.
4. Holbrey, J. D.; Seddon, K. R.; The Phase Behavior of 1-Alkyl-3-methyl-imidazolium Tetrafluoroborates; Ionic Liquids and Ionic Liquid Crystals, *J. Chem. Soc., Dalton Trans.* **1999**, *(13)*, 2133-2139.
5. Bonhôte, P.; Dias, A. P.; Papageorgiou, N.; Kalyanasundaram, K.; Grätzel, M.; Hydrophobic, Highly Conductive Ambient-Temperature Molten Salts, *Inorg. Chem.* **1996**, *35 (5)*, 1168-1178.
6. Holbrey, J. D.; Reichert, W. M.; Swatloski, R. P.; Broker, G. A.; Pitner, W. R.; Seddon, K. R.; Rogers, R. D.; Efficient, Halide Free Synthesis of New, Low Cost Ionic Liquids: 1,3-Dialkylimidazolium Salts Containing Methyl- and Ethyl-Sulfate Anions, *Green Chem.* **2002**, *4 (5)*, 407-413.
7. Awad, W. H.; Gilman, J. W.; Nyden, M.; Harris, R. H.; Sutto, T. E.; Callahan, J.; Trulove, P. C.; DeLong, H. C.; Fox, D. M.; Thermal Degradation Studies of Alkyl-imidazolium Salts and their Application in Nanocomposites, *Thermochim. Acta* **2004**, *409 (1)*, 3-11.
8. Tokuda, H.; Hayamizu, K.; Ishii, K.; Susan, M. A. B. H.; Watanabe, M.; Physicochemical Properties and Structures of Room Temperature Ionic Liquids. 1. Variation of Anionic Species, *J. Phys. Chem. B* **2004**, *108 (42)*, 16593-16600.
9. Crosthwaite, J. M.; Muldoon, M. J.; Dixon, J. K.; Anderson, J. L.; Brennecke, J. F.; Phase Transition and Decomposition Temperatures, Heat Capacities and Viscosities of Pyridinium Ionic Liquids, *J. Chem. Thermodynamics* **2005**, *37 (6)*, 559-568.
10. MacFarlane, D. R.; Forsyth, S. A.; Golding, J.; Deacon, G. B.; Ionic Liquids Based on Imidazolium, Ammonium and Pyrrolidinium Salts of the Dicyanamide Anion, *Green Chem.* **2002**, *4 (5)*, 444-448.
11. Tokuda, H.; Ischii, K.; Susan, M. A. B. H.; Tsuzuki, S.; Hayamizu, K.; Watanabe, M.; Physicochemical Properties and Structures of Room Temperature Ionic Liquids. 3. Variation of Cationic Structures, *J. Phys. Chem. B* **2006**, *110 (6)*, 2833-2839.
12. Fox, D. M.; Awad, W. H.; Gilman, J. W.; Maupin, P. H.; De Long, H. C.; Trulove, P. C.; Flammability, Thermal Stability and Phase Change Characteristics of Several Trialkylimidazolium Salts, *Green Chem.* **2003**, *5 (6)*, 724-727.
13. Tokuda, H.; Hayamizu, K.; Ishii, K.; Susan, M. A. B. H.; Watanabe, M.; Physicochemical Properties and Structures of Room Temperature Ionic Liquids.

2. Variation of Alkyl Chain Length in Imidazolium Cation, *J. Phys. Chem. B* **2005**, *109 (13)*, 6103-6110.

14. Kosmulski, M.; Gustafsson, J.; Rosenholm, J. B.; Thermal Stability of Low Temperature Ionic Liquids Revisited, *Thermochim. Acta* **2004**, *412 (1-2)*, 47-53.

15. Van Valkenburg, M. E.; Vaughn, R. L.; Williams, M.; Wilkes, J. S.; Thermochemistry of Ionic Liquid Heat-Transfer Fluids, *Thermochim. Acta* **2005**, *425 (1-2)*, 181-188.

16. Fox, D. M.; Gilman, J. W.; De Long, H. C.; Trulove, P. C.; TGA Decomposition Kinetics of 1-Butyl-2,3-dimethylimidazolium Tetrafluoroborate and the Thermal Effects of Contaminants, *J. Chem. Thermodynamics* **2005**, *37 (9)*, 900-905.

17. Baranyai, K. J.; Deacon, G. B.; MacFarlane, D. R.; Pringle, J. M.; Scott, J. L.; Thermal Degradation of Ionic Liquids at Elevated Temperatures, *Aust. J. Chem.* **2004**, *57 (2)*, 145-147.

18. Chan, B. K. M.; Chang, N. H.; Grimmett, M. R.; The Synthesis and Thermolysis of Imidazole Quaternary Salts, *Aust. J. Chem.* **1977**, *30 (9)*, 2005-2013.

19. Chowdhury, A.; Thynell, S. T.; Confined Rapid Thermolysis/FTIR/ToF Studies of Imidazolium-Based Ionic Liquids, *Thermochim. Acta* **2006**, *443 (2)*, 159-172.

20. Glenn, A. G.; Jones, P. B.; Thermal Stability of Ionic Liquid BMI(BF$_4$) in the Presence of Nucleophiles, *Tetrahedron Lett.* **2004**, *45 (37)*, 6967-6969.

21. Wooster, T. J.; Johanson, K. M.; Fraser, K. J.; MacFarlane, D. R.; Scott, J. L.; Thermal Degradation of Cyano Containing Ionic Liquids, *Green Chem.* **2006**, *8 (8)*, 691-696.

22. Kroon, M. C.; Buijs, W.; Peters, C. J.; Witkamp, G. J.; Quantum Chemical Aided Prediction of the Thermal Decomposition Mechanisms and Temperatures of Ionic Liquids, submitted for publication to *Thermochim. Acta* **2006**.

23. Earle, M. J.; Esperança, J. M. S. S.; Gilea, M. A.; Lopes, J. N. C.; Rebelo, L. P. N.; Magee, J. W.; Seddon, K. R.; Widegren, J. A.; The Distillation and Volatility of Ionic Liquids, *Nature* **2006**, *439 (7078)*, 831-834.

24. Wavefunction, Inc., 18401 Von Karman Avenue, Suite 370, Irvine, CA 92612, USA

25. Hehre, W. J.; A Guide to Molecular Mechanics and Quantum Chemical Calculations, Wavefunction, Inc.: Irvine (CA), USA, 2003.

8

Limits to Operation Conditions: Electrochemical Stability of Ionic Liquids

8
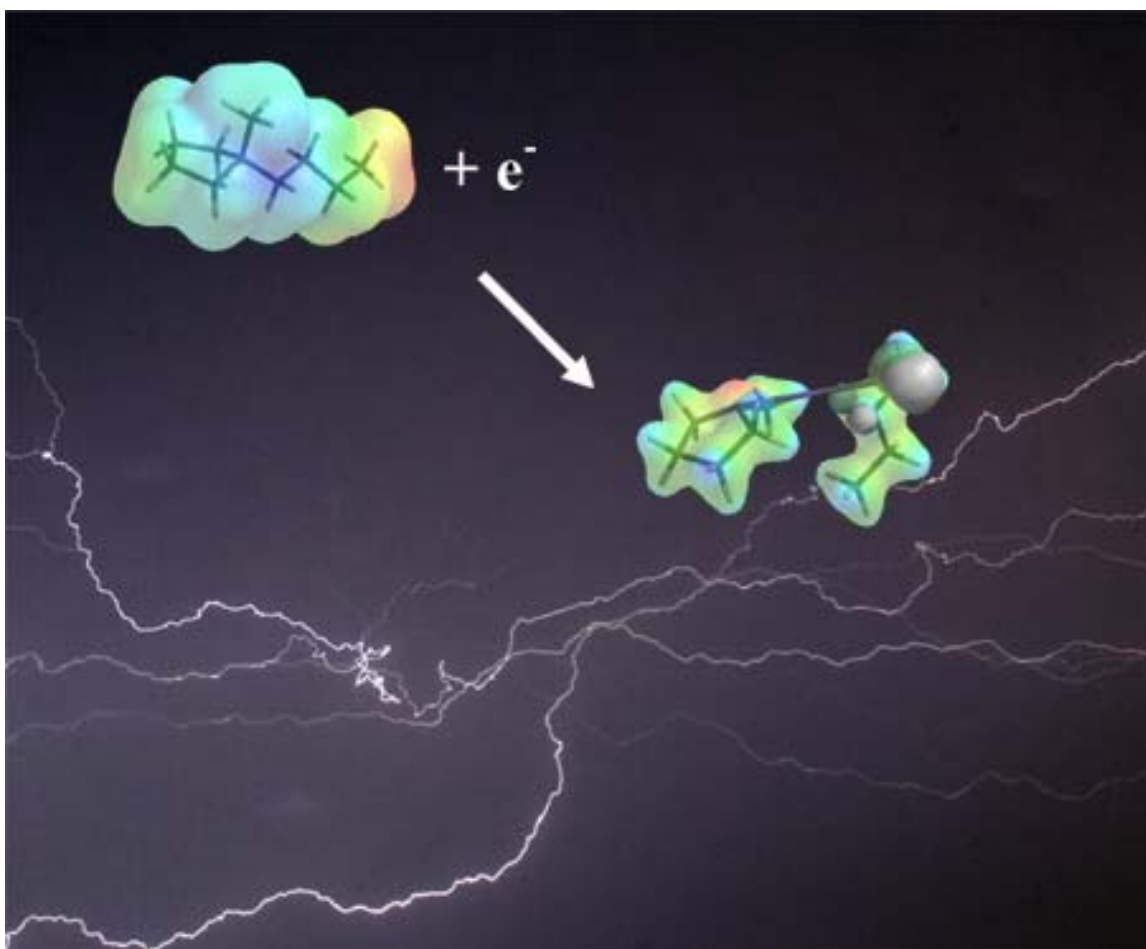
Limits to Operation Conditions: Electrochemical Stability of Ionic Liquids

The stability of ionic liquids with respect to voltage differences is important for their use in electrochemical applications. Ionic liquids decompose when a voltage difference larger than the electrochemical window (4 – 6 V) is applied. However, little is known about the decomposition mechanism and products. In this chapter the electrochemical stability of several ionic liquids is predicted using quantum chemical calculations, including their electrochemical windows and their breakdown mechanisms and products. The predicted electrochemical decomposition products are verified by experiments. The quantum chemical calculations proved to be an excellent method to predict the electrochemical breakdown of ionic liquids.

8. Limits to Operation Conditions: Electrochemical Stability of Ionic Liquids

8.1 Introduction

In the previous chapter, the thermal stability of ionic liquids was successfully predicted using quantum chemical calculations. In this chapter, quantum chemical calculations will be applied to predict the electrochemical stability of ionic liquids[1,2]. The stability of ionic liquids with respect to high voltages is especially important for their use as water-free electrolytes in electrochemical applications. Ionic liquids as water-free electrolytes combine the advantages of the conventional high-temperature molten salt electrolytes and aqueous electrolytes. Ionic liquids have wide electrochemical[3-5] and temperature[6] windows, high ionic conductivities[5,7], can dissolve most metal salts[6] and allow several metals conventionally obtained from high-temperature molten salts to be deposited at room temperature without any corrosion problems[8,9]. Moreover, they may possess lower toxicity, flammability and volatility compared to conventional electrolyte systems[10]. Applications include the use of ionic liquids as electrolytes in fuel cells[11], solar cells[12], electrochemical capacitors[13-15], battery systems[16] and electrochemical synthesis[6]. A high electrochemical stability of ionic liquids is indispensable to reach a high energy and power density of these electrochemical devices.

The electrochemical stability of an ionic liquid is manifested by the width of the electrochemical window. This is the range of voltages over which the ionic liquid is electrochemically inert. Many research groups have measured the electrochemical window of a wide variety of ionic liquids[3-5,10,17-20]. They found that phosphonium-, ammonium-, pyrrolidinium- and piperidinium-based ionic liquids with triflate or triflyl anions have the largest electrochemical windows[4,5,16,17,20]. Moreover, it was found that impurities like residual halides and water have a profound impact on the electrochemical stability of the ionic liquid[6,21]. However, a detailed study on the electrochemical reactions at the cathode and anode limits of different ionic liquids does not exist. Though, it is believed that at these limits, the cathodic reaction is the reduction of the cation[7,19,22], and the anodic reaction is oxidation of the anion[3,7,23]. Further studies are necessary to characterize the reactions at both the cathodic and anodic limits of ionic liquids when voltages larger than their electrochemical window are applied.

Quantum chemical calculations will be used to predict the electrochemical stability of ionic liquids[1,2]. Previously, Koch *et al.*[23] have correlated the electrochemical oxidation potentials of several anions with their respective Highest Occupied Molecular Orbital (HOMO) energies. Here, it will be shown that the potential of the cathode limit (reductive stability) can be correlated to the Lowest Unoccupied Molecular Orbital (LUMO) energy level of the cation[2]. Other data previously obtained by quantum chemical calculations on ionic liquids include structural information[24-27] and vibrational spectra[25-28]. Quantum chemical calculations can also be used to predict reaction paths for all sorts of reacting

_____

systems[29]. For example, they are able to predict the mechanisms of thermal decomposition reactions[30]. However, their use for predicting the electrochemical breakdown reactions and products that occur when voltages higher than the electrochemical window are applied over the ionic liquid has not been described previously.

In this chapter the electrochemical breakdown phenomena in the ionic liquids 1,1-butyl-methylpyrrolidinium bis(trifluoromethylsulfonyl)imide ([bmpyrrol][NTf$_2$]) and 1-butyl-3-methylimidazolium tetrafluoroborate ([bmim][BF$_4$]) on the cathode side under high voltages are predicted using quantum chemical calculations and verified by experiments. It may be complicated to prove that the predicted decomposition products are formed, because it is difficult to separate the decomposition products from the ionic liquid. A reason for this is that these molecules resemble each other. Moreover, ionic liquids do not have a measurable vapor pressure. As a result analytical methods such as gas chromatography (GC) and high performance liquid chromatography (HPLC) are difficult to perform. Therefore, a good design of the experiments on basis of the expected decomposition products is important for the validation of the quantum chemical results.

8.2 Experimental

8.1 Computational methods

All quantum chemical calculations were carried out using the Spartan '04 molecular modeling suite of programs[31]. All structures were fully optimized on the semi-empirical level (PM3)[29], from which the electron density, the HOMO energy level, the LUMO energy level and the spin density (only for radicals) were calculated.

8.2 Materials

The ionic liquid [bmim][BF$_4$] was prepared as described in paragraph 4.2.1 with a purity of >99.5%, measured by boron analysis (ICP-AES) and ^{1}H NMR. The amount of residual chloride was 60 ppm and the moisture content was 30 ppm.

The ionic liquid [bmpyrrol][NTf$_2$] was prepared by a reaction of 1-methylpyrrolidine and 1-chlorobutane in propanol yielding 1,1- butylmethylpyrrolidinium ([bmpyrrol][Cl]), and followed by ion exchange with lithium bis(trifluoromethylsulfonyl)imide in dichloromethane[32]. The two-steps preparation is shown in figure 8.1. All starting materials were bought from Sigma-Aldrich with purities over 99.5%.
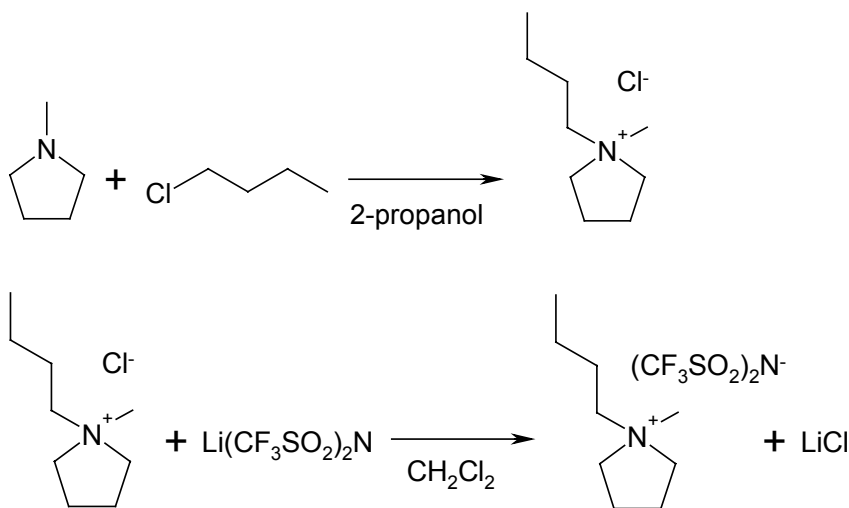
Figure 8.1: Preparation of 1,1-butylmethylpyrrolidinium bis(trifluoromethylsulfonyl)imide

Step 1:
In a round-bottom flask, 195.9 g (2.116 mole) of 1-chlorobutane was added slowly to 163.8 g (1.924 mole) 1-methylpyrrolidine in 2-propanol (200 cm^3). The mixture was then brought to reflux for 24 h. The next day, all the solvent had evaporated (leak in the

_____

system), leaving yellow crystals in the round-bottom flask. The crystals were dissolved in 2-propanol to wash the ionic liquid. Thereafter, the 2-propanol was removed using rotary evaporation, yielding 44.6 g (0.251 mole) of crystalline [bmpyrrol][Cl]. The conversion was only 13.1%, which was due to the evaporation of the reactants during the night.

Step 2:
A solution of 31.1 g (0.175 mole) of [bmpyrrol][Cl] in 50 cm^3 dichloromethane was added to 50.5 g (0.176 mole) of lithium bis(trifluoromethylsulfonyl)imide. The resulting suspension was stirred for 3 days and then filtered to remove the formed lithium chloride crystals. The solvent dichloromethane was evaporated by rotary evaporation yielding 58.2 g (0.138 mole) of [bmpyrrol][NTf$_2$] (conversion = 78.7 %).

The purity of the resulting ionic liquid was measured to be >99.5% using ^{1}H NMR (300.2 MHz., DMSO, TMS): δ 0.92 (t, 3H), 1.33 (m, 2H), 1.69 (m, 2H), 2.11 (s, 4H), 2.98 (s, 3H), 3.29 (m, 2H), 3.44 (m, 4H). The amount of chloride in the ionic liquid was measured with ion chromatography and was 50 ppm. Prior to use the ionic liquid was dried under vacuum conditions in the presence of calcium chloride at room temperature for several days. The water content of the dried ionic liquid was measured using Karl Fischer moisture analysis and was <10 ppm.

8.3 Electrochemical decomposition experiments

An electrochemical cell with two glassy carbon electrodes (inter-electrode distance = 2.5 cm, electrode area = 1.3 cm^2) was filled with ionic liquid. A voltage difference larger than the electrochemical window (8 V) was applied over the ionic liquid at room temperature during 3 hours. Thereafter, the power source was shut down and the electrochemically decomposed ionic liquid was analyzed. The decomposition products from electrochemically decomposed [bmpyrrol][NTf$_2$] were extracted with toluene. Thereafter the toluene phase was analyzed using gas chromatography and mass spectroscopy (GC-MS), type VG70-250SE, operated in the electron impact ionization mode at 70 eV. From the decomposed [bmim][BF$_4$] the ^{1}H and ^{13}C APT (Attached Proton Test) nuclear magnetic resonance (NMR) spectra were measured (Varian Unity Inova 300 s) and compared to the NMR spectra of the pure [bmim][BF$_4$] in order to see the changes in ionic liquid structure.

8.3 Results and discussion

First, a tool to estimate the electrochemical window of an ionic liquid is developed. Because it was previously found that a high energy level of the Highest Occupied Molecular Orbital (HOMO) results in a less stable anion with respect to oxidation (it is easier to remove the electron from this orbital)[23], it was assumed that a low energy level of the Lowest Unoccupied Molecular Orbital (LUMO) results in a less stable cation with respect to oxidation (it is easier to put an additional electron in this orbital). Therefore, it is expected that ionic liquids exhibit a large electrochemical window when the anion possesses a low HOMO energy level and the cation possesses a high LUMO energy level. In that case, the difference between the LUMO energy level of the cation and the HOMO energy level of the anion can be a good measure of the width of the electrochemical window.

In table 8.1 the calculated difference in energy level of LUMO and HOMO of the cation and anion, respectively, of several ionic liquids and their experimentally determined electrochemical windows are given. From figure 8.2 it can be seen that the correlation is excellent with a correlation coefficient of 0.92. Thus the calculated difference in energy level of LUMO of the cation and HOMO of the anion is indeed a good measure to predict the electrochemical window of ionic liquids.

Table 8.1: Calculated (E_{LUMO}-E_{HOMO}) and experimental electrochemical window for several ionic liquids

Cation	Anion	E_{LUMO} cation [eV]	E_{HOMO} anion [eV]	E_{LUMO}- E_{HOMO} [eV]	Cath. limit [V]	Anodic limit [V]	Window [V]	Electrode	Ref. electrode	Ref
[emim$^+$]	[CF$_3$CO$_2^-$]	-4.98	-5.25	**0.27**	-1.1	1.0	**2.1**	Pt	I$^-$/I$_3^-$	7
[emim$^+$]	[CF$_3$SO$_3^-$]	-4.98	-6.39	**1.41**	-1.7	1.9	**3.6**	Pt	I$^-$/I$_3^-$	7
[emim$^+$]	[F(HF)$_{2.3}^-$]	-4.98	-6.59	**1.61**	-1.5	1.7	**3.2**	GC	Ag	10
[emim$^+$]	[F(HF)$_{2.3}^-$]	-4.98	-6.59	**1.61**	-1.8	1.3	**3.1**	GC	ferroc	5
[emim$^+$]	[F(HF)$_{2.3}^-$]	-4.98	-6.59	**1.61**	-0.9	2.5	**3.4**	GC	Al/Al^{3+}	18
[emim$^+$]	[BF$_4^-$]	-4.98	-7.07	**2.09**	-1.8	2.2	**4.0**	Pt	Ag/Ag$^+$	15
[emim$^+$]	[BF$_4^-$]	-4.98	-7.07	**2.09**	-2.1	2.2	**4.3**	Pt	Al/Al^{3+}	19
[bmim$^+$]	[BF$_4^-$]	-4.95	-7.07	**2.12**	-1.7	2.6	**4.3**	Pt	Pt	21
[bmim$^+$]	[BF$_4^-$]	-4.95	-7.07	**2.12**	-1.7	2.5	**4.2**	Pt	Pt	3
[emim$^+$]	[(CF$_3$SO$_2$)$_2$N$^-$]	-4.98	-7.21	**2.23**	-1.8	2.5	**4.3**	Pt	I$^-$/I$_3^-$	7
[emim$^+$]	[(CF$_3$SO$_2$)$_2$N$^-$]	-4.98	-7.21	**2.23**	-2.0	2.1	**4.1**	GC	Ag	13
[emim$^+$]	[(CF$_3$SO$_2$)$_2$N$^-$]	-4.98	-7.21	**2.23**	-2.3	2.0	**4.3**	GC	Pt	16
[edmim$^+$]	[(CF$_3$SO$_2$)$_2$N$^-$]	-4.88	-7.21	**2.33**	-2.0	2.4	**4.4**	Pt	I$^-$/I$_3^-$	7
[empyrrol$^+$]	[F(HF)$_{2.3}^-$]	-4.26	-6.59	**2.33**	-2.1	2.4	**4.5**	GC	ferroc	5
[pdmim$^+$]	[(CF$_3$SO$_2$)$_2$N$^-$]	-4.86	-7.21	**2.35**	-2.0	2.3	**4.3**	GC	Ag	13
[pdmim$^+$]	[(CF$_3$SO$_2$)$_2$N$^-$]	-4.86	-7.21	**2.35**	0.2	5.0	**4.8**	GC	Li/Li$^+$	23
[empip$^+$]	[F(HF)$_{2.3}^-$]	-4.22	-6.59	**2.37**	-2.2	2.4	**4.6**	GC	ferroc	5
[bmpyrrol$^+$]	[F(HF)$_{2.3}^-$]	-4.21	-6.59	**2.38**	-2.2	2.4	**4.6**	GC	ferroc	5
[emim$^+$]	[(C$_2$F$_5$SO$_2$)$_2$N$^-$]	-4.98	-7.40	**2.42**	-2.4	2.1	**4.5**	GC	Ag	13
[bmpip$^+$]	[F(HF)$_{2.3}^-$]	-4.16	-6.59	**2.43**	-2.4	2.4	**4.8**	GC	ferroc	5
[N(1113)$^+$]	[(CF$_3$SO$_2$)$_2$N$^-$]	-4.45	-7.21	**2.76**	-3.0	2.2	**5.2**	GC	Pt	16
[pmpyrrol$^+$]	[BF$_4^-$]	-4.23	-7.07	**2.84**	-2.5	2.3	**4.8**	GC	Ag	17

Continuation of table 8.1: Calculated (E_{LUMO}-E_{HOMO}) and experimental electrochemical window for several ionic liquids

Cation	Anion	E_{LUMO} cation [eV]	E_{HOMO} anion [eV]	E_{LUMO}-E_{HOMO} [eV]	Cath. limit [V]	Anodic limit [V]	Window [V]	Electrode	Ref. electrode	Ref
[bmpyrrol+]	[(CF$_3$SO$_2$)$_2$N-]	-4.21	-7.21	**3.00**	-3.0	2.6	**5.6**	GC	Ag/Ag+	20
[pmpip+]	[(CF$_3$SO$_2$)$_2$N-]	-4.17	-7.21	**3.04**	-3.1	2.3	**5.4**	GC	Pt	16
[N(2226)+]	[(CF$_3$SO$_2$)$_2$N-]	-4.12	-7.21	**3.09**	-2.5	2.8	**5.3**	GC	Ag/Ag+	4
[pdmim+]	[(CF$_3$SO$_2$)$_3$C-]	-4.86	-8.20	**3.34**	0.2	5.5	**5.3**	GC	Li/Li+	23

GC = glassy carbon
ferroc = ferrocene/ferrocenium
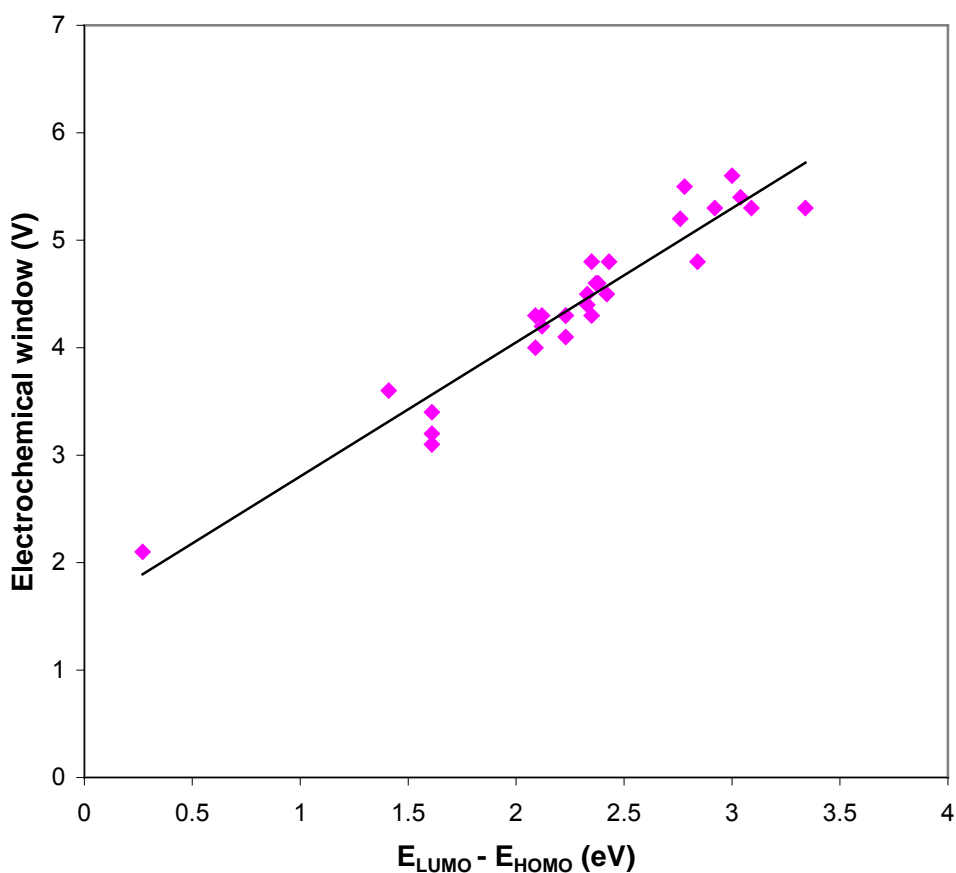
Figure 8.2: Plot of calculated (E_{LUMO}-E_{HOMO}) against electrochemical window. The correlation coefficient is 0.92.

_____

The quantum chemical calculations also show where the ionic liquid will be reduced or oxidized first. Therefore, a map of the absolute value of the HOMO energy level and the LUMO energy level of anion and cation onto the size surface was made, respectively. Colors near red represent large negative values of the mapped property and colors near blue represent large positive values.

A HOMO map shows the regions of the anion where the HOMO is located (blue) and hence are most subject to electrochemical oxidation. In figure 8.3 the HOMO map of the bis(trifluoromethylsulfonyl)imide ($[NTf_2^-]$) anion is shown. It can be seen that this anion will be oxidized first on the nitrogen atom.
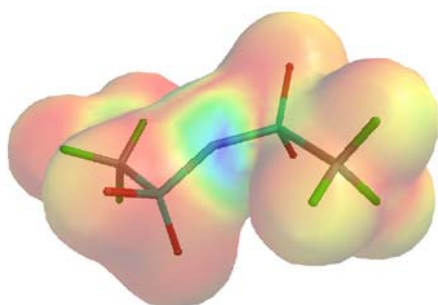
Figure 8.3: HOMO map of the bis(trifluoromethylsulfonyl)imide anion

A LUMO map shows which regions of the cation are most electron-deficient (LUMO density is highest at blue positions) and hence most subject to electrochemical reduction. In figure 8.4 the LUMO maps of the 1-butyl-3-methylimidazolium ($[bmim^+]$) cation and the 1,1-butylmethylpyrrolidinium ($[bmpyrrol^+]$) cation are shown. The $[bmim^+]$ cation will be reduced first on the C2-atom, whereas the $[bmpyrrol^+]$ cation is first reduced on the nitrogen atom.
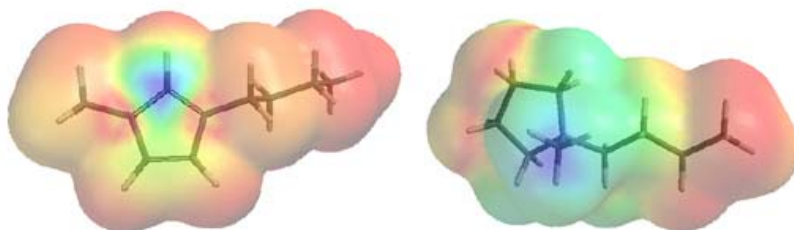
Figure 8.4: LUMO maps of the 1-butyl-3-methylimidazolium cation and the 1,1-butylmethyl-pyrrolidinium cation

_____

Next, the electrochemical reactions that occur at the cathodic limit of the ionic liquids [bmpyrrol][NTf$_2$] and [bmim][BF$_4$] are studied. On the cathodic limit the ionic liquid is reduced, which means that an electron is added to the ionic liquid molecule. For most ionic liquids, it is easier to reduce the cation than the anion (exceptions are the acidic chloroaluminate ionic liquids, where the reduction of the heptachloroaluminate (Al$_2$Cl$_7^-$) anion is the limiting cathode process)[2,6,7,19,22]. The reduction of the cation, in principle, leads to the formation of the analogous radical. Therefore, in order to predict the electrochemical reactions that take place at the cathodic limit, these radicals should be modeled.

Generally, radicals can undergo different types of reactions. First of all, it is possible that the radical itself is not stable and will decompose into a neutral fragment and a smaller more stable radical. Secondly, two radicals can react with each other under the formation of one neutral molecule (radical-radical coupling) or two neutral molecules (disproportionation). Finally, radicals can react with alkenes, where the radical combines with one of the electrons of the π-bond under the formation of a larger radical (radical addition reaction).

When an electron is added to the [bmpyrrol$^+$] cation, the resulting radical is not stable and will decompose into a neutral molecule and a smaller radical, according to quantum chemical calculations (PM3). Three possible decomposition reactions are predicted. The most likely solution (lowest energy level of the formed radical, E = -61 kJ/mol in vacuum) is that the 1,1-butylmethylpyrrolidinium radical will decompose into 1-methylpyrrolidine and a butyl radical (see figures 8.5 and 8.6).

Figure 8.5: Decomposition of the 1,1-butylmethylpyrrolidinium radical into 1-methylpyrrolidine and a butyl radical (surface = electron density of 0.08 e/au^3; property = electrostatic potential). The electron density is high at the red positions (large negative values of the potential) and low at the blue positions (large positive values of the potential). The grey positions indicate a high spin density
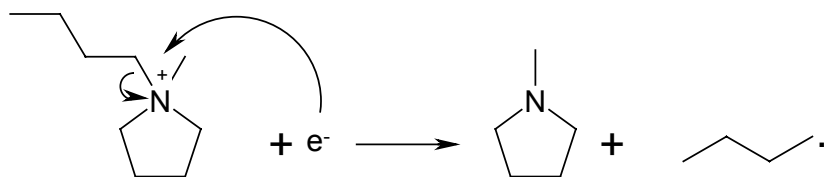
Figure 8.6: Formation of 1-methylpyrrolidine and the butyl radical

_____

Another solution, but less likely than the first one (E = -43 kJ/mol), is that the radical will decompose into a dibutylmethylamine radical by ring opening, where the unpaired electron is located on one of the butyl groups (see figures 8.7 and 8.8).
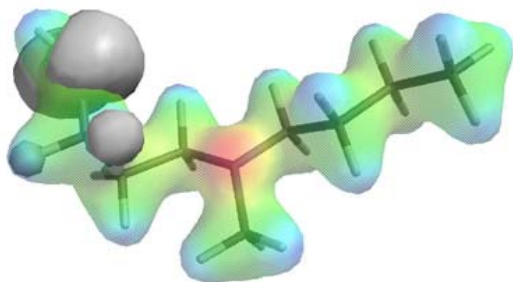
Figure 8.7: Decomposition of the 1,1-butylmethylpyrrolidinium radical into a dibutylmethylamine radical (surface = electron density of 0.08 e/au^3; property = electrostatic potential). The electron density is high at the red positions (large negative values of the potential) and low at the blue positions (large positive values of the potential). The grey positions indicate a high spin density.
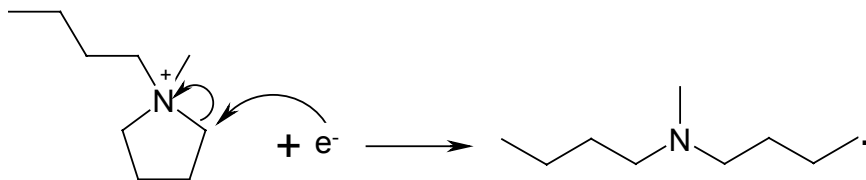
Figure 8.8: Formation of the dibutylmethylamine radical

The last solution with the lowest probability (E = -21 kJ/mol) is that the radical decomposes into 1-butylpyrrolidine and a methyl radical (see figures 8.9 and 8.10).
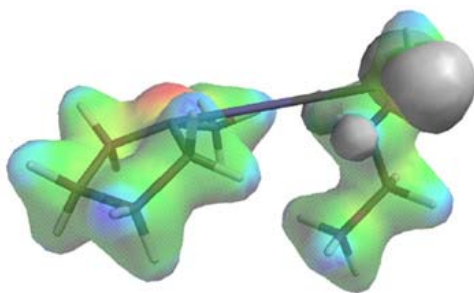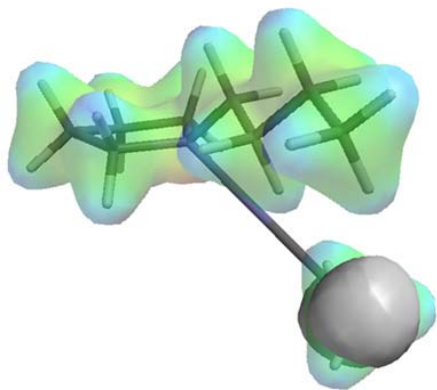

Figure 8.9: Decomposition of the 1,1-butylmethylpyrrolidinium radical into 1-butylpyrrolidine and a methyl radical (surface = electron density of 0.08 e/au^3; property = electrostatic potential). The electron density is lowest at the blue positions (largest positive values of the potential). The grey positions indicate a high spin density.

_____
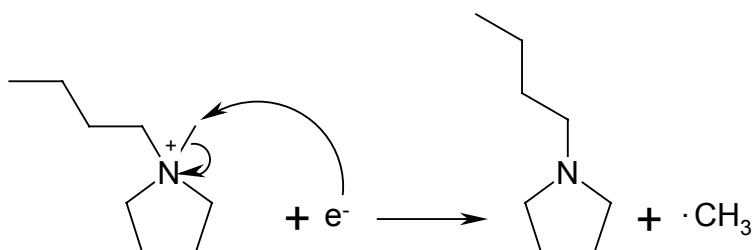
Figure 8.10: Formation of 1-butylpyrrolidine and the methyl radical

However, when an electron is added to the [bmim$^+$] cation, the resulting radical is stable and the radical will not decompose (E = 75 kJ/mol). According to quantum chemical semi-empirical calculations, the unpaired electron is located mainly on the C2 carbon (see figure 8.11).
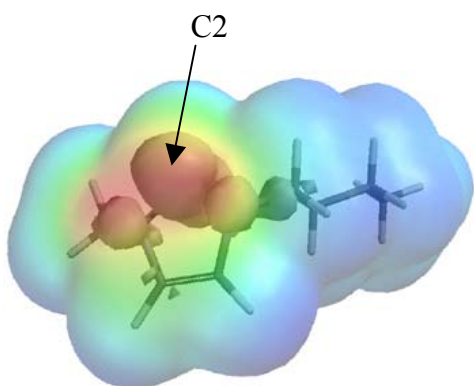
Figure 8.11: Structure and electrostatic potential (surface = electron density of 0.002 e/au^3; property = electrostatic potential) of the 1-butyl-3-methylimidazolium radical (at the semi-empirical PM3 level). The electron density is high at the red positions (large negative values of the potential) and low at the blue positions (large positive values of the potential). The grey lobs (on the C2 atom and adjacent positions) indicate a high spin density.

In contrast to the [bmim$^+$] cation, the 1-butyl-3-methylimidazolium radical has no resonance possibilities and is thus less aromatic (see figure 8.12).
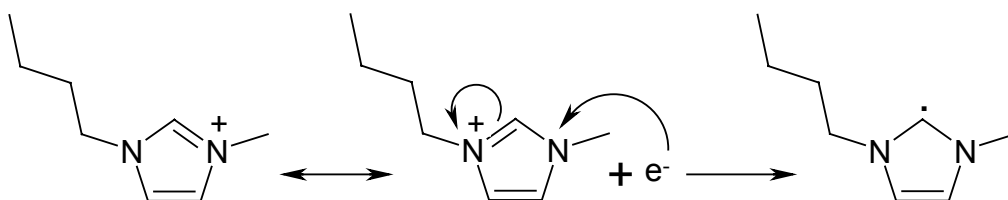
Figure 8.12: Formation of the 1-butyl-3-methylimidazolium radical

_____

The 1-butyl-3-methylimidazolium radical can undergo several reactions. The most probable solution is that two radicals react with each other under the formation of a dimer (radical-radical coupling). Figures 8.13 and 8.14 show the lowest energy conformation (E = 33 kJ/mol) of the dimer.
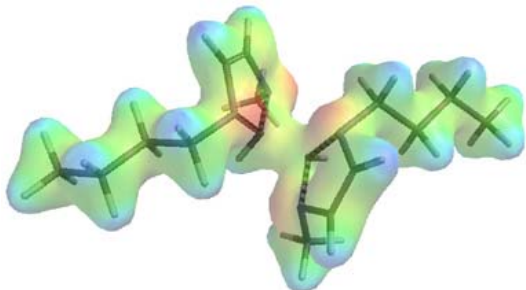
Figure 8.13: 1-Butyl-3-methylimidazolium radical coupling (surface = electron density of 0.08 e/au^3; property = electrostatic potential). The electron density is high at the red positions (large negative values of the potential) and low at the blue positions (large positive values of the potential).
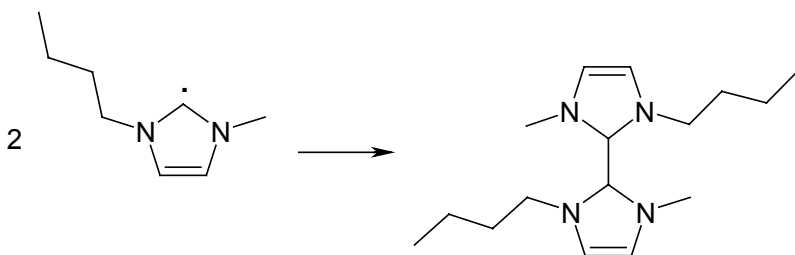
Figure 8.14: Coupling reaction of two 1-butyl-3-methylimidazolium radicals

Another solution (E = 41 kJ/mol) is that the radical picks up a hydrogen atom from another radical present in the system (disproportionation). This transfer of a hydrogen atom from one radical to another results in the formation of an alkane and an alkene (see figures 8.15 and 8.16).
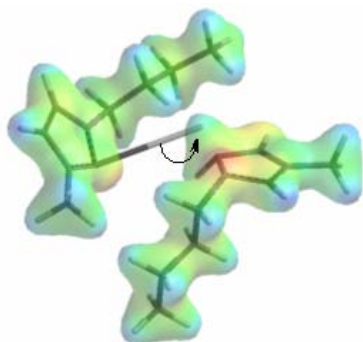
Figure 8.15: Reaction of two 1-butyl-3-methylimidazolium radicals, resulting in hydrogen transfer/ disproportionation (surface = electron density of 0.08 e/au^3; property = electrostatic potential). The electron density is high at the red positions (large negative values of the potential) and low at the blue positions (large positive values of the potential).

_____
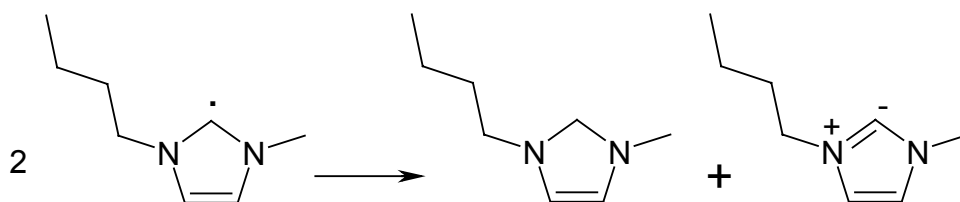
Figure 8.16: Disproportionation reaction of two 1-butyl-3-methylimidazolium radicals

The last solution (but not likely due to the very high energy, E = 235 kJ/mol) is that the radical reacts with the double bond from another radical under the formation of a cage-like structure (see figures 8.17 and 8.18).
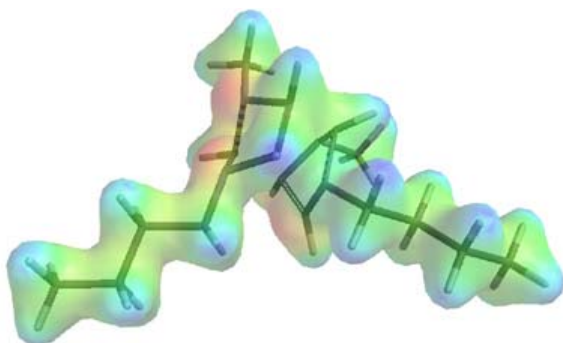
Figure 8.17: Reaction of 1-butyl-3-methylimidazolium radical with the double bond of another radical, leading to cage-formation (surface = electron density of 0.08 e/au^3; property = electrostatic potential). The electron density is high at the red positions (large negative values of the potential) and low at the blue positions (large positive values of the potential).
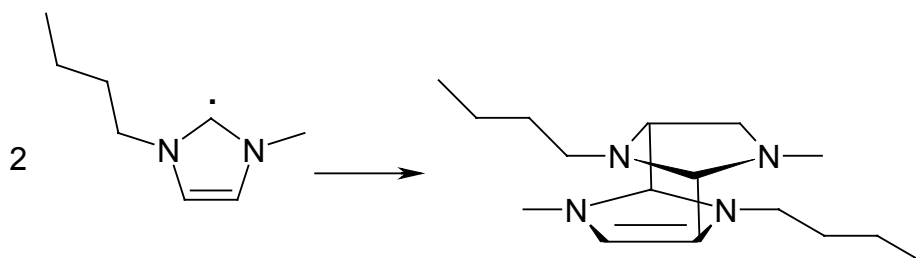
Figure 8.18: Cage-formation reaction of two 1-butyl-3-methylimidazolium radicals

The predicted results for the electrochemical decomposition of both ionic liquids were verified with experiments. Since the predicted electrochemical decomposition products of [bmpyrrol][NTf$_2$] are small and soluble in toluene, but the ionic liquid itself is not, it was decided to extract the decomposition products with toluene. Thereafter, the toluene phase was analyzed with GC-MS, where the different decomposition products were separated and identified. The detected decomposition products are listed in Table 8.2.

Table 8.2: Detected decomposition products of [bmpyrrol][NTf$_2$] using GC-MS

Compound	Peaks
1-Methylpyrrolidine (C$_5$H$_{11}$N)	m/z = 85(M), 57
Octanes (C$_8$H$_{18}$)	m/z = 114(M), 85, 71, 57
Octenes (C$_8$H$_{16}$)	m/z = 112(M), 97, 69, 55
2-Butanol (C$_4$H$_{10}$O)	m/z = 74(M), 59, 45
Dibutylmethylamine (C$_9$H$_{21}$N)	m/z = 143(M), 128, 99, 85, 71, 57
1-Butylpyrrolidine (C$_8$H$_{17}$N)	m/z = 127(M), 84, 55

From Table 8.2 it can be concluded that all three predicted decomposition reactions occur. The presence of 1-methylpyrrolidine, octanes, octenes and 2-butanol in the toluene phase prove that the 1,1-butylmethylpyrroldinium radical has decomposed into 1-methyl-pyrrolidine and a butyl radical. The octanes are formed by a reaction of two butyl radicals with each other (radical-radical coupling). Because a secondary radical is more stable than a primary radical, the unpaired electron in the butyl radical will be located on the 2-position. Therefore, from all possible octane isomers it is most probable that 3,4-dimethylhexane is the main product. The peaks in the mass spectrum indeed correspond with library search results for 3,4-dimethylhexane with a NIST library matching factor of 96.5%. The identified 2-butanol also indicates that 2-butyl radicals are formed during the electrochemical decomposition of [bmpyrrol][NTf$_2$], because 2-butanol is produced by reaction of the 2-butyl radical with chloride, followed by reaction of 2-butyl chloride with water (chloride and water are both impurities present in the ionic liquid in ppm-range). The octenes are formed by reaction of a butyl radical with a butene molecule, which in turn is produced together with butane in a disproportionation reaction of two butyl radicals. No butane was detected in the decomposition product mixture due to its low boiling point. The second decomposition reaction, where the 1,1-butylmethyl-pyrrolidinium radical decomposes by a ring opening reaction, is proven by the presence of dibutylmethylamine in the decomposition product mixture. Even the decomposition reaction with the lowest probability according to quantum chemical calculations has proceeded; 1-butylpyrrolidine was also detected in the toluene phase. So all the expected decomposition reaction products were found and all the found chemicals were predicted. Therefore, it is believed that all decomposition products (except butane) can be dissolved and extracted in toluene. Finally, as a blank the pure ionic liquid [bmpyrrol][NTf$_2$] was extracted with toluene. None of the decomposition compounds could be detected.

_____

Also, the electrochemical decomposition products of [bmim][BF$_4$] predicted by quantum chemical calculations were verified in experiments. Since the predicted decomposition products are large dimers that are very similar to the monomer, it is difficult to separate them using chromatography. Therefore, it was decided to measure a ^{1}H NMR spectrum and a ^{13}C APT spectrum of the electrochemically decomposed [bmim][BF$_4$] and to compare this with the NMR spectrum of pure [bmim][BF$_4$] in order to see the changes in ionic liquid structure.

In Table 8.3 the ^{1}H NMR spectra of electrochemically decomposed and pure [bmim][BF$_4$] are compared. From Table 8.3 it can be concluded that the position of only one peak (the hydrogen attached to the C2 carbon) has changed from $\delta = 8.71$ to lower chemical shifts ($\delta = 5.72$). This means that the hydrogen in the decomposition products is no longer connected to an aromatic carbon, which is consistent with the predicted radical structure (figure 8.12).

Table 8.3: Comparison of ^{1}H NMR spectra of pure [bmim][BF$_4$] and electrochemically decomposed [bmim][BF$_4$] (300.2 MHz, CDCl$_3$, TMS)

δ (^{1}H NMR) pure [bmim][BF$_4$]		δ (^{1}H NMR) electrochemically decomposed [bmim][BF$_4$]	
0.93	(t, 3H)	0.91	(t, 3H)
1.34	(m, 2H)	1.30	(m, 2H)
1.86	(m, 2H)	1.81	(m, 2H)
3.95	(s, 3H)	3.89	(s, 3H)
4.20	(t, 2H)	4.20	(t, 2H)
7.47	(s, 2H)	5.72	(s, 1H)
8.71	(s, 1H)	7.67	(d, 1H)
		7.74	(d, 1H)

The ^{13}C APT NMR spectrum of electrochemically decomposed and pure [bmim][BF$_4$] are compared in Table 8.4. The ^{13}C APT NMR spectra are similar, except for the last peak, which is positive (and small) in the electrochemically decomposed [bmim][BF$_4$], indicating a C or CH$_2$ carbon, and negative (and large) in the pure [bmim][BF$_4$], indication a CH carbon. Therefore, when [bmim][BF$_4$] is electrochemically decomposed, the disproportionation reaction is the most probable decomposition reaction. Dimer formation is also possible, because the peaks from corresponding carbons in both monomers are located exactly at the same position (the corresponding carbons are identical) and no additional peaks are noticed in the ^{13}C spectrum. Cage formation has not taken place, since that would change the chemical nature of the compound and shifts in the peak positions are not detected. This also followed from the quantum chemical calculations that predicted a very high energy barrier for the cage formation.

Table 8.4: Comparison of ^{13}C APT NMR spectra of pure [bmim][BF$_4$] and electrochemically decomposed [bmim][BF$_4$] (300.2 MHz, CDCl$_3$, TMS)

δ (^{13}C NMR) pure [bmim][BF$_4$]		δ (^{13}C NMR) electrochemically decomposed [bmim][BF$_4$]	
13.34	(CH$_3$)	13.18	(CH$_3$)
19.33	(CH$_2$)	18.84	(CH$_2$)
31.93	(CH$_2$)	31.43	(CH$_2$)
36.12	(CH$_3$)	35.68	(CH$_3$)
49.69	(CH$_2$)	48.68	(CH$_2$)
122.57	(CH)	122.27	(CH)
123.87	(CH)	123.58	(CH)
136.07	(CH)	136.53	(C or CH$_2$)

The quantum chemical calculations at the semi-empirical level (PM3) are able to predict the electrochemical decomposition reactions and products of both [bmpyrrol][NTf$_2$] and [bmim][BF$_4$] well. There is no need for a more rigorous quantum chemical method.

_____

8.4 Conclusions

Quantum chemical calculations are an excellent tool to predict the electrochemical window of ionic liquids, which can be correlated to the calculated difference in energy level of LUMO of the cation and HOMO of the anion. Quantum chemical calculations can also be used to predict the possible electrochemical breakdown products of ionic liquids. The electrochemical decomposition of the ionic liquids [bmpyrrol][NTf$_2$] and [bmim][BF$_4$] on the cathode limit were successfully predicted and verified by experiments. [Bmpyrrol][NTf$_2$] decomposes into 1-methylpyrrolidine, octanes, octenes, 2-butanol, dibutylmethylamine and 1-butylpyrrolidine. In the electrochemical breakdown of [bmim][BF$_4$], 1-butyl-3-methylimidazolium radicals are formed, that react with each other in a radical-radical coupling reaction and in a disproportionation reaction. All the expected decomposition reaction products were experimentally found and all the found chemicals were predicted.

8.5 References

1. Kroon, M. C.; Buijs, W.; Peters, C. J.; Witkamp, G. J.; Decomposition of Ionic Liquids in Electrochemical Processing, *Green Chem.* **2006**, *8 (3)*, 241-245.
2. Kroon, M. C.; Buijs, W.; Peters, C. J.; Witkamp, G. J.; Quantum Chemical Aided Design of Ionic Liquids as Electrolytes, Proceedings of the 1st International Congress on Ionic Liquids (COIL 1): Salzburg, Austria, June 2005.
3. Suarez, P. A. Z.; Selbach, V. M.; Dullius, J. E. L.; Einloft, S.; Piatnicki, C. M. S.; Azambuja, D. S.; De Souza, R. F.; Dupont, J.; Enlarged Electrochemical Window in Dialkylimidazolium Cation Based Room-Temperature Air and Water-Stable Molten Salts, *Electrochim. Acta* **1997**, *42 (16)*, 2533-2535.
4. Sun, J.; Forsyth, M.; MacFarlane, D. R.; Room-Temperature Molten Salts Based on the Quaternary Ammonium Ion, *J. Phys. Chem. B* **1998**, *102 (44)*, 8858-8864.
5. Matsumoto, K.; Hagiwara, R.; Ito, Y.; Room-Temperature Ionic Liquids with High Conductivities and Wide Electrochemical Windows; *N*-Alkyl-*N*-methylpyrrolidinium and *N*-Alkyl-*N*-methylpiperidinium Fluorohydrogenates, *Electrochem. Solid State Lett.* **2004**, *7 (10)*, E41-E44.
6. Wasserscheid, P.; Welton, T., Eds. *Ionic Liquids in Synthesis*; Wiley-VHC Verlag: Weinheim, Germany, 2003.
7. Bonhôte, P.; Dias, A. P.; Papageorgiou, N.; Kalyanasundaram, K.; Grätzel, M.; Hydrophobic, Highly Conductive Ambient-Temperature Molten Salts, *Inorg. Chem.* **1996**, 35 (5), 1168-1178.
8. Liao, Q.; Pitner, W. R.; Stewart, G.; Hussey, C. L.; Stafford, G. R.; Electrodeposition of Aluminum from the Aluminum Chloride – 1-Methyl-3-ethylimidazolium Chloride Room Temperature Molten Salt + Benzene, *J. Electrochem. Soc.* **1997**, *144 (3)*, 936-943.
9. Huang, J. F.; Sun, I. W.; Electrodeposition of PtZn in a Lewis acidic $ZnCl_2$ – 1-Ethyl-3-methylimidazolium Chloride Ionic Liquid, *Electrochim. Acta* **2004**, *49 (19)*, 3251-3258.
10. Hagiwara, R.; Ito, Y.; Room Temperature Ionic Liquids of Alkylimidazolium Cations and Fluoroanions, *J. Fluorine Chem.* **2000**, *105 (2)*, 221-227.
11. Hagiwara, R.; Nohira, T.; Matsumoto, K.; Tamba, Y.; A Fluorohydrogenate Ionic Liquid Fuel Cell Operating Without Humidification, *Electrochem. Solid State Lett.* **2005**, *8 (4)*, A231-A233.
12. Papageorgiou, N.; Athanassov, Y.; Armand, M.; Bonhôte, P.; Pettersson, H.; Azam, A.; Grätzel, M.; The Performance and Stability of Ambient Temperature Molten Salts for Solar Cell Applications, *J. Electrochem. Soc.* **1996**, *143 (10)*, 3099-3108.
13. McEwen, A. B.; Ngo, H. L.; LeCompte, K.; Goldman, J. L.; Electrochemical Properties of Imidazolium Salt Electrolytes for Electrochemical Capacitor Applications, *J. Electrochem. Soc.* **1999**, *146 (5)*, 1687-1695.
14. Ue, M.; Takeda, M.; Toriumi, A.; Kominato, A.; Hagiwara, R.; Ito, Y.; Application of Low-Viscosity Ionic Liquid to the Electrolyte of Double-Layer Capacitors, *J. Electrochem. Soc.* **2003**, *150 (4)*, A499-A502.

15. Sato, T.; Masuda, G.; Takagi, K.; Electrochemical Properties of Novel Ionic Liquids for Electric Double Layer Capacitor Applications, *Electrochim. Acta* **2004**, *49 (21)*, 3603-3611.

16. Sakaebe, H.; Matsumoto, H.; N-Methyl-N-propylpiperidinium Bis(trifluoro-methanesulfonyl)imide (PP13-TSFI) - Novel Electrolyte Base for Li Battery, *Electrochem. Commun.* **2003**, *5 (7)*, 594-598.

17. Forsyth, S.; Golding, J.; MacFarlane, D. R.; Forsyth, M.; N-Methyl-N-alkyl-pyrrolidinium Tetrafluoroborate Salts: Ionic Solvents and Solid Electrolytes, *Electrochim. Acta* **2001**, *46 (10-11)*, 1753-1757.

18. Hagiwara, R.; Hirashige, T.; Tsuda, T.; Ito, Y.; A Highly Conductive Room Temperature Molten Fluoride: EMIF·2.3HF, *J. Electrochem. Soc.* **2002**, *149 (1)*, D1-D6.

19. Fuller, J.; Carlin, R. T.; Osteryoung, R. A.; The Room Temperature Ionic Liquid 1-Ethyl-3-methylimidazolium Tetrafluoroborate: Electrochemical Couples and Physical Properties, *J. Electrochem. Soc.* **1997**, *144 (11)*, 3881-3886.

20. MacFarlane, D. R.; Meakin, P.; Sun, J.; Amini, N.; Forsyth, M.; Pyrrolidinium Imides: A New Family of Molten Salts and Conductive Plastic Crystal Phases, *J. Phys. Chem. B* **1999**, *103 (20)*, 4164-4170.

21. Schröder, U.; Wadhawan, J. D.; Compton, R. G.; Marken, F.; Suarez, P. A. Z.; Consorti, C. S.; De Souza, R. F.; Dupont, J.; Water-Induced Accelerated Ion Diffusion: Voltammetric Studies in 1-Methyl-3-[2,6-(S)-dimethylocten-2-yl] imidazolium Tetrafluoroborate, 1-Butyl-3-methylimidazolium Tetrafluoroborate and Hexafluorophosphate Ionic Liquids, *New J. Chem.* **2000**, *24 (12)*, 1009-1015.

22. Nanjundiah, C.; McDevitt, S. F.; Koch, V. R.; Differential Capacitance Measurements in Solvent-Free Ionic Liquids at Hg and C Interfaces, *J. Electrochem. Soc.* **1997**, *144 (10)*, 3392-3397.

23. Koch, V. R.; Dominey, L. A.; Nanjundiah, C.; Ondrechen, M. J.; The Intrinsic Anodic Stability of Several Anions Comprising Solvent-Free Ionic Liquids, *J. Electrochem. Soc.* **1996**, *143 (3)*, 798-803.

24. Meng, Z.; Dölle, A.; Carper, W. R.; Gas Phase Model of an Ionic Liquid: Semi-empirical and Ab Initio Bonding and Molecular Structure, *J. Mol. Struct. (Theochem)* **2002**, *585 (1-3)*, 119-128.

25. Antony, J. H.; Mertens, D.; Breitenstein, T.; Dölle, A.; Wasserscheid, P.; Carper, W. R.; Molecular Structure, Reorientational Dynamics, and Intermolecular Interactions in the Neat Ionic Liquid 1-Butyl-3-methylimidazolium Hexafluoro-phosphate, *Pure Appl. Chem.* **2004**, *76 (1)*, 255-261.

26. Mains, G. J.; Nantsis, E. A.; Carper, W. R.; Ab Initio Bonding, Molecular Structure, and Quadrupole Coupling Constants of Aluminum Chlorides, *J. Phys. Chem. A* **2001**, *105 (17)*, 4371-4378.

27. Katsyuba, S. A.; Dyson, P. J.; Vandyukova, E. E.; Chernova, A. V.; Vidis, A.; Molecular Structure, Vibrational Spectra, and Hydrogen Bonding of the Ionic Liquid 1-Ethyl-3-methyl-1H-Imidazolium Tetrafluoroborate, *Helvetica Chim. Acta* **2004**, *87 (10)*, 2556-2565.

28. Paulechka, Y. U.; Kabo, G. J.; Blokhin, A. V.; Vydrov, O. A.; Magee, J. W.; Frenkel, M.; Thermodynamic Properties of 1-Butyl-3-methylimidazolium

Hexafluorophosphate in the Ideal Gas State, *J. Chem. Eng. Data* **2003**, *48 (3)*, 457-462.

29. Hehre, W. J.; A Guide to Molecular Mechanics and Quantum Chemical Calculations, Wavefunction, Inc.: Irvine (CA), USA, 2003.

30. Kroon, M. C.; Buijs, W.; Peters, C. J.; Witkamp, G. J.; Quantum Chemical Aided Prediction of the Thermal Decomposition Mechanisms and Temperatures of Ionic Liquids, submitted for publication to *Thermochim. Acta* **2006**.

31. Wavefunction, Inc., 18401 Von Karman Avenue, Suite 370, Irvine, CA 92612, USA

32. Lancaster, N. L.; Salter, P. A.; Welton, T.; Young, G. B.; Nucleophilicity in Ionic Liquids. 2. Cation Effects on Halide Nucleophilicity in a Series of Bis(trifluoro-methylsulfonyl)imide Ionic Liquids, *J. Org. Chem.* **2002**, 67 (25), 8855-8861.

9

Economical and Environmental Attractiveness of Ionic Liquid/Carbon Dioxide Processes

9

Economical and Environmental Attractiveness of Ionic Liquid/Carbon Dioxide Processes

The use of ionic liquids in combination with carbon dioxide in chemical processes leads to economical and environmental benefits compared to conventional production processes. Reductions in the use of catalyst and volatile organic solvents lead to lower costs for raw materials and lower waste disposal costs. No expensive purification steps are required to remove catalyst residues from the product. The energy costs for pressurizing the carbon dioxide in ionic liquid/carbon dioxide processes are lower than the energy costs for evaporating the solvent in the conventional process. When the ionic liquid/carbon dioxide process is applied to the production of 1600 ton/year Levodopa, the energy consumption is reduced by 20,000 GJ per year and the waste generation is reduced by 4800 ton of methanol per year and 480 kg catalyst per year. The total variable costs are reduced by 11.3 million euros per year, whereas the investment cost rises with at least 0.91 million euros (for ionic liquid and catalyst investments). The only barrier for adopting the novel approach is the necessary equipment expenditure, but this barrier can be overcome when the ionic liquid/carbon dioxide production process is carried out in existing equipment.

9. Economical and Environmental Attractiveness of Ionic Liquid/Carbon Dioxide Processes

9.1 Comparison of Ionic Liquid/Carbon Dioxide Production Process with Conventional Production Process

In chapter 3 a new method to combine reactions and separation using ionic liquids and carbon dioxide has been described. In the next chapters, it was tried to apply this new process set-up to the production of N-acetyl-(*S*)-phenylalanine methyl ester (APAM) from methyl (*Z*)-α-acetamidocinnamate (MAAC). This reaction is related to the most important step (asymmetric hydrogenation step) in the production of Levodopa, an anti-parkinsonian drug. In this chapter, the production of APAM in ionic liquid/carbon dioxide systems is compared to the conventional production process in order to make an economical and environmental assessment[1].

Conventionally, the asymmetric hydrogenation of MAAC is carried out batch-wise in methanol as the solvent. The kinetics are not known. However, conversion data of the model reaction in methanol are given in literature[2,3]. It is possible to reach a conversion of 100% within 1 hour at 25 °C (298 K) and an initial hydrogen pressure of 2 - 16 bar with 0.25 M solution of MAAC in methanol and a minimum substrate to catalyst ratio of 2000 mole/mole. The enantioselectivity is high (98% ee) due to the use of the efficient chiral Rh-MeDuPHOS as homogeneous catalyst. However, the expensive rhodium-catalyst is very sensitive to oxidation. Because of deactivation, it is only possible to use the catalyst during five batches[2,4]. Total regeneration and recycling of the catalyst is impossible due to catalyst leaches and the regeneration is very energy-intensive. Moreover, an inert nitrogen atmosphere is required for its preparation and handling.

In the conventional production process, the separation and recovery of the Rh-MeDuPHOS catalyst complex from the product APAM is difficult. The product and catalyst cannot be separated by distillation, because their decomposition temperatures are lower than their boiling points. The only possibility to separate the product from the catalyst is by means of extraction with a co-solvent or precipitation with an anti-solvent[4]. In literature three options for product and catalyst recovery are described. The first suggestion is the use of a silica column to remove the catalyst and thereafter evaporating the methanol to obtain the pure product[3], but this recovery method is only used on lab-scale. A more industrially interesting recovery possibility is the addition of water to the reaction mixture, followed by extraction of the product APAM with dichloromethane, while leaving the catalyst in the methanol/water phase. After evaporation of all the solvents, the product and catalyst are recovered[5]. A final option is the addition of huge amounts of hexane/ether as anti-solvent to precipitate the product APAM out of the reaction mixture, followed by filtration and evaporation of the solvents[6]. However, in all these cases some catalyst leaching into the product phase occurs.

_____

The asymmetric hydrogenation of MAAC in ionic liquid/carbon dioxide systems can be carried out either batch-wise or continuously. The reactant MAAC and the rhodium-catalyst are completely dissolved in the ionic liquid, but the hydrogen is only partly pressed into the ionic liquid phase at 50-60 bar and 20 ^{o}C (=293 K)[7]. Carbon dioxide can be added in low concentrations to increase the conversion and enantioselectivity. It is possible to reach conversions and enantioselectivities slightly lower than the conventional process. The rhodium-catalyst is immobilized in the ionic liquid phase and can be reused without significant loss in catalyst activity and selectivity[7] (see paragraph 5.1.2).

The produced APAM can either be extracted or precipitated from the ionic liquid phase (with immobilized catalyst) using supercritical carbon dioxide[8]. It is more difficult to obtain a pure product using precipitation (it is difficult to wash away all ionic liquid from the precipitated product) than using extractions. Therefore, the conventional production process will be compared with the ionic liquid/carbon dioxide production process that uses extraction as a way to separate the product. Extraction of APAM with supercritical carbon dioxide is carried out at 50 ^{o}C (=323 K) and 120 bar. At these conditions, the solubility of APAM in carbon dioxide is 1.78 g APAM per kg CO_2 (see paragraph 5.3.2), whereas ionic liquid and catalyst have negligible solubilities in carbon dioxide. In this way it is possible to extract pure APAM without any ionic liquid or catalyst contamination. A throttling expansion is used to lower the pressure and hence the dissolving power of the carbon dioxide. The product can be precipitated out of the solution at 80 bar, where the solubility of APAM in carbon dioxide has decreased to 0.14 g APAM per kg CO_2 (see paragraph 5.3.2). The carbon dioxide is repressurized and recycled.

The conventional production process of APAM is compared to the ionic liquid/carbon dioxide production process with regard to reaction rate, enantioselectivity, product purity, catalyst stability, process conditions, energy consumption, waste production, ease of handling, ease of catalyst separation, and complexity of the process. The results of the comparison are in table 9.1.

Table 9.1: Comparison of the conventional production process with the ionic liquid/carbon dioxide production process for the production of N-acetyl-(*S*)-phenylalanine methyl ester (very positive aspect: +; aspect that is neither very positive nor very negative: +/-; very negative aspect: -)

Production process property	Conventional production process	Ionic liquid/carbon dioxide production process
Reaction rate	+	+/-
Enantioselectivity	+	+/-
Product purity	-	+
Catalyst stability	-	+
Process conditions	+	+/-
Energy consumption	-	+/-
Waste production	-	+
Ease of handling	-	+/-
Ease of catalyst separation	-	+
Complexity of process	-	+

Reaction rate:
In both the conventional process and the ionic liquid/carbon dioxide process, the reaction is homogeneously catalyzed, because methanol and [bmim][BF$_4$] are both able to dissolve the Rh-catalyst. The thermodynamic equilibrium constant can be calculated from:

$$-\Delta_r G = RT \ln(K) \tag{9.1}$$

with:
$\Delta_r G$ = Gibbs free energy of reaction [J·mol^{-1}]
R = Universal gas constant [J·mol^{-1}·K^{-1}]
T = Temperature [K]
K = Equilibrium constant [-]

The Gibbs free energy of reaction can be calculated from:

$$\Delta_r G = 1 \cdot \Delta_f G_{APAM} - 1 \cdot \Delta_f G_{MAAC} - 1 \cdot \Delta_f G_{H_2} \tag{9.2}$$

where the Gibbs free energy of formation ($\Delta_f G$) of hydrogen is per definition zero at 298 K and 1 atm[9] and the Gibbs free energies of formation of MAAC and APAM at the same conditions can be estimated using the Joback method with an accuracy of ± 10 kJ/mol[10]. This yields $\Delta_f G_{MAAC}$ = −93.09 kJ/mol and $\Delta_f G_{APAM}$ = −167.20 kJ/mol. Using equation (9.2), the Gibbs free energy of reaction at standard conditions is $\Delta_r G$ = -74.11 kJ/mol. The equilibrium constant at room temperature is K = 9.77·10^{12} [-] (equation 9.1), so the thermodynamic reaction equilibrium is totally on the product side. Therefore, differences in reaction rates can only be the result of kinetic effects.

Compared to the conventional process, the reaction rate in the ionic liquid/carbon dioxide system is slightly lower, but it is still industrially feasible[7]. Reason for the lower reaction rate is that the hydrogen solubility in the ionic liquid is lower than the hydrogen solubility in methanol. The reaction rates of the ionic liquid/carbon dioxide processes can be increased by raising the hydrogen pressure (higher hydrogen availability in the ionic liquid phase) and by adding small amounts of carbon dioxide to increase the hydrogen solubility as a result of co-solvency effects and the lower viscosity of the ionic liquid phase.

Enantioselectivity:
The enantioselectivity of the ionic liquid/carbon dioxide process is slightly lower than the enantioselectivity of the conventional process, but this difference is only very small[7]. It is possible to increase the enantioselectivity of the ionic liquid/carbon dioxide process by adding small amounts of carbon dioxide.

Product purity:
The purity of the produced APAM in the conventional process is low. This is a consequence of product contamination by catalyst residues due to catalyst leaching[3,5,6]. The catalyst leaching doesn't only lower the product quality, but the loss of the expensive catalyst is also a serious disadvantage of the conventional process. The purity of the produced APAM in the ionic liquid/carbon dioxide process is very high. The reason is that the ionic liquid with immobilized catalyst does not dissolve in the carbon dioxide, so that pure product is extracted (the amount of ionic liquid and catalyst was below the detection limit of 0.1 ppm)[8].

Catalyst stability:
Compared to the conventional production process, the ionic liquid/carbon dioxide production process shows much higher catalyst stability. In the conventional process the catalyst is highly sensitive towards oxidation. As a result the catalyst is only useful during five batches[2]. In the novel process options the ionic liquid protects the catalyst from oxidation. The expensive chiral catalyst Rh-MeDuPHOS can be reused more than five times without significant changes in activity and selectivity[4,7,11].

Process conditions:
The conventional process is carried out at room temperature and 2-16 bar initial hydrogen pressure[2,3]. The ionic liquid/carbon dioxide production process requires similar temperatures (20 – 50 $^{\circ}$C), but much higher pressures. The asymmetric hydrogenation of MAAC in ionic liquid/carbon dioxide is carried out at 60 bar[7], whereas the extraction takes place with carbon dioxide of 120 bar[8]. Substrate-to-catalyst ratios are in the same order of magnitude for both the conventional and the ionic liquid/carbon dioxide production process[2,7].

Energy consumption:
The conventional process is not energy-efficient. To obtain a pure product without solvent contamination, evaporation of the solvent is always necessary (for all conventional product recovery methods)[3,5,6]. The evaporation of these organic solvents requires a lot of energy. In the ionic liquid/carbon dioxide production process, no energy-intensive evaporation step is needed. Energy is only required for recompressing the carbon dioxide[8]. Even at relatively low solubilities of the product, it is energetically favored to recompress the carbon dioxide over the evaporation of the solvents. The energy consumption can be minimized when the pressure is not totally relieved, but only partly. For example, after extraction the pressure of the carbon dioxide is only released to 80 bar (and not completely to atmospheric pressure), after which it is recompressed to 120 bar to be used again as extractant[8].

Waste production:
The conventional process is not waste conscious. The amount of waste production is high. The waste of the conventional process consists of catalyst disposals and solvent losses. Because the catalyst is only used during five batches[2], the amount of catalyst disposal is significant. Moreover, it is estimated that recovery efficiencies of solvents in the fine chemical industry are in the order of 80%[12]. That means that 20% of the solvent used ends up as emissions into the atmosphere or ground water or is combusted. Efficient recovery of pure solvents is also hindered by the fact that different solvents are used for different reaction steps, leading to cross contamination. In the ionic liquid/carbon dioxide production process, the ionic liquid and catalyst are reused without any emissions into the environment (the ionic liquid is contained, and has no measurable vapor pressure)[13]. This leads to lower costs for raw materials and lower waste disposal costs.

Ease of handling:
In the conventional process an inert atmosphere is required for handling of the air-sensitive catalyst. Therefore, the ease of handling is not high. Moreover, the workers are exposed to inhalation of volatile organic solvents (such as methanol), which are toxic. The ionic liquid/carbon dioxide production process is easier to handle, since no inert atmosphere is required for protection of the catalyst (the catalyst is protected by the ionic liquid)[7]. However, when tetrafluoroborate and hexafluorophosphate ionic liquids are used, moisture-free operation is required, since these ionic liquids are not water-stable[14]. This complicates the handlings in the process. This problem can be overcome when water-stable ionic liquids are used instead. Finally, the ionic liquid/carbon dioxide does not lead to considerable worker's exposure, because ionic liquids do not have a measurable vapor pressure.

Ease of catalyst separation from product:
In the conventional production process it is extremely difficult to separate the catalyst from the product. All suggested recovery options are complex and they always lead to some catalyst leaching into the product phase[3,5,6]. On the contrary, no catalyst leaching will occur in the ionic liquid/carbon dioxide process. The product is removed from the ionic liquid phase by extraction with carbon dioxide, without extraction of ionic liquid and (ionic) catalyst[8].

Complexity of the process:
The recovery of the product and catalyst from the solvent is complex in the conventional production process. The only possibility to separate the product from the catalyst is by means of extraction with a co-solvent or precipitation with an anti-solvent[4]. Additional volatile organic solvents are therefore necessary in the separation step, with associated problems of cross-contamination and catalyst leaching. The ionic liquid/carbon dioxide production process is less complex. The ionic liquid is able to immobilize the catalyst. When the product APAM is extracted from the ionic liquid phase with supercritical carbon dioxide, the ionic liquid with catalyst will not be extracted too, since the ionic liquid and the catalyst have negligible solubilities in carbon dioxide. No catalyst leaching will occur and pure product is obtained without contamination by ionic liquid or catalyst[7,8,13].

9.2 Ecological analysis

The conventional production process generates lot of waste and is energy-intensive. Toxic solvent emissions into the environment are high. More waste is produced by the deactivated catalyst, which contains the transition metal rhodium. The product obtained is not totally pure, because catalyst leaching into the product phase occurs. The evaporation of solvent from the product and catalyst requires a lot of energy.

The use of ionic liquids/carbon dioxide as combined solvents leads to ecological benefits. No waste is produced, because solvent losses and catalyst losses are zero. Moreover, the use of ionic liquids does not lead to cross-contamination and to contamination of the product. The amount of energy needed to recover the product is lower, because energy is only needed to recompress the carbon dioxide, but no energy-intensive evaporation step is needed.

In paragraphs 9.2.1 and 9.2.2 the ecological impact of both processes are quantified and compared.

9.2.1 Waste generation

Waste generation originates from catalyst and solvent losses. The Rh-MeDuPHOS catalyst losses in the conventional process can be estimated in the following way. According to Berger *et al.*[4] a minimum MAAC-to-catalyst ratio of 2000 mole/mole is required. This is equal to a MAAC-to-catalyst ratio of 725 g/g, which means that 1.38 g of Rh-catalyst is required to convert 1 kg of MAAC into 1.01 kg APAM. In the conventional process, it is only possible to use the catalyst during five batches because of deactivation due to oxidation. That means that 1.38/5 = 0.276 g of Rh-catalyst per kilo produced APAM is used as catalyst make-up.

In ionic liquid/carbon dioxide process the catalyst make-up is zero, since the catalyst doesn't significantly deactivate and no catalyst leaching occurs[4,7,11]. However, in the economical evaluation it is assumed that the catalyst has to be replaced each year, since this is generally a more realistic assumption.

The solvent losses in the conventional process are determined in the following way: the amount of used methanol per kilo produced APAM is determined from the starting concentration of MAAC in methanol and it is assumed that the solvent recovery efficiency is 80%[12]. The concentration of MAAC in methanol in the conventional process is 0.25 M[2], which means that 0.25 moles of MAAC are dissolved in 1 liter of methanol. This is equal to 0.316 moles of MAAC per kg methanol (ρ = 0.791 kg/l)[15]. When all MAAC is converted to APAM, the concentration of APAM after reaction will also be 0.316 moles per kg methanol. This is equal to 69.8 g APAM per kg methanol ($M_{w,APAM}$ = 221 g/mole). Therefore, the amount of methanol (kg) is 14.3 times as much as the amount

of APAM (kg). The amount of methanol losses per kg APAM are therefore $0.20 \cdot 14.3 =$ 2.86 kg methanol per kilo produced APAM.

In the ionic liquid/carbon dioxide process, no solvent losses occur. The ionic liquid has no vapor pressure and will neither evaporate nor lead to emissions into the atmosphere. However, in the economical calculation it is also assumed that the ionic liquid has to be replaced each year.

9.2.2 Energy consumption

In the conventional process, at least 14.3 kg methanol per kilo produced APAM has to be evaporated (see paragraph 9.2.1). The amount of energy needed to evaporate 1 kg of methanol consists of the amount of energy to heat the methanol from room temperature (25 ^{o}C) to the boiling point temperature (65 °C) and the heat of evaporation[9]:

$$\Delta H = C_{p,l} \cdot \Delta T + \Delta_{vap} H \tag{9.3}$$

with:

ΔH	=	Amount of energy	[kJ·kg^{-1}]
$C_{p,l}$	=	Specific heat of liquid	[kJ·kg^{-1}·K^{-1}]
ΔT	=	Temperature difference	[K]
$\Delta_{vap} H$	=	Enthalpy of evaporation	[kJ·kg^{-1}]

The specific heat of methanol[15] is $C_{p,l}$ = 2.53 kJ·kg^{-1}·K^{-1} and the enthalpy of evaporation (at boiling point)[15] is $\Delta_{vap} H$ = 1099 kJ·kg^{-1}. Therefore, the total amount of energy that is necessary to evaporate 1 kg of methanol is 1200 kJ/kg (equation 9.3). The amount of energy used per kg produced APAM in the conventional process is $14.3 \cdot 1200 = 17160$ kJ/kg APAM = 17.2 MJ/kg APAM.

The energy consumption in the ionic liquid/carbon dioxide process consists of the amount of energy that is needed to repressurize the carbon dioxide from 80 bar to 120 bar (at 40 ^{o}C). The solubility of APAM in carbon dioxide at 120 bar is 1.78 g/kg. Therefore it is necessary to pressurize 1/0.00178 = 561 kg CO_2 per kilo produced APAM. The amount of energy which is necessary to pressure 1 kg of CO_2 from 80 bar (8.0 MPa) to 120 bar (12.0 MPa) can be estimated in the following way[16]:

$$W = \frac{1}{\eta} \cdot \int \frac{1}{\rho} \cdot dp \approx \frac{\Delta p}{\eta \cdot \rho_{average}} \tag{9.4}$$

with:

W	=	Work	$[J{\cdot}kg^{-1}]$
η	=	Compressor efficiency	$[-]$
ρ	=	Density	$[kg{\cdot}m^{-3}]$
Δp	=	Pressure difference	$[Pa] = [J{\cdot}m^{-3}]$

A compressor efficiency of 75% is assumed. The average density of carbon dioxide in the 80-120 bar range is 628.6 kg/m^3 and the pressure difference is 40 bar (= 4000 kPa). Therefore, the amount of energy to pressurize CO_2 from 80 bar to 120 bar is W = 8.48 kJ/kg (equation 9.4). The total amount of energy necessary per kilo produced APAM in the ionic liquid/carbon dioxide process is 561·8.48 = 4760 kJ/kg = 4.8 MJ/kg APAM, which is 4 times lower than the amount of energy necessary in the conventional process.

In table 9.2 an overview of the waste generation and the energy consumption of both the conventional production process and the ionic liquid/carbon dioxide process is shown.

Table 9.2: Waste generation and energy consumption of the conventional production of APAM compared to the ionic liquid/carbon dioxide production process (annual catalyst and solvent replacement in the ionic liquid/carbon dioxide process will be considered as yearly investment and not as variable cost per kg product)

	Conventional production process	*Ionic liquid/carbon dioxide production process*
Catalyst make-up	0.28 g/kg product	0 g/kg product
Solvent make-up	2.86 kg/kg product	0 kg/kg product
Energy for	Evaporating solvent	Pressurizing carbon dioxide
Energy needed	17.2 MJ/kg product	4.8 MJ/kg product

9.2.3 Total waste and energy savings in the Levodopa production

The ionic liquid/carbon dioxide production process can be used for the production of Levodopa, a medicine for Parkinson's disease. Parkinson's disease is one of the more common diseases of the ageing society, and affects men and women in equal amounts. Approximately 0.5% of the population in the western world suffers from Parkinson's disease[17]. Among the 457 million Europeans and 293 million Americans (2005)[18], there are nearly 4 million people with Parkinson's disease (and this number is rising). While the disease usually develops after the age of 65, it is increasingly diagnosed in people under 50 (presently 15% of all cases)[17].

The most frequently used medicine for treatment of Parkinson's disease is Levodopa, which relieves the symptoms (tremor, muscle stiffness, slowness of movement and loss of balance). Treatment with Levodopa requires 0.4 kg per person per year[19]. Therefore,

the potential market for Levodopa is almost 1600 ton per year. With a price of € 2800,- per kg, the annual Levodopa turnover is predicted to be as high as 4.5 billion euros[17].

In the conventional Levodopa production process, the waste generation in the asymmetric hydrogenation step only, is already almost 3 kg per kg product, and the energy requirement in this step is around 17 MJ per kg product (see paragraphs 9.2.1 and 9.2.2). It is possible to produce Levodopa using the ionic liquid/carbon dioxide production process instead of the conventional production method[13]. In the ionic liquid/carbon dioxide production process, solvent (ionic liquid) losses and catalyst losses in the asymmetric hydrogenation step are zero (compared to a loss of 3 kg methanol and 0.3 g catalyst per kg Levodopa in the asymmetric hydrogenation step of the conventional production process). The energy requirement in this step is only 4.8 MJ per kg product (compared to 17.2 MJ per kg product in the conventional process). Based on the potential market of 1600 ton Levodopa per year, the ionic liquid/carbon dioxide production process conserves in the asymmetric hydrogen step only already 20,000 GJ of energy, and prevents a waste stream of 4800 ton methanol and 480 kg catalyst.

9.3 Economical analysis

The costs of the conventional production process and the ionic liquid/carbon dioxide production process are compared. The total costs of both process methods consist of the fixed costs and the variable costs. The fixed costs include investment costs (equipment, piping, instrumentation, control systems, buildings, etc), whereas the variable costs include costs for raw materials, energy and labor.

9.3.1 Variable costs

The variable costs of both processes include the costs for the reactants MAAC and hydrogen, the costs for the catalyst and solvent make-up, the energy costs and the labor costs. It is expected that both production processes have the same costs for the reactants MAAC and hydrogen, because both operation methods have comparable conversions and enantioselectivities. It is also assumed that the labor costs are the same for both processes, because both process methods have similar problems in the ease of handling (inert or moisture-free atmosphere required to protect the catalyst in the conventional process, and to protect the ionic liquid in the ionic liquid/carbon dioxide process). Therefore these costs will be omitted in the comparison analysis. The remaining variable costs (catalyst and solvent make-up costs and energy costs) will be quantified in the next paragraphs.

In paragraph 9.2.1 it was calculated that the catalyst make-up is 0.28 g Rh-catalyst per kilo produced APAM and that the solvent make-up is 2.86 kg methanol per kilo produced APAM in the conventional production process. According to Chirotech Technology Ltd.[20], the large-scale price of the Rh-MeDuPHOS catalyst is € 20 per gram. Therefore, the costs for the catalyst make-up per kilo produced APAM in the conventional process are 0.28·20 = € 5.52, although this amount might be somewhat lower due to regeneration and recycling of the rhodium. The price of methanol is € 250 per metric ton[21]. This means that the costs for the methanol make-up in the conventional process are 2.86·0.25 = € 0.72 per kg APAM.

In the ionic liquid/carbon dioxide production process the catalyst and solvent make-up costs are zero, because no catalyst and solvent is lost (but ionic liquid and catalyst has to be purchased as an investment). The ionic liquid with immobilized catalyst has no detectable vapor pressure and will neither evaporate nor lead to emissions into the atmosphere.

In paragraph 9.2.2 the energy consumption of the conventional production process and the ionic liquid/carbon dioxide production process were estimated. It was found that the energy consumption of the conventional process is 17.2 MJ per kilo produced APAM, whereas the energy consumption of the ionic liquid/carbon dioxide production process is only 4.8 MJ per kilo produced APAM. The energy consumption can be converted in terms of money using the standard assumption that 1 Nm^3 of natural gas has an exergy

value of 4.9 MJ[22]. The price of 1 Nm³ of natural gas is € 0.3148[23]. This means that the energy costs of the conventional process are € 1.11 per kg APAM and the energy costs of the ionic liquid/carbon dioxide process are € 0.31 per kg APAM.

In table 9.3 an overview of the costs for catalyst and solvent make-up and the energy costs of both the conventional production process and the ionic liquid/carbon dioxide process is shown.

Table 9.3: Catalyst and solvent make-up costs and energy costs of the conventional production of APAM compared to the ionic liquid/carbon dioxide production process

	Conventional production process	Ionic liquid/carbon dioxide production process
Costs for Rh-catalyst make-up	€ 5.52 per kg APAM	€ 0 per kg APAM
Costs for solvent make-up	€ 0.72 per kg APAM	€ 0 per kg APAM
Energy costs	€ 1.11 per kg APAM	€ 0.31 per kg APAM
Total variable costs	**€7.35 per kg APAM**	**€0.31 per kg APAM**

From table 9.3 can be concluded that the variable costs of the ionic liquid/carbon dioxide process are much lower than the variable costs of the conventional process. This difference will only become larger in the future, when the energy prices will further increase. When applying the ionic liquid/carbon dioxide process on the production of Levodopa (with a potential market of 1600 ton per year, see paragraph 9.2.3), the variable costs can be reduced by 1600,000·(7.35 – 0.31) = 11.3 million euros per year. However, the ionic liquid/carbon dioxide process requires a larger investment (see below).

9.3.2 Fixed costs

The fixed costs of the conventional production process consist of costs for the equipment used, including the reaction vessel (withstanding pressures up to 16 bar) and the separation equipment. The separation equipment needed depends on the method of product recovery. However, at least a column to evaporate the solvent and another purification step to remove catalyst residues from the product are needed. The investments for the conventional process are already made which is an advantage for the conventional process.

In the ionic liquid/carbon dioxide production process the fixed costs are made up out of investment costs for the equipment, catalyst and ionic liquid.

The required equipment consists of a high-pressure vessel (withstanding pressures up to 150 bar) and a compressor. Although a high-pressure vessel with large wall thickness is more expensive than an ordinary reaction vessel, the ionic liquid/carbon dioxide process is not complex. No additional columns are needed to separate the solvent and catalyst

from the product. It is likely that the equipment needed for the novel process is not more expensive than the equipment needed for the conventional process. However, the investment still has to be made and this can be a barrier for adoption of the ionic liquid/carbon dioxide process. Since the current economic structure of the chemical industry is such that returns on investment are low, technologies requiring large capital expenditure are unlikely to be adopted. This barrier has seriously limited the more widespread use of many promising technologies. Fortunately, it might be possible to carry out the ionic liquid/carbon dioxide production process in existing equipment. For example, in the fine chemical industry supercritical extraction is already applied[24] and this equipment can also be used to carry out the ionic liquid/carbon dioxide process. In that case, the equipment investment is also already made for the ionic liquid/carbon dioxide production process, resulting in similar investment costs for equipment in both production processes.

However, in the ionic liquid/carbon dioxide production process, investments in the ionic liquid and catalyst have to be made. The ionic liquid and catalyst investment is estimated for the ionic liquid/carbon dioxide production process of Levodopa in the following way: it is assumed that 1 kg Levodopa is dissolved in 14.3 kg of ionic liquid with 1.38 g immobilized catalyst (same weight fractions as in conventional production process). With a potential market of 1600 ton per year, a reaction/separation time of 24 hours (1 day), and 300 operational days per year, the amount of ionic liquid required is $1600^.14.3/300 =$ 76 ton and the amount of catalyst required is $1600^.1.38/300 = 7.4$ kg. The price of ionic liquids is decreasing fast. The first quantities produced in laboratory-scale reflected more the labor costs than the cost of the chemicals. When produced on a large scale, the price of ionic liquids will drop significantly. It is expected that the long-term prices can be as low as € 10 per kilo ionic liquid (or even lower)[14]. The price of the catalyst is € 20,000 per kilo[20]. Therefore, the ionic liquid investment is $76,000^.10 = 0.76$ million euros and the catalyst investment is $7.4^.20,000 = 0.15$ million euros. This means that the total investment in ionic liquid and catalyst is 0.91 million euros. Even when all the ionic liquid and catalyst are replaced once a year, the investment is still much lower compared to the savings in variable costs of 11.3 million euros per year.

In conclusion, it can be said that the ionic liquid/carbon dioxide production process shows economical and ecological advantages over the conventional production process. When the ionic liquid/carbon dioxide process is applied to the production of Levodopa, the variable costs are reduced by 11.3 million euros per year, whereas the investment costs rise at least with 0.91 million euros (for ionic liquid and catalyst investments). The only barrier for adopting the novel approach is the necessary equipment expenditure, but this barrier can be overcome when the ionic liquid/ carbon dioxide production process is carried out in existing equipment.

9.4 References

1. Kroon, M. C.; Peters, C. J.; Sheldon, R. A.; Van Spronsen, J.; Witkamp, G. J.; Economical and Ecological Attractiveness of using Ionic Liquids as Combined Reaction and Separation Media, Proceedings of 6th International Conference on Process Intensification: Delft, The Netherlands, September 2005.
2. Burk, M. J.; Feaster, J. E.; Nugent, W. A.; Harlow, R. L.; Preparation and Use of C2-Symmetric Bis(phospholanes): Production of α-Amino Acid Derivatives via Highly Enantioselective Hydrogenation Reactions, *J. Am. Chem. Soc.* **1993**, *115 (22)*, 10125-10138.
3. Van Den Berg, M.; Minnaard, A. J.; Haak, R. M.; Leeman, M.; Schudde, E. P.; Meetsma, A.; Feringa, B. L.; De Vries, A. H. M.; Maljaars, C. E. P.; Willans, C. E.; Hyett, D.; Boogers, J. A. F.; Henderickx, H. J. W.; De Vries, J. G.; Monodentate Phosphoramidites: A Breakthrough in Rhodium-Catalyzed Asymmetric Hydrogenation of Olefins, *Adv. Synth. Catal.* **2003**, *345 (1-2)*, 308-323.
4. Berger, A.; De Souza, R. F.; Delgado, M. R.; Dupont, J.; Ionic Liquid-Phase Asymmetric Catalytic Hydrogenation: Hydrogen Concentration Effects on Enantioselectivity, *Tetrahedron Asymm.* **2001**, *12 (13)*, 1825-1828.
5. Gladiali, S.; Pinna, L.; Asymmetric Hydroformylation of N-Acyl-1-aminoacrylic Acid Derivatives by Rhodium/Chiral Diphosphine Catalysts, *Tetrahedron Asymm.* **1991**, *2 (7)*, 623-632.
6. Smallridge, A. J.; Trewhella, M. A.; Wang, Z.; The Enzyme-Catalyzed Stereoselective Transesterification of Phenylalanine Derivatives in Supercritical Carbon Dioxide, *Aust. J. Chem.* **2002**, *55 (4)*, 259-262.
7. Shariati, A.; Simons, C.; Sheldon, R. A.; Witkamp, G. J.; Peters, C. J.; Enantio-selective Catalytic Hydrogenation of Methyl α-acetamidocinnamate in [bmim][BF$_4$], submitted for publication to *Green Chem.* **2006**.
8. Kroon, M. C.; Van Spronsen, J.; Peters, C. J.; Sheldon, R. A.; Witkamp, G. J.; Recovery of Pure Products from Ionic Liquids Using Supercritical Carbon Dioxide as a Co-solvent in Extractions or as a Anti-solvent in Precipitations, *Green Chem.* **2006**, *8 (3)*, 246-249.
9. Smith, J. M.; Van Ness, H. C.; Abbott, M. M. *Introduction to Chemical Engineering Thermodynamics*, 5th ed.; McGraw-Hill: New York (NY), USA, 1996.
10. Poling, B. E.; Prausnitz, J. M.; O'Connell, J. P. *The Properties of Gases and Liquids*, 5th ed.; McGraw-Hill: New York (NY), USA, 2001.
11. Guernik, S.; Wolfson, A.; Herskowitz, M.; Greenspoon, N.; Geresh, S.; A Novel System Consisting of Rh-DuPHOS and Ionic Liquid for Asymmetric Hydrogenations, *Chem. Commun.* **2001**, *(22)*, 2314-2315.
12. Reichardt, C. *Solvents and Solvent Effects in Organic Chemistry*, 3rd ed.; Wiley-VHC Verlag: Weinheim, Germany, 2003.
13. Kroon, M. C.; Florusse, L. J.; Shariati, A.; Gutkowski, K. E.; Van Spronsen, J.; Sheldon, R. A.; Witkamp, G. J.; Peters, C. J. On a Novel Class of Production

Processes for the Chemical Industry, to be submitted for publication to *Nature* **2006**.

14. Wasserscheid, P.; Welton, T., Eds. *Ionic Liquids in Synthesis*; Wiley-VHC Verlag: Weinheim, Germany, 2003.
15. Lide, D. R., Ed. *Handbook of Chemistry and Physics*, 78th ed.; CRC Press, New York (NY), USA, 1997.
16. Green, D. W., Ed. *Perry's Chemical Engineers' Handbook*, 7th ed.; McGraw-Hill: New York (NY), USA, 1999.
17. Parkinson's Disease Foundation, Information on Parkinson's disease, http://www. parkinsonsinfo.com/
18. US Census Bureau Database, World population 1950-2050, http://www.census. gov/ipc/www/world.html
19. Challener, C. A., Ed. *Chiral drugs*; Ashgate: Aldershot, UK, 2001.
20. Dowpharma, Chirotech Technology Ltd, Prices of Catalysts and Ligands, http://pharma.dow.com/
21. Methanex, Methanol Price, http://www.methanex.com/products/methanolprice. html
22. Szargut, J. *Exergy Method: Technical and Ecological Applications*; WIT Press: Southampton, UK, 2005.
23. Energie Direct, Natural Gas Price, http://www.energiedirect.nl
24. King, M. B.; Bott, T. R., Eds. *Extraction of Natural Products Using Near-Critical Solvents*, 1st ed.; Chapman & Hall: Glasgow, UK, 1993.

10

Industrial Implementation of Ionic Liquid/Carbon Dioxide Processes Using the Cyclic Innovation Model

10
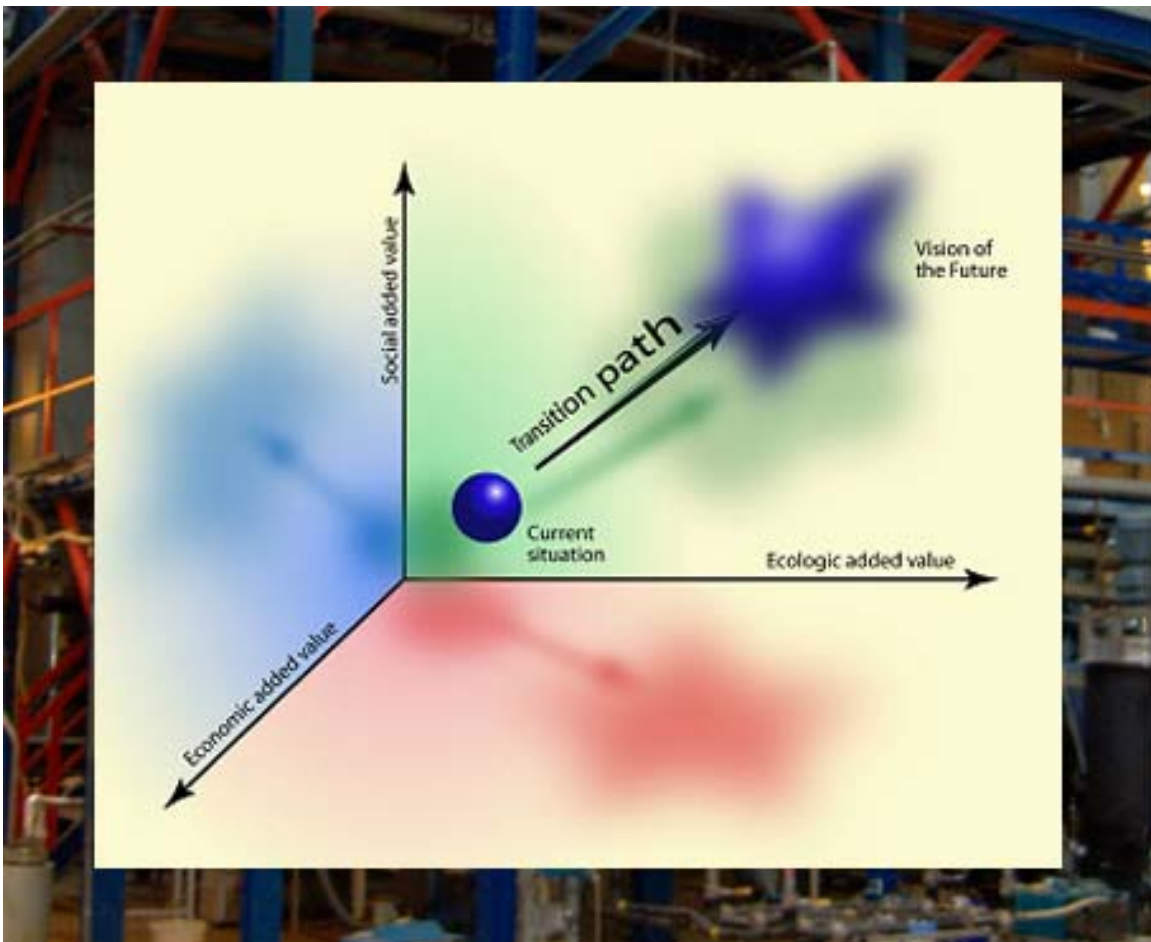
Industrial Implementation of Ionic Liquid/Carbon Dioxide Processes Using the Cyclic Innovation Model

A system concept for managing multi-value innovation is introduced. Multi-value innovation combines economic growth with environmental benefits and social value. Its ambition is to interconnect innovation with sustainability. The concept contains three interdependent components: vision, strategy and execution. The mode of execution is based on the Cyclic Innovation Model. This model does not represent innovation by a linear chain, but by coupled 'circles of change' which connect science and business in a cyclic manner. The Cyclic Innovation Model is applied to the industrial implementation of ionic liquid/carbon dioxide production processes, which are economically and environmentally superior to current production processes. Implementation will lead to a future where more fine chemicals and pharmaceuticals can be safely produced using less raw materials and significantly less energy and yielding less waste. The most important obstacles in the implementation of this new technology are the successful life cycle management of current production plants, the linearity of current innovation thinking and a perceived high risk of adoption. According to the Cyclic Innovation Model, these obstacles can be overcome when developments in all cycles occur in a parallel fashion and all involved actors collaborate in coupled networks.

10. Industrial Implementation of Ionic Liquid/Carbon Dioxide Processes Using the Cyclic Innovation Model

10.1 Introduction

In the Western world, the chemical industry has matured and investments have stabilized. One reason is that the lifetime of production plants is much larger than anticipated due to careful maintenance. Another reason is that smart engineering has increased the capacity of existing plants beyond expectation. Due to excellent life cycle management and maintenance, many current production processes originated about twenty years ago and are not based on the latest state-of-the-art technology. As a consequence, these processes produce too much waste and are too energy-intensive.

Environmental concerns call for new technologies. Recently, new opportunities for radically modified plants have emerged. The production processes involved are more sustainable than the conventional processes due to a more efficient use of resources. Examples are the use of shape-selective catalysts (zeolites) in the butene to isobutene isomerization[1], the use of membrane reactors in the ethylene oxide production[2] and the use of reactive distillation for the methyl acetate production[3]. These processes combine reactions and separations into one process step, and show a higher selectivity toward the main products. The result is less by-product generation (waste) and a lower energy requirement for purification. Despite clear advantages of these new technologies, commercialization is still limited due to the economic success of life cycle management of existing chemical plants.

Another promising technology is the use of ionic liquids and supercritical carbon dioxide as combined reaction and separation media[4-8]. It is possible to carry out highly efficient reactions and separations in ionic liquids, producing less waste and using significantly less energy than conventional alternatives[9-11] (see previous chapters). From an environmental point of view, fast implementation of this technological breakthrough is desired. However, with a conventional plan of execution, implementation could take several decades. One important reason for this long implementation trajectory is that innovations are traditionally considered as linear chains of causal actions, where each stage requires a considerable amount of time. However, when actions take place simultaneously in all stages of the innovation process, the time between invention and successful implementation can be reduced dramatically. For a fast adoption of innovative technologies, execution should be based on an innovation concept that considers the innovation process as coupled 'cycles of change', where developments take place in all cycles simultaneously[12,13]. Such an innovation concept is described and subsequently applied to the commercialization of the ionic liquid technology.

10.2 An integral concept for managing multi-value innovation

Innovation is generally seen by companies as a necessary investment to stay in business. This is the well-known economic aspect of innovation. However, increasing resource use (e.g., energy consumption) and environmental pollution (e.g., waste generation) give rise to a broader, multi-value role of innovation: how to combine economic growth with a more efficient use of natural resources and a decreasing amount of environmental pollution? This multi-value role is especially important in today's society, where energy consumption and waste generation are strongly increasing due to the growth of the world population and the increase in the standard of living (see figure 1.1).

According to Von Weizsäcker *et al.*[14], we could supply the needs of twice as many people using only half the resources, if only we would use better technologies ('Factor 4'). Alternatively, we could increase the quality of life for twice as many people at half the present cost. Therefore, innovation should aim at sustainable business. Multi-value innovation creates economic, ecologic as well as social added-value. It connects three dimensions of societal change (see figure 10.1).
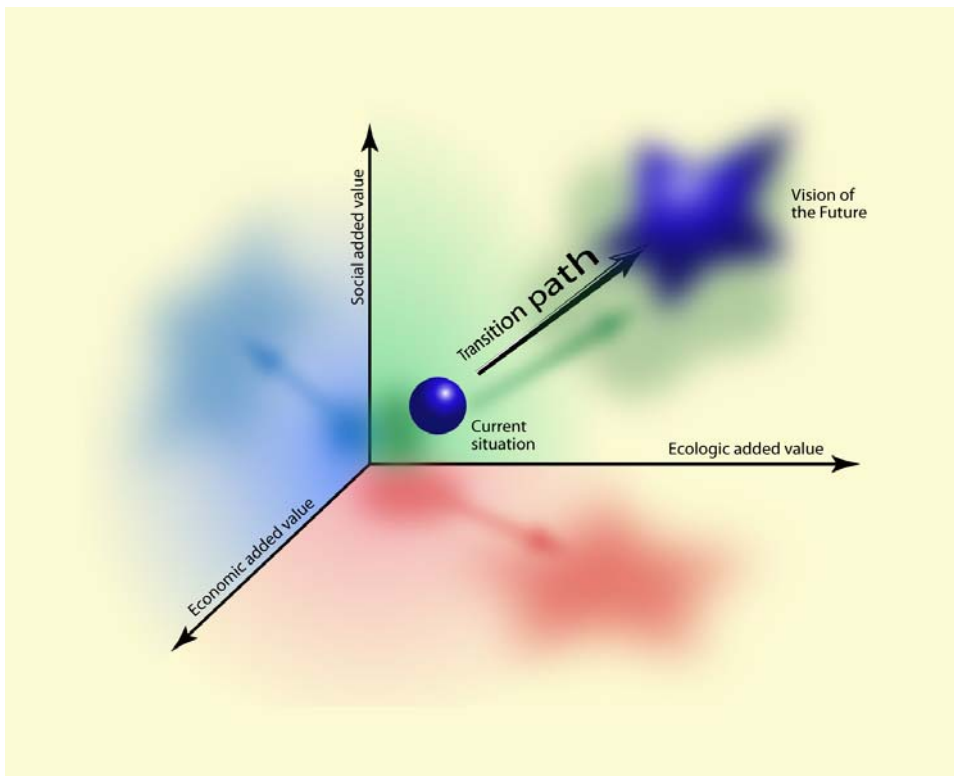
Figure 10.1: Multi-value innovation aims at the creation of economic, ecologic and social added-value. Multi-value innovation is managed by the formulation of a vision for a promising future, the design of a strategy to travel along the transition path from the current situation to the image of the future and the definition of a plan of execution. In this chapter, the vision of the future is a low-energy, waste-free production in the fine chemical industry.

The multi-value innovation concept contains three interconnected parts: a vision of the future, a transition path and a process model for execution[13]. This chapter will concentrate on the process model.

Innovations cause changes in the conventional way of doing things. These changes often threaten vested interests, a phenomenon which Schumpeter[15] called 'creative destruction'. It is therefore not surprising that organizations tend to reinforce the status quo. For example, when a company has successfully invested in an optimized package of technologies for many years, it will not easily change this proven way of working. Innovation requires pulling power to overcome this inertia, as well as the determination to change the old processes. Visions of an attractive future may generate the required pulling power. Such a vision reveals an inspiring new direction and provides a focus on long-term goals. In other words, the vision induces the formulation of a promising image of the future (where we want to be) related to the current situation (where we are now).

Of course, such a vision must be shared by all innovation partners involved. When different actors do not share the same vision, their goals will diverge. This is particularly true for long-term projects. Because innovation is inherently uncertain, returns may not emerge quickly. The risk of decreasing returns in difficult financial periods is large. Only a focus on long-term goals can overcome this problem.

For the industrial implementation of ionic liquid/carbon dioxide production processes, the vision of the future is related to a new method in producing fine chemical and pharmaceutical products. The target is a fast realization of economic growth with a production process that is low-energy and zero-waste.

The process model to realize the change is based on the Cyclic Innovation Model, where innovation activities are no longer described by a linear pipeline but by coupled 'circles of change', connecting science with business as well as technology with markets in a cyclic manner. Parallel developments in all cycles accomplish a fast implementation of new technological concepts.

Based on earlier research on ionic liquids[16-18], we discovered a new way of industrial processing in which pure fine chemicals and pharmaceuticals can be produced efficiently without any waste generation, and using only a very low energy input[10] (see chapter 3). This innovative way of processing makes use of ionic liquids as solvents. It is both economically and environmentally significantly more attractive than conventional production methods (see chapter 9). In addition, the process set-up is safer. Paragraph 10.3 gives an overview of the latest developments in the production of fine chemicals and pharmaceuticals using ionic liquids, formulating an ambitious vision of the future. This is a future where more fine chemicals and pharmaceuticals can be safely produced using less raw materials, significantly less energy and zero waste. A strategy is developed to overcome problems along the transition path. The mode of execution is based on the Cyclic Innovation Model. Paragraph 10.4 contains a summary of this model, which is subsequently applied to the industrial implementation of ionic liquids. Recommendations

that will lead to a fast implementation of this new way of processing are formulated in paragraph 10.5. It should lead to a step forward in the realization of a more sustainable chemical industry.

10.3 How to revolutionize the fine chemical and pharmaceutical production process

10.3.1 Current situation

The chemical industry is under considerable pressure to replace many existing processes by new technologies aiming at a zero environmental footprint (zero emission, zero waste generation, use of renewable resources, energy-efficient). This is especially true for the fine chemical and pharmaceutical industries, which use a lot of energy and generate a large amount of chemical waste per kilogram net product[19,20] (see table 1.1).

Without change, this energy and waste problem will be even larger in the future, because the production of pharmaceuticals will increase dramatically in our ageing society. The world population is increasing; people live longer and will suffer more from infirmities of old age. It is estimated that people over 65 years of age will make up one third of the total population in West Europe after 2020[21]. At the same time, these people can spend more money on medicines that can extend their lives, because their standard of living is increasing[21]. Therefore, the costs of healthcare will rise dramatically. These costs would be even higher if the environmental impact of medicine production was realistically accounted for.

A recent discovery shows that it is possible to produce pharmaceuticals without *any* waste generation and *very low* energy input by using ionic liquids and carbon dioxide as combined reaction and separation media[9,10] (see chapter 3). When ionic liquids are used in combination with supercritical carbon dioxide as co-solvent, it is possible to carry out reactions and separations simultaneously by using the recently discovered miscibility switch phenomenon (see figure 3.3): two immiscible phases (liquid phase and vapor phase) can be forced into one homogeneous liquid phase in the presence of compressed carbon dioxide[22,23]. Using this one-phase/two-phase transformation upon a change in carbon dioxide pressure (or alternatively, carbon dioxide concentration), it is possible to carry out reactions in a homogeneous system, resulting in high reaction rates. Moreover, because ionic liquids can dissolve a wide range of catalysts, a reaction can be carried out with very high selectivity and zero waste production. In the biphasic system the supercritical carbon dioxide is used to extract the pure product from the ionic liquid phase without any contamination by the ionic liquid, because it has negligible vapor pressure. After extraction with carbon dioxide, the product can be separated from the carbon dioxide by further pressure release. The carbon dioxide and the ionic liquid can both be reused[9-11] (see figure 3.4).

This process can produce fine chemicals and pharmaceuticals much more efficiently without any waste generation (no solvent losses). The result is a more cost effective use of the raw materials and no disposal costs. The energy consumption is only 25% of that of the conventional production method (energy is necessary only to pressurize the carbon dioxide, not to evaporate a solvent), resulting in lower operational costs. These savings

lead to a substantially lower cost price. When the new process is carried out in existing equipment, only small investments are required. And the production process is very safe, because there are no toxic volatile organic solvents involved[11] (see chapter 9).

10.3.2 Vision of the future

As mentioned in paragraph 10.2, it is most desirable to replace today's chemical processes by more sustainable alternatives. Processes using ionic liquids are very energy-efficient, eliminate waste and avoid the use of toxic and/or hazardous chemicals. Moreover, because ionic liquids are non-volatile (cannot be inhaled) and can be designed non-flammable (no risk of burning or explosion), these processes are much safer than processes using conventional volatile organic solvents. In terms of figure 10.2, ionic liquids make the business more attractive (economic component), spare the environment (ecological component) and produce medicines safely at lower prices (social component). This vision of the future is shown in figure 10.2. Lower prices of medicines are most welcome at a time when social security systems are under pressure and the cost of healthcare is getting increasingly higher due to the ageing society. The higher affordability of these medicines will improve the quality of life for many people worldwide.
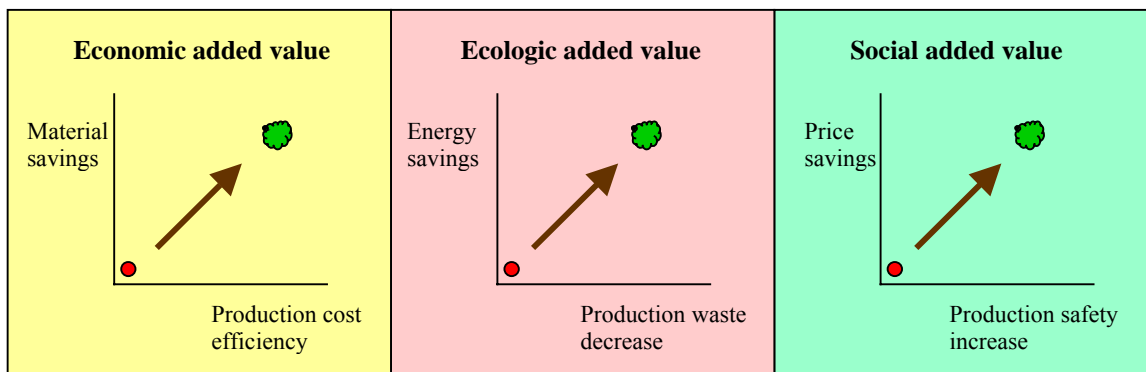

Figure 10.2: Vision of the future: The new production paradigm leads to a future with savings on raw materials, energy and prices. It also leads to a production process with less cost, zero waste and improved safety. Note that this figure shows that each of the three added-value dimensions in figure 10.1 represents itself a two-dimensional parameter space.

10.3.3 Transition path

A strategy has to be designed to travel along the transition path from the current situation (energy-intensive, waste-generating industrial processes) to the vision of the future (low energy, zero-waste industrial processes) with minimum delay. There are a number of obstacles along this transition path that must be overcome to realize a fast implementation. These obstacles are:

- Successful life cycle management of current production plants
- A risk averse chemical industry
- Linear innovation paths causing long times to market

Investment requirements are considered to be an important obstacle in the adoption of the new production process. In the current economic structure of the chemical industry the lifetime of production plants is large and returns on investment are low. Therefore, new technologies requiring large capital expenditure are unlikely to be adopted from an economic point of view. This hurdle has seriously limited a more widespread use of promising technologies in the past.

A second obstacle on the transition path is considered to be uncertainty. A new way of processing always involves risks, because the concept has not yet been proven on a large scale and on the long-term. Therefore, as long as the current production method is making an acceptable profit, industry will be risk averse and stick with optimizing current production concepts. Radical change must primarily come from environmental and social forces, rather than from economical incentives.

Fortunately, the situation for the proposed new ionic liquid/carbon dioxide production process is more positive. Large investments do not have to be made, because the new production process can use existing equipment. In the fine chemical industry, supercritical extraction is already applied[24] and this equipment can also be used to carry out the new process. Moreover, when industry not only takes economic considerations into account but also the environmental and social impact of their activities, the overall advantage of the new investment is even higher.

The obstacle of uncertainty can be overcome by demonstrating the use of ionic liquids under practical conditions for prolonged periods of time. Until recently, the long-term process aspects of ionic liquids (such as the long-term stability, availability, costs and impact on the environment) were unknown[25]. However, cooperation between companies, research institutes and universities has resulted in a 'proof of concept' for a number of ionic liquid processes. In collaboration projects, properties of ionic liquids that are needed for their implementation in industry have been evaluated[26-28]. Considerable progress towards commercialization of ionic liquids has recently been made. Since the supply of ionic liquids is expanding (more types of ionic liquids with increasing availability from multiple vendors), prices are decreasing fast because of economics of scale[29]. At the same time, more ionic liquids are demanded, because new industrial

applications are found. This higher demand does not seem to raise the price, because the supply increases even faster. For example, ionic liquids are currently used in BASF's BASIL® (Biphasic Acid Scavenging using Ionic Liquids) technology for esterifications[30] and in Air Products' GASGUARD® technology for the safe storage of toxic gases[31]. Because of these first commercial applications, ionic liquids are considered less risky, and more as 'proven' technology.

Because the considered obstacles of investment requirements and uncertainty in the adoption of the proposed production process are smaller than perceived, it is possible to accelerate the implementation of the proposed ionic liquid/carbon dioxide production process. Instead of using time-consuming linear innovation paths, an innovation model that considers the innovation process as coupled 'cycles of change' is employed. This will be discussed in the next paragraph.

10.4 Managing the innovation process

10.4.1 The Cyclic Innovation Model

The development of innovation models is generally classified into generations[32-34]. First-generation innovation models represent the innovation process as a pipeline of sequential processes (stage-gate model), starting at scientific research and ending with commercial applications ('technology-push'). Second-generation models reverse this pipeline, starting at the market and ending at scientific research ('market-pull'). Third-generation models are a mixture of the previous two. They combine the 'science-push' and 'market-pull' models and introduce feedback paths in the pipeline. However, innovations do not take place in linear sequences. Instead, innovation creates change, which in turn creates new opportunities and challenges, resulting in innovations that again generate change, etc. Therefore, the mode of execution used in this chapter has a circular architecture and is based on a fourth-generation innovation model, the Cyclic Innovation Model (CIM). This model was introduced by Berkhout[12]. It considers the innovation process as four coupled 'cycles of change', in which parallel developments take place that influence each other. In this way, the innovation path (the transition path from the current situation to the image of the future) can be significantly accelerated.

In CIM, technological research is influenced by two driving forces: scientific exploration and product(ion) development. This influence is not linear (one-way), but shows cyclic interaction (feed-forward and feed-back paths). Therefore, technological research plays a *central* role in connecting sciences with products (upper part of figure 10.3). Technological research is fueled by scientific knowledge in the natural and life sciences ('hard sciences'). In this technical-oriented sciences cycle, technological research is a multi-disciplinary activity: a package of different disciplines from the hard sciences is needed to develop a new technology (many-to-one relationship). In addition, technological research is driven by the needs of technical knowledge on how to create new technical functions (products). In this integrated engineering cycle, product(ion) development is a multi-technology activity: a package of different technologies is used to develop a new product or production process (many-to-one relationship). The dynamics in technological research are thus driven by both new scientific insights (science push) and new requirements in product(ion) development (function pull).

Similarly, market transitions are also influenced in a cyclic way by scientific exploration and product(ion) development. The two linked cycles are shown in the lower part of figure 10.3. Insight in rising and falling markets is fueled by scientific knowledge in the economic and social sciences ('soft sciences'), being directed to the changing needs and concerns in society. In this social-oriented sciences cycle, research is a multi-disciplinary activity: a package of different disciplines from the soft sciences is needed to explain and predict changes in markets (many-to-one relationship). Furthermore, market transitions are driven by the supply of new product/service combinations. In this differentiated service cycle, the supply of new product/service combinations is determined by the

innovative capacity of the business community. The dynamics in market transitions are thus driven by both scientific insight into changing demand and commercial investment in changing supply.
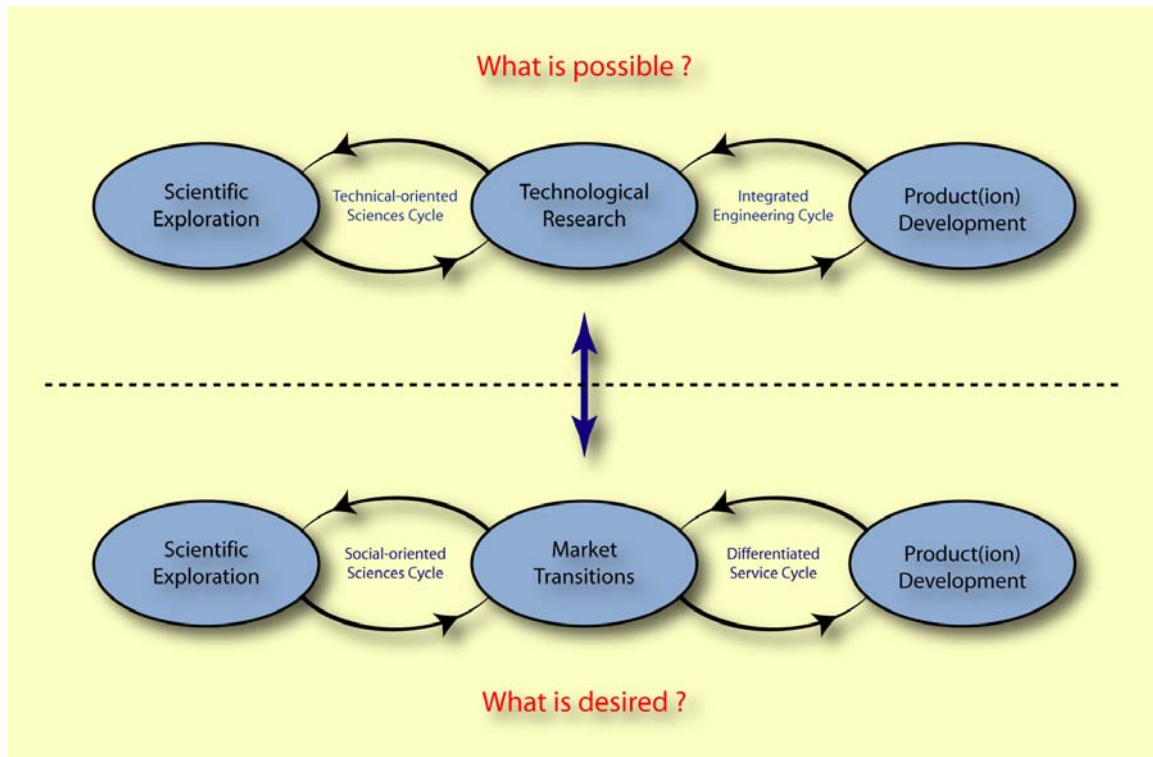
Figure 10.3: Technological research (upper part) is driven by the cyclic interaction between new scientific insights in technologies (technical-oriented sciences cycle) and new requirements in product(ion) development (integrated engineering cycle). Similarly, market transitions (lower part) are driven by the cyclic interaction between new scientific insights in changing demands (social-oriented sciences cycle) and the changing supply of product/service combinations (differentiated service cycle).

Figure 10.3 reveals that both scientific exploration and product(ion) development have a dual nature. Scientific exploration has soft and hard aspects; and product(ion) development has technical and societal aspects. Figure 10.4 combines the upper and lower part of figure 10.3 into the Cyclic Innovation Model: a circle of interacting processes of change, creating interaction between changes in science and industry (interaction between the left and right hand side of the model), as well as technology and markets (interaction between the upper and lower part of the model). The four nodes of change – scientific exploration, technological research, product development and market transitions – are coupled via cyclic interactions, with feed-forward and feedback loops. Technology is very important, but CIM shows that innovation is more than just technology. What is the added value for the user? Note from figure 10.4 that entrepreneurship plays a central role: without entrepreneurship there is no innovation.
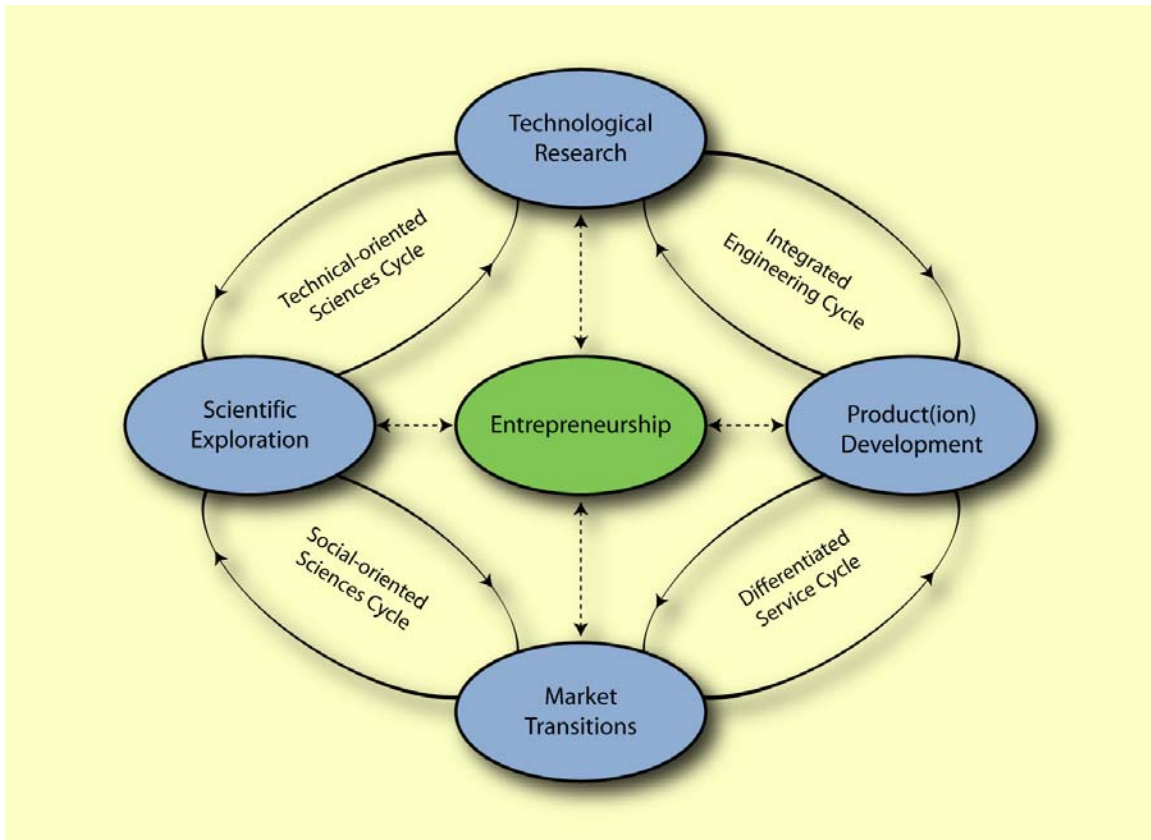
Figure 10.4: In the Cyclic Innovation Model (CIM) changes in science and industry as well as changes in technology and markets are cyclically interconnected. Entrepreneurship plays a central role in the innovation process. Note that the model represents not a chain but a circle, because in practice, innovations build on innovations.

Innovations can be subdivided into classes. Class 1 innovations are based on changes in only one node. For instance, a new marketing concept for an existing product-service combination is a class 1 innovation. Similarly, class 2 innovations are based on changes in two nodes, etc. The most disruptive innovations are of class 4, where all four nodes change and innovations require new scientific discoveries. Industrial application of ionic liquid/carbon dioxide production processes in the chemical industry is a class 4 innovation. The scientific discovery has largely been made, and the technology is maturing. Now, the two remaining CIM nodes (i.e., production development and market transitions) need to change.

In a favorable innovation system there are few barriers between the nodes and cycles. Knowledge, information, labor and capital can take freely flow around the innovation circle, both clockwise and anti-clockwise. However, one or more barriers can disturb this process. Two types of barriers are common: the 'innovation paradox' and 'technical isolation'. The 'innovation paradox' means that a society is not innovative, even though it performs excellent in scientific research (barrier between the left and right hand side of

figure 10.4). 'Technical isolation' means that a society is not innovative, even though it is successful in developing inventive technology (barrier between the upper and lower part of figure 10.4).

10.4.2 Innovating chemical production processes using ionic liquids and carbon dioxide as combined reaction and separation media

Figure 10.5 shows the Cyclic Innovation Model for the implementation of the proposed production process combining carbon dioxide with ionic liquids[35]. It is indicated which actors are responsible for which challenges. Figure 10.6 shows a network representation of the innovation cycles.
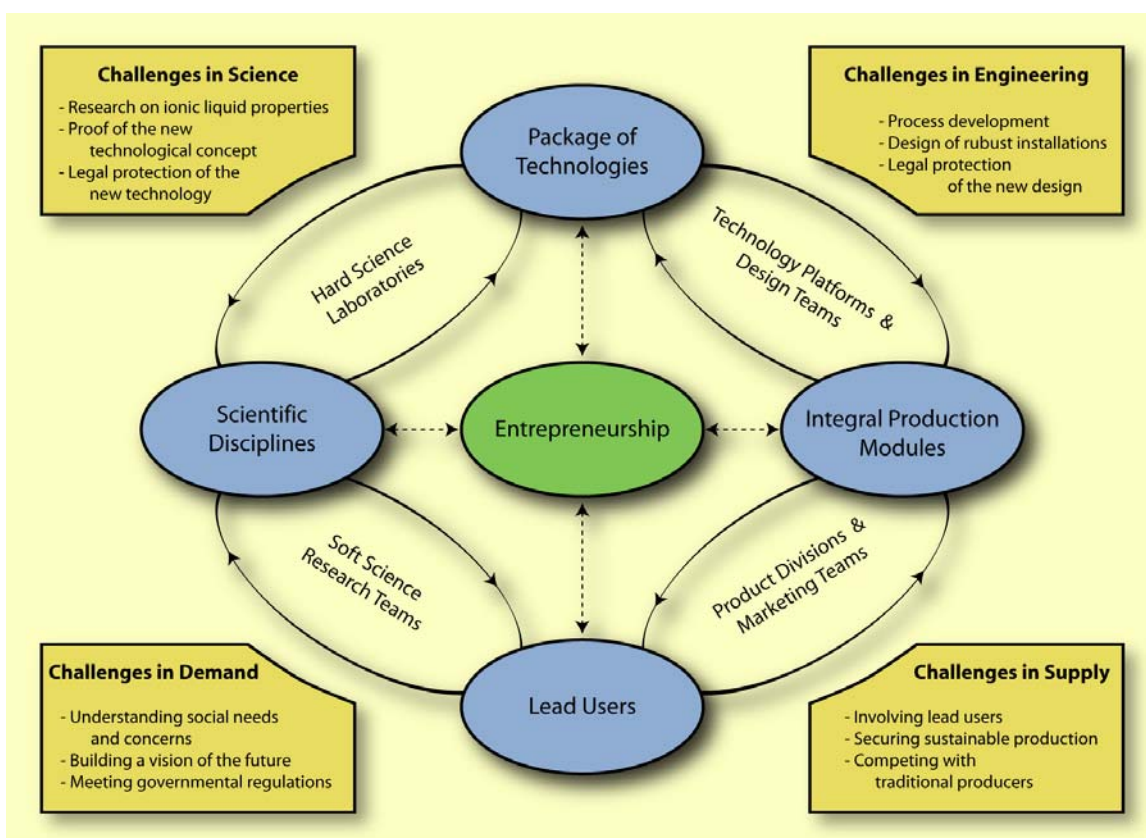
Figure 10.5: The Cyclic Innovation Model for the sustainable production of fine chemicals and pharmaceuticals. Challenges and responsible actors are indicated. Innovation is like playing simultaneous chess on four boards.

Scientific laboratories   Product divisions

Technology driven	Scientific laboratories	Product divisions	
	- Research on ionic liquid properties - Proof of the new technological concept - Protection of the new technology	- Process development - Design of robust installations - Protection of the new design	Technology platforms
Customer driven	- Understanding social needs and concerns - Building a vision of the future - Meeting governmental regulations	- Involving lead users - Securing sustainable production - Competition with traditional producers	Marketing teams

Research-oriented   Product(ion)-oriented

Figure 10.6: Network representation of the innovation cycles for the sustainable production of fine chemicals and pharmaceuticals. There are four interconnected networks, each network having a matrix topology[12].

Challenges in the market
The market of fine chemicals and pharmaceuticals is growing fast, due to the population growth, the trend of aging and the higher standard of living. The latter makes medicines affordable to more people. Conventional production processes in the chemical industry generate too much chemical waste and use too much energy (see table 1.1). Since the environmental awareness is increasing, the fine chemical industry is under pressure to reduce its waste production and energy consumption. Furthermore, lower prices for medicines are demanded to reduce the increasing cost of healthcare. These forces will drive the forthcoming changes.

Looking at the social-oriented sciences cycle, market-oriented research organizations aim in their research to better understand and predict the continuously changing needs and concerns in society. Companies use this knowledge to build a corporate vision of the future. Governments should base their legislation on this understanding, whereas in turn the legislation will again initiate new changes.

For example, governmental legislation can force companies to innovate by setting stricter regulations with regard to safety, health and environment. These regulations should be based on the latest state-of-the-art technology, or, even better, should encourage the development of better technology. Intelligent governmental legislation leads to a faster implementation of multi-value innovation. However, government should design their policies in close collaboration with universities and companies. This is the essence of the triple helix principle[36,37].

Challenges in production
In the differentiated service cycle, companies aim to distinguish themselves with the new production process in order to obtain competitive advantage. Product quality and specifications are set by product divisions in cooperation with lead users. Profitability is a first requirement for securing the sustainable production of fine chemicals and pharmaceuticals. Moreover, marketing groups can use the sustainable image of the company to attract new customers and to confront conventional producers.

The new production process is an example of a process innovation. Industry is not asked to make a new product (it takes at least 10 years of clinical testing before a new medicine is allowed for public use), but to change the way of production. A significant advantage is that the new production method can be carried out by making ample use of existing equipment.

Challenges in engineering
The product divisions (engineers from industry) and technology platforms (applied researchers from the hard sciences) must cooperate in the engineering cycle to develop the ionic liquid technology to maturity. They should test the new production process on a pilot scale and then design robust commercial installations. They must learn all (long-term) process aspects, and know how to optimize the process by smart control. The pharmaceutical industry should share their experiences with the scientific community and stimulate universities to develop solutions to overcome any of the problems that may occur. Also, patent protection of the robust installation design is an important issue.

Challenges in science
Scientific laboratories in cooperation with technology platforms must determine the physical and chemical properties of ionic liquids to select a suitable one for a specific application (technical-oriented sciences cycle). Measuring these properties is time-

consuming and expensive. It is better to develop scientific models for predicting the properties of ionic liquids. Also, the long-term stability of ionic liquids has to be investigated. Furthermore, ionic liquids should be tried as solvents for various reactions and separations. Kinetics and selectivities should be measured. Multi-disciplinary scientific groups (catalysis, thermodynamics, separation technology) should work together to obtain all this information. Based on these data, a proof of concept for the new technology can be reached and applications for the new technology can be found in cooperation with companies. Furthermore, intellectual property protection for the new technology should be arranged.

Class 4 innovation
The new production process is an example of a class 4 innovation. It is based on innovative contributions in all four nodes. Science provides the foundation for the new production process. Basic research on the properties of ionic liquids has generated new insight for the use of these liquids as novel reaction and separation media. Further technological development has resulted in the discovery of a new safe production method without any waste generation and with low energy input. Sustainable industrial production can be secured by the profitability and the 'green' image of the innovation. It is recommended to introduce a certificate that states that the chemical product is produced in an environmentally and socially responsible manner. In this way, customers can recognize that the new production method meets the needs and concerns of society, now and in the future.

10.5 Conclusions

In this thesis a new production process using ionic liquids and carbon dioxide is described that may lead leads to a future where more fine chemicals and pharmaceuticals can be safely produced using less raw materials and significantly less energy and yielding zero waste.

Fast implementation of this sustainable way of production requires the use of a new innovation concept. This concept does not represent innovation by a sequential process, but by coupled networks that connect science and business in a parallel fashion.

10.6 References

1. Pellet, R. J.; O'Young, C. L.; Hazen, J.; Hadowanetz, A. E.; Browne, J. E.; Treated Bound Ferrierite Zeolites for Skeletal Isomerization of *N*-Olefins to Iso-Olefins, US Patent 5523510 (1996).
2. Al-Juaied, M. A.; Lafarga, D.; Varma, A.; Ethylene Epoxidation in a Catalytic Packed-Bed Membrane Reactor: Experiments and Model, *Chem. Eng. Sci.* **2001**, *56 (2)*, 395-402.
3. Huss, R. S.; Chen, F.; Malone, M. F.; Doherty, M. F.; Reactive Distillation for Methyl Acetate Production, *Computers Chem. Eng.* **2003**, *27 (12)*, 1855-1866.
4. Earle, M. J.; Seddon, K. R.; Ionic Liquids. Green Solvents for the Future, *Pure Appl. Chem.* **2000**, *72 (7)*, 1391-1398.
5. Brennecke, J. F.; Maginn, E. J.; Ionic Liquids: Innovative Fluids for Chemical Processing, *AIChE J.* **2001**, *47 (11)*, 2384-2389.
6. Sheldon, R. A.; Lau, R. M.; Sorgedrager, M. J.; Van Rantwijk, F.; Seddon, K. R.; Biocatalysis in Ionic Liquids, *Green Chem.* **2002**, *4 (2)*, 147-151.
7. Wasserscheid, P.; Welton, T., Eds. *Ionic Liquids in Synthesis*; Wiley-VCH Verlag: Weinheim, Germany, 2003.
8. Welton, T.; Ionic Liquids in Catalysis, *Coord. Chem. Rev.* **2004**, *248 (21-24)*, 2459-2477.
9. Kroon, M. C.; Shariati, A.; Florusse, L. J.; Peters, C. J.; Van Spronsen, J.; Witkamp, G. J.; Sheldon, R. A.; Gutkowski, K. E.; Process for Carrying Out a Chemical Reaction, International Patent WO 2006/088348 A1 (2006).
10. Kroon, M. C.; Florusse, L. J.; Shariati, A.; Gutkowski, K. E.; Van Spronsen, J.; Sheldon, R. A.; Witkamp, G. J.; Peters, C. J. On a Novel Class of Production Processes for the Chemical Industry, to be submitted for publication to *Nature* **2006**.
11. Kroon, M. C.; Peters, C. J.; Sheldon, R. A.; Van Spronsen, J.; Witkamp, G. J.; Economical and Ecological Attractiveness of using Ionic Liquids as Combined Reaction and Separation Media, Proceedings of 6$^{\text{th}}$ International Conference on Process Intensification: Delft, The Netherlands, September 2005.
12. Berkhout, A. J. *The Dynamic Role of Knowledge in Innovation. An Integrated Framework of Cyclic Networks for the Assessment of Technological Change and Sustainable Growth*; Delft University Press: Delft, The Netherlands, 2000.
13. Berkhout, A. J.; Hartmann, D.; Van Der Duin, P.; Ortt, R.; Innovating the Innovation Process, *Int. J. Technol. Manage.* **2006**, *34 (3-4)*, 390-404.
14. Von Weizsäcker, E. U.; Lovins, A. B.; Lovins, L. H. *Factor 4, Doubling Wealth, Halving Resource Use*; Earthscan: London, UK, 1997.
15. Schumpeter, J. A. *Business Cycles: A Theoretical, Historical and Statistical Analysis of the Capitalist Process*; McGraw-Hill: New York (NY), USA, 1939.
16. Blanchard, L. A.; Hancu, D.; Beckman, E. J.; Brennecke, J. F.; Green Processing Using Ionic Liquids and CO_2, *Nature* **1999**, *399 (6731)*, 28-29.
17. Liu, F.; Abrams, M. B.; Baker, R. T.; Tumas, W.; Phase-Separable Catalysis Using Room Temperature Ionic Liquids and Supercritical Carbon Dioxide, *Chem. Commun.* **2001**, *(5)*, 433-434.

18. Solinas, M.; Pfaltz, A.; Cozzi, P. G.; Leitner, W.; Enantioselective Hydrogenation of Imines in Ionic Liquid/Carbon Dioxide Media, *J. Am. Chem. Soc.* **2004**, *126 (49)*, 16142-16147.

19. Worrell, E.; Phylipsen, D.; Einstein, D.; Martin, N. *Energy Use and Energy Intensity of the US Chemical Industry*; University of Berkeley: Berkeley (CA), USA, 2000.

20. Sheldon, R. A.; Organic Synthesis – Past, Present and Future, *Chem. & Ind.* **1992**, *(23)*, 903-906.

21. Eurostat, Statistics on population, economics, industry, agriculture, trade, transport, science, technology, and environment of the EU countries, http://epp.eurostat.cec.eu.int/

22. Gauter, K.; Peters, C. J.; Scheidgen, A. L.; Schneider, G. M.; Cosolvency Effects, Miscibility Windows and Two-Phase LG Holes in Three-Phase LLG Surfaces in Ternary Systems: A Status Report, *Fluid Phase Equilib.* **2000**, *171 (1-2)*, 127-149.

23. Peters, C. J.; Gauter, K.; Occurrence of Holes in Ternary Fluid Multiphase Systems of Near-Critical Carbon Dioxide and Certain Solutes, *Chem. Rev.* **1999**, *99 (2)*, 419-431.

24. King, M. B.; Bott, T. R., Eds. *Extraction of Natural Products Using Near-Critical Solvents*, 1st ed.; Chapman & Hall: Glasgow, UK, 1993.

25. Chemical Industry Vision 2020 Technology Partnership, Accelerating Ionic Liquid Commercialization – Research Needs to Advance New Technology, http://www.chemicalvision2020.org/ionic_liquids.html

26. Atkins, M. P.; Davey, P.; Fitzwater, G.; Rouher, O.; Seddon, K. R.; Swindall, J.; (Queen's University Ionic Liquid Laboratories, QUILL), Ionic Liquids: A Map for Industrial Innovation, http://quill.qub.ac.uk/ map/

27. International Union of Pure and Applied Chemistry (IUPAC), Ionic Liquid Projects, http://www.iupac.org/projects/2003/2003-020-2-100.html

28. IUPAC Ionic Liquids Database (IL Thermo), NIST Standard Reference Database # 147, http://ilthermo.boulder.nist.gov/ILThermo/mainmenu.uix

29. Ionic Liquids Database Merck, Ionic Liquids: New Materials for New Applications, http://ildb.merck.de/ionicliquids/en/startpage.htm

30. BASF, BASIL Process (Biphasic Acid Scavenging using Ionic Liquids), http://www.basf.com/corporate/051004_ionic.htm

31. Air Products, GASGUARD Sub-Atmospheric Systems (SAS), http://www.airproducts.com/NR/rdonlyres/ 9D919AAD-DE4F-4614-B3C4-E923C6BF786E/ 0/ GasguardSAS.pdf

32. Rothwell, R.; Towards the Fifth-Generation Innovation Process, *Int. Marketing Rev.* **1994**, *11 (1)*, 7-31.

33. Liyanage, S.; Greenfield, P. F.; Don, R.; Towards a Fourth-Generation R&D Management, Model-Research Networks in Knowledge Management, *Int. J. Technol. Manage.* **1999**, *18 (3-4)*, 372-394.

34. Roussel, P. A.; Saad, K. N.; Erickson, T. J.; *Third Generation R&D. Managing the Link to Corporate Strategy*, Harvard Business School Press: Boston (MA), USA, 1991.

35. Kroon, M. C.; Hartmann, D.; Berkhout, A. J.; Innovating the Innovation Process: How to Revolutionize the Fine Chemical and Pharmaceutical Production Process, submitted for publication to *Green Chem.* **2006**.

36. Etzkowitz, H.; Leydesdorff, L. The Endless Transition: A 'Triple Helix' of University-Industry-Government Relations, *Minerva* **1998**, *36 (3)*, 203-208.

37. Chesbrough, H. W. *Open Innovation: The New Imperative for Creating and Profiting from Technology*, Harvard Business School Press: Watertown (MA), USA, 2003.

11

Conclusions and Outlook

11

Conclusions and Outlook

11. Conclusions and Outlook

11.1 Conclusions

Ionic liquid/carbon dioxide production processes can be an attractive alternative for the wasteful and energy-intensive conventional production processes. Combining reactions and separations using ionic liquids and carbon dioxide lead to considerable process intensification when the miscibility windows phenomenon (carbon dioxide-induced 'single-phase'/'two-phase' transition) is applied. Using this phenomenon, it is possible to carry out reactions in a homogeneous phase, whereas the separation takes place in the biphasic system, where the products are recovered from the phase that does not contain any ionic liquid. Advantages of this new process set-up are the high reaction and separation rates, the low waste generation and energy consumption, the high product quality and the safe working conditions. The occurrence of the miscibility windows phenomenon has been demonstrated for ternary ionic liquid + carbon dioxide + alkanol systems. Since the principle of miscibility windows is a general phenomenon, it is likely that the new process set-up is applicable to many industrial processes.

It was found that the asymmetric hydrogenation of methyl (*Z*)-α-acetamidocinnamate could be carried out in an ionic liquid + carbon dioxide system. Conversions and enantioselectivities were comparable to the conventional production process. The catalyst could be reused without significant loss in activity or selectivity. The product N-acetyl-(*S*)-phenyl-alanine methyl ester was separated from the ionic liquid using carbon dioxide either as co-solvent in extractions (at low carbon dioxide concentrations) or as anti-solvent in precipitations (at high carbon dioxide concentrations). The extracted product contained no detectible amount of ionic liquid or catalyst (<0.1 ppm). Both separation methods work well and can reach a 100% recovery using a proper process lay-out.

A model was developed to predict the phase behavior of ionic liquid systems. This model is based on the truncated Perturbed Chain-Polar Statistical Association Fluid Theory (tPC-PSAFT) equation of state. This model not only describes the carbon dioxide solubility in ionic liquids well, but also gives an indication that the ionic liquid mainly consists of ion pairs instead of separated charged ions.

Quantum chemical calculations were used to develop a tool for prediction of the thermal and electrochemical stability of ionic liquids. The calculated activation energy corresponded well with the measured decomposition temperature and may be used to predict the decomposition temperature of an ionic liquid before it is synthesized. Moreover, it was found that the electrochemical window could be correlated to the calculated difference in energy level of Lowest Unoccupied Molecular Orbital (LUMO) of the cation and Highest Occupied Molecular Orbital (HOMO) of the anion. The electrochemical decomposition reactions of several ionic liquids on the cathode limit were successfully predicted and verified by experiments.

Ionic liquid/carbon dioxide production processes lead to significant economical and environmental benefits compared to the conventional production processes. The operational costs for the production of N-acetyl-(*S*)-phenyl-alanine methyl ester can be reduced by € 7.04 per kilo, because of the lower costs for catalyst and solvent make-up and the lower energy costs in the ionic liquid/carbon dioxide production process. Although the investment costs for the ionic liquid/carbon dioxide production process are higher due to investments in ionic liquid and catalyst, the new production process is economically feasible, especially when the production process is carried out in existing equipment. The most important obstacles in the implementation of the new technology are the successful life cycle management of current production plants, the linearity of current innovation thinking and a perceived high risk of adoption. According to the cyclic innovation model, these obstacles can be overcome when developments in all cycles occur in a parallel fashion and all involved actors collaborate in coupled networks.

11.2 Outlook

Because ionic liquids can be designed for a specific application, it is expected that the production method using ionic liquids and carbon dioxide described in this thesis is applicable to many industrial processes, especially in the fine chemical and pharmaceutical industry. In these industries, the use of ionic liquids could lead to enormous savings in waste generation and energy consumption, whereas at the same time high product qualities are obtained (food-grade, without any ionic liquid contamination). Therefore, it is recommended to extend the research to other systems, preferably with useful products where the new production method would be a solution to the enormous amounts of waste produced and energy consumed, the low purity of the product and the catalyst recovery problem. Moreover, further research should be focused on the control of the reaction and the separation process. For example, the influence of the conditions (temperature, pressure, time, stirrer speed, etc.) on the crystal size and shape of the product after extraction or precipitation is unknown and has to be determined.

The production method described in this thesis is not the only method that shows how ionic liquids can contribute to process intensification. Since the discovery that ambient temperature ionic liquids can be used as solvents for (organic) reactions and separations one decade ago, the number of articles about ionic liquids as 'green' media has been growing steadily (see figure 1.3) and will continue to increase, as ionic liquids are a hot topic in chemistry and chemical engineering. It is expected that new intensified production methods using ionic liquids will be found in the near future.

For example, ionic liquids are promising solvents for the use in ionic liquid membrane reactors (see figure 11.1). Supported ionic liquid membranes are porous solids whose pores are filled with ionic liquid. In the ionic liquid a catalyst can be dissolved that catalyzes the reaction between the gaseous reactants. In principle the reaction can be carried out beyond its equilibrium by continuous removal of (one of) the products, because only the product is able to diffuse through the membrane.
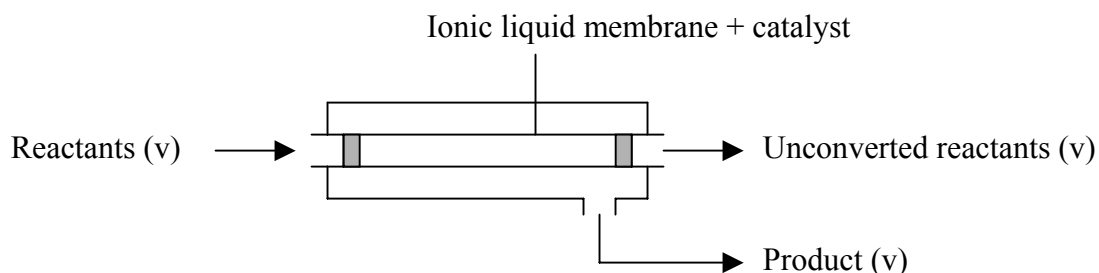

Figure 11.1: Ionic liquid membrane reactor

The advantages of using ionic liquid membranes over normal membranes are the higher stability (the ionic liquid will not evaporate), the higher dispersion of the catalyst without the problem of sintering (ionic liquids stabilize catalysts) and additional separation selectivity (the selectivity of ionic liquids can be optimized by choice of cation and anion).

Another promising field is electrochemical synthesis in ionic liquids. Ionic liquids are suitable solvents for carrying out reduction-oxidation reactions, because of their high electrochemical stabilities and conductivities. The separation is instantaneous, because the different products are formed at different electrodes. Examples are the synthesis of inorganic and organometallic materials and the reduction of carbon dioxide into useful hydrocarbons.

Although many new applications of ionic liquids will be found, it is expected that ionic liquids as solvents will only be industrially applied for the production of specific chemicals, where the ionic liquid offers huge advantages over the conventional solvent. Ionic liquids will not change the whole chemical industry, but they will certainly find their way into a number of industrial processes.

It is essential to know the long-term process aspects for the industrial application of ionic liquids. Therefore, it is expected that ionic liquid research in the near future will be focused on the long-term use and environmental impact of ionic liquids (long-term stability, toxicity, biodegradability, etc.). More models will be developed that predict the physical and chemical properties of ionic liquids based on choice of cation and anion. This makes it possible to select a suitable ionic liquid for each application, without expensive time-consuming experimentation in the laboratory.

It can be expected that the ability to tailor the properties of ionic liquids will be used more and more to design perfect solvents for each application. Certainly, the focus will change from tetrafluoroborate-based and hexafluorophosphate-based ionic liquids to more stable ionic liquids. At this moment especially the 1-hexyl-3-methylimidazolium bis(trifluoromethyl-sulfonyl)imide is at the center of interest. Better alternatives for the base-sensitive imidazolium cation will also be found. Imidazolium is easily deprotonated at the C2-position and the aromatic ring is easily reduced. It is expected that non-aromatic cations without any acidic hydrogen atoms are more stable cations. The choice of cations and anions is enormous, and this choice will be used for an optimal ionic liquid design.

Although a lot of money can be saved by using ionic liquids as industrial solvents, the cost of ionic liquids themselves can be a limiting factor in the development of industrial ionic liquid processes. Currently, ionic liquids are made primarily in laboratory-scale quantities and sell for around € 1,000 per kilo. To be competitive with conventional solvents, the price of ionic liquids will have to be reduced by a factor of 100 or more. The price can drop to about € 10 per kilo or even less, when larger quantities of ionic liquids are produced, depending on composition, purity and quantity. But this price is still high compared to conventional organic solvents. However, the attention for safety, health and

environment will make the use of ionic liquids in industry economically more attractive than the use of conventional organic solvents, which have high flammabilities and high volatilities leading to high emissions, high costs for pollution and high solvent make-up costs.

Acknowledgements

De tijd is gevlogen. Ik kan me nog goed herinneren dat ik als nuldejaars aankwam in Delft in 1999, niet wetende hoe leuk ik mijn studietijd en promotietijd zou vinden. Vele mensen hebben invloed gehad op de keuzes die ik tijdens mijn ontwikkeling tot scheikundig ingenieur heb gemaakt. Mijn eerste woord van dank gaat uit naar Hedzer van der Kooi, die mijn interesse voor de thermodynamica al in mijn derde studiejaar aanwakkerde. Hij was mijn coach tijdens mijn fabrieksvoorontwerp voor Shell, mijn begeleider gedurende mijn research-practicum bij Purac, en mijn adviseur gedurende mijn stagetijd bij Toshiba. Het was ook Hedzer die mij voor het eerst in contact bracht met Cor Peters.

Vanaf de dag dat ik Cor Peters ontmoette in Tokyo, konden we het goed met elkaar vinden. Cor deed ook interessant onderzoek bij de vakgroep thermodynamica. Hij liet mij voor het eerst kennis maken met het vakgebied van de ionische vloeistoffen. Ik besloot niet alleen mijn scriptie en afstudeerproject aan dit onderwerp te wijden, maar zelfs nog wat langer door te gaan gedurende mijn promotieonderzoek. Ik wil Cor hartelijk bedanken voor alle begeleiding tijdens mijn scriptie, afstudeerproject en promotieproject. Cor, het was een genoegen om met je samen te werken. Ik heb veel van je geleerd, zowel op technisch en wetenschappelijk gebied, als op sociaal gebied. Je hebt zo veel contacten in de wereld en ik heb er bewondering voor hoe je je groep door moeilijke reorganisatorische tijden hebt geleid.

Tijdens mijn afstudeerproject en promotieproject werd ik ook begeleid door Geert-Jan Witkamp. Op het moment dat ik met mijn onderzoek naar ionische vloeistoffen begon, kende ik Geert-Jan nog niet. Maar dat veranderde snel. Geert-Jan, ik wil je bedanken voor je enorme belangstelling in het onderzoek en al je technische adviezen. Door jou werden al mijn artikelen tot op de letter nauwkeurig doorgenomen. Ik wil je ook bedanken voor vriendschap die we in de jaren hebben opgebouwd, de gezellige avondjes die we hadden, en het uitwisselen van leuke leesboeken. In jou heb ik een leesgenoot gevonden die dezelfde smaak qua literatuur heeft.

Besides Cor, Geert-Jan and myself, many other people were involved in the ionic liquid project. I would like to thank Ali Shariati (section Physical Chemistry and Molecular Thermodynamics), Roger Sheldon (section Biocatalysis and Organic Chemistry), Jaap van Spronsen (section Process Equipment), Guus Berkhout (section Technology, Strategy and Entrepreneurship), Wim Buijs (section Catalysis Engineering), Ioannis Economou (Demokritos), Anneke Levelt Sengers (NIST), Geert Woerlee (Feyecon) en Gary Meima (Dow) for their advice and their input. Technische ondersteuning heb ik gekregen van Louw Florusse, Gerard Hofland en Andréanne Bouchard. Dank jullie wel voor alle hulp. Ik wil ook graag Michel van den Brink, Paul Durville, Michiel Janssen, Chrétien Simons, Ron Penners, Adri Knol en Anton van Estrik bedanken voor hun hulp bij de syntheses en analyses. Furthermore, I would like to thank Vincent Toussaint, Dap Hartmann, Eirini

Karakatsani and Marco Constantini for their contributions to the experimental and modeling work.

During my PhD research I also worked several times outside Delft. First of all, I would like to thank Ioannis Economou for giving me the opportunity to work in his group at the National Center for Scientific Research 'Demokritos', Greece. I was a pleasure working in Athens with you and your group. Secondly, I would like to thank Anneke Levelt Sengers for her hospitality during my stay at the National Institute of Standards and Technology in Gaithersburg, Maryland, USA. Anneke, I learned a lot from you, and I admire your technical work and your fight for women in science.

It is not only the interesting work that made my PhD time such a wonderful period, but also the interaction with the group members of the different groups I worked with. I had a very nice time at the section Physical Chemistry and Molecular Thermodynamics in Delft. I still remember our trip to Bavaria with the nice product confrontation, the bowling night, the BBQs at Theo's home, and the nice evenings at Cor's place (Adri, ik vind het echt superleuk dat je ons iedere keer weer bij jullie thuis uitnodigt). Cor, Ali, Sona, Eliane, Khalik, Lola, Eugene (biertje doen?), Louw, Theo, Rita, Vincent, Luc, Bianca, Astrid, Laura, Karin, Aleidus, Felix, Berend, Marco and all the other Erasmus-students working in our group, thank you for the wonderful time!

I also would like to thank my colleagues at the former 'Apparatenbouw voor de Procesindustie' for the nice time I had in Delft. Jaap, je bent een geweldige kamergenoot, reisgezel en vriend. Bedankt voor alle gezelligheid. Furthermore, I would like to thank my fellow PhD and MSc students (Pepijn, Raimo, Elif, Marcos, Martijn, Vanesa, Jelan, Richard, Albert, Andréanne, Hélène and all the others) for their kindness and their friendship. En natuurlijk wil ik ook de mensen van de werkplaats en de veiligheids-commissie bedanken voor alle hulp en gezelligheid, met name André, Jan, Martijn, Stefan, Gerard, Daniel, Leen, Michel, Bert en alle anderen.

Jan en Tineke, bedankt voor jullie onvoorwaardelijke steun. Jullie zijn altijd geïnteresseerd in alles waar ik mee bezig ben. Zonder jullie aanmoediging en ondersteuning was ik nooit zover gekomen. Ik vind het ook geweldig dat ik jullie aan de email, msn en skype heb gekregen, zodat de afstand tussen ons altijd klein zal zijn, zelfs als ik even in het buitenland ben.

Tot slot wil ik jou bedanken, Jeroen. Jij hebt mijn hele promotietijd van het dichtste bij meegemaakt, zowel inhoudelijk als persoonlijk. Ik durf te wedden dat niemand mijn proefschrift en artikelen beter heeft gelezen dan jij. Ik wil je daarvoor bedanken. Maar mijn grootste dank gaat uit naar het plezier en de ontspanning die je me hebt kunnen geven tijdens mijn gehele promotietijd. Onze vakantie naar Vama Veche was één van de hoogtepunten. Bedankt voor alles!

Curriculum Vitae

Identity:

Name: Maaike Christine Kroon

Born: December 31th, 1980, Rotterdam, The Netherlands

Education:

1993 – 1999:   Pre-university education at the 'Willem van Oranje' in Oud-Beijerland, The Netherlands (graduated cum laude)

1999 – 2002:   Bachelor Chemical and Biochemical Engineering at the Delft University of Technology, The Netherlands (graduated cum laude)

2002 – 2004:   Master Chemical Engineering at the Delft University of Technology, The Netherlands (graduated cum laude)

2003 – 2005:   Honor's track program 'Innovative Developments in Chemical Engineering' at Delft University of Technology (graduated cum laude)

2004 – 2006:   Ph.D. at the section Physical Chemistry and Molecular Thermodynamics and the section Process Equipment at the Delft University of Technology, The Netherlands

Awards:

Sept. 1999:   Scholarship of Delft University of Technology on the basis of the results for final examinations at pre-university education

Sept. 2000:   CIVI-prize of encouragement 2000 (Central Institute For Industrial Development) of the 'Hollandse Maatschappij der Wetenschappen' for the best propaedeutics in chemistry/chemical engineering in The Netherlands

Sept. 2000:   Propaedeutics-prize of Delft University of Technology for obtaining the certificate of the propaedeutics in chemical engineering cum laude

Sept. 2003:   Admission to the honour's track program, an additional individual program around a certain theme for students who finish their Bachelor-program cum laude

April 2005:   Study prize of the faculty Applied Sciences of the Delft University of Technology for most innovative Master's research

Nov. 2005:   Unilever Research Prize for remarkable study results of young promising graduates

Nov. 2005:   Master's-prize of Delft University of Technology for the best Master in Chemical Engineering in 2004-2005

Nov. 2005:   Prize for best Master graduate student of the Delft University of Technology in 2004-2005

June 2006:   Admission as participant to the Meeting of Nobel Prize Winners in Chemistry in Lindau, Germany

Sept. 2006:   Study prize of the 'Bataafsch Genootschap der Proefondervindelijke Wijsbegeerte' for the best graduate student of the Delft University of Technology in 2004-2006

Publications

Patents

- M. C. Kroon, A. Shariati, L. J. Florusse, C. J. Peters, J. van Spronsen, G. J. Witkamp, R. A. Sheldon, K. E. Gutkowski, Process for Carrying Out a Chemical Reaction, International Patent WO 2006/088348 A1 (2006).

Reviewed Papers

- M. C. Kroon, A. Shariati, M. Costantini, J. van Spronsen, G. J. Witkamp, R. A. Sheldon, C. J. Peters, High-Pressure Phase Behavior of Systems with Ionic Liquids: Part V. The Binary System Carbon Dioxide + 1-Butyl-3-methyl-imidazolium Tetrafluoroborate, *J. Chem. Eng. Data* **2005**, *50 (1)*, 173-176.

- M. C. Kroon, C. J. Peters, R. A. Sheldon, J. van Spronsen, G. J. Witkamp, Economical and Ecological Attractiveness of Using Ionic Liquids as Combined Reaction and Separation Media, *Proceedings of 6th International Conference on Process Intensification*, Delft, September 27-29 (2005).

- M. C. Kroon, J. van Spronsen, C. J. Peters, R. A. Sheldon, G. J. Witkamp, Recovery of Pure Products from Ionic Liquids using Supercritical Carbon Dioxide as Co-solvent in Extractions or as Anti-solvent in Precipitations, *Green Chem.* **2006**, *8 (3)*, 246-249.

- M. C. Kroon, W. Buijs, C. J. Peters, G. J. Witkamp, Decomposition of Ionic Liquids in Electrochemical Processing, *Green Chem.* **2006**, *8 (3)*, 241-245.

- M. C. Kroon, E. K. Karakatsani, I. G. Economou, G. J. Witkamp, C. J. Peters, Modeling of the Carbon Dioxide Solubility in Imidazolium-Based Ionic Liquids with the tPC-PSAFT Equation of State, *J. Phys. Chem. B* **2006**, *110 (18)*, 9262-9269.

- M. C. Kroon, L. J. Florusse, A. Shariati, K. E. Gutkowski, J. van Spronsen, R. A. Sheldon, G. J. Witkamp, C. J. Peters, On a Novel Class of Production Processes for the Chemical Industry, to be submitted for publication to *Nature* **2006**.

- M. C. Kroon, D. Hartmann, G. Berkhout, Innovating the Innovation Process: How to Revolutionize the Fine Chemical and Pharmaceutical Production Process, submitted for publication to *Green Chem.* **2006**.

- M. C. Kroon, W. Buijs, C. J. Peters, G. J. Witkamp, Quantum Chemical Aided Design of the Electrochemical Window of Ionic Liquids, to be submitted for publication to *Green Chem.* **2006**.

- M. C. Kroon, W. Buijs, C. J. Peters, G. J. Witkamp, Quantum Chemical Aided Prediction of the Thermal Decomposition Mechanisms and Temperatures of Ionic Liquids, submitted for publication to *Thermochim. Acta* **2006**.

- M. C. Kroon, V. A. Toussaint, A. Shariati, L. J. Florusse, G. J. Witkamp, C. J. Peters, Fluid Phase Equilibria of Ternary Systems with Ionic Liquids, Carbon Dioxide and Some Organic Compounds of Pharmaceutical Interest, to be submitted for publication to *J. Chem. Eng. Data* **2006**.

Non-Reviewed Papers

- M. C. Kroon, A. Shariati, V. A. Toussaint, G. J. Witkamp, R. A. Sheldon, C. J. Peters, A Novel and Environmentally Benign Approach to Combine Reactions and Separations, *Proceedings of the Netherlands Process Technology Symposium 4 (NPS 4)*, Veldhoven, The Netherlands, October 26-27 (2004).

- A. Shariati, M. C. Kroon, V. A. Toussaint, G. J. Witkamp, R. A. Sheldon, C. J. Peters, Atom-Efficient Reactions and Environmentally Benign Separations Using Ionic Liquids and Supercritical Carbon Dioxide, *Proceedings of the AIChE 2004 Annual Meeting*, Austin (TX), USA, November 7-12 (2004).

- M. C. Kroon, W. Buijs, C. J. Peters, G. J. Witkamp, Quantum Chemical Aided Design of Ionic Liquids as Electrolytes, *Proceedings of the 1st International Congress on Ionic Liquids (COIL 1)*, Salzburg, Austria, June 19-22 (2005).

- A. Shariati, M. C. Kroon, V. A. Toussaint, J. van Spronsen, R. A. Sheldon, G. J. Witkamp, C. J. Peters, Asymmetric Hydrogenation and Catalyst Recycling Using the Ionic Liquid [bmim][BF$_4$] and Supercritical Carbon Dioxide, *Proceedings of the 21st European Symposium on Applied Thermodynamics (ESAT 2005)*, Jurata, Poland, June 1-5 (2005).

- M. C. Kroon, W. Buijs, C. J. Peters, G. J. Witkamp, Quantum Chemical Aided Design of Ionic Liquids as Electrolytes for the Reduction of Metal Salts, *Proceedings of the Netherlands Process Technology Symposium 5 (NPS 5)*, Veldhoven, The Netherlands, October 25-26 (2005).

- M. C. Kroon, J. van Spronsen, C. J. Peters, R. A. Sheldon, G. J. Witkamp, Recovery of Pure Products from Ionic Liquids using Supercritical Carbon Dioxide as Co-solvent in Extractions or as Anti-solvent in Precipitations, *Proceedings of the 8th Conference on Supercritical Fluids and Their Applications*, Ischia, Italy, May 28-31 (2006).

- M. C. Kroon, E. K. Karakatsani, I. G. Economou, G. J. Witkamp, C. J. Peters, Modeling of the Carbon Dioxide Solubility in Imidazolium-Based Ionic Liquids with the PC-PSAFT Equation of State, *Proceedings of the 22nd European Symposium on Applied Thermodynamics (ESAT)*, Elsinore, Denmark, June 28 – July 1 (2006).

- M. C. Kroon, E. K. Karakatsani, I. G. Economou, G. J. Witkamp, C. J. Peters, Modeling of the Carbon Dioxide Solubility in Imidazolium-Based Ionic Liquids with the PC-PSAFT Equation of State, *Proceedings of the Thermo International 2006 Conference*, Boulder (CO), USA, July 30 – August 4 (2006).

- M. C. Kroon, W. Buijs, C. J. Peters, G. J. Witkamp, Decomposition of Ionic Liquids in Chemical Processing, *Proceedings of the Thermo International 2006 Conference*, Boulder (CO), USA, July 30 – August 4 (2006).

- M. C. Kroon, L. J. Florusse, A. Shariati, K. E. Gutkowski, J. van Spronsen, R. A. Sheldon, G. J. Witkamp, C. J. Peters, A Novel Method of Chemical Processing; Miscibility Windows in Ionic Liquids, *Proceedings of the Thermo International 2006 Conference*, Boulder (CO), USA, July 30 – August 4 (2006).

- M. C. Kroon, W. Buijs, C. J. Peters, G. J. Witkamp, Thermal Stability of Ionic Liquids, *Proceedings of the 2006 EUCHEM Conference on Molten Salts and Ionic Liquids*, Hammamet, Tunesia, September 16-22 (2006).

- M. C. Kroon, E. K. Karakatsani, I. G. Economou, G. J. Witkamp, C. J. Peters, Modeling-Based Design of Ionic Liquid/Carbon Dioxide Processes, *Proceedings of the Netherlands Process Technology Symposium 6 (NPS 6)*, Veldhoven, The Netherlands, October 24-25 (2006).

- I. G. Economou, M. C. Kroon, E. K. Karakatsani, C. J. Peters, G. J. Witkamp, Modeling Carbon Dioxide – Imidazolium-Based Ionic Liquid Phase Equilibria with the tPC-PSAFT Equation of State, *Proceedings of the 2006 AIChE Annual Meeting*, San Fransisco (CA), USA, November 12-17 (2006).

- M. C. Kroon, W. Buijs, C. J. Peters, G. J. Witkamp, Decomposition of Ionic Liquids in Chemical Processing, *Proceedings of the 2006 AIChE Annual Meeting*, San Fransisco (CA), USA, November 12-17 (2006).